

INSTITUTE
FOR
AEROSPACE STUDIES

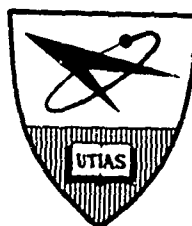
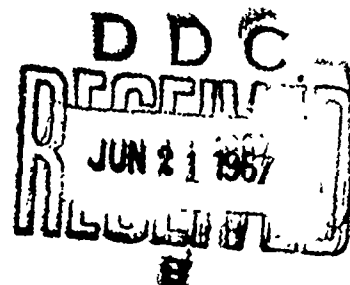
UNIVERSITY OF TORONTO

AN ATTITUDE CONTROL SYSTEM TO CONSTRAIN THE SKIN TEMPERATURE
OF A MANNED LIFTING SPACECRAFT DURING REENTRY INTO THE EARTH'S ATMOSPHERE

by

Jerome H. Fine

AD 654732



This document has been approved
for public release and sale; its
distribution is unlimited.

JULY 1967

UTIAS REPORT NO. 126
AFOSR 67-0858

RECEIVED

JUL 21 1967

CFST

151

AN ATTITUDE CONTROL SYSTEM TO CONSTRAIN THE SKIN TEMPERATURE
OF A MANNED LIFTING SPACECRAFT DURING REENTRY INTO THE EARTH'S ATMOSPHERE

by

Jerome H. Fine

Manuscript received March 9, 1967.

JULY 1967

UTIAS REPORT NO. 126
AFOSR 67-0858

ACKNOWLEDGEMENTS

I express my sincere appreciation to Prof. B. Etkin for his help and guidance throughout the investigation and for the considerable time and effort which he expended on my behalf. I would also express my gratitude to Dr. G. N. Patterson for the opportunity to carry out the research at the UTIAS.

Special thanks are tendered to the staff at the University of Toronto Institute of Computer Science who operated the IBM 7094 and to Dr. C.C. Gottlieb who made the time available on the computer.

Financial support for this work was received from the United States Air Force, Office of Scientific Research, Applied Mathematics Division, under grants AF-AFOSR-222-63, 64, 66. The National Research Council of Canada provided support in the form of a scholarship.

SUMMARY

An attitude control system to regulate the temperature of a manned lifting spacecraft during reentry into the Earth's atmosphere is proposed. Its use prevents the peak skin temperature that is experienced during the reentry from rising moderately beyond that which would occur during an equilibrium glide of the same vehicle.

The effects of Earth rotation and oblateness upon the performance of the attitude control system were found to be moderate and predictable. The maximum temperature increment associated with them was found to be only 100 F° for the worst set of initial conditions. The cross range shift of the footprint due to rotation was found to be within 70 miles of the value that would occur for the corresponding orbit in vacuum. Oblateness could generally be accounted for by using the effective initial glide angle relative to the Earth's surface rather than the geocentric initial value relative to the central coordinate system.

The results of density variations in the Earth's atmosphere were not serious. Large increases in the maximum skin temperature occurred only when extremely large spatially random density disturbances were encountered by the vehicle.

TABLE OF CONTENTS

	<u>Page</u>
NOTATION	vi
I. INTRODUCTION	1
1.1 Historical Background	1
1.2 Types of Protection Against Heating	2
1.3 Footprint Terminology	2
1.4 Choice of Vehicle and Basic Path	4
1.5 CONTAC System	4
1.6 Comparison with Other Systems	5
1.7 Trajectory Phases	6
1.8 Phase I - Pre-Atmospheric Flight	7
1.9 Phase II - Overall Down Range Control	8
1.10 Phase III - Equilibrium Glide Attainment	9
1.11 Phase IV - Attitude Control Release	10
1.12 Phase V - Final Range Control	11
II. ATTITUDE CONTROL LOGIC	12
2.1 Introduction	12
2.2 Choice of Attitude Limits	13
2.3 CONTAC Program Flow Diagram (see Fig. 12)	15
2.4 Vehicle Implementation	16
2.5 Vehicle Attitude Control	18
III. VEHICLE CHARACTERISTICS	19
3.1 Introduction	19
3.2 Vehicle Geometry	19
3.3 Vehicle Aerodynamics	20
3.4 Equilibrium Nose Stagnation Point Temperature	21
IV. GEOPHYSICAL ENVIRONMENT	22
4.1 Introduction	22
4.2 Rotation of the Earth	23
4.3 Earth's Oblate Gravitational Field	23
4.4 Oblate Shape of the Earth	26
4.5 Mean Standard Atmosphere	27
4.6 Atmospheric Density Variations	28
V. EQUATIONS OF MOTION	29
5.1 Basic Reference System	29
5.2 Conversion Between Reference Systems	30
5.3 Vector Equation of Motion	30
5.4 Expansion of the Single Vector Equation of Motion	31
5.5 Numerical Procedures	35

	<u>Page</u>
VI. RESULTS AND DISCUSSION FOR A CIRCULAR, NON-ROTATING EARTH	37
6.1 Introduction	37
6.2 Footprint Optimization	37
6.3 Effect of Non-Standard Initial Conditions	42
VII. RESULTS AND DISCUSSION - OBLATE, ROTATING EARTH	44
7.1 Introduction	44
7.2 Effect of the Earth's Rotation	44
7.3 Effect of the Earth's Oblate Shape	45
7.4 Effect of the Earth's Oblate Gravity Field	46
7.5 Effect of the Earth's Rotation and Oblateness	47
VIII. RESULTS AND DISCUSSION - DENSITY PERTURBATIONS	48
8.1 Introduction	48
8.2 Effect of Different Basic Models	48
8.3 Effect of Altitude Dependent - Perturbations in the Density	49
8.4 Effect of Random Density Perturbations	49
IX. CONCLUSIONS	50
9.1 Validity of the CONTAC System Concept	50
9.2 Effects of Adverse Conditions on the Reentry	51
REFERENCES	52
APPENDIX A - The Equilibrium Glide Trajectory	
APPENDIX B - The Effective Initial Glide Angle	
APPENDIX C - Program Listings	
APPENDIX D - Sample Output	

NOMENCLATURE

Roman Letters

C_D	drag coefficient ($D/\frac{1}{2}\rho V^2 S$)
$C_{D_{min}}$	minimum drag coefficient (at zero angle of attack)
$C_{n,m}$	general spherical harmonic coefficient - see Eq. (4.1)
$C_{2,0}$	spherical harmonic coefficient associated with polar flattening
C_L	lift coefficient ($L/\frac{1}{2}\rho V^2 S$)
C_p	pressure coefficient in Newtonian flow - see Eq. (3.1)
D	aerodynamic drag on the vehicle (lb_f)
F	force (lb_f)
F_A	total aerodynamic force acting on the vehicle (lb_f)
f_c	defined by Eq. (4.17)
f_f	defined by Eq. (4.18)
f_p	the Earth's polar flattening $\left(\frac{R_o - R_{pole}}{R_o} = \frac{1}{298.28} \right)$
f_q	the Earth's equatorial flattening $\left(\frac{R_{major} - R_{minor}}{R_o} \approx 10^{-5} \right)$
f_r	defined by Eq. (4.16)
GM	the Earth's gravitational constant (ft^3/sec^2)
g	total acceleration due to the Earth's gravitational field (ft/sec^2)
g_r	acceleration in the direction of the geocentric radius - see Eq. (4.4a) (ft/sec^2)
g_{λ}	acceleration in the direction of the geocentric latitude - see Eq. (4.4b) (ft/sec^2)
g_{θ}	acceleration in the direction of the geocentric longitude - see Eq. (4.4c) (ft/sec^2)
$\{\bar{h}, \bar{j}, \bar{v}\}$	third intermediate reference system - see Fig. 21
I_{α}	vehicle moment of inertia about the pitch axis ($slug/ft^2$)
$\{\bar{i}, \bar{j}, \bar{k}\}$	basic reference system - see Fig. 18
$\{\bar{i}', \bar{j}', \bar{k}'\}$	first intermediate reference system - see Fig. 21
$\{\bar{i}, \bar{j}, \bar{k}\}$	flight axes reference system - see Fig. 20

K	parameter defined by Eq. (A.8)
k_{α}	angular acceleration in pitch (sec^{-2})
k_{ϕ}	angular acceleration in roll (sec^{-2})
L	aerodynamic lift on the vehicle (lb_f)
L/D	ratio of lift to drag
M	moment exerted by the pitch reaction jets ($\text{lb}_f \times \text{ft}$)
m	mass of the vehicle (slugs)
$\frac{\bar{m} \bar{c}}{\bar{s}}$	heat capacity of the skin of the vehicle (BTU/ft^2)
$\{\bar{n}, \bar{e}, \bar{v}\}$	second intermediate reference system - see Fig. 21
P_n^m	general spherical harmonic - see Eq. (4.2)
Q	parameter defined by equation (3.9)
q	convective heating rate at any point on the vehicle ($\text{BTU}/\text{ft}^2 \text{ sec}$)
q_n	nose stagnation point convective heating rate ($\text{BTU}/\text{ft}^2 \text{ sec}$)
R_n	radius of curvature of the nose stagnation point (feet)
R_o	average equatorial radius (feet)
r	geocentric distance to the vehicle (feet)
S	reference wing area of the vehicle (ft^2)
$S_{n,m}$	general spherical harmonic coefficient - see Eq. (4.1)
s	distance along the flight path starting at the initial position (feet)
T	radiation-equilibrium nose stagnation point temperature (degrees Rankine or degrees Fahrenheit if specified)
\hat{T}	actual skin temperature at any point on the vehicle (degrees Rankine)
T_{lastmax}	the higher of the present temperature and the values measured since testing for a local maximum started - see Fig. 12
T_{lastmin}	the lower of the present temperature and the values measured since testing for a local minimum started - see Fig. 12
T_{deadband}	the allowable temperature variation before any action is taken - see Fig. 12

t	time starting at the initial point (seconds)
U	Earth's gravitational potential - see Eq. (4.1)
V	vehicle speed - see Fig. 19
y	perpendicular distance to the surface of the Earth from the vehicle - defined by Eq. (4.12) (feet)

Greek Letters

α	angle of attack of the vehicle (radians or if specified degrees)
γ	geocentric (with respect to the local geocentric horizontal) glide angle of the velocity vector - see Figs. 19 and 20 (radians or if specified degrees)
γ_e	initial geocentric glide angle - see Fig. 37
γ_{eff}	effective initial glide angle, defined by Eq. (B2) - see Fig. 37
Δt	defined by Eq. (2.4)
Δy	the difference in the perpendicular distance to the Earth's surface from the vehicle for the two latitude positions at the beginning and end of Phase II as measured at the average geocentric radius - see Fig. 37 (feet)
$\Delta\alpha$	defined by Eq. (2.6)
ϵ	emissivity of the material on the surface of the vehicle
θ	geocentric longitude of the position of the vehicle relative to the Prime Meridian - see Fig. 19 (radians or if specified degrees)
$\theta_{2,2}$	longitude of the equatorial major axis (radians or if specified degrees)
λ	geocentric latitude of the position of the vehicle - see Fig. 19 (radians or if specified degrees)
ρ	density of the atmosphere (slugs/ft ³)
σ	Stefan-Boltzmann constant (4.756×10^{-13} BTU/ft ² sec °R ⁴)
ϕ	angle of roll of the vehicle (radians or if specified degrees)
ψ	geocentric azimuth of the position of the vehicle - see Fig. 19 (radians or if specified degrees)
Ω	angular velocity of the $\{\bar{I}, \bar{J}, \bar{K}\}$ flight axes system relative to the $\{\bar{I}, \bar{J}, \bar{K}\}$ basic reference system (radians/sec)
ω	angular velocity of the Earth on its axis (radians/sec or if specified degrees/sec)

Superscripts

- ($\dot{}$) first derivative of a variable with respect to time
($\ddot{}$) second derivative of a variable with respect to time
($\vec{}$) denotes three-dimensional vector

Subscripts

- ()_{max} maximum value
()_{min} minimum value
()_s value when the last use of the reaction jets was started

I. INTRODUCTION

1.1 Historical Background

When the problems of manned space flight were being solved in the late 1950's and the early 1960's, the state of the art with regard to protecting reentry nose cones was oriented toward an ablative type of material since the heat pulse for ballistic missiles is characterized by intense heating rates which normally last for quite short intervals of time. Thus, the occurrence of manned space flight so soon after the successful implementation of the ballistic missile program produced technological solutions based primarily on concepts developed for the ICBM system. As a consequence, the heat shield concept which is presently associated with the manned capsule configuration seemed both a natural and logical extension of the techniques which were and still are generally accepted practice.

However, the capsule shape is able to attain only a very low ratio of lift to drag (L/D). Therefore, only very limited manoeuvring capability is available to the pilot. He is unable to land the spacecraft outside a relatively small area once the retro rockets have been fired and the deboost phase has been completed. As a result, only a small portion of the Earth's surface can be reached during any given twenty-four hour period. This is because each successive orbital track is displaced by about 22.5 degrees as a result of the Earth's rotation. Therefore, during that time period there would be only about sixteen passes over the whole Earth each yielding only a thin strip of coverage.

As a result of the above restrictions, a large pickup and recovery force must be maintained in the principal landing zone during the entire course of an exercise in case of an emergency. This procedure is unsatisfactory for many reasons. First, and perhaps the most obvious, is the sheer cost. However, and this reason is probably of greater importance, weather conditions may dictate the choice of landing area and a sudden storm might require the movement of the pickup force to a more suitable position within an impossibly short time interval. Other difficulties are also apparent upon even a preliminary analysis. The efficient solution to the landing problem appears to require a different shape of reentry vehicle. The basic requirement is greater manoeuvrability, which requires a higher L/D. Thus, the capsule configuration must be abandoned in favour of a winged vehicle or lifting body.

Another obvious requirement for space flight for the foreseeable future will be the minimization of space vehicle weight. It is not necessary to point out in any detail the well-known correlation between the cost of the first stage booster and the mass of the final payload. Therefore, the first step is to design a vehicle with a moderate L/D which possesses no excess protection to enable it to reenter the Earth's atmosphere and land on the Earth's surface. Considering the minimal degree of protection available, the basic flight path upon which the preliminary design is based should be a simple trajectory for which the problems of protecting the spacecraft and its occupants are as moderate as possible. However, when the choice for the basic path and the method of protection is being made, consideration must be given to incorporating provision for departures from the basic path. The departures are necessary to allow the vehicle to manoeuvre to landing sites other than the basic terminal position.

Before considering the choice of the vehicle and the basic path, two general areas should be reviewed. The concepts involved in protecting the

vehicle against extreme heating rates will be presented first. Then, the manoeuvring capability or 'landing footprint' available to a vehicle will be discussed.

1.2 Types of Protection Against Heating

There are two basic methods of withstanding reentry heating. Ablation materials have successfully been used on both ICBM nose cones and the current series of manned capsules in addition to other classes of vehicles. Very broadly speaking, the basic principle is to use a material which has a large heat of sublimation in order to absorb as large a total heat load as possible for a given mass. The actual heating rates experienced during the reentry are usually unimportant for such a design. However, the maximum heat load is very strictly defined. When exceeded, the heat shield will fail and the spacecraft will disintegrate.

On the other hand, a radiative material can withstand much higher total heat loads as long as the maximum heating rate does not exceed the capability of the material. The permissible heating rate is primarily a function of the temperature versus time capability of the material (see Fig. 1), its emissivity, and (for higher than average heating rates of a short duration) its heat capacity. If the material is thin enough, its heat capacity may be neglected and the temperature then assumes the radiation - equilibrium value. In this situation, the rate at which heat is absorbed locally by the skin of the spacecraft equals the rate at which heat is being radiated from its surface. Changes in the heating rate are then quickly reflected by a change in the skin temperature. A higher rate requires a higher temperature to radiate more heat and vice versa. In general, the position at which the heating rate is most severe is the nose stagnation point of the vehicle, since the nose cap has the smallest effective radius of curvature. Therefore, the nose stagnation point will have the highest temperature on the spacecraft. Thus, if a suitable material can be found for the nose stagnation point, it can safely be assumed that the rest of the vehicle can also be adequately protected. Consequently, unless explicitly stated, the radiation-equilibrium nose stagnation point temperature will be the value to which reference is being made whenever temperature is referred to in this paper.

Two other points which should be mentioned in comparing ablative and radiative cooling. The materials which employ the latter method must always be replaced after use. On the other hand, while recoating may be necessary for a severe reentry, it should be possible to reuse in a conventional manner a vehicle which employs radiation cooling. It should be noted, however, that ablative materials are able to handle very large heating rates (until the maximum heat load is reached) that are usually far larger than the heating rates which the maximum temperature of a radiation cooled material can support.

1.3 Footprint Terminology

In order to initiate a return to the Earth's surface, an orbiting spacecraft will fire its retro rockets. Once this deboost phase is over, the vehicle becomes a hypersonic glider which is capable of influencing the position of its landing site only by means of aerodynamic force controlled by the attitude of the vehicle. A representative manoeuvre boundary or footprint from Ref. 1 is shown in Fig. 2. Note that the initial position is at the altitude at which aerodynamic forces begin to affect the path of the reentry vehicle. Throughout this investigation, the computations were started when the perpendicular distance to the Earth's surface was 350,000 feet. As a consequence, the reentry

values of velocity and glide angle at the initial position were treated independently of the orbital altitude at which retro-fire takes place. The actual flight path is effectively separated for computational purposes from the point and conditions of retro-fire. The only restriction is that the deboost cannot occur at an altitude that is greater than the maximum height which is compatible with conditions at the initial position.

In Fig. 3, additional terminology is given regarding the projection of the footprint onto an imaginary sphere which is used in place of the Earth's surface. Geocentric spherical trigonometry is used to define the geographical position over the imaginary sphere. Since the footprint boundary is given for an altitude of about 100,000 feet, the usual conversion problems of positioning the vehicle in terms of its geodetic latitude and longitude and of determining the distance travelled over an oblate Earth can be avoided.

The actual method of presenting the results requires some explanation. Assume for the moment that the initial position of the vehicle is in the Earth's equatorial plane and that the initial azimuth is either due East or West. Note that the initial glide angle is quite immaterial to the range definition (although it is of great importance to the pilot since too large a value would cause the spacecraft to disintegrate through overheating). In this situation, the equatorial plane, the great circle projection, the orbital track projection, and the footprint midline all coincide. The 'down range' is the absolute value of the longitude change from the initial position (by definition, down range is positive). The cross range is the final latitude (cross range may be positive or negative) if the initial azimuth was due East and the negative of the final latitude if the initial azimuth was due West. Note that the definition must be consistent with the reentry trajectory track over the Earth's surface, not with the Earth's co-ordinate system. A third range parameter, the azimuth or heading angle change, may also be simply defined in this situation as the final azimuth minus (or plus in the case of a due West reentry) ninety degrees.

At the initial position (which has been arbitrarily defined to be the point over the Earth's surface when the vehicle's altitude is 350,000 feet), the initial values of speed, altitude, glide angle, azimuth, latitude, and longitude define the path which the vehicle will travel over the Earth's surface. For a non-rotating, spherical Earth, the final pattern or shape of the projection of the path on the Earth's surface will not be affected by the initial values of the last three parameters. The resultant equivalent down range, cross range and azimuth change must be the same as for the case of the due East equatorial reentry with the same initial values of speed, altitude, and glide angle. For this situation, the great circle projection, the orbital track projection, and the footprint midline will still coincide with each other, but they will no longer coincide with the equatorial plane. However, for a rotating, oblate Earth, all three will tend to diverge. In this situation, the great circle projection remains in the same relative position. Consequently, all range parameters are measured in equivalent degrees over the imaginary sphere relative to the great circle projection through the initial position. Figure 3 illustrates a typical footprint over a rotating, oblate Earth. The subroutine which computes these range values is listed in Appendix C under the name of SUBROUTINE RANGE.

1.4 Choice of Vehicle and Basic Path

The type of vehicle chosen can be seen in Fig. 4. It satisfies the requirement of moderate lift to drag ratio since $(L/D)_{\max}$ can range from 1.3 to 1.7 for this type of configuration.

With regard to the choice of the basic path, the manoeuvrability requirement is first used to determine the method of preventing the spacecraft from burning up during the reentry. When the vehicle must reach landing zones corresponding to large down range distances, prolonged flight times must result. Consequently the total heat input to an ablative material would be extremely large and might become prohibitive. However, in a design which radiates most of the heat away from the vehicle, the total heat load is not an important consideration. Therefore, a wide variation in the time interval over which the heating occurs will have a negligible effect on the vehicle design as long as the peak temperature experienced during the flight is independent of the point at which the spacecraft lands. Consequently, radiation cooling offers the only practical solution for protecting the vehicle against the extreme heating which is encountered during the reentry. This method then requires a trajectory that satisfies the requirement on the peak temperature.

An equilibrium glide was chosen as the basic path. This trajectory is characterized (see Appendix A for a more comprehensive discussion) by the absence of any long period or 'phugoid' oscillations along the trajectory. This situation results from the equality between the lift force and the difference between gravitational and centrifugal forces. There were a number of important reasons for the choice of the equilibrium glide. First, it satisfies the requirement that it be a simple trajectory since it is a fixed-attitude reentry. Second, it offers the lowest possible value for the peak temperature which is experienced by the vehicle during its reentry without the introduction of a sophisticated optimal programming procedure. Third, the equilibrium glide also satisfies the requirement that departures from this basic path may easily be made in order to provide the manoeuvring capability necessary to land at sites other than the basic terminal position.

The reader should also note the simple analytical result for the peak temperature which is experienced during an equilibrium glide (see Appendix A). The ease of obtaining this comparison standard and its simplicity of definition will greatly outweigh the benefits of obtaining any reduction in the standard peak temperature by complex optimal procedures.

1.5 CONTAC System

The problem, then, is to conceive of as simple a procedure as possible which will allow the next generation of reentry vehicles the freedom to manoeuvre to their desired landing zones. Ideally, implementation of this procedure will not require any additional protection for the pilot or the vehicle.

As a solution to this problem, the author proposes a CONstant Temperature Attitude Control (CONTAC) system which will limit the peak temperature which is experienced by the vehicle during a reentry to a value which is only moderately (by 20°F or 30°F) greater than the peak temperature in a standard equilibrium glide. As a consequence, the CONTAC system will operate within the constraint that a negligible weight penalty is incurred relative to an

equilibrium glide, which it is assumed the vehicle can safely fly. A further constraint will be that neither predictive nor memory logic (with a minor exception) will be used by the CONTAC system. This requirement means that the CONTAC system must produce the solution on a real time basis when operating in the actual reentry environment.

It will be shown that the CONTAC system gives the pilot the extensive manoeuvrability which he requires in order to land the spacecraft at any point under or near the orbital envelope (Fig. 5). When coupled with the proper range controller, the complete system will provide automatic guidance to the final destination and prevent any dangerous temperature peaks which might destroy the vehicle. In addition, no undue waiting periods will be required. For most landing areas within the orbital envelope, the delay before retro-fire will be less than twelve hours and no point will require more than twenty-four hours. For orbits of small inclination to the equatorial plane the waiting times would be usually less than one orbital period. Furthermore, the peak temperature will always be very near to the peak value encountered during an equilibrium glide except in those cases for which the atmospheric density variations about the mean are both large and random. Under these extreme conditions, it will be impossible to prevent a moderate rise in the peak temperature whenever the CONTAC system encounters a sequence of density variations for which no further correction by means of attitude control is available (i.e. when the optimum attitude - optimum angle of attack and zero roll angle - has already been assumed). Since adverse conditions which occur randomly are impossible to predict, a statistical result must be given and vehicle protection provided for the worst sequence of events which might occur with a certain design probability.

1.6 Comparison with Other Systems

As detailed in Ref. 1, a number of authors have studied the problem of guiding a spacecraft to its final destination. However, this investigation is not primarily concerned with the actual guidance, but rather with the means by which the heating problems may be minimized. In addition, the effects of Earth rotation and oblateness upon both the heating and the guidance problem will be ascertained. Finally, a test to determine the effect of random variations in atmospheric density will be presented.

With regard to the heating problem, a solution for minimizing the total heat load can be found in Refs. 2 and 3. However, since these solutions must operate within the inherent limitation imposed by the maximum allowable heat load, the manoeuvring capability is restricted to landing sites which are relatively close to the initial position.

The only other solution for minimizing peak temperatures that has been found in the open literature is a Temperature Rate Flight Control System which has been developed by Stalony-Dobrzanski (Ref. 4). The results show that the TRFCS is also able to prevent the peak temperature which occurs during a reentry from becoming greater than the value which is experienced during an equilibrium glide. (The use of the equilibrium glide as the basic path for the TRFCS is an additional reason for its choice as the standard of comparison in the present investigation.) However, in order to implement the TRFCS, the derivative of the temperature is required along with an elaborate analogue system to analyze the rate of temperature change. The attitude of the vehicle is adjusted using either the angle of attack or the bank angle as the primary control variable.

In contrast, the CONTAC system uses a simple digital program to analyze directly the actual temperature. In addition, the attitude is controlled via pitch and roll channels simultaneously.

With regard to the effects on the Earth's rotation and oblateness, there are no papers available which analyze the resulting changes in the footprint when constraints upon the peak temperature (or for that matter maximum heat load) are present. There have been a few studies which analyzed the effects of the Earth's rotation, but no constraints in connection with heating problems were incorporated.

Due to the lack of significant statistical data, the influence of density variations in the Earth's atmosphere is still extremely difficult to analyze. A number of average curves of density versus altitude are available for both summer and winter for latitudes from the equator to 75°N. Based on this type of information, a number of papers have appeared which deal with the effect of a constant percentage change in the density upon the guidance problem. However, even if heating effects were included in these investigations, the results cannot take account of the fact that the atmosphere is a dynamic system whose state can only be described in a statistical manner. With regard to the effects of random density variations about an average curve of density versus altitude, the author is not aware of any other studies which deal with the heating problem either from an optimal point of view (such as those represented by Refs. 2 and 3) or from a system approach (such as proposed by Stalony-Dobrzanski). Indeed, from a detailed examination of the way in which optimal procedures are applied, the inclusion of random density variations would seem to rule out this concept. The iteration procedure used depends on accurate external environmental specifications. If the density is a random quantity, it would not be possible under the presently used procedures to arrive at a final solution. Only a real time approach inherent in both the TRFCS and the CONTAC system can attempt to provide a solution. The present investigation will include the results of the attempts by the CONTAC system to deal with random density variations as well as constant percentage changes in the density.

1.7 Trajectory Phases

In order to simplify the description and analysis of the various aspects of the CONTAC system, the reentry trajectory has been divided into five rather distinct phases. Each phase is described rather briefly at this point in order to acquaint the reader with the overall concept. What the CONTAC system is capable of doing is also explained. In addition, problems which it cannot solve are mentioned and some suggestions are made regarding the solution of these difficulties.

It is assumed that the vehicle is under the primary control of a navigation and guidance system, that monitors and adjusts the two primary attitude angles, α and ϕ , in order to home on the desired landing site. At certain short but critical periods of the flight, the CONTAC system, as a result of monitoring vehicle temperature, automatically cuts in and overrides the navigation system. This situation occurs only during the portions of Phases III and IV of the reentry when the CONTAC system is in active operation. There are, of course, additional constraints on the attitude angles. These will be presented during the discussion of each phase.

The five phases of the trajectory are shown in Fig. 6. Although no such sharply defined divisions will occur during an actual flight, it is simpler to divide the reentry into the five parts shown for the purpose of explaining what takes place within each phase.

The CONTAC system has been designed for space vehicles entering the Earth's atmosphere from altitudes up to five hundred miles. It is conceivable that some application might be found for reentries from positions higher than this altitude. However, the primary requirement is that the maximum convective heating rate first experienced during the reentry (Fig. 6) must not produce a temperature greater than the peak value which would be experienced during an equilibrium glide. If this constraint is satisfied, the CONTAC system is capable of preventing all subsequent maximum temperatures from becoming very much greater than the peak experienced during an equilibrium glide. But, if the deboost altitude is above five hundred miles, the spacecraft must reenter the atmosphere at a speed which is substantially greater than the circular value. In order to prevent skipout, the reentry glide angle must also be increased. As a result, the first maximum experienced for the convective heating rate exceeds the peak for an equilibrium glide. Unless this single pulse can be tolerated, the vehicle fails.

Therefore, the CONTAC system is intended to be used for reentries from low orbital altitudes, up to about five hundred miles, with vehicles that use radiative cooling as the primary protection against failure due to heating. Examples of this type of operation include shuttle service for space stations, low orbit reconnaissance, and low orbit satellite service and repair.

1.8 Phase I - Pre-Atmospheric Flight

It should be noted at this point that although the CONTAC system may go into operation as soon as the retro rockets have been fired (or some other method is used to push the spacecraft out of its vacuum orbit), the angle of attack of the vehicle is quite immaterial for a period of between ten and thirty minutes, depending on the height of orbital ejection. This delay is due to the fact that aerodynamic forces do not become appreciable until an altitude of about 350,000 feet is reached (Fig. 7). Thus the pilot will have ample time to jettison any service modules or extraneous externals and to perform the tasks associated with the alignment of the spacecraft prior to the buildup of atmospheric density.

One point of importance which is associated with this phase is the deboost attitude alignment and velocity increment. Both values must be carefully computed and equally carefully implemented since a large error in either could cause excessive heating rates leading to the failure of the spacecraft. Figure 8 shows the effect of errors in retro-fire attitude alignment and velocity increment. However, past experience in the Gemini program indicates that the required accuracies for attitude alignment and velocity increment will not be difficult to achieve. Interpretation of the results indicates that the Gemini retro-fire system experienced maximum errors of one degree in attitude alignment and three feet per second in velocity increment (Ref. 5). A simultaneous maximum error in both would yield a maximum resultant error at the end of Phase I at 350,000 feet of 0.1 degrees in flight path angle, 10 feet per second in speed and 2 degrees in down range. Cross range might also be affected but to a negligible extent; the maximum error could amount to only 0.2 degrees. Note that all of the above nominal error values are maximum and would be very unlikely to occur simultaneously.

Since experience has proven that a highly accurate calculation of the alignment attitude and velocity increment values is possible, there should be no difficulty in this area. However, it may be necessary to change the method by which the calculation is made. Consequently, the allowable margin of error is described and discussed in Section VI where the effects of incorrect reentry conditions at the beginning of Phase II are considered.

1.9 Phase II - Overall Down Range Control

For the purposes of this investigation, the reentry begins at 350,000 feet. This is due to the fact that for all practical purposes, the atmosphere has no effect on the flight path until the spacecraft reaches this altitude. Since the pilot has no control over the trajectory between the time he fires the retro rockets and the time he descends to this height, it is best to separate the problems associated with achieving the correct reentry conditions at 350,000 feet (by the proper attitude alignment and retro velocity increment at orbital altitudes) from the problems associated with controlling the vehicle's down range (by the proper angle of attack once lift and drag become appreciable). In fact, in order to simplify the problem even further, the portion of the flight within the atmosphere has been sub-divided into four parts, Phases II, III, IV, and V of the reentry.

During Phase II, the CONTAC system must be in operation; however, it exercises no actual control except to signal the end of Phase II at the point when the first q_{max} is reached (Fig. 9). At this position, the CONTAC system switches from passive to active operation and Phase III begins. Therefore, during Phase II, the pilot (or the automatic guidance system) has the function of devising the angle of attack program that will eliminate down range errors which may initially be present or which may occur during Phase II due to the Earth's departure from a circular, non-rotating sphere with a standard time invariant atmosphere. Since Phase II lasts for about four minutes, there is ample time for any down range corrections which are required in order to ensure that the vehicle lands on target.

To some extent, it will be possible to compensate, by adjustment of the initial retro-fire, for down range errors which it is anticipated will occur during Phase II due to some of the above non-ideal conditions. As a first approximation, a constant angle of attack can be used during the calculation for Phase II. In this situation, down range errors which will occur due to rotation and oblateness can be evaluated rather easily for this portion of the flight. The same calculation procedure can also be used to find the down range errors which will occur during Phase I. Thus, at the deboost position, it should be feasible to make the necessary corrections for down range errors which will occur during Phases I and II due to Earth rotation and oblateness. Note that the time of retro-fire may also be varied in addition to the attitude alignment and velocity increment. This additional parameter will probably provide most of the necessary correction.

Errors in down range which occur during Phase II due to variations in the atmospheric density are much more difficult to evaluate. Since it is unlikely that an accurate prediction of the density can be made, an estimate based on the available statistical data should be made. It may then be possible to compensate for the anticipated down range error by adjusting the retro-fire parameters.

The only restriction on the angle of attack during Phase II (angle of roll is zero) is that it must not be so low as to cause the first q_{max} to exceed the maximum allowable value nor so high as to endanger the rear portion of the vehicle from excessive heating rates. In general, the optimum value lies very near the angle of attack which yields the maximum lift coefficient. Larger values for the angle of attack will reduce the down range and smaller values will increase it. For the vehicle studied, the optimum angle of attack was 55 degrees. The largest angle of attack used during Phase II was 65 degrees and the smallest value was 35 degrees. These two limits yielded a down range interval of about 75 degrees or about 5000 nautical miles.

It should be noted that almost all of the incremental down range achieved by modulating the angle of attack during Phase II is not apparent until the end of Phase III. This is because the primary effect of varying the entry angle of attack is a variation in the vehicle's speed at the end of Phase II without any major difference in altitude, glide angle, or down range distance (Fig. 9). A comprehensive discussion and analysis of this point is given in Sec. 6.2.

1.10 Phase III - Equilibrium Glide Attainment

The most critical portion of the reentry is Phase III, the various sections of which are shown in Fig.10. During this part of the flight, the CONTAC system must remove energy from the vehicle at a rate designed to place the vehicle on or very near to an equilibrium glide trajectory. However, the rate of energy dissipation must also be flexible enough to allow the pilot (or the automatic guidance system) to control the vehicle's range in order to counteract all departures from non-ideal conditions as well as any errors present at the start of Phase III. Failure of the CONTAC-guidance combination to cope with adverse conditions will result in the vehicle over-heating during the flight or landing at the wrong location, either of which could be disastrous.

The actual details of the CONTAC system are given in Section II. At this point, it is sufficient to state that the phugoid or long period oscillation can be completely eliminated before the peak temperature is experienced and as a result, that value is very nearly minimized.

For most reentries, the attitude which is adopted subsequent to the first q_{max} is held for between two and four minutes. During this period, the pilot again has an opportunity to continue correcting any down range errors as well as beginning to reduce any cross range discrepancy. The additional incremental down range available during Phase III varies from about 1500 miles when the entry angle of attack is 65 degrees up to about 5000 miles when the entry angle of attack is 35 degrees. It should be repeated that practically all of the down range increment available due to Phase II attitude control actually occurs during Phase III due to the variation in speed at the beginning of Phase III. The pilot or the guidance system must be aware of and be able to compensate for this speed difference.

During Phase III, a number of pairs of values are used for the upper and lower limits on the attitude angles of the vehicle. These pairs of values are inputs to the CONTAC system and may be regarded as constants within this system. During an actual or simulated reentry in which a pilot or range controller is available, the attitude limits will be changed to provide the

necessary range control in order to land the spacecraft at the proper point on the Earth's surface. It is a feature of the CONTAC system that it is unaffected by the values for these limits as long as the upper and lower values of certain key pairs do not coincide. As long as this requirement is satisfied, the CONTAC system can damp the long period oscillations from the trajectory and place the vehicle on the equilibrium glide before the peak temperature occurs.

In very simple terms, the pilot will select the upper and lower limits for the angles of attack and roll which best fit the choice of the landing area toward which he desires to proceed, although certain practical considerations will restrict the pilot's freedom of choice (the upper and lower limits must not coincide for both pitch and roll). The CONTAC system then automatically adjusts the attitude angles (or the pilot himself if the associated control hardware should fail, but not the temperature readout equipment) to some value between the upper and lower limits of the angles of pitch and roll.

It has definitely been determined that the CONTAC system will hold the temperature at very nearly a constant value as long as the vehicle's attitude has not reached either an upper or lower limit. A single skip usually occurs just after the first q_{max} , but this is quite intentional, and is designed to provide down range control capability during the early part of the reentry. Indeed, in some situations, this short skip is completely eliminated in order to substantially reduce the down range.

Thus, by the time the vehicle descends to about 260,000 feet, it has been placed upon an equilibrium glide corresponding to the attitude at which the spacecraft is currently being held. The lowest value for the peak temperature is achieved by using the optimum attitude. It occurs at maximum vertical force (see Appendix A) which is at 55 degrees angle of attack and zero roll angle. This optimum attitude is then held by the CONTAC system quite automatically until the peak temperature is attained. At that point, Phase IV begins and the attitude is changed to provide down range and cross range manoeuvring capability. In practically all the re-entries studied, Phase IV began at an altitude of about 245,000 feet. However, in cases where the density variations were quite large, Phase IV began at an altitude as much as 30,000 feet lower than the above value.

1.11 Phase IV - Attitude Control Release

There will, of course, be problems associated with unpredictable increases in air density which may drive the temperature during this phase beyond its previous maximum. In such a situation, it might be expected that the CONTAC system would have to revert to Phase III operation. However, the reader may recall that no such sharply defined division occurs during the actual flight. Therefore, since the CONTAC system has neither memory nor predictive logic, it is impossible for any such division to exist in the controlling concept. When in operation, the CONTAC system is attempting to keep the temperature constant, and if an increase occurs, whatever the cause, the CONTAC system will change the attitude so as to reduce the temperature. If the attitude is already at its optimum value and the CONTAC system is unable to prevent a further increase in the temperature, then the conclusion to be drawn is quite obvious, i.e. Phase III had not yet been completed. But the reversion is only with respect to the author's arbitrary division of the flight. The CONTAC system is not affected.

In fact, the pilot (or the automatic guidance system) need not in principle even know that the CONTAC system exists, let alone how it operates. Naturally, he would wonder why he is unable to assume a particular attitude for range control during certain portions of the reentry. However, the CONTAC system is completely automatic so that it can cope with unpredictable situations about which the pilot may be unaware.

The pilot would, of course, actually be informed about both the existence and the operation of the CONTAC system and he may, therefore, depend on it to properly reduce the attitude from the optimum position at the beginning of Phase IV to the desired values of pitch and roll sometime before the end of Phase IV. In addition, with regard to where Phase III ends and Phase IV begins, the pilot can leave this quite arbitrary decision entirely to the built-in logic of the CONTAC system. It is quite immaterial, as far as he is concerned, just where the peak temperature occurs during the flight. The only problem is to prevent that value from becoming any larger than necessary, and this problem the CONTAC system will solve all by itself.

Therefore, during Phase IV, the CONTAC system will gradually reduce the angles of pitch and roll until at some particular point in the flight, both values are under the complete control of the pilot. The transfer of this control may be revoked at any time after it is first made; however, after the temperature has fallen several hundred degrees, the pilot will realize that the transfer is complete and that the CONTAC system is no longer in operation. This transfer always occurs by the time the speed and height have dropped to values in the vicinity of 12,000 feet per second and 150,000 feet, respectively. At that time, a procedure to increase the cross range will have come into effect. A paper by Wagner (Ref. 6) discusses the variation of the bank angle of the spacecraft in relation to cross range control. The results indicate that large angles of roll should be used at the beginning of the reentry when the speed is high and that small angles of roll are best near the end of the flight when the speed is low. Various modes of dependence between the angle of roll and the flight parameters speed, altitude, and energy, were investigated to determine the best relationship. The calculations showed that a simple linear variation of bank angle versus speed gives the best overall performance.

1.12 Phase V - Final Range Control and Touchdown

As this paper is being written, the procedures for the final landing of a spacecraft are being developed in principle and tested in practice. However, an analysis of this phase is outside the scope of this investigation. It is therefore, of little value to speculate upon the best method to reach the landing site and perform the touchdown. Several papers (among them Refs. 7, 8, and 9) have appeared which deal with this manoeuvre so that some ideas are already available concerning the problems which may be encountered and the methods of solution.

To this date, all of the flight experience in the supersonic regime has been with the X-15 vehicle. Thus, it may be quite some time before the best solutions to the various problems are found. However a basic outline of the final phase has emerged from this test program. The additional local down range which can be attained is about 200 miles for the conditions given in Fig. 3 for the footprint boundary. But, it may be noted that the final azimuth is approximately perpendicular to the boundary line. Consequently, the footprints which are presented in Sections VI and VII are a conservative estimate of the

vehicle's capability. One point of considerable importance should be noted. At the end of Phase IV, the values of speed and altitude within and on the footprint boundary are independent of the final position. Consequently, the same procedure can always be used for the approach during Phase V.

II. ATTITUDE CONTROL LOGIC

2.1 Introduction

This section discusses the detailed concepts behind the CONTAC system. The methods by which the system may be implemented on the spacecraft itself will also be suggested although the actual details may require modifications in order to conform to hardware requirements.

In order to give the reader some insight as to why the CONTAC system is used, a typical reentry is shown in Fig. 11a in which no attitude control was attempted except at the first skip point. At this position, the angle of attack was reduced from the optimum value of 55 degrees and zero roll angle to 22.7 degrees with a roll angle of 50 degrees to the left in order to obtain greater down range and to produce some cross range. However, due to the reduction in the angle of attack, a phugoid oscillation is initiated which results in a large temperature oscillation as well. Because the latter is synchronized almost exactly with the phugoid, it was logical to attempt to control both the phugoid and the temperature oscillations by monitoring only the temperature. The reason for the use of the temperature as the controlling variable is that this value can be measured directly on board the spacecraft with a high degree of accuracy. On the other hand, the altitude is a very difficult quantity to measure when the vehicle is still 250,000 feet above the Earth's surface. In addition, the temperature oscillations are the ones which must be controlled. It is quite immaterial whether or not the phugoid oscillation is controlled and damped out as soon as possible or is amplified and made larger so long as the temperature peaks are reduced. Of course, the fact that the elimination of the temperature oscillation also results in the elimination of the phugoid (Fig. 11b) is an added bonus which results in greater range control over the vehicle by the pilot.

It may be of interest to note that attitude control based upon altitude measurements was also investigated at an early stage in the development of the CONTAC system. In view of the results, which were inferior to the CONTAC concept, and the difficulty associated with the measurement of the altitude during an actual reentry, all effort on this aspect was abandoned.

A discussion of the basic philosophy behind the CONTAC system will provide a greater understanding of how it works. The main purpose is to dissipate as much of the vehicle's kinetic energy at as high an altitude as possible. In order to achieve this result, the CONTAC system is designed to prevent any decrease in the temperature after the first maximum is reached during the initial pass into the atmosphere. In order to prevent the decrease, the angle of attack is reduced which increases the L/D (actually the ratio of vertical force to drag, but at constant bank angle, L/D is just as appropriate) and thereby extends the glide path over a longer distance at the higher altitudes. However, the angle of attack eventually reaches its minimum value and at that point the temperature will begin to fall. However, when at some later time the temperature again starts to rise, a decision must be made as to when is the best time to increase

the angle of attack in order to prevent a subsequent temperature peak from exceeding the highest temperature experienced prior to that point in the flight. With no prediction scheme available, the best choice of the time to increase the angle of attack is immediately, i.e. as soon as the temperature again begins to rise. Keeping the temperature constant from that point on implies a gradual reduction in L/D which in turn may result in lower altitudes sooner than is desirable. There may be an optimum period of time to wait before initiating any increase in the angle of attack. However the absence of both memory and predictive logic within the CONTAC system precludes any use of a time delay interval.

In summary, the CONTAC system operates on the principle that the best place to lose speed is at as high an altitude as possible. Therefore, the angle of attack is gradually reduced in such a manner as to prevent the temperature from falling after it achieves a local peak value. That action results in an extension of the glide path at higher altitudes due to the resulting higher values of L/D . On the other hand, it was found best (by increasing the angle of attack) to prevent for as long as possible any subsequent rise in temperature after a minimum value occurs. The result is a system which always attempts to keep the temperature constant as long as angle of attack changes are possible, i.e. as long as the angle of attack was at neither its lower nor upper limit following a maximum or minimum, respectively, in the equilibrium nose stagnation point temperature.

The same principles are also used to control the bank angle in conjunction with the angle of attack. The only difference is that the "wings level" position is substituted for the upper limit since the maximum value for the ratio of vertical force to drag occurs for zero bank angle. On the other hand, the minimum value for this ratio occurs at the largest angle of roll. Therefore, the "lower limit" is the largest bank angle to the right or left depending on which direction the landing zone is situated with respect to the orbital track.

2.2 Choice of Attitude Limits

There are certain practical limitations on the freedom of choice for the upper and lower limits for both the angle of attack and the bank angle. Most of the limitations are due to the problems associated with obtaining as small a value as possible for the peak temperature experienced during the reentry of the spacecraft. In addition, the allowable range of values for the upper and lower limits changes with each phase of the reentry. Consequently, the best procedure will be to take each phase in turn and describe the reasons for the restrictions during that part of the trajectory.

(a) During Phase I, there are no restrictions and no practical limitations since the atmosphere is not effective in controlling the trajectory. The only point at which the attitude must be controlled is at the beginning of Phase I during the retro-fire. At that time, the attitude control must be quite precise, but there is, of course, no restriction on the choice of the angles. Near the end of Phase I, however, the angle of attack should be somewhere near the value to be used during Phase II since, otherwise, stability and control problems might be encountered.

(b) During Phase II, the bank angle should always be zero in order to produce the maximum possible vertical force for a given angle of attack. It might be feasible to introduce some aerodynamic side force on the vehicle at this

time, but the results would hardly be worth the added complexity necessary in the guidance system. This is because only large angles of roll would really be effective in producing cross range at this high a speed (Ref. 6), but the associated reduction in vertical force could not be tolerated.

The angle of attack should always be near the optimum value of 55 degrees which gives the maximum lift coefficient. In the presence of a pre-determined atmosphere in which there were no density variations about the mean curve of density versus altitude, it would be possible to determine the desired angle of attack which would then be held throughout Phase II. However, in general, the guidance system will probably be making small changes throughout Phase II in order to compensate for predicted errors in the terminal down range position. Since the CONTAC system does not go into active operation until the end of Phase II, the angle of attack is completely under control of the guidance system during this time.

The largest angle of attack which was used herein during Phase II was 65 degrees. However, values as high as 75 degrees would probably be feasible if the spacecraft could withstand the resulting higher heating rates at the rear of the undersurface of the vehicle. The smallest value used was 35 degrees. When still smaller values were tried, the first maximum temperature was higher than the peak temperature for an equilibrium glide.

The designation of the upper limit on the attitude (no lower limit was used) was the entry angle of attack (which varied between 35 degrees and 65 degrees) and the entry angle of roll (which was always zero).

(c) During Phase III, the CONTAC system is in active operation about half the time. The vehicle is initially rolled to one side or the other and the nose pitched down in order to prevent the temperature from falling.

The lower limits are designated as the "skip angle of attack" and the "skip bank angle". The reason for this terminology is that the spacecraft usually performs a nearly constant altitude glide at the beginning of Phase III, involving a very small skip, or increase in altitude, of between zero and 20,000 feet. For some situations, especially when the entry angle of attack is large, the skip does not occur; however, the designation is still retained.

Note that the skip angle of attack and the skip bank angle are controlled by the range guidance system. These attitude angles are always the actual values held by the vehicle whenever the temperature is falling. The skip angles may, of course, be changed at any time during Phase III, but an immediate change in predicted down range will not result if the skip angles are not in current use due to override by the CONTAC system.

The largest value used for the skip angle of attack was 55 degrees; the smallest value was 5 degrees. The smallest value might require adjustment if its use results in upper surface heating which cannot be tolerated.

The "largest" value used for the skip angle of roll was zero and the "smallest" value was -90 degrees. Notice that the use of a bank angle to the left preserves the algebraic definition of largest and smallest. If roll angles to the right are employed, the largest would still be zero and the "smallest" would then become +90 degrees. The key point to keep in mind is that the largest roll angle must always occur for the maximum vertical force (which obviously forces

the largest roll angle to be zero) and the "smallest" bank angle for the minimum vertical force.

The upper limits during Phase III are simply designated the "upper limits". The values are always the ones which give the maximum vertical force which is, of course, obtained at the angle for the maximum lift coefficient. Therefore, the upper limit for the angle of attack is 55 degrees and the upper limit for the bank angle is zero.

(d) Phase IV always starts with the attitude at the upper limits, the same as the upper limits for Phase III.

The lower limits for Phase IV are designated "lower limits". They are used when the speed falls appreciably and the CONTAC system goes into passive operation. Within the limitations imposed by the stability and available aerodynamic control of the vehicle, the guidance system is free to choose any values which it finds necessary to control the range. In general, the lower limit for the angle of attack will lie in the vicinity of the angle for $(L/D)_{\max}$ while the lower limit for the bank angle is varied in the way which will result in the maximum cross range (if necessary).

(e) During Phase V, the CONTAC system is no longer in operation. All values for the attitude are dictated by guidance and control problems.

2.3 CONTAC Program Flow Diagram (see Fig. 12)

The basic purpose of the CONTAC system is to prevent a change in the temperature. The digital implementation of the basic concept is quite simple. The program to simulate and test the concept is, of course, much more detailed only because of other requirements such as program error checks and printouts of intermediate calculations. In general, conflicts often occur and the extra effort to take account of the numerous possibilities is considerable.

In the absence of these other details, the CONTAC system logic is shown in Fig. 12. There must be some memory (but no predictive requirement) so that the system can remember whether it is testing for a local minimum or maximum, and for the storage of $T_{\text{last min}}$ or $T_{\text{last max}}$, respectively. If the latter is currently being experienced, then when the temperature has fallen below the current local maximum by a reasonable margin (T_{deadband}), corrective action is taken. The determination of a local minimum is similar.

However the simulation of the CONTAC system by a digital computer is prone to difficulties in logic flow and numerical calculation which have no counterpart in the real situation. The basic cause is the method by which a digital computer must perform the calculations. As opposed to a continuous value for all variables, as is found in the output of an analogue computer, or analogue instruments, a digital computer calculates the flight path only at specific points along that path. As a consequence, the deadband test shown in Fig. 12 may not be satisfied at one point in the calculation, but will be satisfied by too great a margin at the next point. If the digital calculation is proceeding in steps of two or three seconds, the time lag introduced by the digital calculation is totally unacceptable (Fig. 13) and measures must be found

to correct the situation*. The simplest method would be to reduce the time interval (actually, the flight path distance) between the points in the calculation. However, what value should be used? A step size small enough to satisfy the deadband test requirement produces an unacceptably large increase in computing time on the machine. A step size which increases computer time by only a reasonable amount will not always be able to provide an acceptably short time delay.

The solution adopted was to provide the calculation section with backup capability. As shown in Fig. 14, new points are calculated at shorter and shorter intervals until both questions (Fig. 12) are satisfied. At that point, the distance travelled and the corresponding time delay between the actual position and the position at backup point No. 5 (Fig. 14) is acceptable and the commands to adjust the angle of attack and the bank angle are calculated and implemented.

The backup capability allows the calculation section to proceed with step sizes which are as large as calculation errors permit and thereby perform the calculation as fast as possible. The choice of the smallest step size for the test is based upon practical experience with the runs and usually results in a maximum time delay of between ten and twenty milliseconds. During test runs to determine the maximum acceptable value, it was found that delays which were an order of magnitude greater produced results which were only negligibly different. However, for still larger time delays, a discrepancy was noted sometimes.

2.4 Vehicle Implementation

The problems of isolating the control logic from the details of the calculation will, of course, disappear once the system is placed on board the spacecraft and actually put into operation. As shown in Fig. 15, the calculation section of Fig. 12 will be replaced by the vehicle dynamics. The vehicle sensors will provide the forward interface to the control hardware and the reaction jets will be the rearward interface. In the case of a digital control system, the sampling rates for the analogue to digital convertor will probably be on the order of ten milliseconds or less for the temperature. Other variables need to be sensed less often and perhaps only when needed.

The absence of inner return loops in the vehicle control logic merely indicates that no signal is necessary until the appropriate test is satisfied. However, since the calculation will be in real time, a great deal of attention must be given to the way in which the available computational time is divided. Because the CONTAC system is often in the passive mode, i.e. no active attitude control is being performed, time sharing procedures will probably make the best use of the available computational capacity. The range controller will undoubtedly use the major share of the computer's time for predictive calculations since in view of the complex corrections required by the disturbing effects of the Earth's rotation and oblateness it is doubtful whether any simple predictive scheme would be satisfactory for the size of footprint within which the CONTAC system is able to operate. However, a simple interrupt system

* It is not so much the length of the time lag that complicates the situation, but the fact that it is unpredictable and varies from zero to perhaps five or even ten seconds. Since no real system will possess such a random variation in the size of the deadband, results computed on this basis would be highly suspect.

will allow for the monitoring of the temperature on a scheduled basis and the subsequent calculation of the attitude control moments when required.

The control scheme proposed here requires the measurement or computation of angles of attack and roll and their derivatives. No specific means are recommended for obtaining this information. However, one possibility is to compute them from the outputs of an inertial platform, which can provide both velocity and attitude in inertial space. Other techniques are also possible within the state of the art. When the CONTAC system commands a change of α or ϕ , it is assumed that pitch or roll jets are turned on, producing a constant moment with zero time lag. Both $|\dot{\alpha}|$ and $|\dot{\phi}|$ are constrained to be less than certain selected maxima, and when these are reached, the control jets are turned off.

An extensive effort to produce a thermocouple which is capable of measuring the temperature at the nose stagnation point of the vehicle is described in Ref. 4. Actual tests were conducted which showed that such a device was able to measure values in excess of 3500°F for several minutes. Since the peak temperature which occurred for the vehicle used in this investigation was usually below 3000°F, there will not be any difficulty in procuring a satisfactory measuring instrument.

Another basic problem is to determine the actual stagnation point temperature. The position of the thermocouple is, of necessity, fixed in the nose of the vehicle. When changes are made in the angle of attack, the thermocouple will no longer be at the stagnation point and some method must be found to determine the actual stagnation point temperature.

The solution to this problem is also given in Ref. 4. The relationship between the measured and the stagnation point temperatures is given by

$$T_{\text{measured}} = T_{\text{stagnation}} \cos^{3/8} (\alpha - \alpha_{\text{stagnation}})$$

At high Mach numbers and for positions up to 40 degrees off the stagnation point, this relationship is in excellent agreement with both theoretical and experimental data for both hemispheres and swept cylinders. When the CONTAC system is active, the maximum variation in the angle of attack was from 5 degrees to 55 degrees. The thermocouple position could be at the stagnation point when the angle of attack of the vehicle is at 30 degrees. Consequently, the maximum offset would be only 25 degrees. For a stagnation point temperature of 3000°F, the temperature measured when the angle of attack of the vehicle is 55 degrees is only 4.2 percent less or 2875°F. The derivative of the temperature with respect to the angle of attack is also very small. The corresponding value would be 9.7 F° / degree change in angle of attack.

In general, the vehicle will experience a small, but variable degree of side slip, owing to the presence of inadvertent yawing movements from asymmetries and control action. Consequently, two extra thermocouples could be provided to measure the sideslip angle and to control reaction jets which would achieve a null angle. The suggested positions are on the wing leading edges; offset nose positions would also be satisfactory.

Note that regardless of the position used for the thermocouples, several extra sensors would be used in parallel at each location in order to guarantee reliability.

2.5 Vehicle Attitude Control

As part of any simulation of a complex physical situation, a decision must be made as to just how accurately the mathematical model should be able to duplicate the real situation. In the case of the attitude control system, information is available (Refs. 10 and 11) which makes possible a considerable simplification in the complexity of the mathematical model. These references indicate that the short period mode possesses time constants orders of magnitude greater than the characteristic times of the CONTAC system. As a result, most of the terms in the general equations describing the attitude of the vehicle may be eliminated - in particular, both the damping and spring constants are deemed negligible. Consequently, only the inertial term remains in the equations for rotation about any axis. It is also assumed that both the Earth's rotation and the movement of the vehicle within the Earth's reference system will have a negligible effect on the attitude equations.

In keeping with the above assumptions, the equations of motion for the attitude become very simple. Only the equation for the angle of attack will be developed since the bank angle equation is similar. The basic equation is

$$I_{\alpha} \ddot{\alpha} = M \quad (2.1)$$

where M is the constant pitching moment supplied by the pitch control jets when they are turned on. Thus

$$\ddot{\alpha} = k_{\alpha} \quad (2.2)$$

where k_{α} is zero when the control jets are off, positive when set for nose-up change, and negative for nose-down change.

Assuming that the angle of attack was decreasing when the pitch jets were first turned on and that the angle of attack should now begin to increase (i.e. k_{α} is positive), integration gives

$$\alpha = \begin{cases} \dot{\alpha}_s + k_{\alpha}(t-t_s) & (t-t_s) < \Delta t \end{cases} \quad (2.3a)$$

$$\alpha_{\max} \quad (t-t_s) \geq \Delta t \quad (2.3b)$$

where

$$\Delta t = (\dot{\alpha}_{\max} - \dot{\alpha}_s)/k_{\alpha} \quad (2.4)$$

A final integration yields

$$\alpha = \begin{cases} \alpha_s + \dot{\alpha}_s(t-t_s) + \frac{1}{2}k_{\alpha}(t-t_s)^2 & (t-t_s) < \Delta t \end{cases} \quad (2.5a)$$

$$\alpha_s + \Delta\alpha + \dot{\alpha}_{\max} [(t-t_s) - \Delta t] \quad (t-t_s) \geq \Delta t \quad (2.5b)$$

where

$$\Delta\alpha = (\dot{\alpha}_{\max} + \dot{\alpha}_s)(\dot{\alpha}_{\max} - \dot{\alpha}_s)/2k_{\alpha} \quad (2.6)$$

Figure 16 shows the various relationships. Since equations (2.5a) and (2.5b) are simple analytical expressions which are a function only of time, they are easily introduced into the equations of motion presented in Section V. One point which may require explanation is the reason for the limit placed on $\dot{\alpha}$. On the one hand, as large a value as possible is desirable in order to be able to respond as quickly as possible to rapid changes in atmos-

pheric density that require a rapid adjustment of the angle of attack. On the other hand, if the inertia of the vehicle (with its negative angular velocity - remember that α_s was negative) is to be quickly overcome, Eq. (2.4) shows that a large $\dot{\alpha}_{\max}$ requires a large angular acceleration. In addition, high angular rates lead to frequent cycling of the control which requires a high fuel expenditure for the reaction jets. Consequently, a reasonable compromise must be found between $\dot{\alpha}_{\max}$, the available angular acceleration, and the available mass of fuel. The values used in this investigation were quite conservative. Appendix D gives a sample set of values prior to the actual output.

Slight variations in sign in Eqs. (2.3) to (2.6) are required when k_α is negative. Also, two sets of bank angle equations are required, one for positive k_ϕ and one for negative k_ϕ . The bank angle equations are a little more complicated to use since the optional right or left hand turn requires additional logic within the digital computer program. For a left hand turn, all the α symbols need only be replaced by ϕ to convert equations (2.3) to (2.6) into bank angle equations for a positive k_ϕ . Of course, the basic equation for the bank angle

$$\ddot{\phi} = k_\phi \quad (2.7)$$

which is exactly the parallel of Eq. (2.2) and applies equally to all situations.

III. VEHICLE CHARACTERISTICS

3.1 Introduction

In recent years, the general trend in lifting vehicle programs has been a shift away from configurations with relatively high lift to drag ratio ($L/D > 2.5$), such as the X-20 Dynasoar, to a lifting body style as typified by the M2-F2, the HL-10, and the SV-5 (Ref.12) wingless reentry vehicles. The reasons for the choice seem to have been based primarily upon the advantages associated with much lower temperatures resulting from the elimination of small nose cap and leading edge radii. The disadvantages caused by a much smaller footprint or landing area capability are not severe enough to cause serious concern. By reason of the Earth's rotation under what is essentially a fixed inertial orbit, these wingless vehicles are still able to land at any point on the Earth which falls underneath or at least near the orbital envelope (Fig. 5) without having to wait more than 24 hours. Naturally, the coverage is severely restricted for equatorial or near-equatorial orbits; but even the Dynasoar could not claim complete coverage for equatorial orbits without incurring extremely high temperatures.

3.2 Vehicle Geometry

The vehicle chosen for this study is quite similar to current design concepts. Its mass and wing area never individually enter the equations of motion; consequently, they have been left in the form of the wing loading ratio. This parameter was then chosen from about the middle of the range which is presently under review. The value of 40 lb/ft^2 is, therefore, simply representative.

The actual vehicle configuration is a delta wing planform with a leading edge sweep of about 70 degrees. Although the mass and wing area are not needed for the equations of motion, nevertheless some estimate of the nose cap and leading edge radii is desirable. A mass of about 8000 lb. gives a wing area of about 200 sq. ft. which would then lead to a base length of about 17 ft.

However, the body would be only about 20 ft. long since around 5 ft. of the nose would probably be cut off to provide a nose cap radius in the vicinity of 2.5 ft. The leading edge radius would also lie in this region.

3.3 Vehicle Aerodynamics

One of the most vital requirements for any investigation which seeks to predict the reentry flight path of a spacecraft with a reasonable degree of accuracy is a proper representation of aerodynamic forces throughout all phases of the trajectory. However, since the primary object of this study is to determine the effectiveness of the CONTAC system under varying operating conditions, only that portion of the flight where the heating rates are extreme will require highly accurate models for the aerodynamic forces which are exerted on the vehicle. Portions of the trajectory that are relatively unimportant to the primary purpose of the analysis may employ a model which is able to give only a reasonable approximation for the lift and drag coefficients.

Such is the case with the aerodynamic model chosen to represent the lift and drag forces on the vehicle under consideration. Several experimental studies (Refs. 13 to 15) show that expressions based on Newtonian theory adequately represent the sum total of the aerodynamic forces which are developed over a spacecraft during its reentry into the Earth's atmosphere as long as the Mach number is greater than about six or eight. As a result, a number of authors (Refs. 3, 16, and 17) have used either an exact or modified form of the flat plate, hypersonic, Newtonian approximation. Based on Ref. 14, the best estimate for the pressure coefficient on a flat plate is

$$C_p = 1.75 \sin^2 \alpha \quad (3.1)$$

The value assigned to the minimum drag coefficient, $C_{D_{min}}$, is determined by the vehicle configuration, primarily by the degree of nose cap and leading edge bluntness. The nose cap radius should be as large as possible in order to reduce heating (See Sec. 3.4); however, a large value will produce a maximum lift-drag ratio which is too small to permit the required manoeuvrability. The compromise value of nose radius given in Sec. 3.2 yields a value for the minimum drag coefficient of

$$C_{D_{min}} = 0.0625 \quad (3.2)$$

If the value of the nose cap radius which has been suggested does not produce the above value for $C_{D_{min}}$, an adjustment to the former may easily be made without unduly affecting the peak temperature, since the latter varies only as the eighth root of the nose radius (see Eq. 3.7).

The use of the preceding values for C_p and $C_{D_{min}}$ gives the modified Newtonian expressions for the lift and drag coefficients, which are

$$C_L = 1.75 \sin^2 \alpha \cos \alpha \quad (3.3)$$

$$C_D = 0.0625 + 1.69 \sin^3 \alpha \quad (3.4)$$

These expressions are valid for $0 < \alpha < 90$ degrees and are quite accurate down to Mach numbers of six or seven. For Mach numbers smaller than five, there is every indication that Eqs. (3.3) and (3.4) continue to be quite representative even down through the transonic region. References 18 to 20 indicate that for

angles of attack below about twenty or thirty degrees, the lift and drag coefficients continue to exhibit the same general pattern while the L/D slowly increases with decreasing Mach number. Consequently, Eqs. (3.3) and (3.4) may continue in use down through the high subsonic range if conservative estimates of manoeuvring capability are acceptable.

3.4 Equilibrium Nose Stagnation Point Temperature

Since the primary goal of this investigation is to determine the applicability of the CONTAC system, the exact numerical magnitude of the nose stagnation point convective heating rate is relatively unimportant. Indeed, it is even questionable whether extremals in the stagnation point temperature (see Fig. 14 as to how a maximum or minimum T is handled) which occur as a result of reversals in the gradient of the heating rate must be accurately predicted by the model which has been adopted. On the other hand, the heating rate must be simulated in a way which is sensitive to changes in atmospheric and flight conditions, especially at the times when the model predicts that the maximum rate is being experienced. In other words, it is not at all important that the predicted heating rate reach a maximum or minimum at precisely the same time that the actual heating rate reaches its extremal values (in fact, it is very dubious whether any model which simulates the heating rate, no matter how complex or sophisticated it might be, could predict the exact time at which the heating rate derivative changes sign); it is only necessary that if the heating rate is to remain relatively constant as a result of attitude control for the simulated model that this condition also occur in the real situation and at about the same time in the flight. This rather lax requirement is due to the adaptive nature of the CONTAC system which must only prevent any large changes in the heating rate as long as possible, i.e. as long as the attitude angle has not reached its upper or lower limit.

The particular form of the nose stagnation point convective heating rate which is used in this investigation has also been adopted by several other authors (Refs. 3, 17, 21, and 22) as being sufficiently representative of experimental results. The basic relationship is

$$q_n = \frac{17,600}{\sqrt{R_n}} \left(\frac{V}{26,000} \right)^{3.15} \left(\frac{\rho}{0.002378} \right)^{0.5} \quad (3.5)$$

Since the value which is to be measured on board the vehicle is the temperature, this heating rate is then inserted into the temperature rate equation which is

$$\frac{\bar{m} \bar{c}}{S} \frac{dT}{dt} = q - \epsilon \sigma T^4 \quad (3.6)$$

The radiation-equilibrium temperature is defined by setting the left hand side of Eq. (3.6) equal to zero. When an actual measurement is being made, the equilibrium value is produced by using such a small value of $\bar{m} \bar{c}/S$ at the temperature sensor that the left hand side becomes negligible and an excellent approximation to the equilibrium value is achieved very quickly. The data in Ref. 4 indicates that there will be a relatively negligible time lag in reaching the equilibrium temperature since the time constants associated with the cyclic commands produced by the CONTAC system are of the order of five to ten seconds.

Then, setting to zero the left hand side of Eq. (3.6) and substituting Eq. (3.5) for the heating rate, q_n , gives the radiation-equilibrium nose

stagnation point temperature as

$$T^4 = \frac{17,600}{\epsilon \sigma \sqrt{R_n}} \left(\frac{V}{26,000} \right)^{3.15} \left(\frac{\rho}{0.002378} \right)^{0.5} \quad (3.7)$$

The only terms which must have values assigned are ϵ and R_n . Normally, ϵ is between 0.5 and 0.8 while R_n is about 2.5 feet for the vehicle under consideration. Thus, the products of $\epsilon \sqrt{R_n}$ would range from 0.8 to 1.25 due to the uncertainty in ϵ . As a consequence, a "standard" value for the temperature is used for which a value of unity is taken for $\epsilon \sqrt{R_n}$. The advantage is a standard from which the proper result for the temperature may be computed when the correct values of ϵ and R_n are known without the disadvantage of being greatly in error. This standard stagnation point temperature is used in all the calculations as a measure of the actual temperature which would result for a device (e.g. a sophisticated thermocouple) placed at the nose stagnation point of the spacecraft. This variable will henceforth be referred to simply as the "temperature" (as already noted in Section 1.2). Then, in view of the above assumptions, the temperature is given by

$$T^4 = Q V^{3.15} \sqrt{\rho} \quad (3.8)$$

where

$$Q = 17,600 / \sigma 26,000^{3.15} \sqrt{0.002378} \quad (3.9)$$

or

$$Q = 9,397 \quad (3.10)$$

IV. GEOPHYSICAL ENVIRONMENT

4.1 Introduction

One of the most important goals of this investigation is to study the effect of non-ideal conditions upon the peak temperature, primarily with a view to determining the extent to which these conditions impair the performance of the CONTAC system.

There are two distinct types of non-ideal conditions which are of concern. The first includes all the effects which may be predicted well in advance of the reentry. These effects include the Earth's rotation, the Earth's oblateness (i.e. the distortions of both shape and gravitational potential), and the geographical variations of the time average density (which are a function of both latitude and longitude as well as altitude). The second type includes those effects which are the result of departures from the time averaged mean values of the density.

A third source of disturbance is atmospheric wind. No data could be found showing the spatial gradient of the wind at the altitudes of concern of this investigation (the same problem was encountered with density variations and will be discussed in Sec. 4.6). However, local wind velocities of up to 500 feet per second do exist. Actually, almost all values are lower than 250 feet per second, but on isolated occasions they approach the higher figure. Assuming a step increase of 500 feet per second (from -500 to +500 feet per second seems far too large a difference to support even if both conditions did occur within a reasonable proximity), the percentage increase in the velocity at a speed of 20,000 feet per second would amount to only $2\frac{1}{2}$ percent. The

resulting increase in temperature would be slightly less (see Eq. 3.8). The percentage increase would be greater at lower velocities, but by the time the speed falls below about 16,000 feet per second, the temperature is no longer a problem. Since it would be the changes in wind speed that cause the difficulties (see Sec. 8.4), it is clear that winds should not present a problem for the CONTAC system.

4.2 Rotation of the Earth

There is a relative pseudowind present due to the Earth's rotation. The West to East speed at the equator amounts to about 1500 feet per second relative to inertial space. For the calculation of aerodynamic heating and forces, this relative velocity may be subtracted from the initial entry speed for equatorial West to East reentries and provides a small but not insignificant reduction in the peak temperature experienced during the flight.

The actual rotational motion of the Earth is quite complex. Parvin (Reference 23) has done an excellent summary of the various motions and lists five separate parts to the rotation of the Earth.

The primary motion is, of course, the familiar rotation of the Earth about its axis which produces the normal sunrise and sunset. This movement takes by definition, exactly one solar day to complete. However, the rotational speed of interest is with respect to inertial space and for this figure the sidereal day may be used. The length of time taken for one revolution in inertial space is 23 hours, 56 minutes, and 4.09 seconds. This works out to a rotational speed of 0.00417807 degrees of longitude per second.

The other four parts of the rotation will be mentioned for interest, but are all negligible with regard to the effect they have on the reentry of a spacecraft. First, there is the precessional rotation about the 23.5 degree inclination to the ecliptic pole which takes about 25,800 years. Second, other bodies in the solar system tend to cause a slight irregularity in the precessional rate called nutation; one component with less than ten seconds of arc has a period of nineteen years while the other component with less than one-half second of arc has a period of only two weeks. Next, the pole itself wanders, which would tend to affect the alignment of the Earth's axis; however, although the two periods are relatively short - twelve and fourteen months - the angles are less than four seconds of arc. Finally, there is an additional revolution due to the spiral motion of the galaxy which occurs once approximately every 200 million years. A better and much more complete description of these four additional motions may be found in the reference. It is quite clear, however, that they are too small to have any effect on the reentry.

4.3 Earth's Oblate Gravitational Field

During the past ten years, the use of artificial satellites to measure the potential field of the Earth has shown the inadequacy of representing the gravitational attraction as a simple central force. Using the notation of this paper, the general representation of the Earth's potential field as given by Kozai (Ref. 24) is

$$U = \frac{GM}{r} \left[1 + \sum_{m=2}^{\infty} \sum_{n=0}^{\infty} \left(\frac{R_0}{r} \right)^n P_n^m(\sin \lambda) \{C_{n,m} \cos m \theta + S_{n,m} \sin m \theta\} \right] \quad (4.1)$$

where

$$P_n^m(\sin \lambda) = \frac{1}{2^n n!} \cos^m \lambda \frac{d^{n+m}(\sin^2 \lambda - 1)^n}{d(\sin \lambda)^{n+m}} \quad (4.2)$$

are spherical harmonics. Several other formulations exist, but all are essentially the same in that they use an infinite series of spherical harmonics to represent the potential field.

The gravitational vector is divided into its three principal components which results in (see Sec. 5.2 for a definition of the $\{\bar{n}, \bar{e}, \bar{v}\}$ reference system)

$$\bar{g} = \bar{n} g_\lambda + \bar{e} g_\theta - \bar{v} g_r \quad (4.3)$$

and requires the expressions for each of the gravitational components which are defined by the spherical gradient of the potential as

$$g_r = \frac{\partial U}{\partial r} \quad (4.4a)$$

$$g_\lambda = \frac{1}{r} \frac{\partial U}{\partial \lambda} \quad (4.4b)$$

$$g_\theta = \frac{1}{r \cos \lambda} \frac{\partial U}{\partial \theta} \quad (4.4c)$$

Substitution of U into equations (4.4a), (4.4b), and (4.4c) and expansion of the spherical harmonics by means of Eq. (4.2) is tedious, but can easily be carried out. The result for the first few terms in the series is shown in order to provide the reader with some idea of the actual results. When all the substitutions are made, Eq. (4.3) for \bar{g} becomes

$$\begin{aligned} \bar{g} = \bar{v} \frac{GM}{r^2} & \left[1 + \left(\frac{R_0}{r} \right)^2 \left\{ \frac{3}{2} (3 \sin^2 \lambda - 1) C_{2,0} + 9 \cos^2 \lambda (C_{2,2} \cos 2\theta + S_{2,2} \sin 2\theta) \right\} \right. \\ & + \left(\frac{R_0}{r} \right)^3 \left\{ 2(5 \sin^3 \lambda - 3 \sin \lambda) C_{3,0} \right. \\ & + 2(15 \sin^2 \lambda - 3) \cos \lambda (C_{3,1} \cos \theta + S_{3,1} \sin \theta) \\ & + 60 \sin \lambda \cos^2 \lambda (C_{3,2} \cos 2\theta + S_{3,2} \sin 2\theta) \\ & + 60 \cos^3 \lambda (C_{3,3} \cos 3\theta + S_{3,3} \sin 3\theta) \left. \right\} + \dots \left. \right] \end{aligned}$$

$$\begin{aligned}
& + \bar{n} \frac{GM}{r^2} \left[\left(\frac{R_0}{r} \right)^2 \left\{ 3 \sin \lambda \cos \lambda C_{2,0} - 6 \sin \lambda \cos \lambda (C_{2,2} \cos 2\theta + S_{2,2} \sin 2\theta) \right\} \right. \\
& + \left(\frac{R_0}{r} \right)^3 \left\{ \frac{1}{2} (15 \sin^2 \lambda - 3) \cos \lambda C_{3,0} \right. \\
& + \frac{3}{2} (11 - 15 \sin^2 \lambda) \sin \lambda (C_{3,1} \cos \theta + S_{3,1} \sin \theta) \\
& + 15 (1 - 3 \sin^2 \lambda) \cos \lambda (C_{3,2} \cos 2\theta + S_{3,2} \sin 2\theta) \\
& + 45 (\sin^2 \lambda - 1) \sin \lambda (C_{3,3} \cos 3\theta + S_{3,3} \sin 3\theta) \left. \right\} + \dots \left. \right] \\
& + \bar{e} \frac{GM}{r^2} \left[\left(\frac{R_0}{r} \right)^2 \left\{ 6 \cos \lambda (S_{2,2} \cos 2\theta - C_{2,2} \sin 2\theta) \right\} \right. \\
& + \left(\frac{R_0}{r} \right)^3 \left\{ \frac{1}{2} (15 \sin^2 \lambda - 3) (S_{3,1} \cos \theta - C_{3,1} \sin \theta) \right. \\
& + 30 \sin \lambda \cos \lambda (S_{2,2} \cos 2\theta - C_{2,2} \sin 2\theta) \\
& + 45 (1 - \sin^2 \lambda) (S_{3,3} \cos 3\theta - C_{3,3} \sin 3\theta) \left. \right\} + \dots \left. \right] \quad (4.5)
\end{aligned}$$

Although the forces due to even higher order harmonics will influence the orbit of an artificial satellite to some extent, the presence of terms other than those containing $C_{2,0}$ has a negligible effect upon the reentry of a spacecraft. By neglecting all such terms, the complexity of the gravitational vector is considerably reduced, with the $\{\bar{e}\}$ component disappearing altogether. The result is

$$\begin{aligned}
\bar{g} = \bar{v} \frac{GM}{r^2} & \left[1 + \left(\frac{R_0}{r} \right)^2 \frac{3}{2} (3 \sin^2 \lambda - 1) C_{2,0} \right] \\
& + \bar{n} \frac{GM}{r^2} \left[\left(\frac{R_0}{r} \right)^2 3 \sin \lambda \cos \lambda C_{2,0} \right] \quad (4.6)
\end{aligned}$$

The three remaining constants are given by

$$\begin{aligned}
GM &= 3.986032 \times 10^{20} \text{ cm}^3/\text{sec}^2 \\
\text{or} \quad GM &= 1.407654 \times 10^{16} \text{ ft}^3/\text{sec}^2 \quad (4.7)
\end{aligned}$$

$$\begin{aligned}
R_0 &= 6.378196 \times 10^8 \text{ cm} \\
\text{or} \quad R_0 &= 20,925,840 \text{ feet} \quad (4.8)
\end{aligned}$$

$$C_{2,0} = -1.08248 \times 10^{-3} \quad (4.9)$$

They were taken as the best average of all the values suggested by Refs. 24 to 26.

4.4 Oblate Shape of the Earth

The primary departure of the Earth from a perfect sphere is the flattening of the poles. Several papers by Kaula (Refs. 25 and 26 in particular) have also indicated the additional distances by which the Earth departs from its ellipsoidal shape, which in turn gives rise to the additional coefficients in Eq. (4.1). The variations are systematic to the extent that they indicate a triaxial tendency. Wagner (Refs. 27 to 29) has done extensive work on this subject with, however, conflicting results. Consequently, only an approximate (one figure accuracy) average was adopted with the major axis at about twenty degrees longitude west and a minor axis about 210 feet shorter ($f_q = 10^{-5}$) situated at seventy degrees longitude east.

In order to calculate the perpendicular height above a triaxial ellipsoid, it is sufficient to know the geocentric geographical position. The three variables will be the geocentric radius, the geocentric latitude, and the geocentric longitude. Several different methods were found in the literature which provided suggestions on how to calculate the perpendicular height above an oblate spheroid. While most were unnecessarily complex, a very simple solution is given by Baker (Ref. 30) which is deemed to be the best. In the notation of this paper, the suggested equation is

$$y = r - R_0 \left[1 - f_p \sin^2 \lambda - \frac{1}{2} (f_p)^2 \left(\frac{R_0}{r} - \frac{1}{4} \right) \sin^2 2\lambda \right] \quad (4.10)$$

where y is the perpendicular height above an ellipsoidal Earth.

In order to compensate for the triaxial tendency of the Earth's equator, an additional term of the form $R_0 f_q \sin^2 \theta$ (which is derived in the same way as the $R_0 f_p \sin^2 \lambda$ term for the polar flattening) is required. The higher order term in f_q^2 is, of course, negligible in comparison. This additional term must then be multiplied by $\cos^2 \lambda$ in order to reduce the triaxial effect to zero at the poles. A biasing constant is also required in order to raise the major axis and lower the minor axis above and below, respectively, the Earth's average equatorial radius, R_0 . This biasing constant (of $\frac{1}{2}$) in equation (4.11) is required due to the definition of f_q as given in the nomenclature.

In addition, $\sin^2 2\lambda$ is expanded using the usual trigonometric relationship in order to adapt the formula for digital computation (both $\sin \lambda$ and $\cos \lambda$ are already available, but $\sin 2\lambda$ would have to be calculated). The result is

$$\begin{aligned} y = r - R_0 + R_0 f_p \sin^2 \lambda + (f_r/r + f_c) \sin^2 \lambda \cos^2 \lambda \\ + R_0 f_q \{ \sin^2 (\theta - \theta_{2,2}) - \frac{1}{2} \} \cos^2 \lambda \end{aligned} \quad (4.11)$$

An exact procedure which required several iterations to yield the result and which was not, therefore, useful during the actual computation of trajectories was then compared with the answer from Eq. (4.11). The exact procedure indicated that a correction factor should be added to take account of higher order terms which were omitted from the power series approximation given in Eq. (4.10). The actual formula used during calculation of trajectories was

$$\begin{aligned} y = r - R_0 + R_0 f_p \sin^2 \lambda + \{ f_r/r + f_c + f_f (\sin^2 \lambda - \frac{1}{2}) \} \sin^2 \lambda \cos^2 \lambda \\ + R_0 f_q \{ \sin^2 (\theta - \theta_{2,2}) - \frac{1}{2} \} \cos^2 \lambda \end{aligned} \quad (4.12)$$

where

$$R_o = 6.378196 \times 10^8 \text{ cm} \quad (4.13)$$

or

$$R_o = 20,925,840 \text{ feet}$$

$$f_p = 1/298.28 \quad (4.14)$$

$$f_q = 10^{-5} \quad \theta_{2,2} = -20 \text{ degrees} \quad (4.15)$$

were taken as the best average of all the values suggested by Refs. 24 to 29.

$$\text{Also} \quad f_r = \frac{1}{2}(R_o f_p)^2 \quad (4.16)$$

$$f_c = R_o (f_p)^2 / 8 \quad (4.17)$$

$$\text{And} \quad f_f = -3.328 \quad (4.18)$$

was optimized for the adopted values of R_o and f_p .

In practice, Eq. (4.12) evaluated the last three terms in single precision arithmetic and then used double precision addition when adding all five values together to achieve the final result. Comparison with the exact iterative procedure showed that the accuracy achieved with Eq. (4.12) was always better than 0.05 feet over the tested altitude range of zero to one million feet.

4.5 Mean Standard Atmosphere

In this investigation, the basic model used to define the variation of density with altitude was the U.S. Standard Atmosphere, 1962 (Ref. 31). As far as corrections for oblateness were concerned, the true perpendicular altitude above the surface was used to define the height as per Eq. (4.12). In essence, the atmosphere was assumed to be a uniformly thick blanket enveloping the Earth. Figure 17 from a report by Cole and Kantor (Ref. 32) gives ample evidence to support his assumption.

Additional information regarding standard atmospheres for different latitudes has recently appeared in the literature (Ref. 33). However, in view of the lack of detail concerning the space between each mean set of values, the additional accuracy afforded by the extra reference curves would not have been worth the additional programming effort necessary to make them available to the program calculating the flight trajectories. In addition, there must certainly be longitudinal variations, as well as those associated with latitude, and the current absence of information about these is further justification for ignoring both effects. Perhaps the most important point in favour of using a single standard atmospheric model over the whole Earth is the necessity of determining the effects of departures from a non-rotating, circular Earth in a manner which distinguishes them from those due to atmospheric density variations.

4.6 Atmospheric Density Variations

The presence of spatial density variations about some mean values in the atmosphere poses a problem with which any control system must cope. Whether the purpose of the control system is to achieve lower temperatures, a terminal position, or any other of several possibilities, the most difficult part of the problem is the fact that the density variations about the mean are random and can only be specified by way of statistical data. Since this paper deals with the feasibility of the CONTAC system rather than with the exact details of the hardware, a single mean curve, the U.S. Atmosphere, 1962, was deemed sufficiently representative for all but a few reentries. Then, the problem was to find a model that would permit a reasonably accurate picture of the spatial density variations to be found in the atmosphere about the mean curve of density versus altitude.

One question that was deemed important, however, was whether the shape of the mean curve of density versus altitude was itself of any great importance. In order to answer it, a number of quite arbitrary exponential curves were used with widely varying values of the scale height. Actually, each new reference curve was composed of two exponentials. The higher altitude portion was defined by the scale height and the point at which it intersected the U.S. Standard Atmosphere, 1962. The lower curve was defined by the cut-off point for the upper curve and a second point of intersection with the U.S. Standard Atmosphere, 1962 which was below the cut-off point. The results are given in Sec. 8.2.

Two types of spatial density variations about the mean were used. One was based on altitude and the other was generated as a set of Gaussian random numbers which were spaced at equal intervals along the flight path length. Considerable attention was paid to the choice of these two types due to the almost complete lack of data regarding spatial density variations in the atmosphere. A great many papers could be found which gave day to day variations at a given point. Other investigators gave the results of calculations which defined new mean atmospheres at various latitudes. However, Cole and Cantor (Ref. 32) did provide some information regarding the maximum spatial density variations about the mean which might be expected as well as the distances over which the departures might occur.

For the density variations based on altitude, an actual experimental result shown in Ref. 32 confirmed a suggestion by Etkin (Ref. 34) that a simple sinusoidal variation about the mean of density versus altitude would be realistic. The necessary parameters were the amplitude of the variation about the mean, the wave length, and the point of zero variation or the nodal position. A range of values were used and the results can be found in Sec. 8.3.

In the case of random departures from the basic curve, a statistical approach was required. The method chosen to simulate the variations about the mean was a series of random numbers representing fractional deviations from the mean, with a Gaussian distribution. After specifying the variance of the series, the numbers were then assigned to equidistance positions along the flight path. In the absence of any other data, linear interpolation was used between the points to find the fractional departure from the mean value for the density. The fraction could be positive or negative, but was limited to an absolute magnitude of three times the variance (which it would be less than 99%

of the time in any case) in order to prevent bizarre results such as a negative density. In order to provide a statistical result, a number of trajectories was computed, one for each of several different series of random numbers having the same variance and correlation interval. (The effect of the random density model is presented in Sec. 8.4.)

While the above method of simulating the random variation to be expected in the atmosphere is certainly not the best possible model, it should at the very least be adequate. In any case, the lack of any concrete data upon which to base a more realistic model does not warrant a more sophisticated approach. It is, of course, possible that the information exists in classified reports. If so, the results presented in Sec. 8.4 will provide an immediate answer as to whether the CONTAC system will perform in a satisfactory manner under all expected atmospheric variations. On the other hand, if such data actually does not exist, then an evaluation of the CONTAC system must wait until it has been determined.

V. EQUATIONS OF MOTION

5.1 Basic Reference System

The choice of a basic reference system from among the multitude of possibilities is usually dictated by the problem which is to be solved as well as by the methods of solution which are available. In many situations, as in the present case, the choice is easily made due to the many restrictions imposed by unfavourable reference systems which might require an unnatural set of equations or perhaps extra terms in the equations. Initially, this investigation was begun using an analogue computer of limited capacity. When the problem outgrew the available equipment, a large scale digital computer was substituted. The original reference system was retained, however, due to the background of experience and confidence.

The basic reference system chosen is a set of axes $\{\bar{I}, \bar{J}, \bar{K}\}$ fixed at the mass centre of a rotating Earth (Fig. 18). Thus, the position of the vehicle is naturally expressed in terms of the geocentric latitude, λ , the geocentric longitude, θ (positive to the East), and the geocentric radius, r (Fig. 19); the velocity of the vehicle is then given by the geocentric azimuth, ψ (heading with respect to the North-positive to the East), the glide angle, γ (angle between the local geocentric horizontal and the velocity vector-positive downward), and the magnitude of the velocity vector, \bar{V} (Fig. 19). However, since all aerodynamic data is always referenced to a set of axes which are aligned in some way with the vehicle, a second reference system which will be termed flight axes $\{\bar{i}, \bar{j}, \bar{k}\}$ must be introduced (Fig. 20). It should be noted that these flight axes are not fixed to the body; on the contrary, the $\{\bar{j}\}$ axis always remains in the local geocentric horizontal plane, thereby forcing the $\{\bar{i}, \bar{k}\}$ axes to remain in the local geocentric vertical plane. In order to complete the orientation requirements, the $\{\bar{i}\}$ axis is directed along the velocity vector, \bar{V} , and the $\{\bar{k}\}$ axis is directed downward (in this study $|\gamma| < 90$ degrees). As a consequence of this definition for the flight axes, the side force equation will include the component of the lift in that direction, namely: $L \sin \phi$. For those readers who have not encountered this vehicle reference system of flight axes (for example, Refs. 35 and 36), it should again be mentioned that this investigation is concerned with a three degree of freedom system of equations

for a point mass vehicle. Since the pitch, roll, and yaw angles which are dependent variables in a six degree of freedom system are now control variables, it is rather useful to simplify the three force equations by using the required components of the lift and drag. The point mass vehicle is then rotated in pitch and roll (sideslip is assumed negligible and the yaw angle is, therefore, set identically equal to zero) so as to develop these required lift and drag components. The validity of the assumption regarding the representation of aerodynamic forces has been examined in Section III.

5.2 Conversion Between Reference Systems

Since the equations of motion are written in the flight axes reference system, it is necessary to find the components of all forces in this final reference system. (Fig. 21). Thus the conversion matrices from any of the basic or intermediate reference systems to the flight axes reference system must be found. A rotation about the $\{\bar{K}\}$ axis (Fig. 22) gives the transformation from the $\{\bar{I}, \bar{J}, \bar{K}\}$ set of axes to the $\{\bar{I}', \bar{J}', \bar{K}\}$ set of axes. The second rotation about the $\{\bar{J}'\}$ axis (Fig. 23) gives the transformation to the $\{\bar{n}, \bar{e}, \bar{v}\}$ set of axes. The third rotation about the $\{\bar{v}\}$ axis (Fig. 24) gives the transformation to the $\{\bar{h}, \bar{j}, \bar{v}\}$ set of axes. Finally, the fourth rotation about the $\{\bar{j}\}$ axis gives the transformation to the $\{\bar{i}, \bar{j}, \bar{k}\}$ reference system of flight axes (Fig. 25). These four rotations naturally require the four simple conversion matrices given with each figure. The overall conversion matrices from any of the intermediate reference systems are then easily found to be

$$\begin{pmatrix} \bar{h} \\ \bar{j} \\ \bar{v} \end{pmatrix} = \begin{pmatrix} \cos\gamma & 0 & -\sin\gamma \\ 0 & 1 & 0 \\ \sin\gamma & 0 & \cos\gamma \end{pmatrix} \begin{pmatrix} \bar{i} \\ \bar{j} \\ \bar{k} \end{pmatrix} \quad (5.1)$$

$$\begin{pmatrix} \bar{n} \\ \bar{e} \\ \bar{v} \end{pmatrix} = \begin{pmatrix} \cos\gamma\cos\psi & -\sin\psi & -\sin\gamma\cos\psi \\ \cos\gamma\sin\psi & \cos\psi & -\sin\gamma\sin\psi \\ \sin\gamma & 0 & \cos\gamma \end{pmatrix} \begin{pmatrix} \bar{I} \\ \bar{J} \\ \bar{K} \end{pmatrix} \quad (5.2)$$

$$\begin{pmatrix} \bar{I}' \\ \bar{J}' \\ \bar{K} \end{pmatrix} = \begin{pmatrix} \cos\gamma\cos\psi\sin\lambda & -\sin\psi\sin\lambda & -\sin\gamma\cos\psi\sin\lambda \\ +\sin\gamma\cos\lambda & & +\cos\gamma\cos\lambda \\ -\cos\gamma\sin\psi & -\cos\psi & \sin\gamma\sin\psi \\ \cos\gamma\cos\psi\cos\lambda & -\sin\psi\cos\lambda & -\sin\gamma\cos\psi\cos\lambda \\ -\sin\gamma\sin\lambda & & -\cos\gamma\sin\lambda \end{pmatrix} \begin{pmatrix} \bar{I} \\ \bar{J} \\ \bar{K} \end{pmatrix} \quad (5.3)$$

The conversion matrix between the basic reference system $\{\bar{I}, \bar{J}, \bar{K}\}$ and the flight axes reference system $\{\bar{i}, \bar{j}, \bar{k}\}$ could be found and expressed in the same manner; however, it is unnecessary since it is not used.

5.3 Vector Equation of Motion

An evaluation was made of the relative magnitudes of all forces which may act upon a spacecraft during a reentry into the Earth's atmosphere. Forces due to other planetary bodies including the moon, the solar wind, and magnetic fields often have an appreciable effect on the orbits of particular satellites when these forces are experienced over long periods of time. However,

for a reentry trajectory, it can easily be shown (Ref. 38) that only aerodynamic forces and the Earth's gravitational field have a non-negligible effect upon the flight path. In addition, based on the information in Ref. 23, it may be assumed that the basic reference system, $\{\bar{I}, \bar{J}, \bar{K}\}$ (see Fig. 18), is rotating in inertial space at a constant angular velocity.

The single vector equation of motion which is required for a point mass moving in such a rotating reference system is given by (Ref. 39)

$$\frac{\bar{F}}{m} = \bar{a} + 2(\bar{\omega} \times \bar{V}) + \bar{\omega} \times (\bar{\omega} \times \bar{r}) \quad (5.4)$$

where \bar{a} is the acceleration relative to the $\{\bar{I}, \bar{J}, \bar{K}\}$ reference system, i.e. relative to the Earth.

The only external forces are either aerodynamic or gravitational. It is appropriate, therefore, to separate the left hand side of Eq. (5.4) and write

$$\bar{F} = \bar{F}_A + m\bar{g} \quad (5.5)$$

The relative acceleration, \bar{a} , in the $\{\bar{I}, \bar{J}, \bar{K}\}$ system has components along the $\{\bar{i}, \bar{j}, \bar{k}\}$ axes that are obtained by the rule for transforming a derivative between rotating frames of reference (Ref. 40), i.e.

$$\bar{a} = \dot{\bar{V}} + (\bar{\Omega} \times \bar{V}) \quad (5.6)$$

where $\bar{\Omega}$ is the angular velocity of the $\{\bar{i}, \bar{j}, \bar{k}\}$ system relative to the $\{\bar{I}, \bar{J}, \bar{K}\}$ and the components of \bar{V} are the rates of change of the components of \bar{V} along the $\{\bar{i}, \bar{j}, \bar{k}\}$ axes.

Equations (5.4) to (5.6) can be combined to give

$$\frac{\bar{F}_A}{m} + \bar{g} = \dot{\bar{V}} + (\bar{\Omega} \times \bar{V}) + 2(\bar{\omega} \times \bar{V}) + \bar{\omega} \times (\bar{\omega} \times \bar{V}) \quad (5.7)$$

5.4 Expansion of the Single Vector Equation of Motion

The expansion of each of the terms in Eq. (5.7) in the $\{\bar{i}, \bar{j}, \bar{k}\}$ flight axes system is not difficult although it is somewhat involved and lengthy. The three components of each term will first be found in whichever axes system is most convenient then, if necessary, transferred to the $\{\bar{i}, \bar{j}, \bar{k}\}$ flight axes system, and finally collected to give the three complete force equations. Starting with the first term, the results are as follows.

The aerodynamic forces are given by

$$\begin{aligned} \bar{F}_A = & -\bar{I} C_D(\alpha) \frac{1}{2} \rho(y) V^2 S \\ & + \bar{J} C_L(\alpha) \frac{1}{2} \rho(y) V^2 S \sin \varphi \\ & - \bar{K} C_L(\alpha) \frac{1}{2} \rho(y) V^2 S \cos \varphi \end{aligned} \quad (5.8)$$

$C_L(\alpha)$ and $C_D(\alpha)$ are given by Eqs. (3.3) and (3.4). The expression for the density, $\rho(y)$, has been discussed in Sec. 4.5 and the evaluation of the height y , above a triaxial ellipse is given by Eq. (4.12).

The gravitational force vector is given by Eq. (4.3) in the $\{\bar{h}, \bar{e}, \bar{v}\}$ reference system. Transforming the components from this intermediate reference system to the $\{\bar{i}, \bar{j}, \bar{k}\}$ flight axes system via equation (5.2) gives the gravity vector as

$$\begin{aligned}\bar{g} = & \bar{i} (-g_r \sin \gamma + g_\lambda \cos \gamma \cos \psi + g_\theta \cos \gamma \sin \psi) \\ & + \bar{j} (-g_\lambda \sin \psi + g_\theta \cos \psi) \\ & + \bar{k} (-g_r \cos \gamma - g_\lambda \sin \gamma \cos \psi - g_\theta \sin \gamma \sin \psi)\end{aligned}\quad (5.9)$$

The expressions for g_r , g_λ , and g_θ are developed and stated in Sec. 4.3. Although, as noted in Sec. 4.3, g_θ is too small to affect the reentry trajectory of a spacecraft, the expressions have purposely been left in a generalized form so that the precise effect of any term in the series may be ascertained should it be desirable at some future date. In addition, the values of g_r and g_λ will normally include only the major effect of the Earth's oblate gravity potential, namely $C_{2,0}$ term. However, here again, the expressions are left in their generalized form. The truncated expressions which were actually used in the calculations may be found by a comparison of Eqs. (4.3) and (4.6) to be

$$g_r = -\frac{GM}{r^2} \left[1 + \left(\frac{R_0}{r}\right)^2 \frac{3}{2} (3 \sin^2 \lambda - 1) C_{2,0} \right] \quad (5.10)$$

$$g_\lambda = \frac{GM}{r^2} \left[\left(\frac{R_0}{r}\right)^2 3 \sin \lambda \cos \lambda C_{2,0} \right] \quad (5.11)$$

$$g_\theta = 0 \quad (5.12)$$

The terms on the right hand side of Eq. (5.7) are either very simple or quite complex. The first term is simply

$$\dot{\bar{V}} = \bar{i} \dot{V} \quad (5.13)$$

Before proceeding with the next term, the expression for $\bar{\Omega}$ should be found. With reference to Figs. 22 to 25, it can easily be seen that the sum total of all the rotations which are required to rotate from the $\{\bar{I}, \bar{J}, \bar{K}\}$ basic reference system to the $\{\bar{i}, \bar{j}, \bar{k}\}$ flight axes reference system yields the relative rotational velocity which is

$$\bar{\Omega} = \bar{K} \dot{\theta} + \bar{J}' \dot{\lambda} + \bar{v} \dot{\psi} - \bar{j} \dot{\gamma} \quad (5.14)$$

The negative sign in the last term is required due to the rotation of \bar{h} into \bar{v} which is in the opposite sense from the normal right hand rule.

At this point, the three kinematic relationships for the position of the vehicle \dot{r} , $\dot{\lambda}$ and $\dot{\theta}$ should be defined since the last two are required immediately. They are

$$\dot{r} = -V \sin \gamma \quad (5.15)$$

$$\dot{\lambda} = \frac{V}{r} \cos \gamma \cos \psi \quad (5.16)$$

$$\dot{\theta} = \frac{V \cos \gamma \sin \psi}{r \cos \lambda} \quad (5.17)$$

Then, in order to transform $\bar{\Omega}$ into the $\{\bar{i}, \bar{j}, \bar{k}\}$ flight axes system, the trans-

formation given in Eqs. (5.2) and (5.3) must be used, along with the substitution of Eqs. (5.16) and (5.17). The result is

$$\begin{aligned}\bar{\Omega} = & \bar{i}(\dot{\psi}\sin\gamma - \frac{V}{r\cos\lambda}\sin\gamma\cos\gamma\sin\lambda\sin\psi) \\ & + \bar{j}(-\dot{\gamma} - \frac{V}{r}\cos\gamma) \\ & + \bar{k}(\dot{\psi}\cos\gamma - \frac{V}{r\cos\lambda}\cos^2\gamma\sin\lambda\sin\psi)\end{aligned}\quad (5.18)$$

Finally, combining the expression for $\bar{\Omega}$ with $\bar{V} = \bar{i} V$ yields the desired cross product for the second term on the right hand side of Eq. (5.7). The result is

$$\begin{aligned}(\bar{\Omega} \times \bar{V}) = & \bar{i}(0) \\ & + \bar{j}(\dot{\psi}V\cos\gamma - \frac{V^2}{r\cos\lambda}\cos^2\gamma\sin\lambda\sin\psi) \\ & + \bar{k}(\dot{\gamma}V + \frac{V^2}{r}\cos\gamma)\end{aligned}\quad (5.19)$$

The next term is somewhat easier to express. It is easily seen (Fig. 23) that

$$\bar{\omega} = \bar{K} \omega \quad (5.20)$$

which upon substitution of Eq. (5.3) and combination with $\bar{V} = \bar{i} v$ results in

$$\begin{aligned}2(\bar{\omega} \times \bar{V}) = & \bar{i}(0) \\ & - \bar{j}(2\omega V[\sin\gamma\cos\lambda\cos\psi + \cos\gamma\sin\lambda]) \\ & + \bar{k}(2\omega V\cos\lambda\sin\psi)\end{aligned}\quad (5.21)$$

Finally, the last term is easiest to expand in the reverse direction. It is also easy to see (Fig. 23) that

$$\bar{r} = -\bar{v} r \quad (5.22)$$

or

$$\bar{r} = \bar{i}'r\cos\lambda - \bar{k}r\sin\lambda \quad (5.23)$$

which upon combination with Eq. (5.20) gives

$$\bar{\omega} \times (\bar{\omega} \times \bar{r}) = \bar{i}'\omega^2 r\cos\lambda \quad (5.24)$$

and after substitution of Eq. (5.3) results in

$$\begin{aligned}\bar{\omega} \times (\bar{\omega} \times \bar{r}) = & \bar{i}(\omega^2 r\cos\lambda[\sin\gamma\cos\lambda + \cos\gamma\sin\lambda\cos\psi]) \\ & - \bar{j}(\omega^2 r\cos\lambda\sin\lambda\sin\psi) \\ & + \bar{k}(\omega^2 r\cos\lambda[\cos\gamma\sin\lambda - \sin\gamma\sin\lambda\cos\psi])\end{aligned}\quad (5.25)$$

All of the terms in Eq. (5.7) have now been expanded into the $\{\bar{i}, \bar{j}, \bar{k}\}$ flight axes reference system. Since each of the three components are

independent of the other, three first order, non-linear, differential equations may be written by collection of all the terms in Eqs. (5.8), (5.9), (5.13), (5.19), (5.21), and (5.25). The result is

$$\dot{V} = -C_D(\alpha)\frac{1}{2}\rho(y)V^2S/m - g_r\sin\gamma + g_\lambda\cos\gamma\cos\psi + g_\theta\cos\gamma\sin\psi - \omega^2r\cos\lambda(\sin\gamma\cos\lambda + \cos\gamma\sin\lambda\cos\psi) \quad (5.26)$$

$$\begin{aligned} \dot{\gamma}V = & -C_L(\alpha)\frac{1}{2}\rho(y)V^2\frac{S}{m}\cos\varphi - \frac{V^2}{r}\cos\gamma - g_r\cos\gamma - g_\lambda\sin\gamma\cos\psi \\ & - g_\theta\sin\gamma\sin\psi - \omega^2r\cos\lambda(\cos\gamma\cos\lambda - \sin\gamma\sin\lambda\cos\psi) \\ & - 2\omega V\cos\lambda\sin\psi \end{aligned} \quad (5.27)$$

$$\begin{aligned} \dot{\psi}V\cos\gamma = & C_L(\alpha)\frac{1}{2}\rho(y)V^2\frac{S}{m}\sin\varphi + \frac{V^2\cos^2\gamma\sin\lambda\sin\psi}{r\cos\lambda} - g_\lambda\sin\psi + g_\theta\cos\psi \\ & + \omega^2r\cos\lambda\sin\lambda\sin\psi + 2\omega V(\sin\gamma\cos\lambda\cos\psi + \cos\gamma\sin\lambda) \end{aligned} \quad (5.28)$$

In addition to the above three differential equations, and the positional differential equations (5.15), (5.16), and (5.17), several other relationships are required which have already been stated or developed previously. For convenience, they will be mentioned again at this point. Equations (3.3) and (3.4) give the relationship between the lift and drag coefficients, $C_L(\alpha)$ and $C_D(\alpha)$, and the angle of attack, α . The relationship between the density, $\rho(y)$, and the perpendicular height above the Earth's surface, y , has been discussed in Sections 4.5 and 4.6. The perpendicular height above the surface of a triaxial Earth, y , is given by Eqs. (4.12) to (4.18). Finally, the expressions for g_r , g_λ , and g_θ are given by Eqs. (5.10), (5.11), and (5.12). Should it be desirable to include additional terms in the oblate gravity field of the Earth, equations (4.1) to (4.5) will serve to illustrate the manner by which it may be done.

At this point in the development of the equations of motion, it was found to be convenient to make a change in the independent variable from time, t , to path length along the trajectory, s . The original reasons for making this change are no longer a justification for it. However, it was convenient to maintain the new independent variable and the following first order, non-linear, differential equations were the ones which were actually integrated.

The three force equations become

$$\begin{aligned} \frac{d(V^2)}{ds} = & -\frac{C_D(\alpha)S}{m}\rho(y)V^2 - 2(g_r\sin\gamma - g_\lambda\cos\gamma\cos\psi - g_\theta\cos\gamma\sin\psi) \\ & - 2\omega^2r\cos\lambda(\sin\gamma\cos\lambda + \cos\gamma\sin\lambda\cos\psi) \end{aligned} \quad (5.29)$$

$$\begin{aligned} \frac{d\gamma}{ds} = & -\frac{C_L(\alpha)S\cos\varphi}{2m}\rho(y) - \left(\frac{1}{r} + \frac{g_r}{V^2}\right)\cos\gamma \\ & - \frac{1}{V^2}(g_\lambda\sin\gamma\cos\psi + g_\theta\sin\gamma\sin\psi) \\ & - \frac{\omega^2r\cos\lambda}{V^2}(\cos\gamma\cos\lambda - \sin\gamma\sin\lambda\cos\psi) \\ & - \frac{2\omega}{V}\cos\lambda\sin\psi \end{aligned} \quad (5.30)$$

$$\begin{aligned} \frac{d\psi}{ds} = & \frac{C_L(\alpha)S\sin\varphi}{2m} \rho(y) \frac{1}{\cos\gamma} + \frac{\cos\gamma\sin\psi/\sin\lambda}{r\cos\lambda} \\ & - \frac{1}{v^2\cos\gamma} (g_\lambda\sin\psi - g_\theta\cos\psi) + \frac{\omega^2 r\cos\lambda}{v^2} \frac{\sin\lambda\sin\psi}{\cos\gamma} \\ & + \frac{2\omega}{V} \left(\frac{\sin\gamma\cos\psi\cos\lambda}{\cos\gamma} + \sin\lambda \right) \end{aligned} \quad (5.30)$$

The three positional equations become

$$\frac{dr}{ds} = -\sin\gamma \quad (5.32)$$

$$\frac{d\lambda}{ds} = \frac{\cos\gamma\cos\psi}{r} \quad (5.33)$$

$$\frac{d\theta}{ds} = \frac{\cos\gamma\sin\psi}{r\cos\lambda} \quad (5.34)$$

Also, the differential equation for the time is

$$\frac{dt}{ds} = \frac{1}{V} \quad (5.35)$$

5.5 Numerical Procedures

A major problem in the development of digital computer programs is the problem of retaining accuracy during the course of the computation while keeping the number of points (and therefore the computation time) as low as possible. In particular, the calculation of flight trajectories of reentry vehicles often requires an accuracy of six or eight figures in the altitude or geocentric radius, respectively. The latter requirement certainly exceeds the precision of numbers in most scientific computers when round-off error* inherent in all integration schemes is taken into account. Truncation-error is easily reduced by using one of the standard, high-accuracy integration techniques such as the fourth order Runge-Kutta method and the proper size of interval. However, round-off error proves much more difficult to eliminate, especially when a small enough interval size (and therefore a large number of points) is used to reduce the truncation-error. Consequently, a practical method must be found for reducing round-off error and also of reducing the number of integration points while simultaneously keeping the truncation-error to a minimum.

* Error is introduced from two sources:

- (a) Truncation-error may be defined as the difference between the true value and the value obtained from the numerical integration formula which takes use of a finite number of terms from an infinite Maclaurin's or Taylor's series.
- (b) Round-off error is the result of the limited accuracy (usually 8 figures) available within the computer.

The solution to the problem of round-off error took advantage of the basic characteristic of digital calculations. All numerical integration schemes involve adding small increments to the variables in order to find the next value after each step. Accordingly, these increments possess far more absolute accuracy than their respective variables. Thus, if the variables could take advantage of this increased absolute accuracy when incrementation took place, the round-off error would be greatly reduced. Notice that the incrementation stage would be the only one at which the increased accuracy (and therefore greater computation time) would be used since the calculation of the increments would use the variables only to their original accuracy.

In practical computational terms (using popular languages such as FORTRAN), the scheme merely involves the use of double-precision addition whenever the increments are added to the variables. Normal single-precision computation of the increments makes use only of the most significant part of the variables. In addition, an analysis of the whole program should be made as other sections may benefit from this technique. An example is the calculation of the altitude over an oblate Earth when only the geocentric latitude and the geocentric radius are available. Having calculated the "corrections" in single precision, they should be added in double precision.

A major reduction in the number of steps is also possible, by using a continuously varying interval step size dictated by truncation-error. It has been found that the truncation-error depends on how quickly the variables are changing as well as the step size. In the calculation of flight trajectories of entry vehicles using geographical coordinates, the key variables are the glide angle, the azimuth, and the latitude. Experience has shown that whenever all of these variables are reasonably stationary, the interval step size can be rather large. The criterion which was used to determine the interval size (within a certain preset range) was that the change in all these angles per step should be kept below a certain minimum value. By varying the interval size parameter, the value could be found for which the truncation-error was acceptable, since the double-precision incrementation always reduced the total round-off error to a negligible value.

Two basic methods were used to check the results of the computations. First, the atmosphere was removed (by setting the density to zero) and orbits were calculated for all the situations for which simple analytical solutions were known. Circular and elliptical orbits were compared over non-rotating and rotating Earth reference systems. In every case, the additional terms involving the Earth's rotation produced the proper result when changes were expected. On the other hand, parameters such as the orbital period and the major axis (for elliptical orbits) remained the same. Typical accuracies were six or seven figures over several orbits. These latter results also gave confidence in the numerical integration procedure referred to above. The check on the accuracy of Eq. (4.12) was made via the test program developed to check the original validity of its results.

In order to check the accuracy of the digital program when the atmosphere was present, the terms due to rotation and oblateness were removed. The equations were then further simplified (the atmosphere was made exponential, only zero roll angles were considered, and gravity was held constant at its average value) and the results compared with the output of the identical equations which had been wired into an analogue computer. Over the range for which the density approximation on the analogue computer was reasonably accurate (from 150,000 feet up to 300,000 feet) there was no discernable difference between the two results.

VI. RESULTS AND DISCUSSION FOR A CIRCULAR, NON-ROTATING EARTH

6.1 Introduction

The next three sections of this paper present an analysis of the performance of the CONTAC system with results obtained from the digital computer program listed in Appendix C. Section VI is devoted to presenting the overall capabilities of the CONTAC system as well as its limitations.

The method of presenting the results has been discussed in Sec. 1.3. Apart from the peak temperature, the two main quantities of interest are the equivalent down range and cross range. These values are illustrated and defined in Fig. 3.

In order to give the reader a better understanding of the way in which the CONTAC system works, a detailed history of all important variables is given in Figs. 11b and 11c. Figure 11a is a similar history of an uncontrolled reentry and may be used as a comparison. It is quite clear that the CONTAC system is easily able to control the temperature and prevent the additional rise of 650°F which occurred for the uncontrolled reentry.

In order to provide the details of the way in which the altitude angles are controlled, an expanded scale has been used for a portion of the reentry in Fig. 11d. Notice first that the line of time vs. down range is straight over this small portion of the reentry. Consequently, the abscissa of the graph has been labelled as time in addition to down range in order to provide a better feeling for the time scale of the cycling of the angle of attack by the CONTAC system. The most important information to be gained from Fig. 11d is the rates involved in the process. Notice that the fuel economy will be quite high due to infrequent use of the reaction jets.

6.2 Footprint Optimization

The standard reentry conditions at 350,000 feet altitude were chosen to be 26,000 feet per second for the speed and 1.0 degree for the glide angle. It might be noted that the speed is between 250 and 300 feet per second greater than the orbital velocity at this height, which therefore allows the spacecraft the possibility of having reached this position from an altitude of between 250 and 300 miles. A slight increase in the initial speed or glide angle would allow higher initial orbital altitudes up to 500 miles if that condition were desirable.

Two criteria were used in determining the best flight path which could be obtained from the initial conditions. The most important factor was to prevent throughout the reentry, the occurrence of a temperature greater than the peak value experienced during an equilibrium glide. In general, this requirement was slightly relaxed to allow temperature peaks which were greater by 20°F or 30°F . The second principal requirement was to obtain as large a cross range as possible throughout the whole extent of the down range capability.

In addition, some effort was added to increase the available down range increment. It is here that a further reason for the choice of 26,000 feet per second as the initial velocity was found. On Fig. 9, it is shown that the speed lost up to the point of the first temperature maximum can easily be controlled to a value between 150 and 175 feet per second by the use

of the proper entry angle of attack. As noted in Sec. 1.9, this reduction in the vehicle's speed at the end of Phase II can be produced without causing a significant difference in altitude, glide angle, or down range distance at that position. This condition results from the variation of the drag coefficient with the angle of attack while the lift coefficient remains essentially constant. Consequently, due to the choice of speed at the initial position, the speed at the end of Phase II is either very slightly above (when low angles of attack with relatively low drag coefficients were used) or just below (when high angles of attack with much larger drag coefficients were used) circular orbital velocity. In a vacuum, the former speed results in a perigee condition which would produce an additional revolution around the Earth yielding 360 degrees of down range increment before the spacecraft descends to the same altitude. On the other hand, even in a vacuum, the latter speed would produce an apogee condition which brings about an immediate decrease in altitude. However, it is quite obvious that the presence of atmospheric drag will tend to alter the situation. Except when complicated by Earth oblateness, even the use of a very small angle of attack (at 5° , $C_D \approx C_{D_{min}}$) for the former situation results only in an extended glide at practically constant altitude (the rise is limited to 30,000 feet) until the speed falls below the circular value by about 1000 feet per second. On the other hand, the continued use of a high angle of attack for the latter situation reduces the speed very quickly resulting in very little incremental down range. In both extreme situations as well as any between, the incremental down range which is available by means of subsequent attitude control, is very nearly the same once the speed falls below the circular value by about 1500 feet per second. Therefore, any small speed variations at the end of Phase II on the order of one hundred or even fifty feet per second will result in large variations in incremental down range during Phase III of the reentry. As a consequence, the situation provides the guidance system with the capability of large down range increments, without interference from the CONTAC system, due to the possibility of an extended glide at very low angles of attack during which the speed is lost very slowly.

It should be noted that the above discussion is not altered by the inclusion of Earth rotation. The immunity is due to the fact that although the relative speed can change by up to ± 1500 feet per second at the equator for initially due West or due East reentries, respectively, the relative circular orbital speed also changes by exactly the same value. For other initial azimuths, the same relative change also occurs. Consequently, the same perigee and apogee conditions result upon the use of low and high entry (i.e., during Phase II) angles of attack, respectively.

With regard to satisfying the first criterion, the CONTAC system behaved very well. The operational limits were difficult to obtain since impractical situations had to be imagined before any degradation was found in the peak temperature performance. The discussion of the parameters which were varied during the reentry is confined to the attitude at this particular point; the result of the differences or errors in initial conditions is presented in Sec. 6.3.

The entry angle of attack was limited to a maximum of 65 degrees in order to prevent excessive heating rates at the rear of the spacecraft. It may be questionable whether larger pitch angles could be maintained due to problems of stability and control. However, assuming that these problems can be solved, there is no reason why angles as high as 75 or even 80 degrees cannot be used.

The lower limit for the entry angle of attack was approximately 35 degrees. When smaller values were used, the first maximum temperature was too large, since too little lift was developed to prevent the vehicle from descending too low on the initial penetration into the atmosphere.

The entry roll angle was always held at zero during this investigation. It is probable that a moderate roll angle during Phase II could increase the cross range without affecting the peak temperature control. Further investigation into this question might prove useful.

The skip angle of attack (which is controlled by the guidance system) is employed as the lower limit during Phase III. The largest value was the lesser of 55 degrees and the entry angle of attack. The lowest value used was 5 degrees. The guidance system might employ even smaller values down to zero if the upper surface of the spacecraft is not subject to or can cope with large heating rates. It should be noted that when the large entry angles of attack of 55 or 65 degrees were used, the CONTAC system often prevented the vehicle from assuming the skip angle of attack. As soon as it commences active operation at the beginning of Phase III, the CONTAC system disallows lower limits if they would permit too high a peak temperature. Again, it is noted that this operation is completely automatic.

The skip angle of roll (which is also controlled by the guidance system) is employed as the lower limit during Phase III. The "smallest" value was a full minus ninety degrees to the left (or plus ninety to the right). Smaller values were not used since they resulted in less cross range which was not in accordance with the second criterion. The "largest" value used was zero degrees. The CONTAC system often prevented the vehicle from assuming the skip bank angle when it was near ninety degrees; the conditions which led to this situation were the same as those which prevented very small skip angles of attack from being used and again the CONTAC system automatically disallowed the value and prevented the temperature from achieving too high a value.

The upper limit on the angle of attack during both Phases III and IV was 55 degrees. This value was fixed at the attitude which yielded the maximum vertical force. The upper limit for the bank angle was also the value which yielded maximum vertical force, namely zero degrees. The reasons for this choice have already been given in Sec. 1.10.

The lower limit for both the angle of attack and the bank angle did not affect the operation of the CONTAC system. Therefore, the choice of the values used will be discussed under the second criterion of cross range optimization.

While operating within the above values for the attitude, the CONTAC system performed the task of restraining the peak temperature experienced during the reentry without any degradation in performance for any combination of these values. As shown in Fig. 26, the peak temperature experienced during the reentry varied only ± 20 Fahrenheit degrees about the peak value experienced during an equilibrium glide. At the same time, cross range was practically constant (between 9 degrees and 11 degrees) throughout most of the available down range. Therefore, it is possible to obtain an "isothermal footprint" (with regard to the peak temperature experienced during the reentry) of considerable area when the CONTAC system is employed to constrain the temperature during

the flight. The dimensions are over one hundred degrees equivalent longitude in down range and about twenty degrees equivalent latitude in cross range. Considering the fact that the continental United States has a "length" of only forty degrees in equivalent longitude and is less than eighteen degrees of equivalent latitude wide, this "isothermal footprint" is about three times the area of that country. Consequently, during any given 12 (or at most 24) hour period, enough range control is available when using the COMIAC system to land at any point within or near the United States, as long as the terminal position is underneath or at least near the orbital envelope.

The attainment of the second criterion, the maximum possible cross range, was attempted by programming the skip bank angle (Phase III) and the lower limit for the angle of roll (Phase IV) within the restraints imposed by the first criterion. During each Phase of the reentry, several possibilities were investigated until the best overall performance was attained throughout the flight.

Note that the final results for cross range presented in this paper should not be considered the maximum possible values since it was not feasible to consider every parameter combination. In addition, the calculation was terminated at approximately 100,000 feet where the speed was about 3000 feet per second. As a consequence, about 3 degrees of equivalent latitude or about 200 miles of additional cross range is available before the final touchdown. However, as pointed out in Section 1.12, this final portion of the flight has not been included in the investigation. Therefore, no details for Phase V can be given.

On the other hand, density variations in the atmosphere and other sources of error may reduce the anticipated cross range. It was invariably found that when the relationships which yielded maximum cross range were incorrectly adjusted, the result was not only a decrease in cross range, but also either increased or decreased down range depending on the direction of the mismatch. Therefore, it may be necessary to sacrifice a portion of the cross range capability in order to retain a degree of down range mobility in the latter phases of the flight.

At this point, a detailed description of the methods used to maximize the cross range will be given for Phases I to IV.

During Phase I, no cross range control is available by means of attitude adjustments since atmospheric forces are negligible. In conjunction with the rotation of the Earth, it might seem possible to provide additional cross range by appropriately delaying or advancing the retro-fire time. For instance, in the case of a polar orbit with the landing zone near the equator, a retro-fire delay of 20 minutes would appear to provide 5 additional degrees of cross range. However, the results in Sec. 7.2 are contrary to such a possibility since the midline of the footprint closely follows the vacuum orbital track over the Earth's surface.

During Phase II, no cross range control was attempted. For entry angles of attack in the vicinity of 35 degrees, a very slight increase in cross range may be possible by trading off some vertical force for small amounts of side force. However, the speed is so great that only large forces will produce a turning radius with any appreciable effect. Thus, since large bank angles cannot be used without degrading the vehicle's peak temperature performance, there is too little to be gained from complicating the reentry with an additional parameter.

During Phase III, about ten to twenty percent of the cross range may be realized by using the optimum bank angle. Figure 27 shows that the best value for the skip angle of roll is about 75 degrees and this value was adopted for all subsequent trajectories. Another possibility for producing the most cross range was that of using a bank angle based on speed or perhaps altitude as suggested by Wagner (Ref. 6). However, the result was usually so close to 75 degrees that the additional complexity was not considered worth while.

It is during Phase IV that most of the cross range capability is realized. The lower limits for the angle of attack and the bank angle are not, of course, used until well after the beginning of Phase IV. This is because the CONTAC system retains control of the attitude until so much energy has been dissipated that the convective heating rate will continue to decline regardless of the attitude assumed. Once this condition has been reached, the guidance system will assume full control.

The basic concept behind the attempt to maximize the cross range is the relationship proposed by Wagner (Ref. 6). The problem in this investigation was how to implement the procedure on a practical basis. The method which was adopted is to base the maximum allowable bank angle (either left or right) on a variable connected with the shape of the trajectory. The three variables considered were the speed, the altitude, and the glide angle. The energy was also considered in order to combine both speed and altitude in some manner. However, the glide angle was rejected on the grounds that its variation during this part of the flight was an increase while a decrease in the bank angle was obviously required. This left the speed, altitude, and energy of the vehicle as a basis upon which to proceed.

The next step was to find the best angle of attack for the lower limit during Phase IV. The value found to yield the largest cross range was the angle for $(L/D)_{\max}$ which occurs at 22.7 degrees for the vehicle under study. This value could be anticipated due to the fact that the maximum down range also results from the use of this angle.

At this point, a number of simultaneous tradeoffs were investigated. No attempt is made to justify the procedure nor even the final result. However, very briefly, it involved the determination of which power relationship (square root, linear, or quadratic) between the bank angle and one of the speed, the altitude, or the energy would yield the most cross range. The result that was consistently best for all the reentries studied is the relationship shown in Fig. 28 in which the bank angle was a linear function of the speed over the interval shown. A few results were found for which a slightly greater cross range was achieved by using the square root of the speed over the specified interval; however, there was no way of predicting when the result would be larger. Therefore, the linear variation was adopted as the best solution.

In general, the above combination of the angle of attack for $(L/D)_{\max}$ and the relationship shown in Fig. 28 for the bank angle as the lower limits during Phase IV proved a proper choice in one other way. In most situations, the azimuth change at 100,000 foot altitude was about 70 degrees. A slight additional increase until a speed of 1000 feet per second is reached during Phase V would yield a final azimuth change of about 80 to 90 degrees. It is certainly convenient to be heading in the proper direction to achieve the maximum possible additional cross range if it is required during the last stages of the reentry.

However, no calculations were made for Phase V of the reentry. But, it is worth mentioning that any procedures which are used to optimize the cross range must take into account the final approach and landing. Certainly, some cross range capability must be sacrificed in order to obtain a sensible landing pattern and a touchdown with a margin of safety and an allowance for adverse conditions at the landing site.

6.3 Effect of Non-Standard Initial Conditions

The results presented in this section deal with the effects produced by a difference between the desired and the actual initial values of the speed and the glide angle. The cause of the difference has been dealt with in some detail in Section 1.8. However, the investigation should not be confined only to that limited range of errors in attitude misalignment and incorrect retro-fire velocity increment that have occurred in recent flights. Therefore, the results of large deviations in the speed and the glide angle will be examined.

Before any results are presented, it should be noted that there are actually two problems to consider. The more important is whether the CONTAC system can cope with the deviations from the expected initial values. This question is easily answered. If the peak temperature during the reentry does not exceed by more than a small value the peak temperature which is experienced during an equilibrium glide, then this test is successful. If unsuccessful, the first temperature maximum is always higher than the standard peak temperature. On the other hand, when the test is successful, the peak which occurs during the flight (whether it be the first or a subsequent maximum) will be equal to the standard peak value.

The second question is whether or not the vehicle may still land at its original destination. Due to changes in the initial conditions, the shape, size, and position of the footprint is altered. The alterations are analyzed and the basic differences in the footprint are given. It can then be determined whether or not the footprint still contains the desired landing site.

Figure 29 shows the results of deviations in the initial speed which range from 25,700 to 26,300 feet per second. With respect to the first problem, it can be concluded that positive errors in the initial speed will not cause any degradation in the performance of the CONTAC system. However, peculiarly enough, it is the negative errors (due to a lower than normal initial speed) which cause some difficulty. For small errors, between zero and -100 feet per second, the increase in the peak temperature is also small, amounting to only 50F° for most points on the footprint and only 90F° for the extreme down range positions. However, for errors in the vicinity of -300 feet per second, the performance definitely begins to decline; peak temperatures are 200F° greater for most points on the footprint and at the extreme down range position, the peak is another sixty degrees higher still. Calculations could be made for even greater errors in the initial speed, but a simple check on the initial altitude from which such a reentry could be initiated reveals that even for an error of -300 feet per second (i.e. an initial speed at 350,000 feet of 25,700 feet per second), the maximum height from which the vehicle could have descended is only 130 miles. In addition, the errors in retro-fire alignment attitude would have to be about 30 degrees in alignment and about 250 feet per second in velocity increment. Such large errors would lie outside the normal

operating conditions. Finally, still larger errors (on the negative side at least) have no chance at all of occurring unless some deliberate action to decrease the speed is taken at an altitude below 100 miles. Since this height is below normal orbiting altitudes, the action would have to take place subsequent to retro-fire and is not considered a feasible possibility in the production of errors.

With regard to the position of the altered footprint, no problems are apparent. The maximum down range possible with the -300 feet per second error is still 60 degrees of equivalent longitude greater than the minimum down range with the +100 feet per second error. And with the latter error, global down range is already available. Therefore, with the +300 feet per second error, the guidance system will only have to take the vehicle around the Earth one additional orbit if the minimum down range position is past the landing site. With regard to cross range, it is quite clear that no problems exist here either. The minimum footprint width is still almost equal to the equivalent latitude span of the United States. Also, note that the minimum down range increment or footprint length is still greater than the equivalent longitude span of that country.

Figure 30 shows the results of deviations in the initial glide angle which range from 0.65 to 1.5 degrees. Reference 5 indicates that such an interval is far larger than would be expected due to normal errors in attitude alignment and velocity increment. However, Fig. 8 shows that this interval is to be expected if large retro-fire errors are present. Negative errors in the initial glide angle are easily handled by the CONTAC system and without any degradation in performance. But for positive errors even as small as 0.25 degrees, the CONTAC system fails to prevent the peak temperature from rising beyond the standard peak value. An analysis of the actual trajectories indicates that in every case the first temperature maximum is higher than the standard peak value due to the inability of the spacecraft to produce enough vertical force. As a result, the vehicle descends to a lower than standard height in the atmosphere at that position. The decrease in height results in a higher density without a compensating decrease in speed. Therefore, although the CONTAC system is not directly responsible for the temperature increase (recall that it does not go into active operation until the beginning of Phase III and these temperature peaks occur at the end of Phase II), nevertheless, the vehicle must be designed to withstand the additional rise in the peak temperature of 200°F if the initial glide angle may be as high as 1.25 degrees. However, it should be noted that the additional rise for an initial glide angle of 1.5 degrees is only about 300°F over the standard peak temperature. Consequently, the relationship is highly non-linear.

With regard to the position of the altered footprint there may be a problem for initial glide angles greater than about 1.4 degrees. Beyond this value, the maximum down range may be less than the minimum down range for initial glide angles less than 0.75 degrees. Whether the additional down range (obtainable from permitting the vehicle to travel once around the Earth in order to overlap the original down range position) can be usefully employed by the down range guidance scheme is a question which must be answered by simulated real time runs. The cross range is not a problem; there is more than the usual value.

A few additional points which apply to both Figs. 29 and 30 should be mentioned. First, there has been no attempt to optimize the upper and lower limits for the attitude when incorrect initial conditions in the speed or glide angle were present. Second, the results of an incorrect initial value for the down range position has not been taken into account. A one degree error in the initial down range would require about a twelve second error in retro-fire time assuming that the initial conditions of speed and glide angle were correct. However, the initial down range is also affected by the conditions which produce errors in the initial reentry values. For instance, an increased initial glide angle of 1.35 degrees (which results in a decreased down range over the whole footprint) is accompanied by a decreased down range at the initial position of eleven degrees of equivalent longitude when the retro-fire takes place at 250 miles. Consequently, it can be seen that the range control problem may be quite difficult to solve, but a solution should be available which is also compatible with the concept and operation of the CONTAC system.

VII. RESULTS AND DISCUSSION - OBLATE, ROTATING EARTH

7.1 Introduction

Section VI presented the problems associated with variations in the initial reentry conditions of speed and glide angle. However, it will certainly be possible to design for the spacecraft the equipment necessary to compute the proper attitude alignment and retro-fire velocity increment at the given orbital position. Therefore, these problems should not be considered to be very serious. On the other hand, the effects of Earth rotation and oblateness must be compensated for this task; may not be simple in all situations.

In order to understand the individual effects of the Earth's rotation and oblateness, calculations were performed in which only one of these was present at a time. All the effects were then combined and the overall effect noted.

7.2 Effect of the Earth's Rotation

Figure 31 gives the results of calculations for a number of different reentry positions and directions when it was assumed that the Earth was circular, but rotating.

An analysis of the peak temperatures shows that the CONTAC system encounters a little difficulty in controlling the temperature when rotation and an initial Westerly heading along the equator combine to increase the initial relative speed between the vehicle and the atmosphere. On the other hand, this effect is reversed for an initial Easterly heading and lower than normal peak temperatures result. However, since the maximum difference in each case amounts to only $\pm 125^\circ \text{F}$ for due West and due East equatorial reentries, respectively, the effect of rotation on temperature peaks cannot be considered a major problem. In most situations, the effect will probably be beneficial since the loss in inertial velocity during launch does not favour the establishment of orbits which travel in a Westerly direction against the rotation of the Earth.

With respect to the shape of the footprint, the most obvious part of the result is the shift towards negative values of cross range without any substantial change in down range. A comparison should be made (Fig. 29). In those cases, for a non-rotating Earth, errors in the initial speed of ± 300 feet per second produced large shifts in final down range. For these cases in which there is a ± 1500 feet per second change in speed relative to the Earth due to an initial Westerly or Easterly heading, respectively, along the equator, the down range shift averages only about ± 8 degrees of equivalent longitude which is only about four percent of the total down range distance. It may be concluded, therefore, that for a given set of initial conditions, the Earth's rotation is not a significant factor with respect to the final down range position of the vehicle. The physical explanation has already been presented in Sec. 6.2.

However, with regard to the cross range, an important shift occurs in the footprint. Fortunately, the extent of the shift is quite predictable. A comparison has been made with orbital tracks for vacuum trajectories. In almost every case studied, the extent of the shift is either the same as or algebraically less (i.e. whether the actual shift is positive or negative) by up to 1 degree than the value which would be found due to the rotation of the Earth under the equivalent circular orbit (Fig. 3). In most cases, the agreement was better than $\frac{1}{2}$ degree. The example easiest to visualize is the case for which the vehicle is initially heading due north from the equator. For a circular vacuum orbit through the initial position, the Earth will have rotated -10.8 degrees by the time the spacecraft reaches the equator again at 180 degrees down range. The actual shift in this case also amounts to -10.8 degrees. A check upon all other cases yields similar results.

The observed result may be explained as follows. In symmetric flight, with zero bank and sideslip, neither the lift nor the drag have a horizontal component perpendicular to V . Thus the only force available to produce horizontal curvature of the path (in an Earth-fixed reference frame) is the Coriolis force. This is the same whether the atmosphere is present or not, (except for the gradual reduction of V by the drag). Hence the horizontal curvature of the path is largely unaffected by the atmosphere.

7.3 Effect of the Earth's Oblate Shape

Figure 32 gives the results of calculations for a number of different reentry positions and directions when it was assumed that the Earth's poles were depressed to give the correct oblate shape, but that the gravitational field was purely a central force and the Earth was not rotating.

An analysis of the peak temperatures shows that the CONTAC system also encountered a little difficulty when the oblate shape of the Earth caused the effective initial glide angle (see Appendix B) to be larger than normal. For situations in which the effective initial glide angle is smaller than normal, the CONTAC system was able to maintain the peak temperature at the standard value.

The situation may be compared directly with the results of Fig. 30 in which both smaller and larger than normal values were used for the geocentric initial glide angle. The extreme negative difference between the effective and the geocentric initial glide angle is -0.18 degrees, and occurred for an initial latitude of 30 degrees North and an initial heading of due

North. The peak temperature for both this footprint and the one where the geocentric initial glide angle was 0.75 degrees is the normal peak value. In addition, the cross range is the same for each. However, down range achieved in the oblate Earth case is a relatively small but significant amount less at both ends of the footprint than for the case of the geocentric initial glide angle of 0.75 degrees. This difference is in good agreement with the expected result.

The extreme positive difference between the effective and the actual initial glide angle is +0.18 degrees, and occurred for an initial latitude of 60 degrees South and an initial heading of due North. For this reentry, the peak temperature for both this footprint and the one where the initial glide angle was 1.25 degrees is somewhat greater than the standard peak value, but the difference is, as expected, less for the case of the oblate Earth reentry. The peaks were about 160F° - 190F° greater. On the other hand, both the down range and the cross range achieved under both situations is substantially the same, which indicates that the continued decrease in the height due to the oblate shape has a continued effect on range while for peak temperatures, the effect ceases at the first temperature maximum (which occurs at about 18.5 degrees down range from the initial position).

The use of other geographical locations for the initial position produced similar results. A slight rise in the peak temperature was noted for the South-to-North trajectory, which produces an increase in the effective initial glide angle of only 0.07 degrees. The equator-to-pole reentry, which produces a decrease of 0.07 degrees, experiences a slight increase in down range.

In general, the results due to the shape oblateness of the Earth often showed that much of the effect can be accounted for by the difference between the effective and the geocentric initial glide angle. In addition, although there is a substantial difference in many situations between results for the same effective (over an oblate Earth) and geocentric (over a spherical Earth) initial glide angles, there is at least qualitative agreement in all cases. However, it should not be considered serious if the correction factors for non-normal values of the effective and the geocentric initial glide angles do not agree. The guidance system must reduce to zero either type of error. Since they are equal in magnitude, errors due to non-normal values in the actual initial glide angle will provide the necessary information on the extent of the errors which may be expected on account of the shape oblateness of the Earth.

There is another possible approach to the problem of shape oblateness. Rather than relying on the CONTAC - guidance system to correct for the errors introduced by incorrect values in the effective initial glide angle, it should be possible to produce the correct down range by an appropriate adjustment of the actual geocentric initial glide angle. The adjustment would have to take account of the geographical location of the initial position. The change in the actual initial glide angle could be produced by correcting the retro-fire attitude alignment and velocity increment.

7.4 Effect of the Earth's Oblate Gravity Field

The results of including the oblateness term in the gravitational field for the Earth showed a negligible difference between the various foot-

prints which result from different initial positions and initial heading directions. Consequently, it may be concluded that even the $C_{2,0}$ coefficient has a negligible effect on the reentry of a spacecraft and that all other terms may be completely ignored.

One minor effect was found which tends to cancel the shape oblateness contraction in down range which resulted when proceeding from polar to equatorial regions. For these cases, the small reduction in gravitational force on the vehicle due to the additional distance between the vehicle and the equatorial bulge resulted in a small increase in down range of the order of 5 degrees at the minimum down range position and 10 degrees at the maximum down range position. Since this increase amounted to less than 5% of the total, and no other results were affected, it was not considered significant. Note that in the case of shape oblateness, the decrease in down range was double this value when the initial position was at the pole.

7.5 Effect of the Earth's Rotation and Oblateness

Figure 33 gives the results of calculations for a number of different reentry positions and directions for a rotating oblate Earth.

An analysis of the peak temperatures shows that the CONTAC system again encountered the same expected difficulty in controlling the peak temperature when rotation and the initial heading combine to increase the relative speed between the vehicle and the atmosphere. In these situations, an initial heading which is due West together with an initial equatorial position results in an increase in the peak temperature of about $100F^{\circ}$ above the standard peak temperature. Almost exactly the same result occurred in the case of a circular, but rotating Earth. Also, the decrease of $100F^{\circ}$ due to an initial Easterly heading is again present.

In addition, the expected increase in the peak temperature also occurs when the effective initial glide angle is larger than normal although in the rotating Earth environment the increase is relatively small. The worst situation studied occurred for an initial latitude of 60 degrees South with an initial heading of due North; for this case, the rise was only a modest $100F^{\circ}$ over all but the extreme down range portion of the footprint for which a rise of $200F^{\circ}$ was incurred.

It is conceivable that a higher temperature increase would result if the initial heading and initial latitude combined to produce both a higher than normal effective initial glide angle together with a higher than normal effective initial speed. However, in order to produce the former, almost due North initial headings are required while the latter requires almost due West values. The latitude must also be large if the former is to be significant, which in turn reduces the latter. Therefore, it is deemed quite unlikely that peak temperature will be more than $100F^{\circ}$ above the standard peak during reentries for which the inertial initial conditions are a speed of 26,000 feet per second and a flight path angle of 1.0 degrees. Finally, even if the effective initial glide angle is greater than 1.0 degrees and increases in the peak temperature higher than $100F^{\circ}$ occur, it would be possible to compensate for this in advance of the reentry by the appropriate adjustment in the retro-fire attitude alignment and velocity increment.

With regard to the shape and position of the footprint, the combined effects of rotation and oblateness upon both the down range and the cross range do produce a situation which is difficult to analyze. However, the results may be considerably simplified with the aid of Figs. 31 and 32 and the analysis which applies to each. Very broadly speaking, the two effects seem to combine in an almost linear fashion and produce the range distortions associated with shape oblateness together with the cross range shift due to rotation. For example, the rotational case used in Sec. 7.2 in which the vehicle is initially heading due North from the equator results in the identical cross range shift of 10.8 degrees of equivalent latitude at 180 degrees of equivalent longitude down range; in addition, this same case now manages to have an extended footprint with almost the same maximum down range as the oblate shape case. Continuing with this same footprint, the cross range shift at 360 degrees of equivalent longitude down range is 21.4 degrees as compared to 21.7 degrees for the circular orbit in vacuum which goes through the initial position. The above results are illustrated in Fig. 33a. Many more examples (there were 40 pairs of point to choose from as well as the general outline of each footprint) far too numerous to mention bear out the conclusions that the effects of rotation and oblateness combine with very little interaction.

In conclusion, it should be noted that the effects of both rotation and shape oblateness upon the shape and size of the footprint are large. The effect of gravitational oblateness is usually negligible and is so completely masked by shape oblateness that it is never significant. With regard to shape oblateness, the primary effect is to change the down range position and span of the footprint without producing any major change in the cross range. On the other hand, rotation produces a dramatic cross range shift without any major effect upon the down range. However, the cross range shift due to rotation is accurately predicted by the vacuum orbital track over the Earth's surface of an object which passes through the initial position of the vehicle. It must have the same azimuth and also possess the correct speed (the glide angle should be zero) relative to the Earth's surface to place the object in a circular orbit. Consequently, although the cross range shift is quite large and cannot be ignored if accurate navigation is to be achieved, the guidance system will be able to predict the extent of the shift as a function of the down range.

VIII. RESULTS AND DISCUSSION - DENSITY PERTURBATIONS

8.1 Introduction

As noted in Sec. 4.6, there is very little data available on spatial density variations in the Earth's atmosphere. As a result, several different types of variations were proposed and calculations carried out to determine if they caused any degradation in the CONTAC system performance. Each sub-section gives a detailed account of the extent of the variation for which the CONTAC system could correct, so that its limitations are established.

8.2 Effect of Different Basic Models

An attempt was made to determine just how small the atmospheric scale height had to be before the CONTAC system would be unable to correct for larger than normal density gradients. The details of the density versus altitude relationship are shown in Fig. 34. Scale heights between 14,000 feet and 26,000 feet were used during the initial portion of the reentry. It can be

seen that the increase in density at 230,000 feet due to the use of the smallest scale height produced a density increase of about 250% which is an extreme value in view of the available data (Ref. 33).

The results were very satisfactory. The use of the CONTAC system resulted in no increase in the peak temperature larger than 10°F above the standard peak value and the range results were within 2% of the values found when using the U.S. Standard Atmosphere, 1962. The 1959 ARDC Standard Atmosphere was also used. Again, as expected, there was no effect noted.

8.3 Effect of Altitude-Dependent Perturbations in the Density

In order to simulate variations dependent upon the altitude, information found in Ref. 32 was adopted. The resemblance to a sine wave suggested the curve shown in Fig. 35. The variations are all about the U.S. Standard Atmosphere, 1962. After the reentry was calculated for this shape, a number of others were investigated. The wave length was varied from 25,000 feet to 100,000 feet. The amplitude was increased to give a fractional variation of ± 0.2 and the nodal point was shifted to test the sensitivity to all phase relationships.

The most severe case used a wave length of 25,000 feet and an amplitude of 0.2 for the fractional variation. The above values together with a scale height of 18,000 feet for parts of the U.S. Standard Atmosphere, 1962 yield a density increase of 45% in an altitude range of 4,250 feet in the region one-half of a wave length from the nodal point. Since Ref. 32 indicates that the "density may vary by as much as 50 percent when descending through an altitude increment of 4,250 feet" and that this is the maximum increase to be expected, it was felt that further calculations were not necessary.

Again, the results were completely satisfactory in that the CONTAC system was able to maintain control of the temperature. The down range, however, did vary by as much as 5% from the values obtained by using the U.S. Standard Atmosphere, 1962.

8.4 Effect of Random Density Perturbations

The simulation of random spatial density variations presented an unavoidable difficulty. Data is not available from which to set up a realistic model of the variations which might be expected. A little information combined with intuitive judgements was used to postulate a random variability model based upon the distance travelled by the spacecraft during the reentry. The detailed description of the model is given in Sec. 2.6.

The results may best be described by reference to Fig. 36. The combination of variance and correlation interval above the hatched zone usually resulted in situations with which the CONTAC system could not cope. Increases in the peak temperature of about 300°F usually resulted for variances which were 0.05 to 0.1 greater than the variance shown acceptable for a given correlation interval. For combinations in the hatched zone, the peak temperature was usually less than 25°F greater than the standard peak value; however, in isolated examples, an increase of between 50°F and 100°F was experienced. For variances which were 0.05 to 0.1 less than the variance immediately under the hatched region, the peak temperature was always equal to the standard peak value.

An exhaustive study could not be made due to the statistical nature of the problem. A complete set of results would have required over a thousand individual runs, each requiring up to three or four minutes of computer time.

A large number of runs is needed because a probability analysis is required. For each combination of variance and correlation interval, a number of different random density distributions would have to be used, and a graph deduced of the probability of exceeding a given temperature for that combination. Repeating for a number of variance-correlation pairs would provide the data for a Figure like 36, in which the hatched area would be bounded by curves of constant probability of exceeding a set temperature, e.g., 1% and 10% probability of exceeding a 300F° rise. In order to have a reasonable degree of confidence in the results, a great many individual runs must be made for each pair of values for the variance and correlation interval. Since certain results would occur infrequently, the suggested figure for the number of runs in each set is one hundred. It seems likely that at least ten pairs or sets would be required. For the graph presented, about 2½ hours of time was used to make about 50 individual runs for 7 pairs of values for the variance and correlation interval.

One additional factor of importance must be noted. In addition to the radiation-equilibrium temperature, the actual temperature based on Eq. (3.6) was calculated for the nose stagnation point. In general, the equilibrium temperature is held at a constant value by the CONTAC system for a lengthy period. For this situation, the difference between the real peak temperature (in which the skin possesses some heat capacity) and the equilibrium peak temperature is usually less than 5F°. For this reason, the real peak temperature has heretofore been ignored. However, when random spatial density variations were encountered which had a correlation interval less than 200 miles (and especially when this distance was less than 100 miles - at 20,000 feet/sec, 100 miles are traversed in only 26 seconds), there was often a large difference between the two peak values. In one instance when the equilibrium peak temperature was about 300F° greater than the standard value, a heat capacity of 2.0 BTU/ft² (which might be provided by a 0.03 inch thick skin of Molybdenum weighing 1.6 lb/ft²) reduced the excess temperature by 20% to about 240F°. Only a few of the 50 runs provided a situation for which this result could occur. Consequently, no definitive conclusions could be drawn. But it will certainly be very fruitful to determine the extent to which even a limited heat capacity for the vehicle's skin can reduce excess peak temperatures caused by random spatial density variations in the Earth's atmosphere.

IX. CONCLUSIONS

9.1 Validity of the CONTAC System Concept

The results of this investigation indicate that the CONTAC system which has been proposed is a highly effective method for reducing the peak temperature experienced during the reentry of a manned, lifting spacecraft. The maximum temperature which a vehicle experiences during a fixed attitude reentry is lowest for an equilibrium glide. This maximum is taken as the standard peak value. The CONTAC system prevents the actual peak temperature experienced during the reentry from exceeding that value as long as the initial conditions are not such as to produce a value for the first temperature maximum

that is higher than the peak value for the equilibrium glide. In addition, if the first peak temperature is higher, then the CONTAC system is able to prevent all subsequent peaks from exceeding the first.

With regard to range control, the CONTAC system is intended for use with any type of guidance scheme which uses closed loop control. The available down range increment for the vehicle in this study (which is similar to the M2-F2 now currently under investigation) is in excess of 100 degrees of equivalent longitude. The combined cross range for turns both to the left and to the right is greater than 20 degrees of equivalent latitude throughout all of the above value for down range. Within these limits, the footprint is essentially isothermal, i.e. the temperature experienced during the reentry is the same regardless of the terminal position of the vehicle within the footprint.

9.2 Effects of Adverse Conditions on the Reentry

The performance of the CONTAC system has been investigated under several types of adverse conditions. The first type is errors in the initial values of speed and glide angle. The second consists of those effects which can be predicted in advance, such as the Earth's rotation and oblateness. The third type consists of variations from standard values of the atmospheric density which are both altitude dependent and random.

Large errors in the initial speed and glide angle are considered unlikely since they can be produced only by extremely large retro-fire errors. (Past experience shows that retro-fire errors can be kept quite small.) At the deboost position, attitude alignment must be in error by about 5 degrees or the velocity increment must be in error by about 50 fps before any significant changes in the initial speed and glide angle are noted at the reentry altitude of 350,000 feet. However, if large retro-fire errors are present, the following results are noted. Negative errors in the initial speed up to 100 feet per second (larger errors are improbable) could cause an increase in the peak temperature up to 100 F°. However, an increase in the initial glide angle of 0.5 degrees causes an increase of 300 F° in the peak temperature.

The Earth's rotation causes a maximum increase of about 100 F° in the peak temperature when the Earth's rotation and the initial heading combine to produce an effective initial speed 1500 feet per second above the standard value of 26,000 feet per second. When the Earth's oblateness and the initial heading and latitude combine to produce an effective initial glide angle of 0.18 degrees greater than the standard value of 1.0 degree, the maximum increase in the peak temperature is again about 100 F°. However, the rotational condition is unlikely to occur in practice since satellite orbits are usually in the same sense as the Earth's rotation, and the oblateness effect may be compensated for in advance of the reentry by an appropriate adjustment of the retro-fire attitude alignment and velocity increment.

Atmospheric density perturbations based on altitude did not, within reasonable limits, produce any situations for which the CONTAC system could not correct. The maximum likely vertical density gradients had no effect on the CONTAC system performance. On the other hand, random spatial (roughly horizontal) density variations produced a very different result. The investigation described a basis for judging the adequacy of the CONTAC system when sufficient information about random density variations in the Earth's atmosphere become available. Insufficient data could be found for the altitudes of concern, namely between 220,000 feet to 290,000 feet, in order to arrive at a firm conclusion at this time.

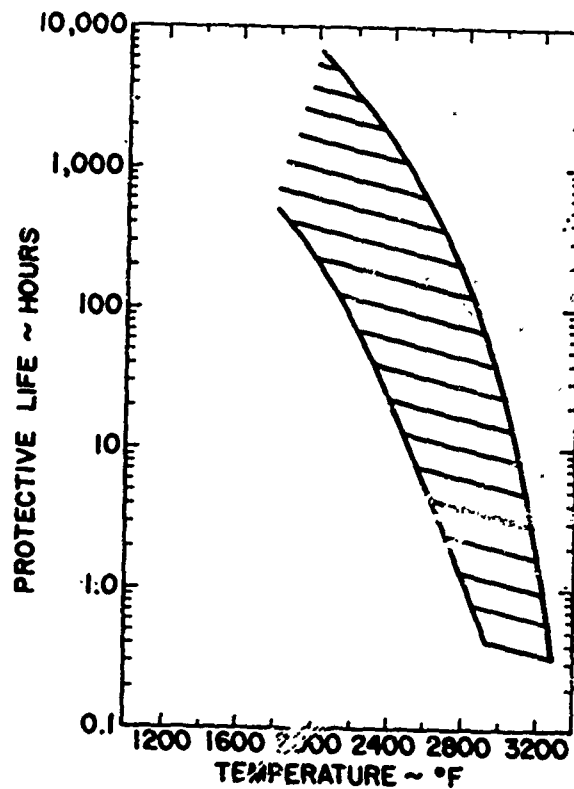
REFERENCES

1. Wingrove, R.C. A Survey of Atmospheric Reentry Guidance and Control Methods, IAS 31st Annual Meeting, January 21-23, 1963, New York, N.Y., IAS Paper No. 63-86.
2. Bryson, A.E.
Denham, W.F.
Carrol, F.J.
Mikami, Kinya Determination of Lift or Drag Programs to Minimize Re-Entry Heating, Journal of the Aerospace Sciences, Vol. 29, No. 4, April, 1962.
3. Levinsky, E. S. Application of Inequality Constraints to Variational Problems of Lifting Re-Entry, IAS 29th Annual Meeting, January 23 - 25, 1961, New York, New York, IAS Paper No. 61-21.
4. Stalony-Dobrzanski, J. Re-Entry Guidance and Control Using Temperature Rate Flight Control System, AIAA 2nd Aerospace Sciences Meeting, January 25-27, 1965, New York, N.Y., AIAA Paper No. 65-47.
5. Collins, R. R.
Dotts, H.W.
Hoyler, W.F.
Hecht, K.F. Guidance, Control, and Propulsion Systems, Gemini Mid-program Conference Including Experimental Results, February 23-25, 1966, Manned Spacecraft Center, Houston, Texas, NASA SP-121.
6. Wagner, W.E. Roll Modulation for Maximum Re-Entry Lateral Range, Journal of Spacecraft, Vol. 2, No. 5, September-October 1965.
7. Smith, R.H.
Menard, J.A. Supercircular Entry and Recovery with Maneuverable Manned Vehicles, National IAS, ARS Joint Meeting, June 13-16, 1961, Los Angeles, California, IAS Paper No. 61-114-1808.
8. Gaines, L.M.
Surber, T.E. Prediction of Optimum Approach and Landing Techniques for Manned Re-Entry Gliders, National IAS, ARS Joint Meeting, June 13-16, 1961, Los Angeles, Calif. IAS Paper, No. 61-114-1809.
9. Thompson, M.O.
Weil, J.
Holleman, E.C. An Assessment of Lifting Reentry Flight Control Requirements during Abort, Terminal Glide, and Approach and Landing Situations, AGARD Specialists' Meeting on Stability and Control, Sept. 20-23, 1966, Cambridge, England.
10. Etkin, B. Longitudinal Dynamics of a Lifting Vehicle in a Circular Orbit, UTIAS Report No. 65, AFOSR TN 65-191, Feb. 1960.
11. Drummond, A.M. Performance and Stability of Hypervelocity Aircraft on a Minor Circle, UTIAS Report to be published.

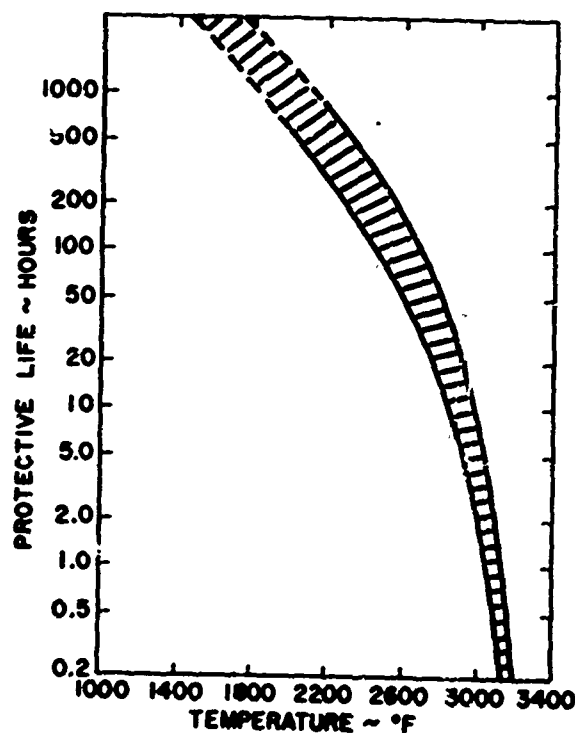
12. Technology Week Including Missiles and Rockets, American Aviation Publications, Inc., Vol. 19, No. 20, July 25, 1966.
13. Geiger, R.E. Experimental Lift and Drag of a Series of Glide Configurations at Mach Numbers 12.4 and 17.5, IAS National Summer Meeting, June 28-July 1, 1960, Los Angeles, California, IAS Paper No. 60-92.
14. Felterman, D.E.
Neal, L, Jr. An Analysis of the Delta-Wing Hypersonic Stability and Control Behaviour at Angles of Attack Between 30° and 90° , NASA TN D-1602, March 1963.
15. Wells, W.R.
Armstrong, W.O. Tables of Aerodynamic Coefficients Obtained from Developed Newtonian Expressions for Complete and Partial Conic and Spheric Bodies at Combined Angles of Attack and Sideslip with Some Comparisons with Hypersonic Experimental Data, NASA TR R-127, 1962.
16. Smith, R.H.
Menard, J.A. Supercircular Entry and Recovery with Maneuverable Manned Space Vehicles, IAS-ARS Joint Meeting, June 13-16, 1961, Los Angeles, Calif., IAS Paper No. 61-114-1808.
17. Chapman, D.R. An Analysis of the Corridor and Guidance Requirements for Supercircular Entry into Planetary Atmospheres, NASA TR R-55, 1960.
18. Mugler, J.P. Jr.
Olstad, W.B. Static Longitudinal Aerodynamic Characteristics at Transonic Speeds of a Blunted Right Triangular Pyramidal Lifting Reentry Configuration for Angles of Attack up to 110° , NASA TN D-797, June 1961.
19. Fournier, P.G. Wind-Tunnel Investigation at High Subsonic Speed of the Static Longitudinal Stability Characteristics of a Winged Reentry Vehicle Having a Large Negatively Deflected Flap-Type Control Surface, NASA TN D-2030, October, 1963.
20. Ware, G. M. Low-Subsonic-Speed Static Stability of Right-Triangular-Pyramid and Half-Cone Lifting Reentry Configurations, NASA TN D-646, February 1961.
21. Crabtree, L.F.
Donnett, R.L.
Woodley, J.G. Estimation of Heat Transfer to Flat Plates, Cones and Blunt Bodies, Royal Aircraft Establishment Technical Report No. 65137, July 1965.
22. Leo Rute A Study of Aerodynamic Effects of Isothermal and Temperature Gradient Atmospheres on Reentry Trajectories, Polytechnic Institute of Brooklyn Department of Aerospace Engineering and Applied Mechanics, PIBAL Report No. 738, March 1962.
23. Parvin, R.H. The Earth and Inertial Space, Part I - Motions of the Earth, Aerospace Engineering, Vol. 18, No. 4, April 1959.

24. Kozai, Yoshihide Numerical Results on the Gravitational Potential of the Earth from Orbits, Proceedings of the First International Symposium on the Use of Artificial Satellites for Geodesy, April 26 - 28, 1962, Washington, D.C.
25. Kaula, W.M. Tesseral Harmonics of the Gravitational Field and Geodetic Datum Shifts Derived from Camera Observations of Satellites, NASA TN D-1848, June 1963.
26. Kaula, W.M. Improved Geodetic Results from Camera Observations of Satellites, Journal of Geophysical Research, Vol. 68, No. 18, Sept. 15, 1963.
27. Wagner, C.A. The Drift of a 24-Hour Equatorial Satellite Due to an Earth Gravity Field Through 4th Order, NASA TN D-2103, February 1964.
28. Wagner, C.A. The Equatorial Ellipticity of the Earth as Seen from Four Months of Syncom II Drift Over the Western Pacific, NASA TN D-3313, July 1966.
29. Wagner, C.A. The Equatorial Ellipticity of the Earth from Two Months of Syncom II Drift Over the Central Pacific, NASA TN D-3315, July 1966.
30. Baker, R.M. Jr. Three-Dimensional Drag Perturbation Technique, ARS Journal, Vol. 30, No. 8, August 1960, AFOSR TN 59-767, July 1, 1959.
31. Staff U.S. Standard Atmosphere, 1962.
32. Cole, A. E.
Kantor, A.J. Horizontal and Vertical Distribution of Atmospheric Density Up to 90 km, Air Force Surveys in Geophysics, No. 157, AFRCRL-64-483, June 1964.
33. Cole, A.E.
Court, A.
Kantor, A.J. Model Atmospheres (Chapter 2, Handbook of Geophysics and Space Environment), Air Force Cambridge Research Laboratories, E.G. Hanscom Field, Bedford, Massachusetts.
34. Etkin, B. Private Communications, 1966.
35. Sommer, S.C.
Short, B.J. Point Return from a Lunar Mission for a Vehicle that Maneuvers Within the Earth's Atmosphere, NASA TN D-1142, November 1961.
36. Nielsen, J.N.
Goodwin, F.K.
Mersam, W.A. Three-Dimensional Orbits of Earth Satellites, Including Effects of Earth Oblateness and Atmospheric Rotation, NASA MEMO 12-4-58A, December 1958.
37. Fine, J.H. Stability of Flight Paths of Lifting Vehicles During Entry into Planetary Atmospheres, UTIAS Technical Note No. 48, July 1961, AFOSR 1488.

38. Brown, R.C.
Brulle, R.V.
Giffin, G.D. Six-Degree-of-Freedom Flight Path Study Generalized
Computer Program, Part I, Problem Formulation, WADD
Technical Report No. 60-781, Part I, May 1961.
39. Etkin, B. Dynamics of Flight, J. Wiley & Sons, Inc., New York,
1959.
40. Etkin, B. Dynamics of Flight, Appendix A-6, - Derivative of a
Vector.



Protective capability of aluminide-base coatings for molybdenum.



Protective capability of the chromium-iron-silicon coating for columbium alloys.

FIGURE 1 ENDURANCE TIME vs TEMPERATURE FOR COATED REFRACTORY METALS
 (From 'Refractory Metals and their Protection', Thomas D. Cooper and Oscar O. Sharp, Aerospace Engineering, Vol. 22, No. 1, January 1963.)

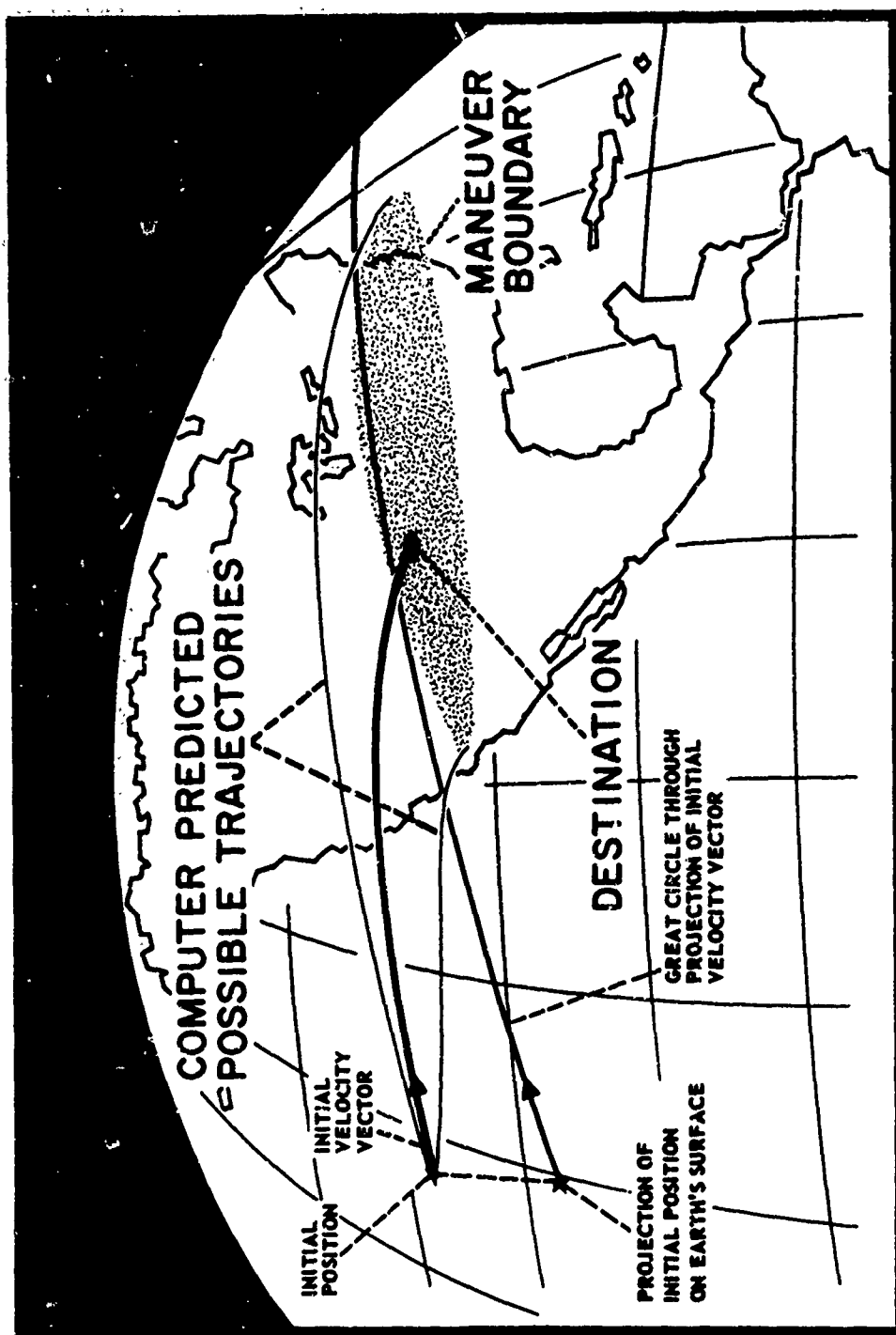
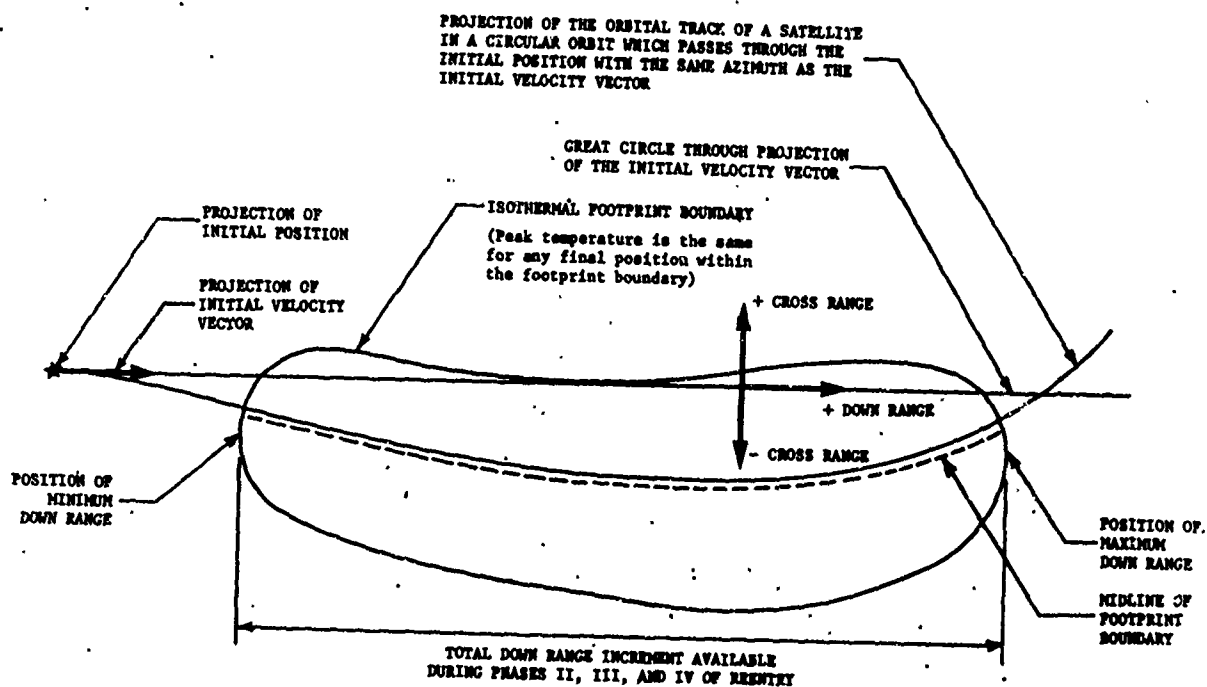


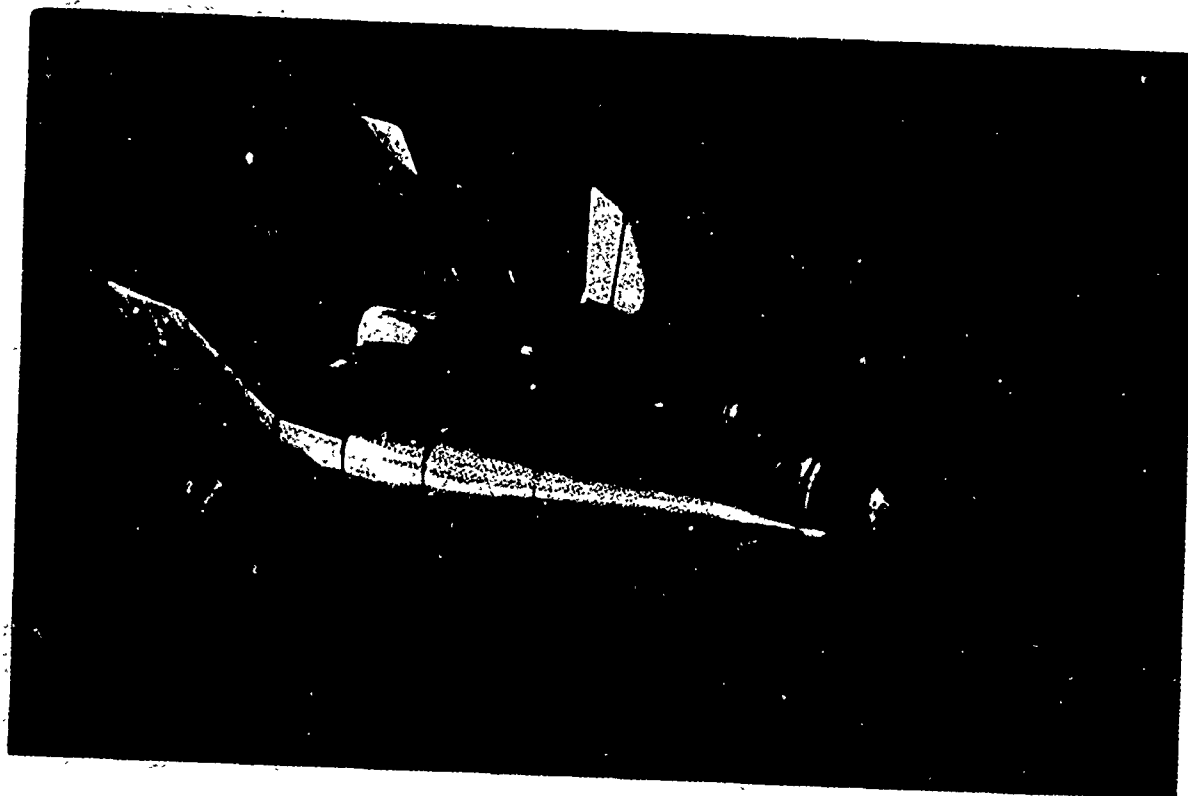
FIGURE 2 TYPICAL MANOEUVRE BOUNDARY OR FOOTPRINT
 (From 'A Survey of Atmospheric Reentry Guidance and Control Methods',
 Rodney C. Wingrove, IAS 31st Annual Meeting, January 21-23, 1963,
 New York, N.Y., IAS Paper No. 63-86.)



NOTES:

1. All positions of down range and cross range are given in degrees of equivalent longitude and latitude, respectively, relative to the great circle through the projection of the initial velocity vector.
2. Down range is always positive. It is in the direction parallel to the great circle.
3. Cross range is measured in the direction perpendicular to the great circle.
4. Conditions on the footprint boundary are as follows:
 - (a) Energy of Vehicle = 250,000 ft lb_f / lb_m
(Nominal Speed = 3,000 ft/sec)
(Nominal Altitude = 100,000 feet)
 - (b) Heading is approximately perpendicular to the footprint boundary (± 20 degrees)

FIGURE 3 FOOTPRINT TERMINOLOGY



HL-10 Artistic Representation
Northrop North, Hawthorne, California
January, 1966

FIGURE 4 TYPICAL VEHICLE CONFIGURATION

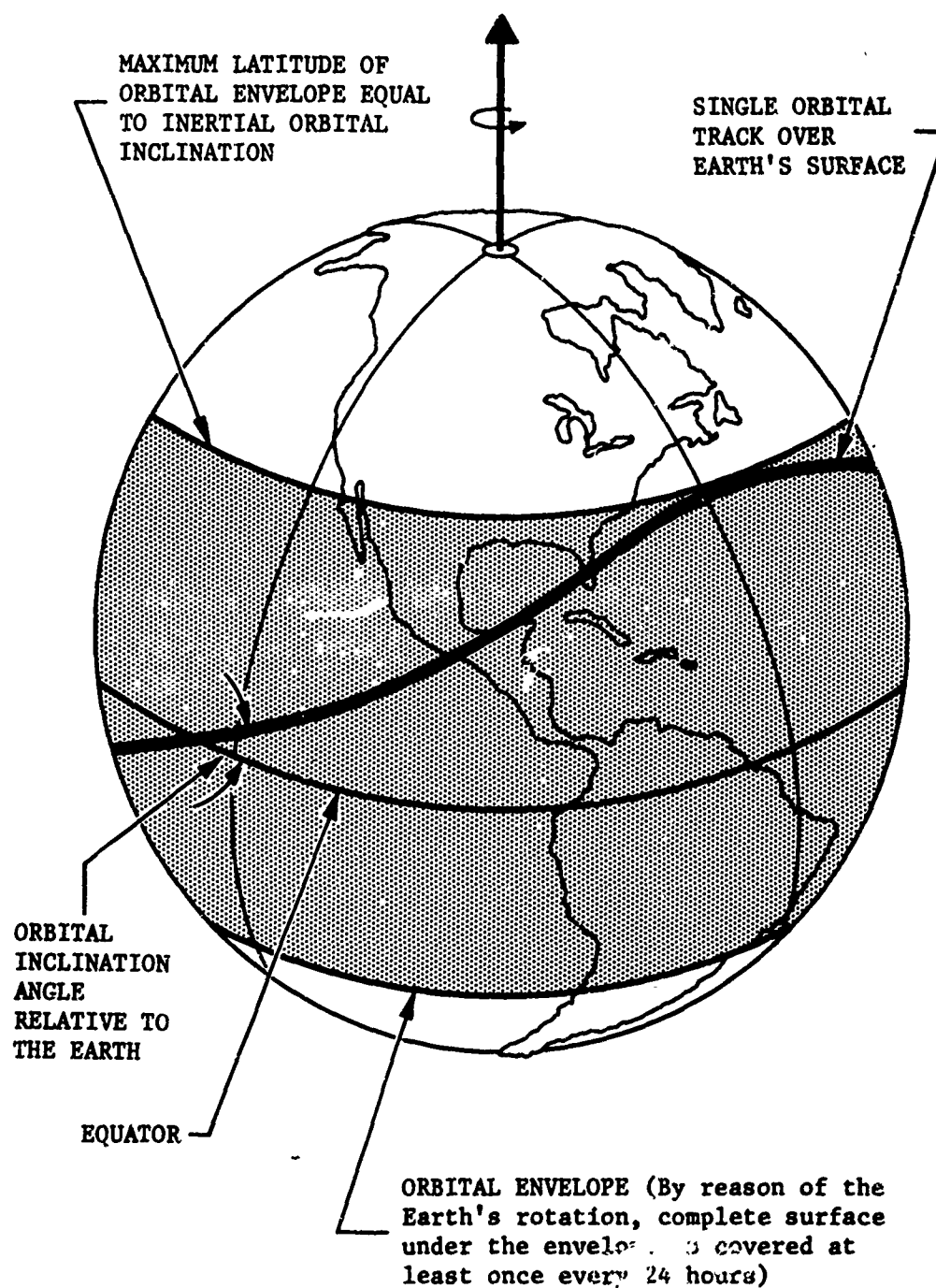


FIGURE 5 ORBITAL ENVELOPE

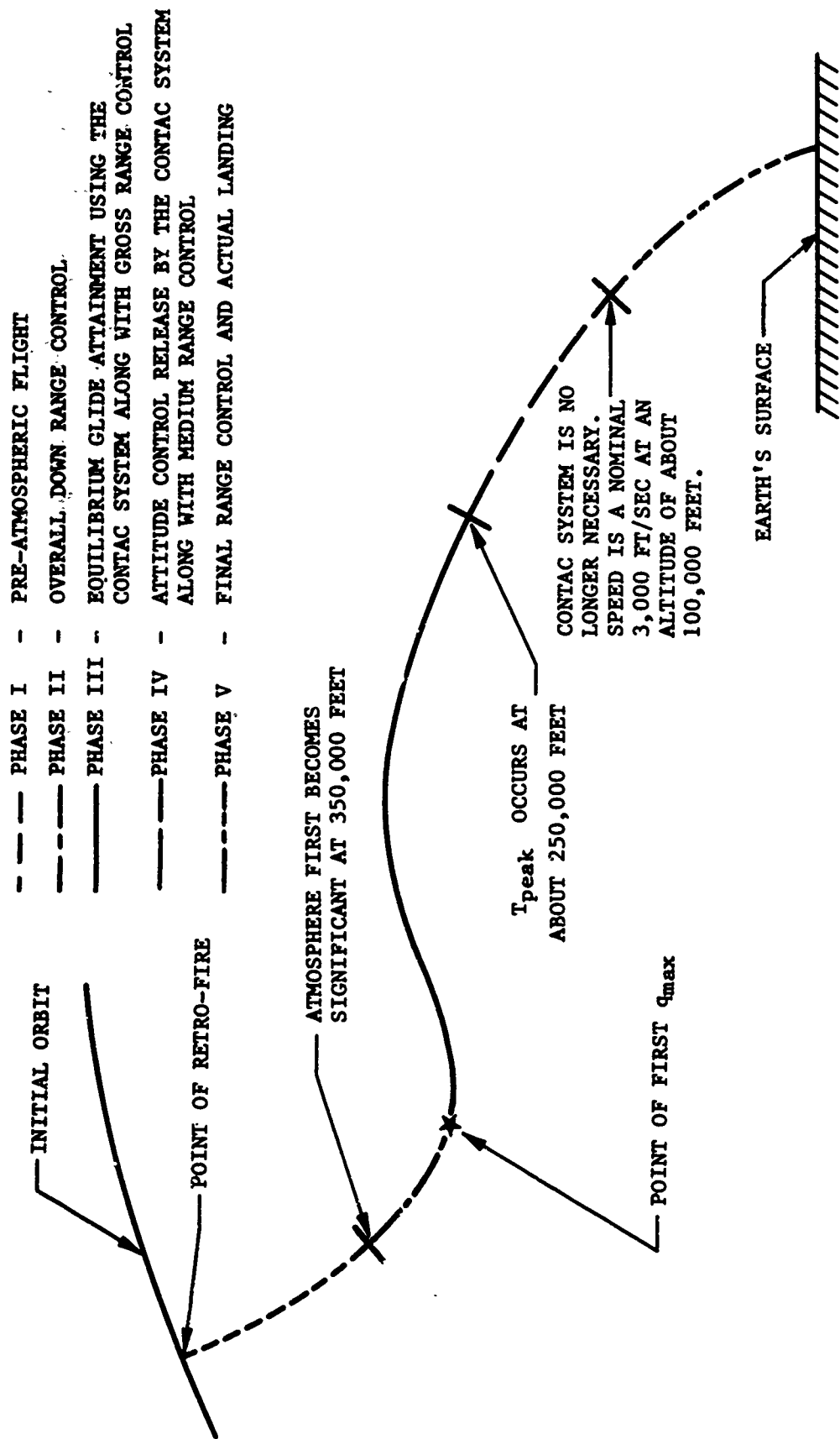


FIGURE 6 THE FIVE REENTRY PHASES
(Not To Scale)

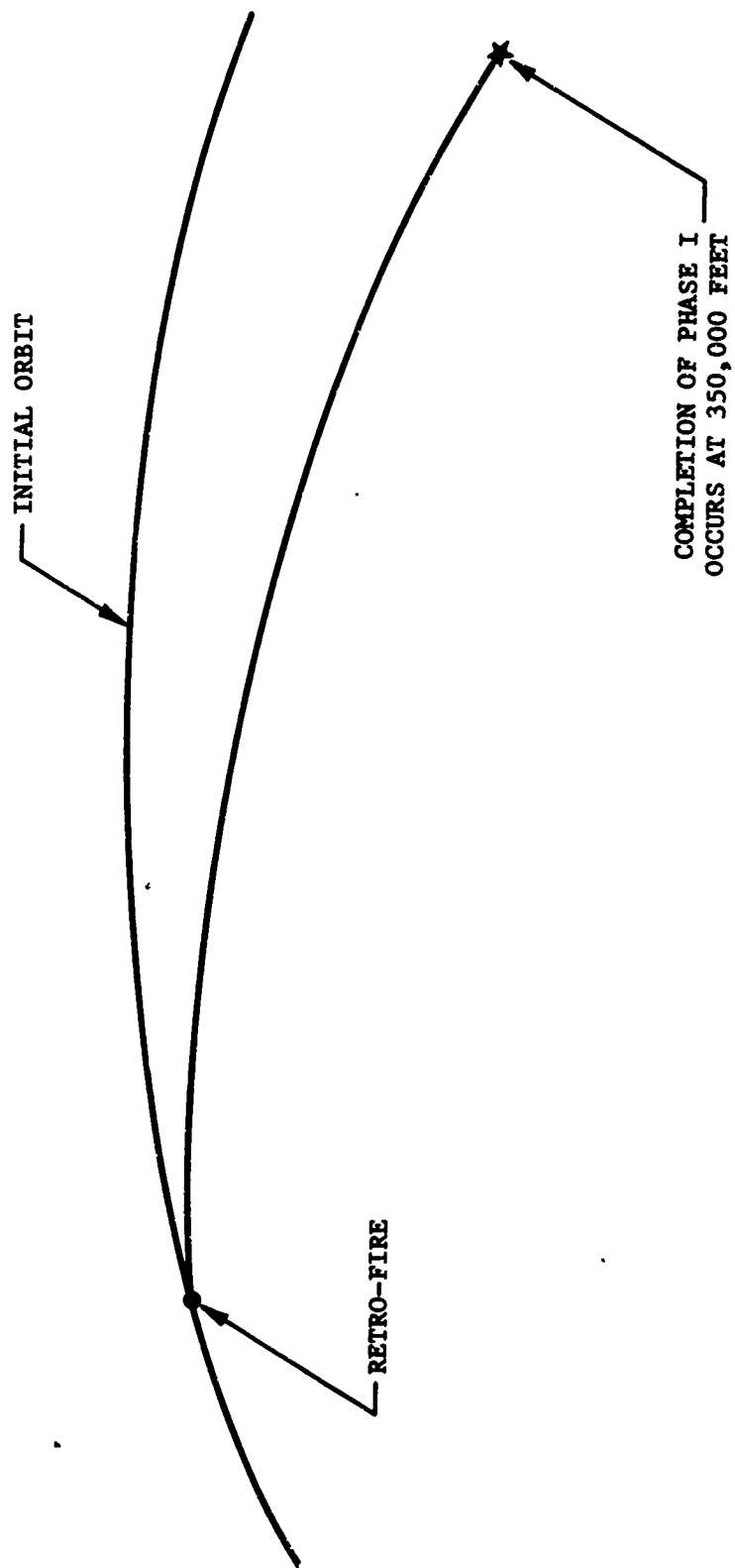


FIGURE 7 PHASE I - PRE-ATMOSPHERIC FLIGHT

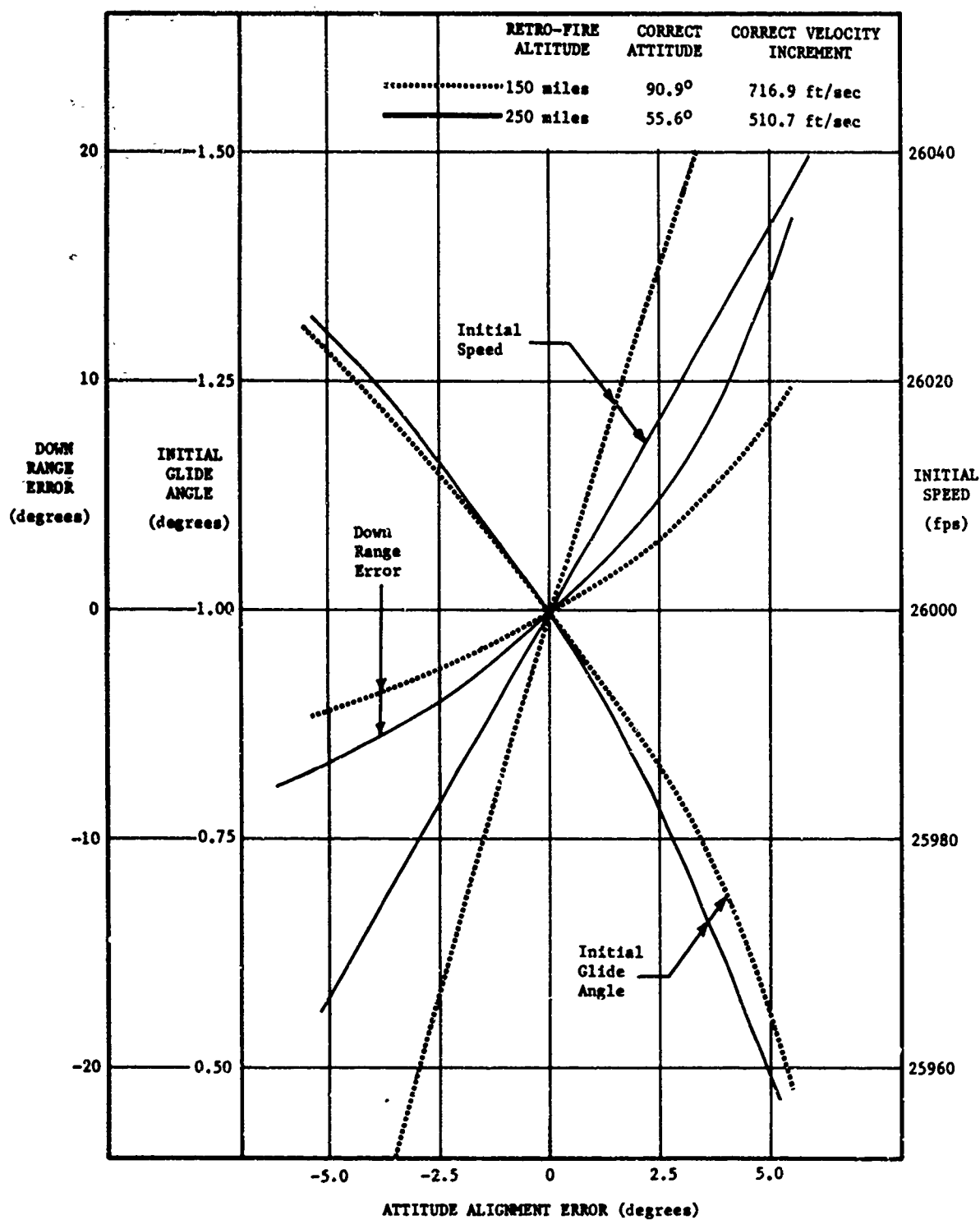


FIGURE 8a INITIAL CONDITIONS AT 350,000 FEET vs RETRO-FIRE ATTITUDE ALIGNMENT ERROR FOR AN INITIALLY CIRCULAR ORBIT

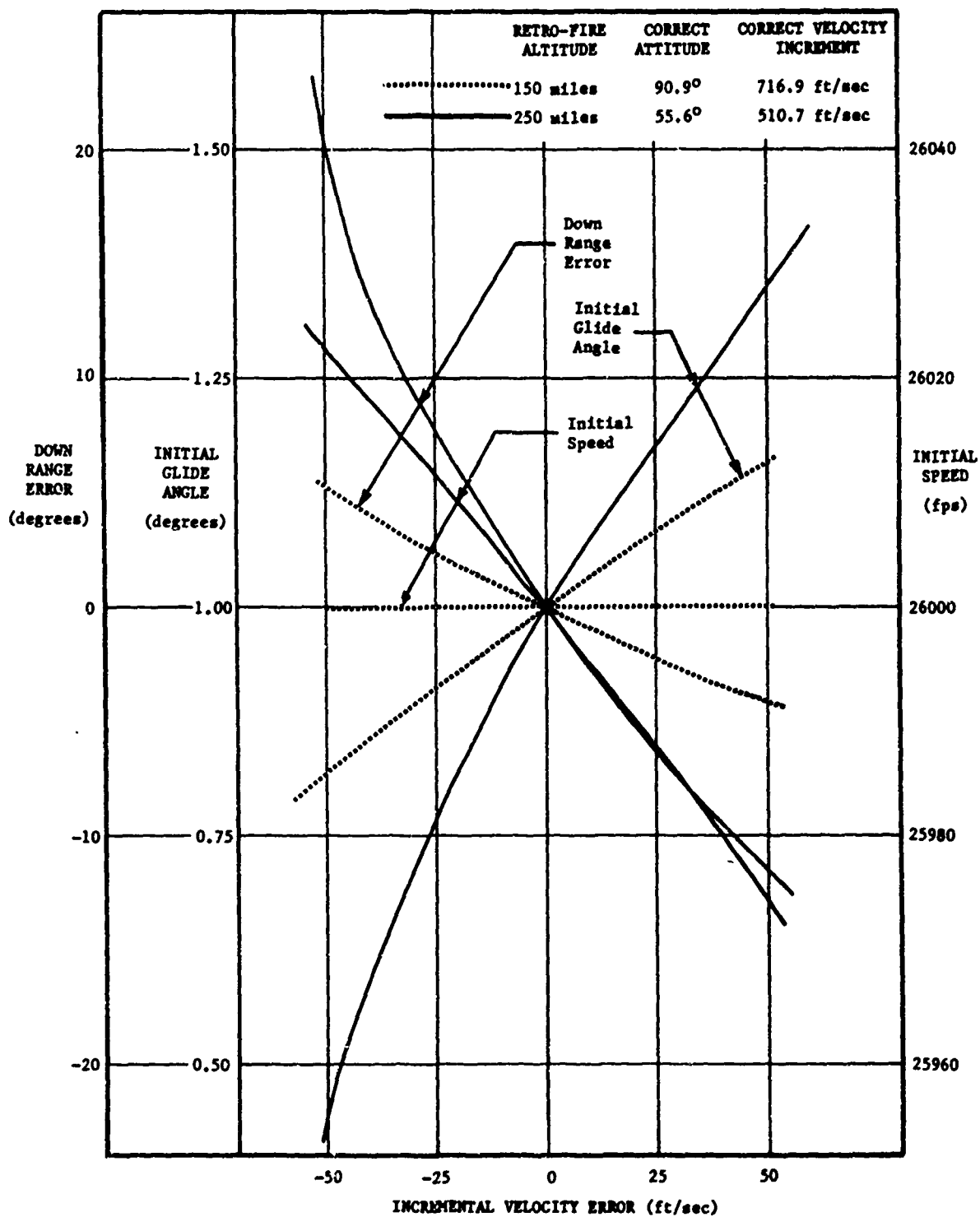


FIGURE 8b INITIAL CONDITIONS AT 350,000 FEET vs RETRO-FIRE INCREMENTAL VELOCITY ERROR FOR AN INITIALLY CIRCULAR ORBIT

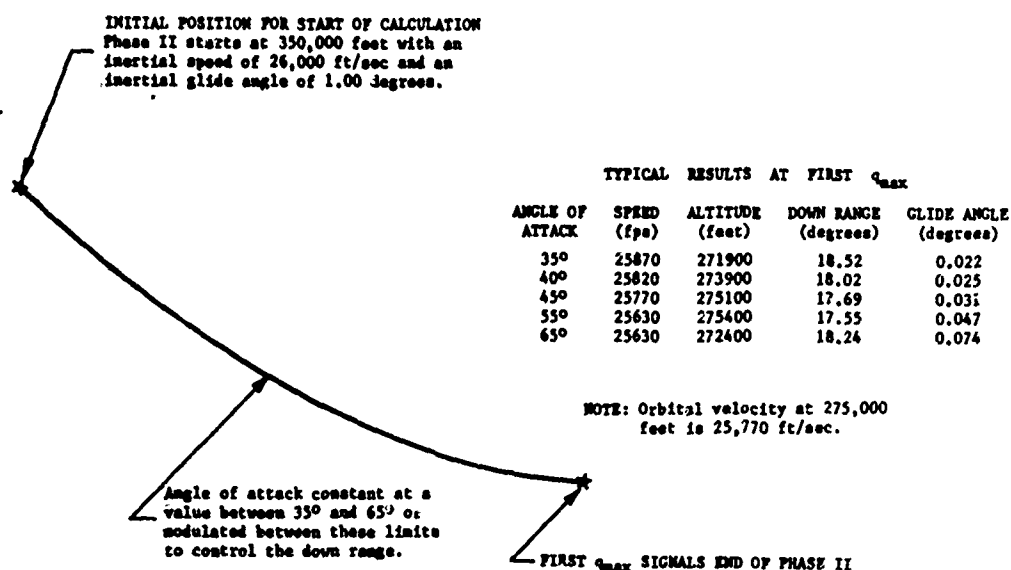


FIGURE 9 PHASE II - OVERALL DOWN RANGE CONTROL

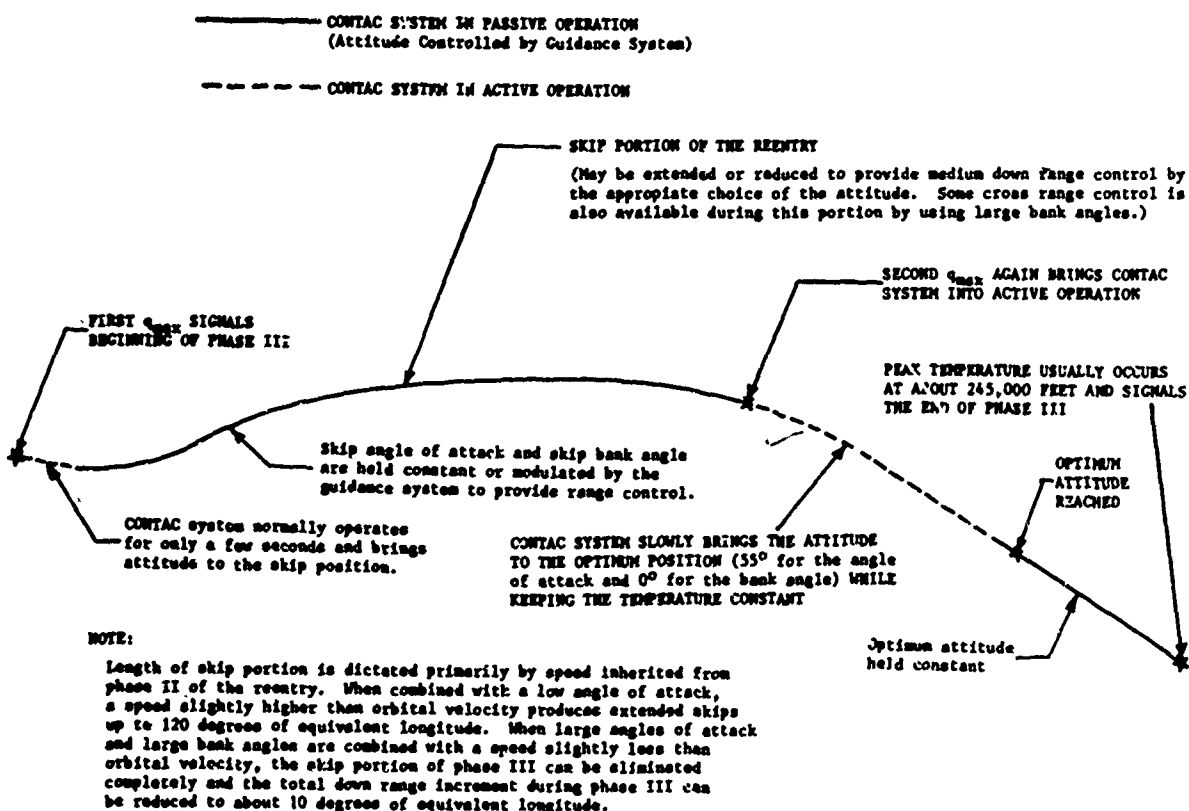


FIGURE 10 PHASE III - EQUILIBRIUM GLIDE ATTAINMENT

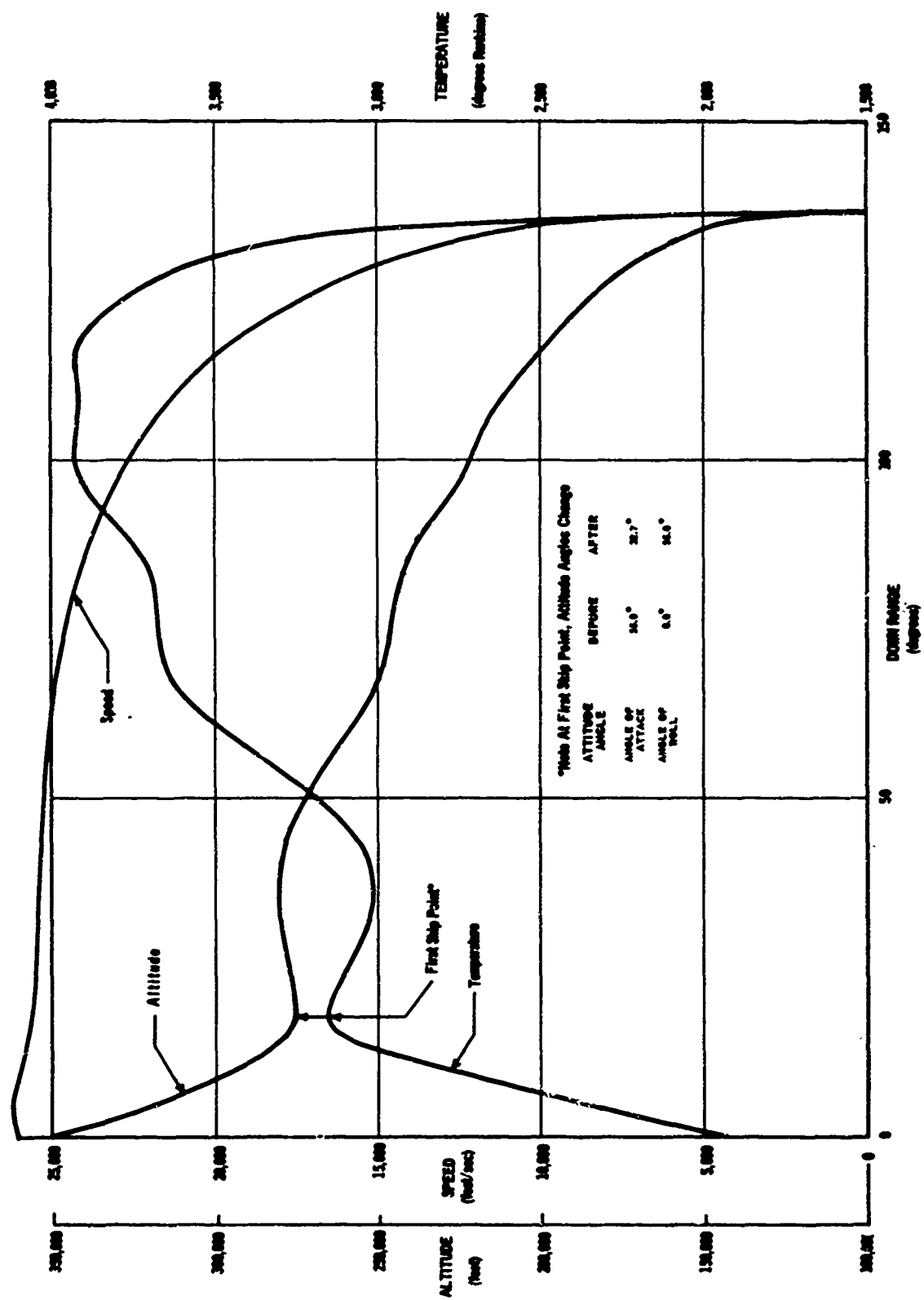


FIGURE 11.3 FLIGHT PARAMETERS FOR AN UNCONTROLLED REENTRY

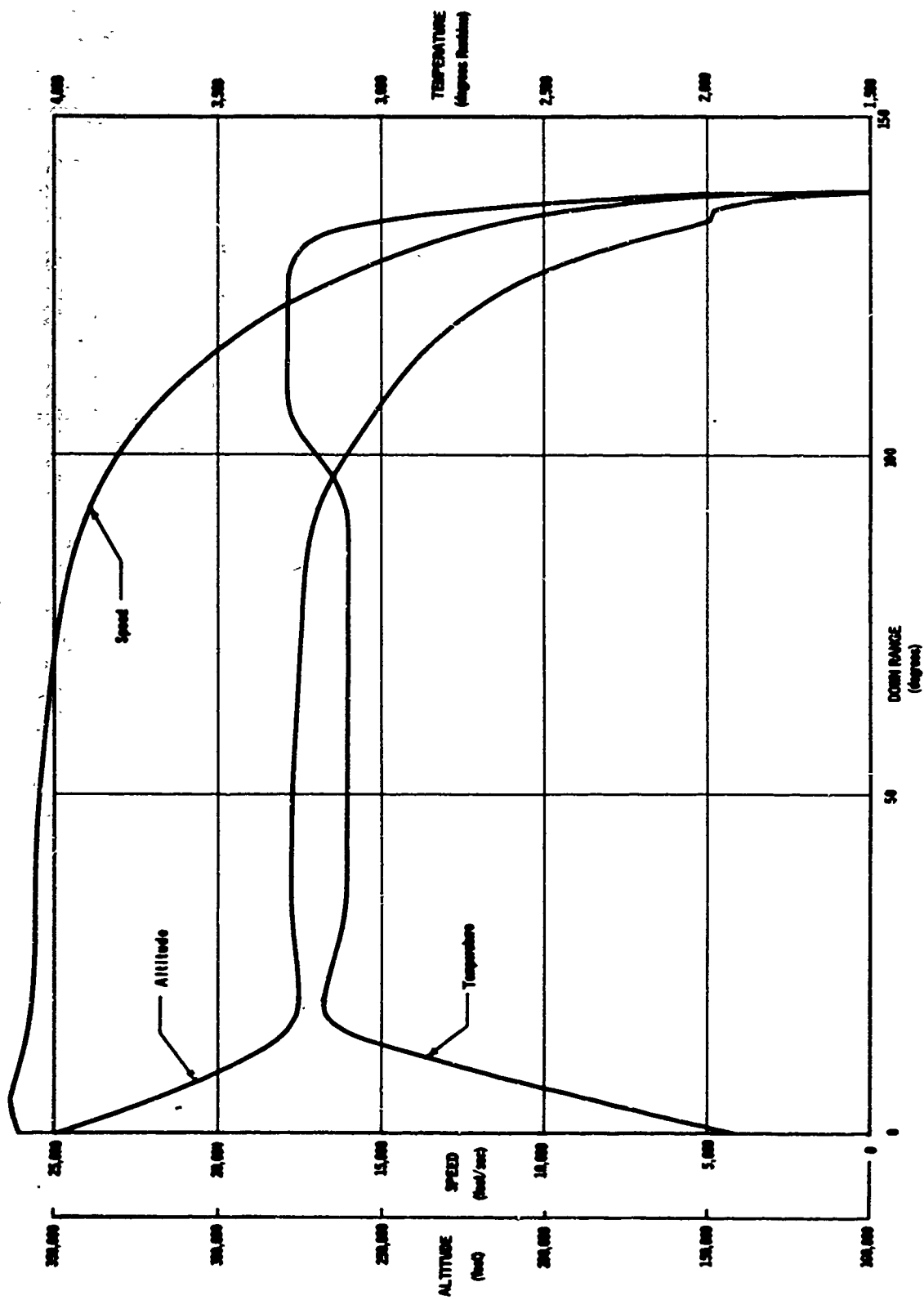


FIGURE 11b FLIGHT PARAMETERS FOR A CONTACT CONTROLLED REENTRY

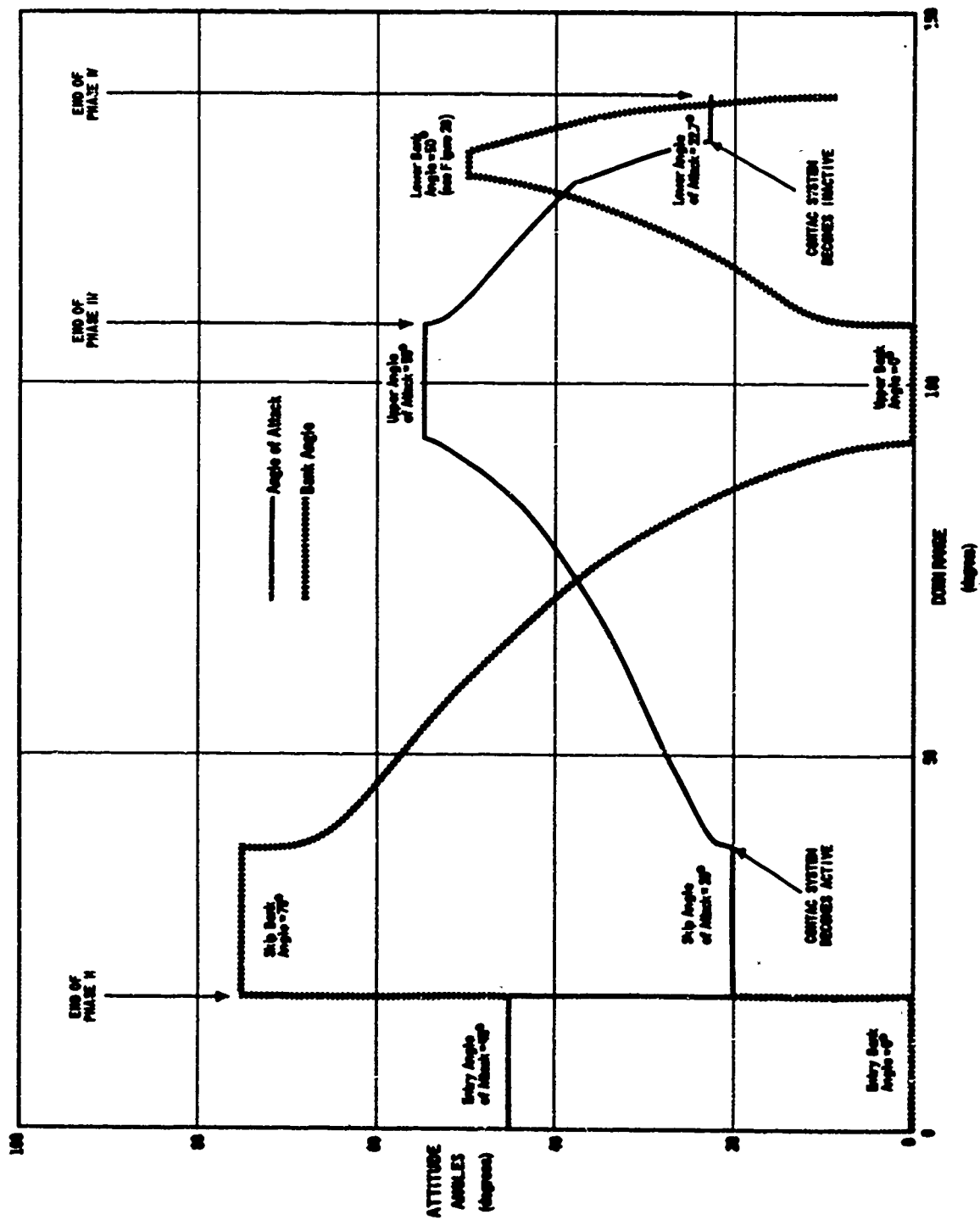


FIGURE 11c HISTORY OF ATTITUDE ANGLES FOR A CONTROLLED REENTRY

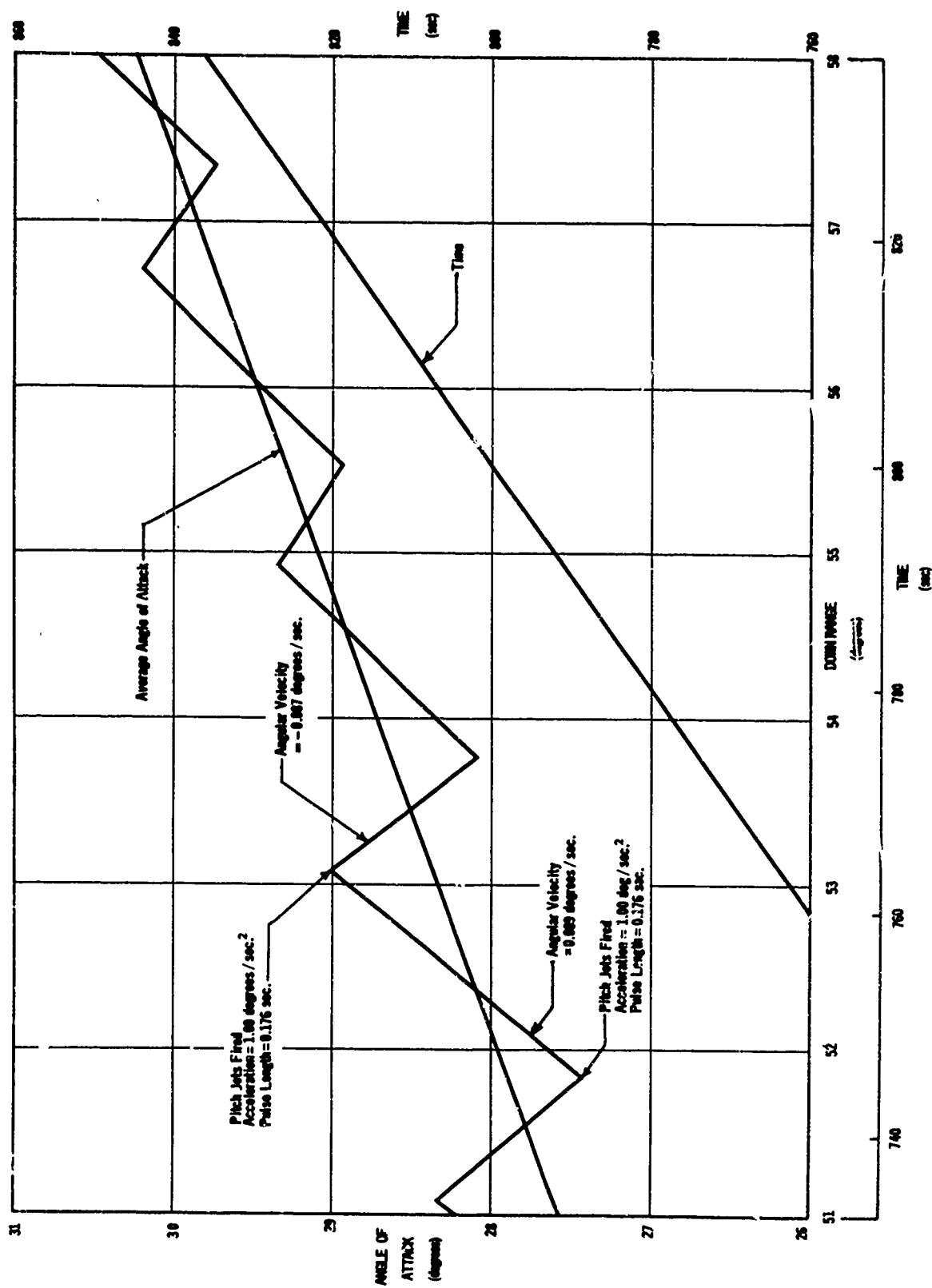


FIGURE 11.4 DETAILED HISTORY OF ANGLE OF ATTACK FOR A PORTION OF A CONTROLLABLE REENTRY

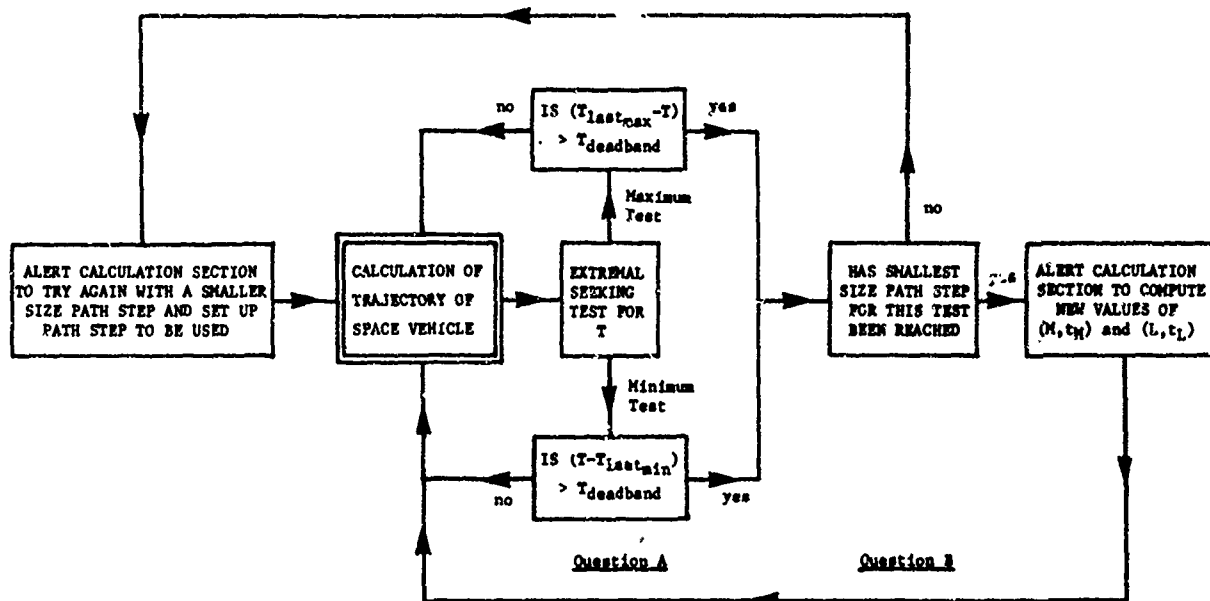


FIGURE 12 CONTAC SYSTEM PROGRAM FLOW DIAGRAM

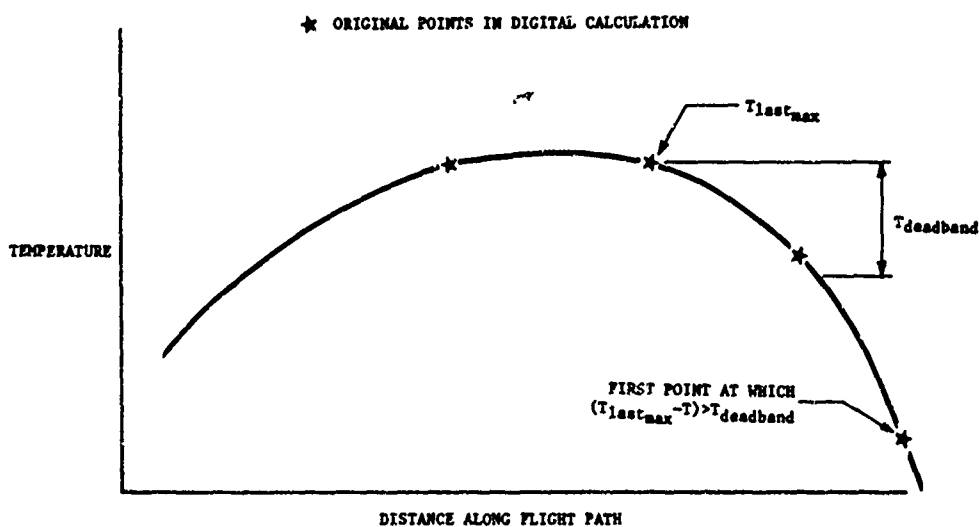


FIGURE 13 TEMPERATURE vs DISTANCE ALONG FLIGHT PATH
DIGITAL POINTS AND $T_{deadband}$ DIFFICULTY

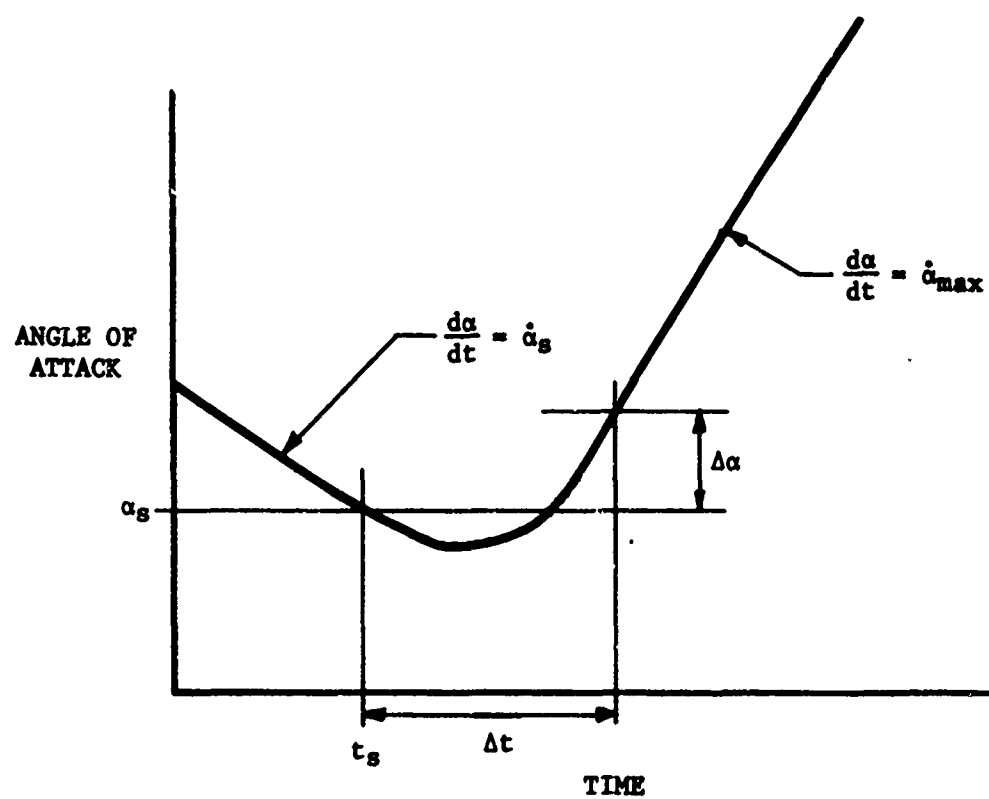


FIGURE 16 CONTAC SYSTEM CONTROL OF THE ANGLE OF ATTACK

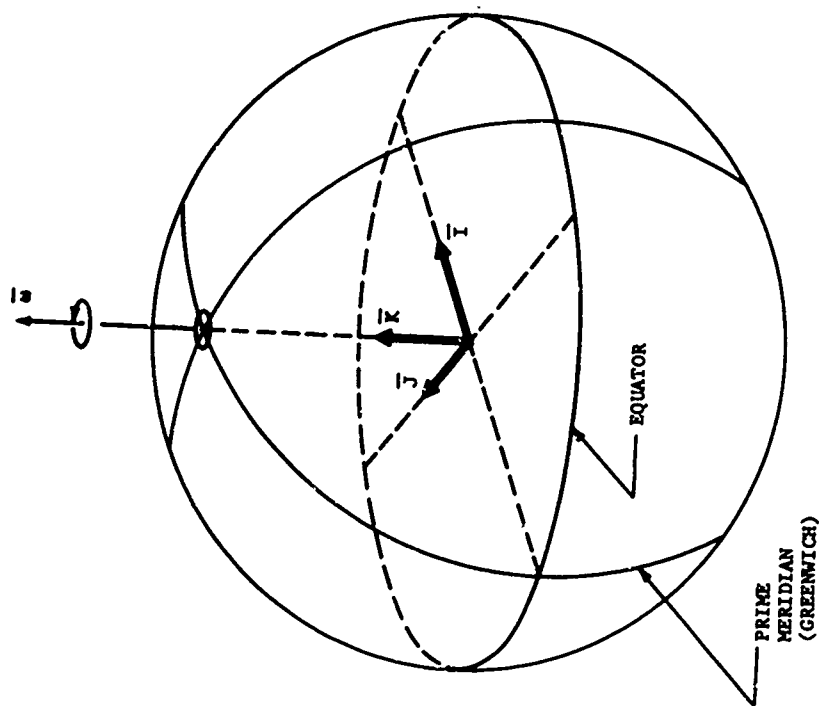


FIGURE 18 BASIC REFERENCE SYSTEM

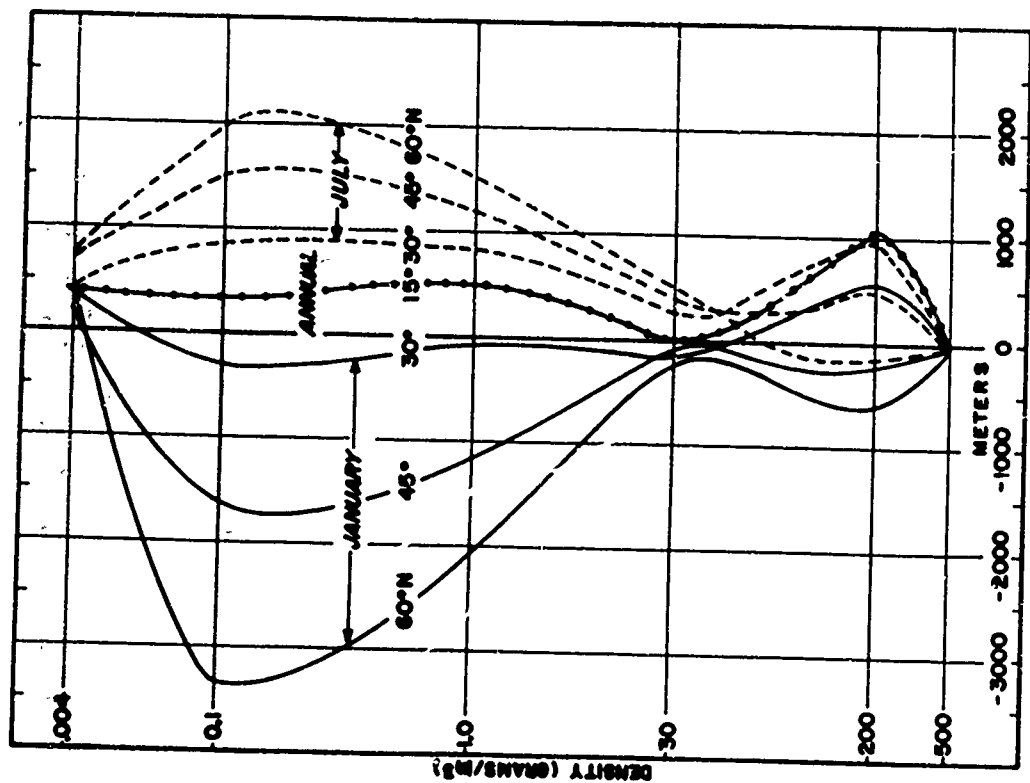


FIGURE 17 DEPARTURES IN THE HEIGHT OF SPECIFIC DENSITY SURFACES FROM U.S. STANDARD ATMOSPHERE, 1962.

(From 'Horizontal and Vertical Distribution of Atmospheric Density up to 50 km', Allen E. Cole and Arthur J. Kantor, Air Force Surveys in Geophysics, No. 157, AFRCL-64-483, June 1964.)

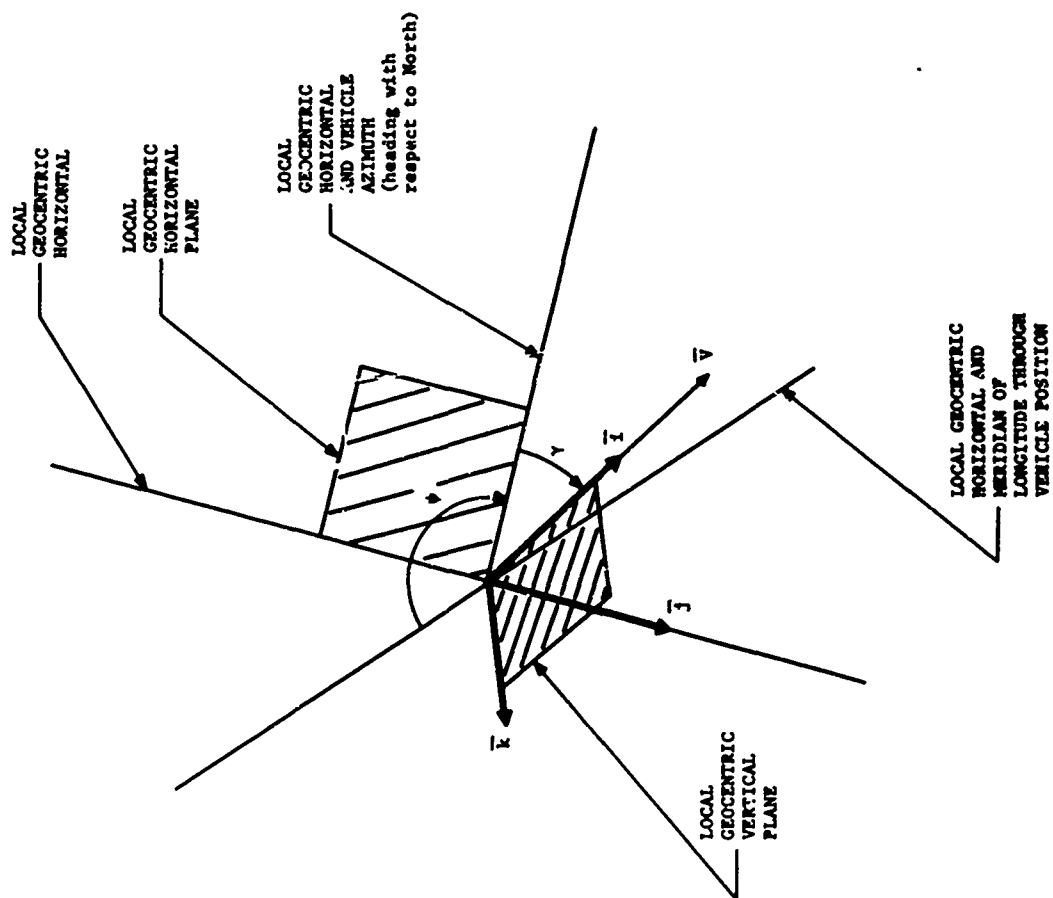


FIGURE 20 FLIGHT AXES COORDINATE REFERENCE SYSTEM

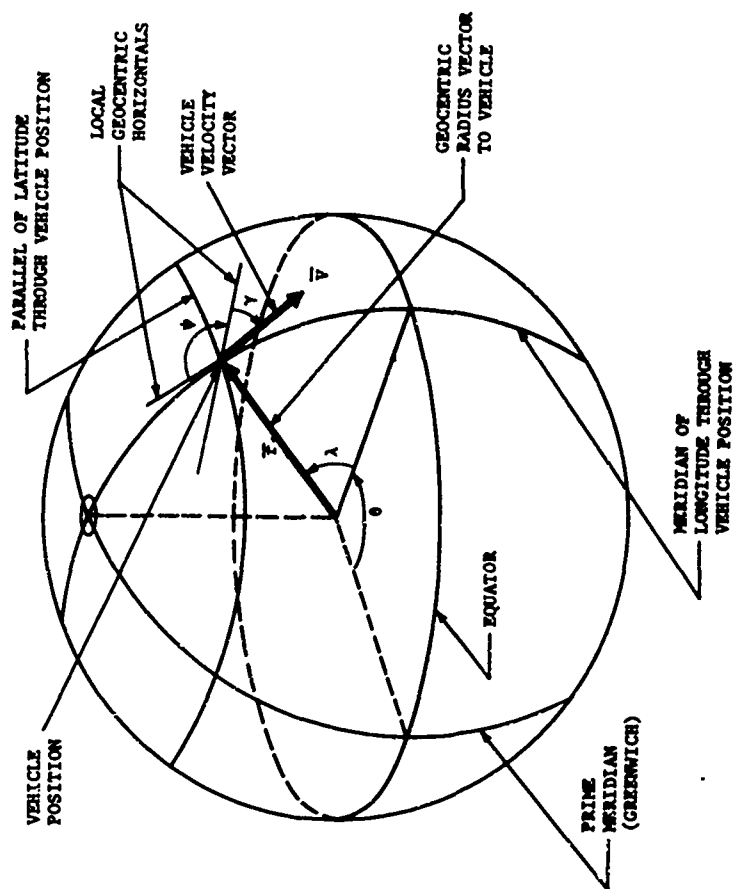


FIGURE 19 GEOCENTRIC COORDINATES FOR POSITION AND VELOCITY

1. $\{\bar{K}\}$ axis is pointing out of page from indicated position

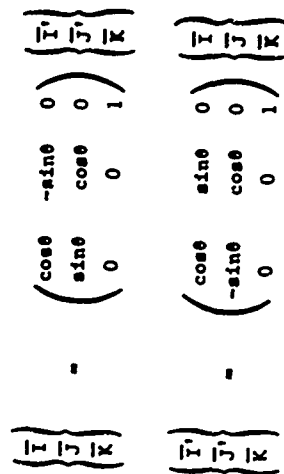


FIGURE 22 CONVERSION BETWEEN BASIC REFERENCE SYSTEM $(\bar{I}, \bar{J}, \bar{K})$ AND FIRST INTERMEDIATE REFERENCE SYSTEM $(\bar{I}', \bar{J}', \bar{K}')$

1. \bar{I} , \bar{J} , \bar{I}' , and \bar{J}' are all in the equatorial plane.

2. \bar{n} , \bar{e} , \bar{h} , and \bar{j} are all in the local geocentric horizontal plane.

3. \bar{h} , \bar{v} , \bar{i} , and \bar{k} are all in the same local geocentric vertical plane.

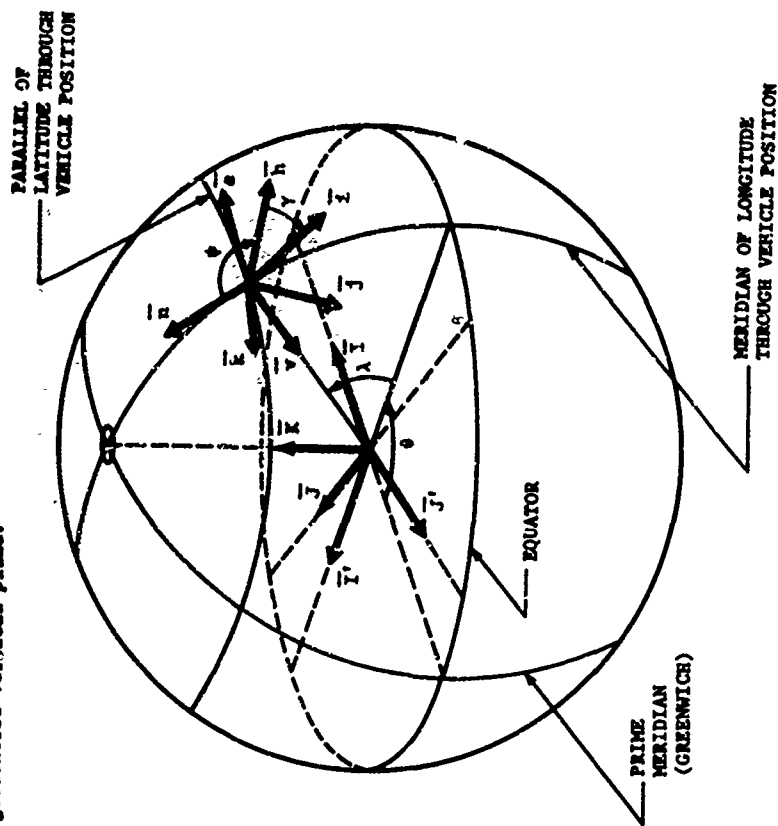


FIGURE 21 REFERENCE SYSTEMS

BASIC:

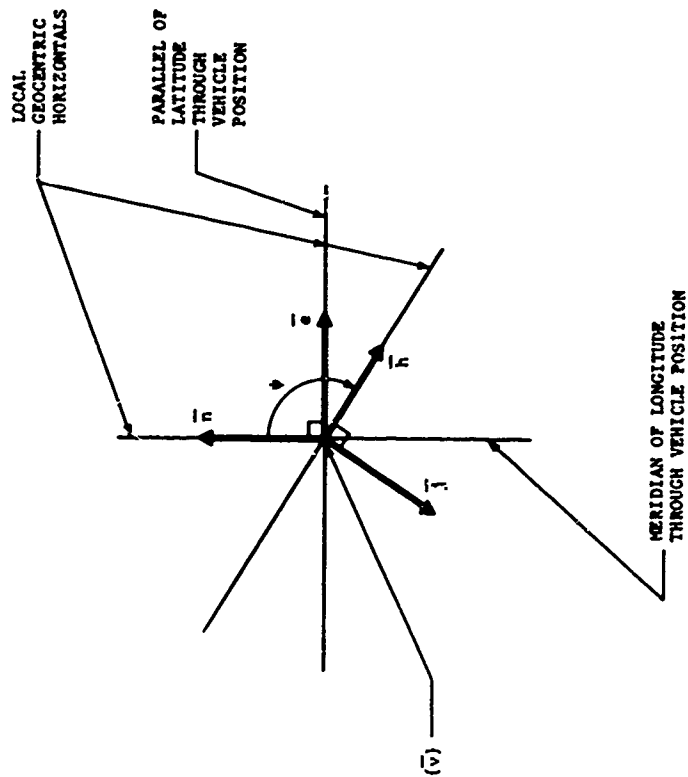
 $\{\bar{I}, \bar{J}, \bar{K}\}$

INTERMEDIATE: $\{\bar{I}', \bar{J}', \bar{K}\}, \{\bar{n}, \bar{e}, \bar{v}\}, \{\bar{h}, \bar{j}, \bar{v}\}$

FLIGHT: $(\bar{i}, \bar{j}, \bar{k})$

NOTE:

1. (\bar{v}) axis is pointing into page at indicated position.



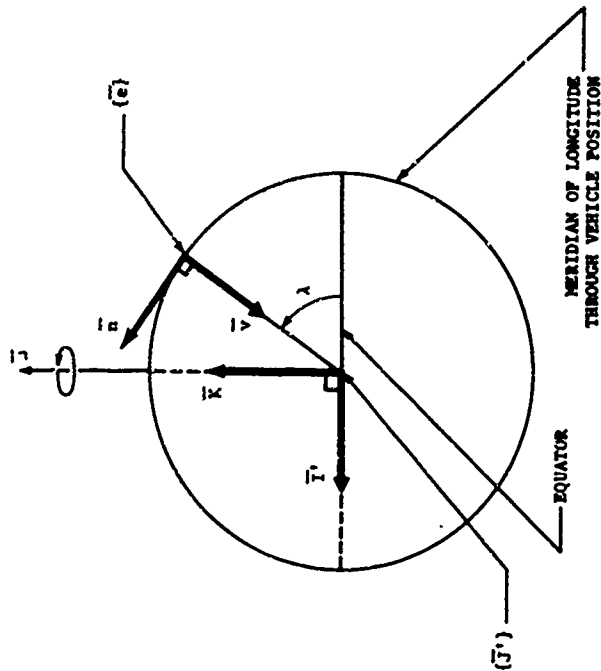
$$\begin{Bmatrix} \bar{n} \\ \bar{j} \\ \bar{v} \end{Bmatrix} = \begin{pmatrix} \cos\psi & -\sin\psi & 0 \\ \sin\psi & \cos\psi & 0 \\ 0 & 0 & 1 \end{pmatrix} \begin{Bmatrix} \bar{n} \\ \bar{j} \\ \bar{v} \end{Bmatrix}$$

$$\begin{Bmatrix} \bar{n} \\ \bar{j} \\ \bar{v} \end{Bmatrix} = \begin{pmatrix} \cos\psi & \sin\psi & 0 \\ -\sin\psi & \cos\psi & 0 \\ 0 & 0 & 1 \end{pmatrix} \begin{Bmatrix} \bar{n} \\ \bar{j} \\ \bar{v} \end{Bmatrix}$$

FIGURE 24 CONVERSION BETWEEN SECOND INTERMEDIATE REFERENCE SYSTEM ($\bar{n}, \bar{e}, \bar{v}$) AND THIRD INTERMEDIATE REFERENCE SYSTEM ($\bar{n}, \bar{j}, \bar{v}$)

NOTES:

1. (\bar{i}) axis is pointing out of page from indicated position.
2. (\bar{e}) axis is pointing into page at indicated position.



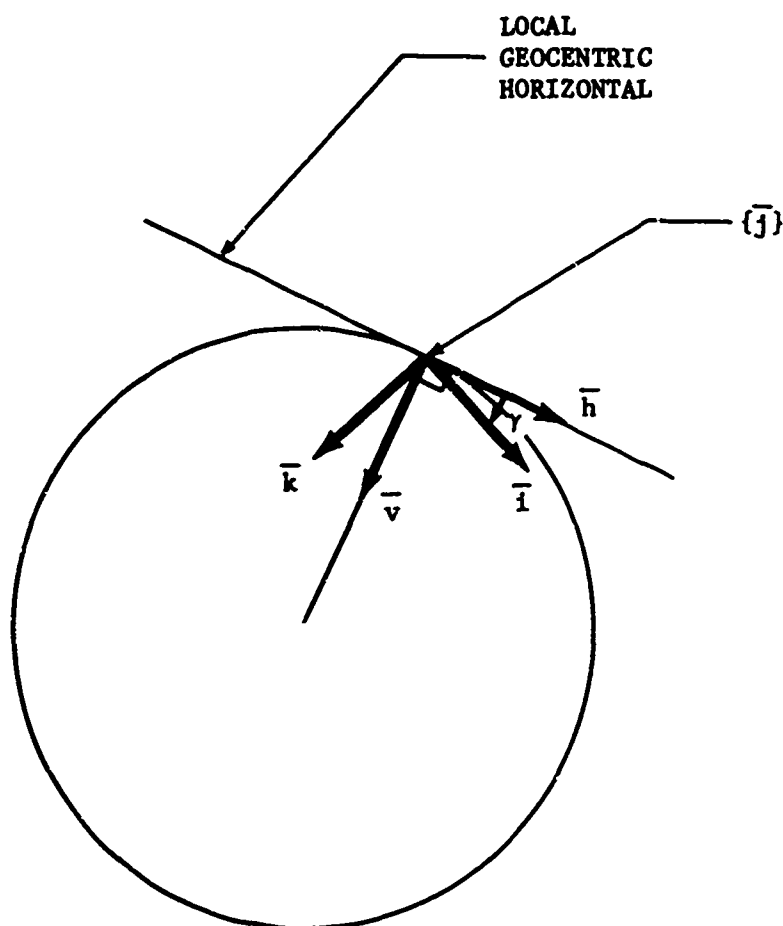
$$\begin{Bmatrix} \bar{i} \\ \bar{j} \\ \bar{k} \end{Bmatrix} = \begin{pmatrix} \sin\lambda & 0 & \cos\lambda \\ 0 & -1 & 0 \\ \cos\lambda & 0 & -\sin\lambda \end{pmatrix} \begin{Bmatrix} \bar{n} \\ \bar{e} \\ \bar{v} \end{Bmatrix}$$

$$\begin{Bmatrix} \bar{n} \\ \bar{e} \\ \bar{v} \end{Bmatrix} = \begin{pmatrix} \sin\lambda & 0 & \cos\lambda \\ 0 & -1 & 0 \\ \cos\lambda & 0 & -\sin\lambda \end{pmatrix} \begin{Bmatrix} \bar{i} \\ \bar{j} \\ \bar{k} \end{Bmatrix}$$

FIGURE 23 CONVERSION BETWEEN FIRST INTERMEDIATE REFERENCE SYSTEM ($\bar{i}, \bar{j}, \bar{k}$) AND SECOND INTERMEDIATE REFERENCE SYSTEM ($\bar{n}, \bar{e}, \bar{v}$)

NOTE:

1. $\{\bar{j}\}$ axis is pointing out of page from indicated position



$$\begin{pmatrix} \bar{i} \\ \bar{j} \\ \bar{k} \end{pmatrix} = \begin{pmatrix} \cos \gamma & 0 & -\sin \gamma \\ 0 & 1 & 0 \\ \sin \gamma & 0 & \cos \gamma \end{pmatrix} \begin{pmatrix} \bar{h} \\ \bar{j} \\ \bar{v} \end{pmatrix}$$

$$\begin{pmatrix} \bar{h} \\ \bar{j} \\ \bar{v} \end{pmatrix} = \begin{pmatrix} \cos \gamma & 0 & \sin \gamma \\ 0 & 1 & 0 \\ -\sin \gamma & 0 & \cos \gamma \end{pmatrix} \begin{pmatrix} \bar{i} \\ \bar{j} \\ \bar{k} \end{pmatrix}$$

FIGURE 25 CONVERSION BETWEEN THIRD INTERMEDIATE REFERENCE SYSTEM $\{\bar{h}, \bar{j}, \bar{v}\}$ AND FLIGHT AXES REFERENCE SYSTEM $\{\bar{i}, \bar{j}, \bar{k}\}$

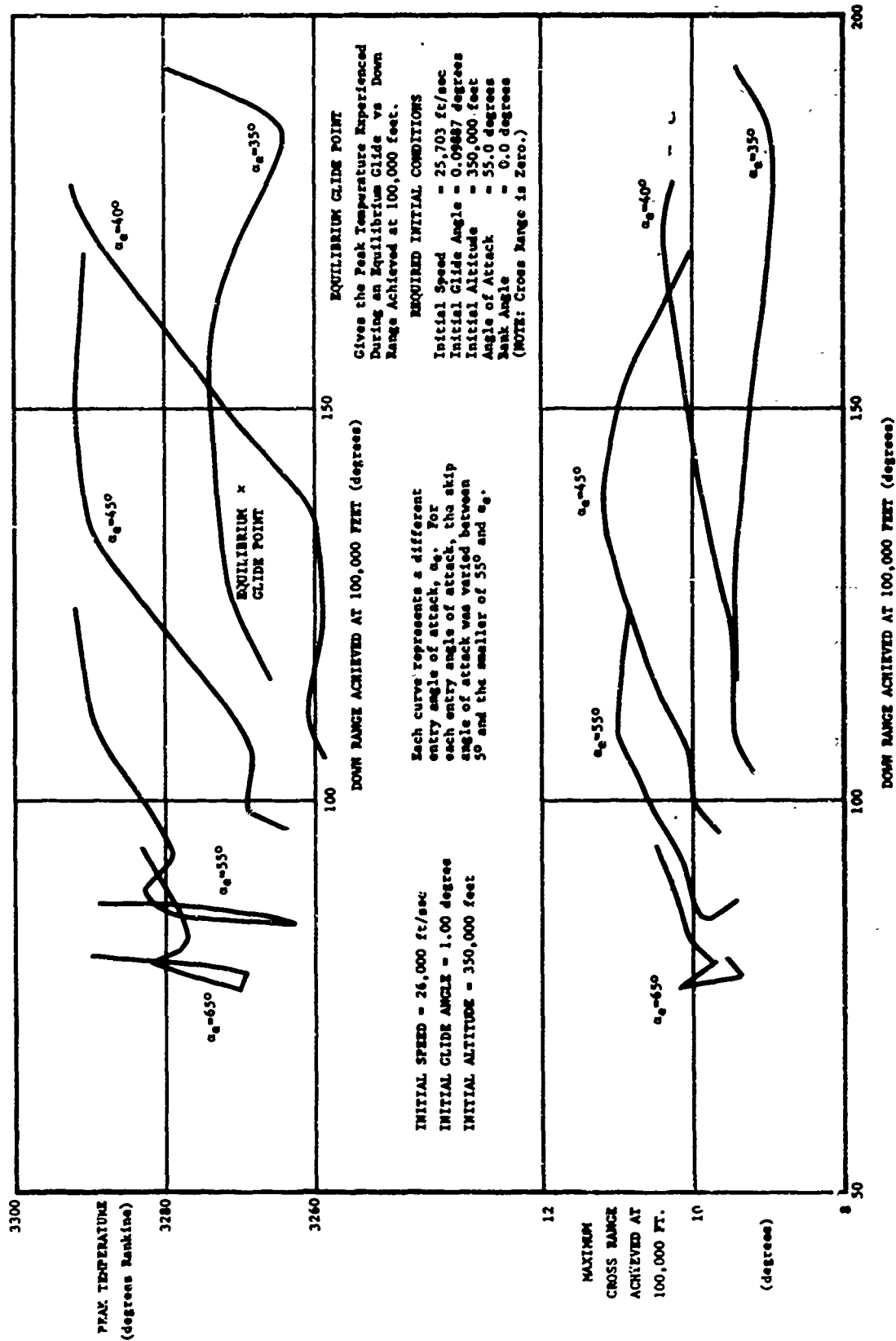


FIGURE 26 VEHICLE PERFORMANCE FOR VARIOUS ENTRY AND SKIP ANGLES OF ATTACK

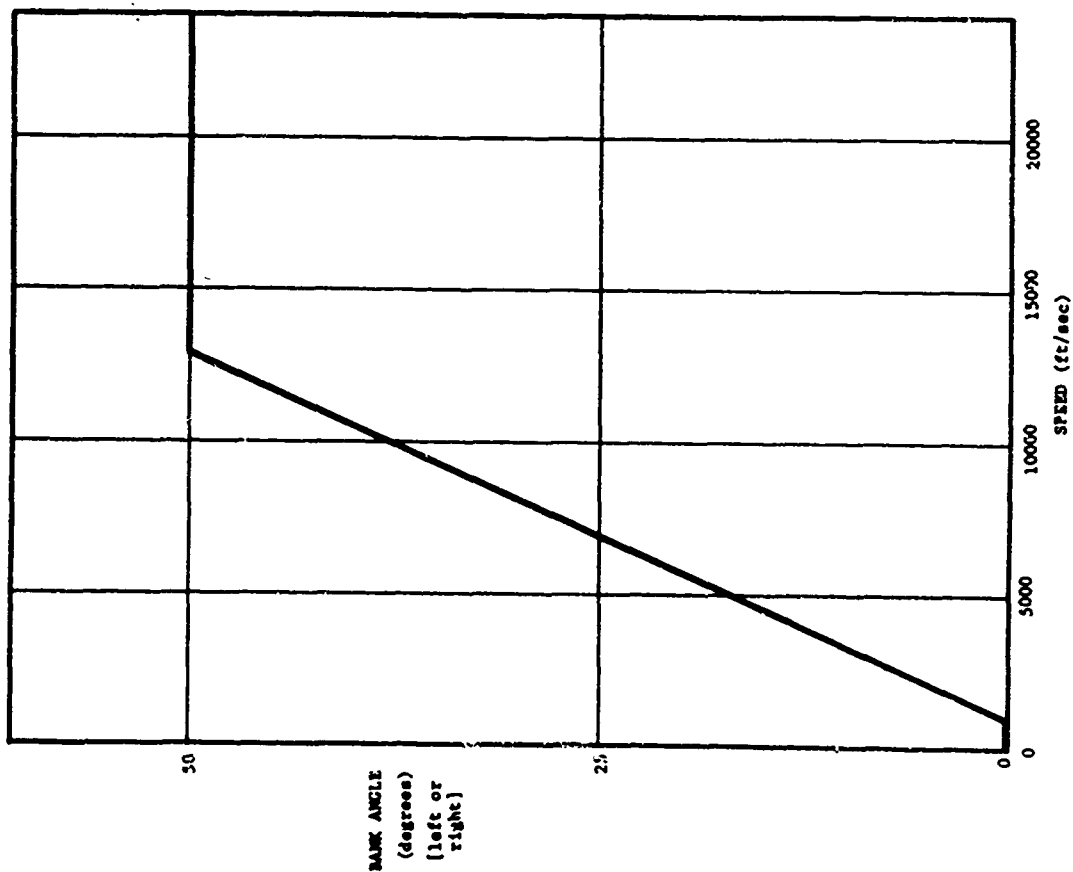


FIGURE 28 VARIATION OF LOWER LIMIT FOR THE BANK ANGLE vs SPEED DURING PHASE IV OF THE REENTRY

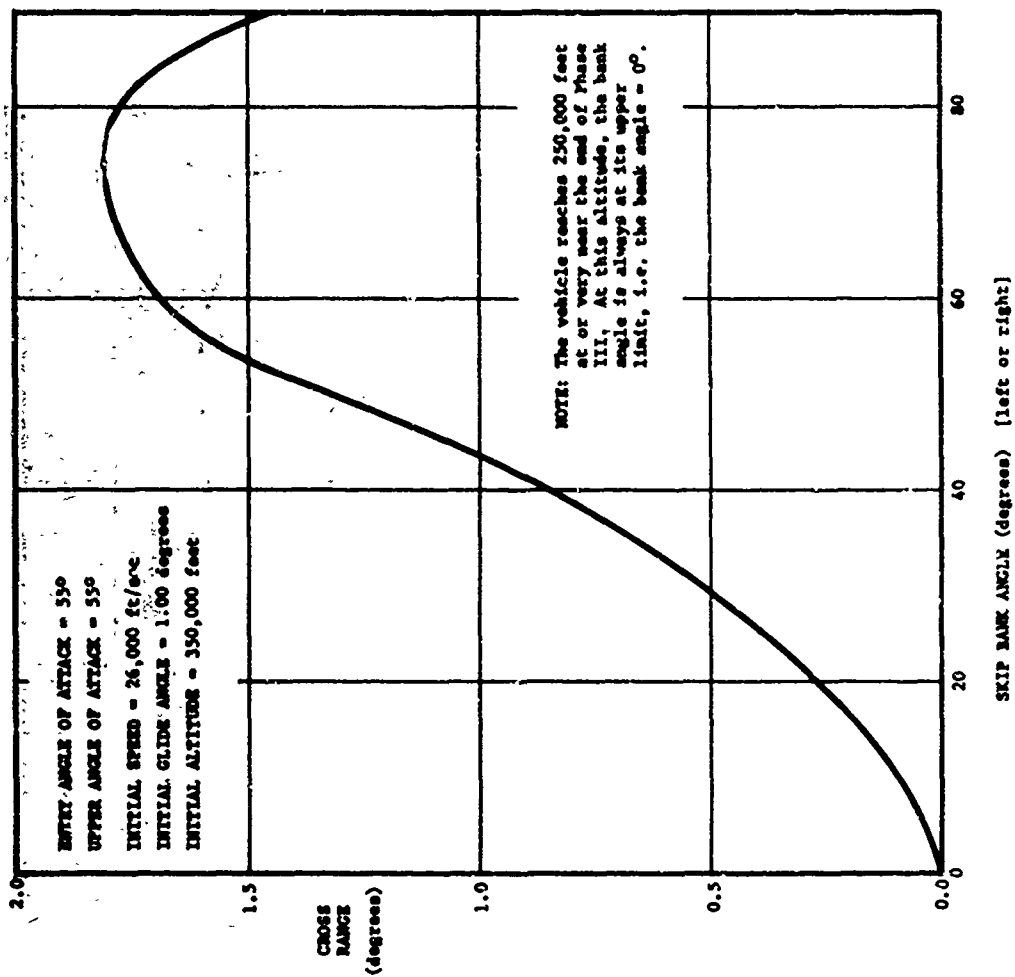


FIGURE 27 VARIATION OF CROSS RANGE AT 250,000 FEET WITH SKIP BANK ANGLE

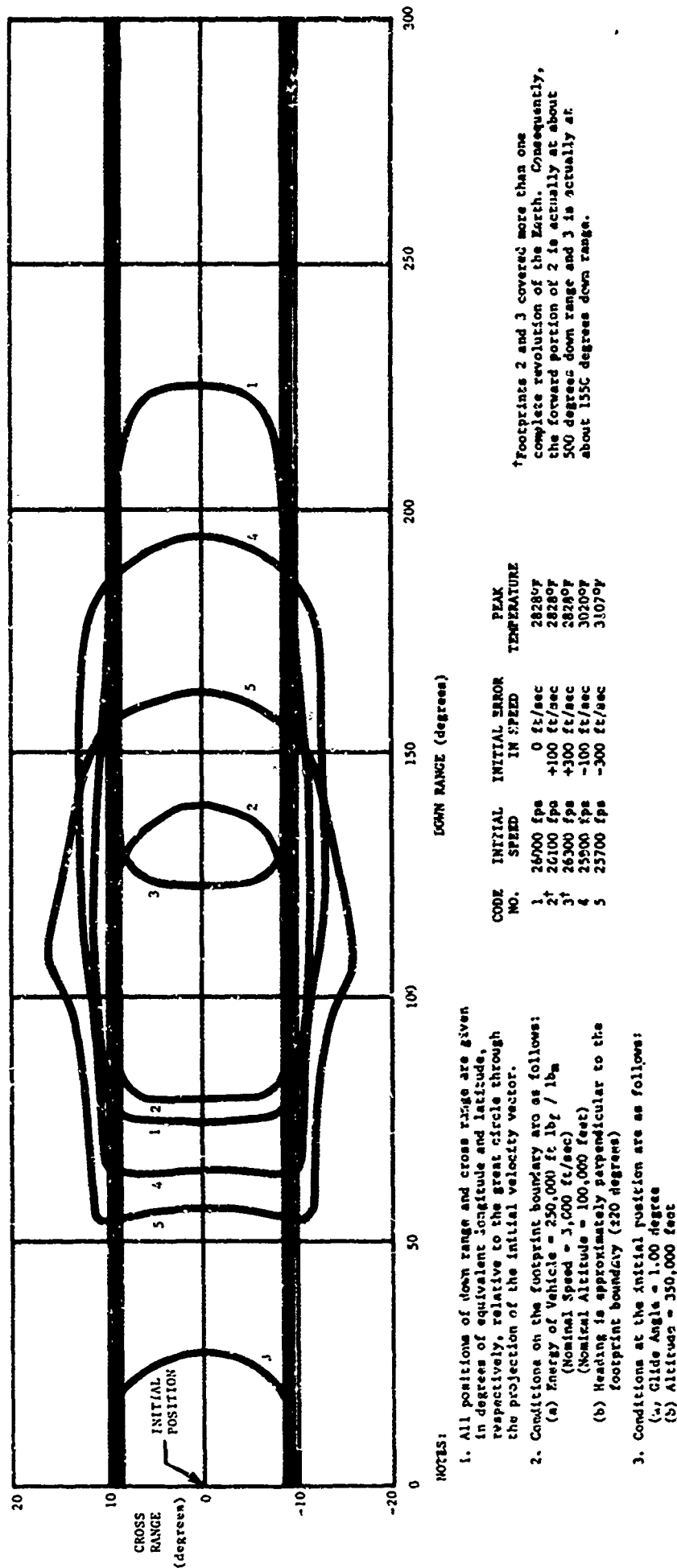
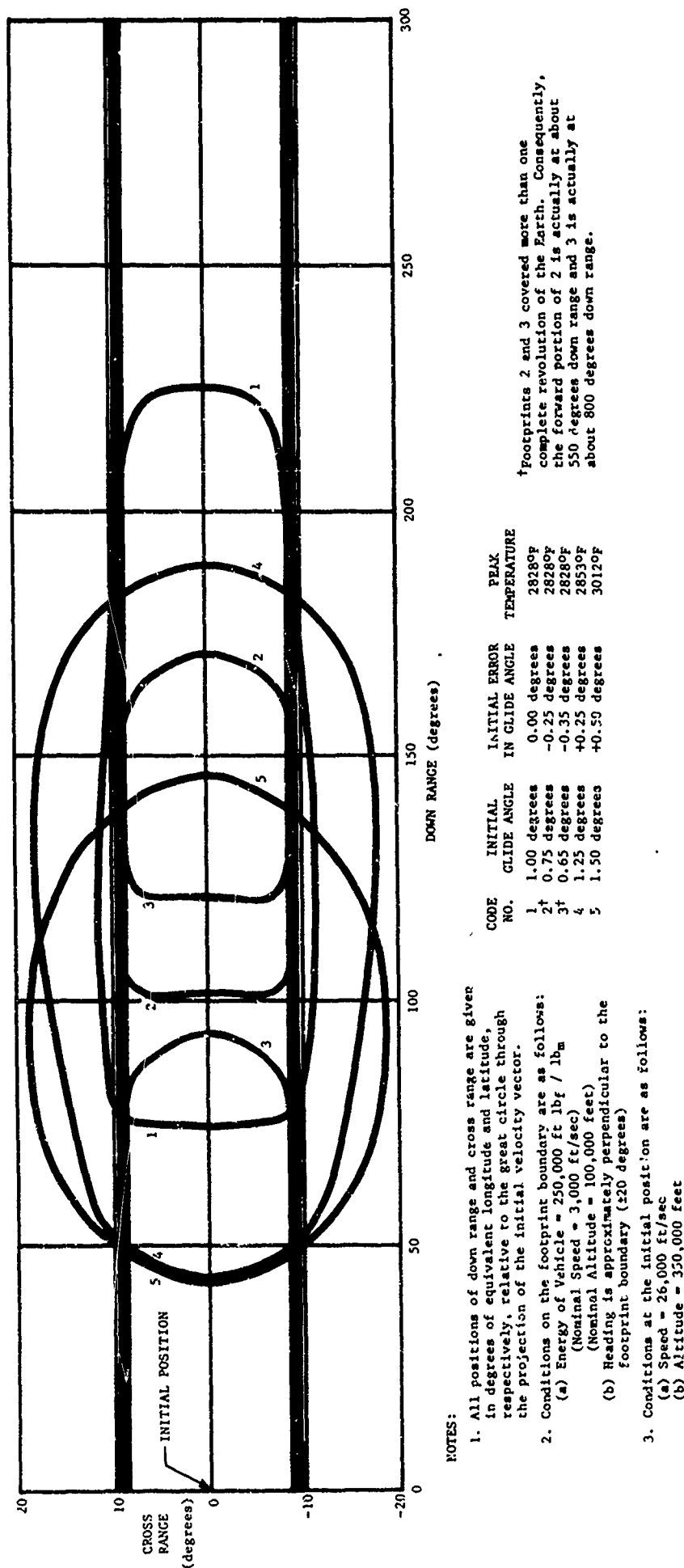


FIGURE 29 CROSS RANGE VS DOWN RANGE FOR VARIOUS INITIAL SPEEDS OVER A CIRCULAR, NON-ROTATING EARTH

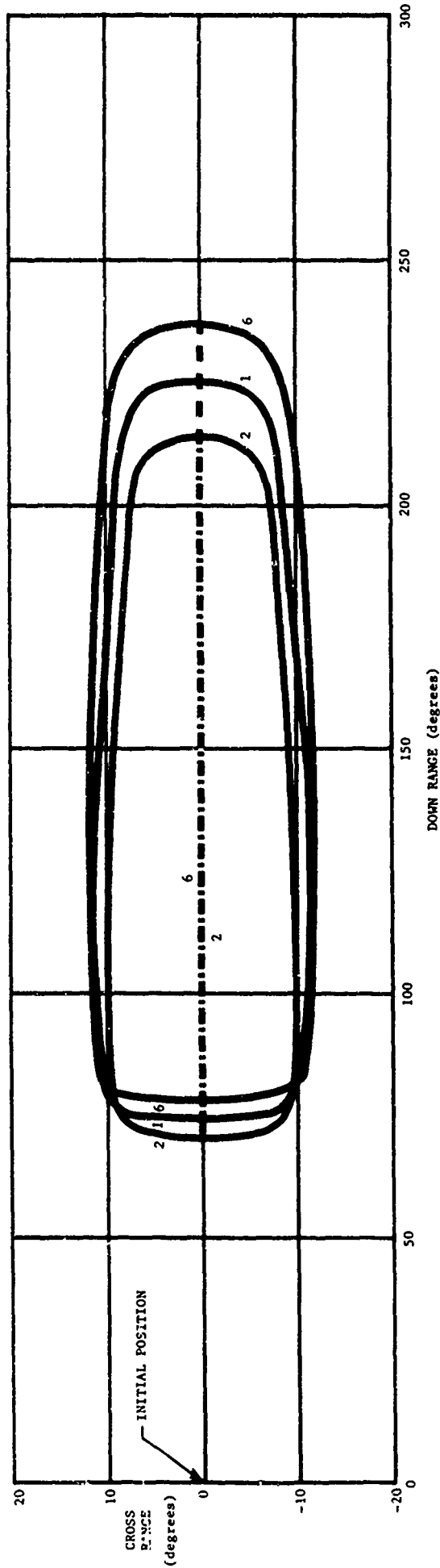


NOTES:

1. All positions of down range and cross range are given in degrees of equivalent longitude and latitude, respectively, relative to the great circle through the projection of the initial velocity vector.
2. Conditions on the footprint boundary are as follows:
 (a) Energy of Vehicle = 250,000 ft lb_f / lb_m
 (Nominal Speed = 3,000 ft/sec)
 (Nominal Altitude = 100,000 feet)
 (b) Heading is approximately perpendicular to the footprint boundary (±20 degrees)
3. Conditions at the initial position are as follows:
 (a) Speed = 26,000 ft/sec
 (b) Altitude = 350,000 feet

†Footprints 2 and 3 covered more than one complete revolution of the Earth. Consequently, the forward portion of 2 is actually at about 550 degrees down range and 3 is actually at about 800 degrees down range.

FIGURE 30 CROSS RANGE VS DOWN RANGE FOR VARIOUS INITIAL GLIDE ANGLES OVER A CIRCULAR, NON-ROTATING EARTH



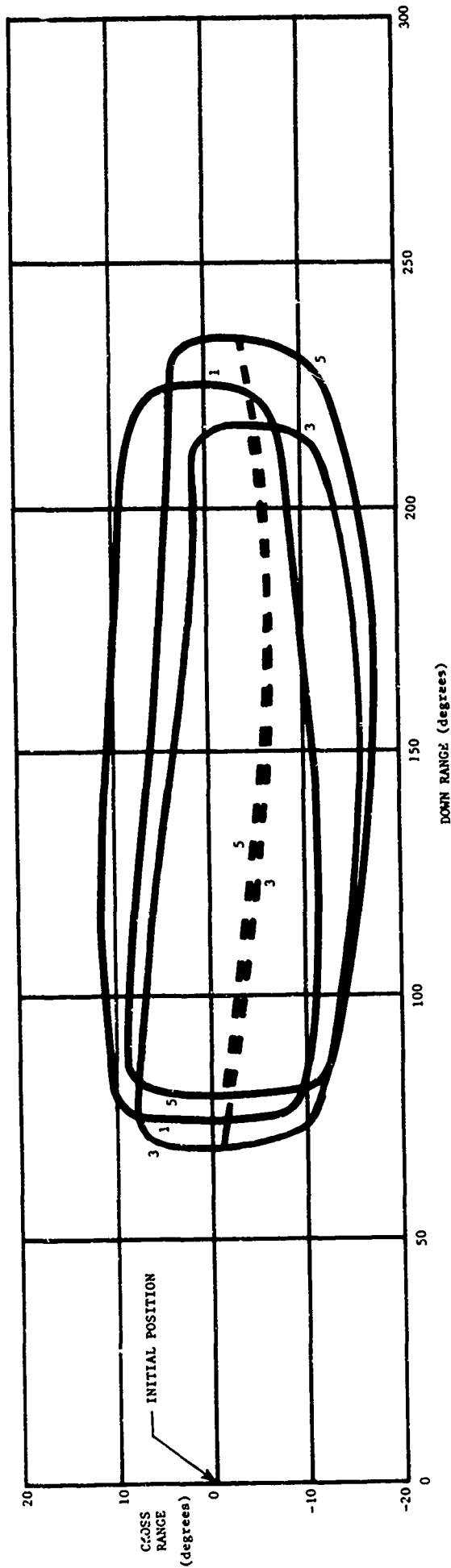
NOTES:

1. All positions of down range and cross range are given in degrees of equivalent longitude and latitude, respectively, relative to the great circle through the projection of the initial velocity vector.
2. Conditions on the footprint boundary are as follows:
(a) Energy of Vehicle = 250,000 ft lb_f / lb_m
(Nominal Speed = 3,000 ft/sec)
(Nominal Altitude = 100,000 feet)
(b) Heading is approximately perpendicular to the footprint boundary (±20 degrees)

CODE NO.	INITIAL LATITUDE	INITIAL AZIMUTH	PEAK TEMPERATURE
1	0°	90°	2828°F
2	0°	90°	2700°F
6	0°	-90°	2954°F

3. Inertial conditions (relative to inertial space) at the initial position are as follows:
(a) Inertial Speed = 26,000 ft/sec
(b) Inertial Glide Angle = 1.00 degree
(c) Altitude = 350,000 feet
(d) Inertial Azimuth is value given in the table; no correction is necessary for these two reentries.
4. Solid lines are the boundaries of the footprints.
5. Broken lines are the midlines of the footprints. They show the extent of the shift in cross range due to the Earth's rotation.

FIGURE 31 a CROSS RANGE vs DOWN RANGE FOR TWO INITIAL POSITIONS OVER A CIRCULAR, ROTATING EARTH



NOTES:

1. All positions of down range and cross range are given in degrees of equivalent longitude and latitude, respectively, relative to the great circle through the projection of the initial velocity vector.
2. Conditions on the footprint boundary are as follows:
 - (a) Energy of Vehicle = 250,000 ft lb_f / lb_m
(Nominal Altitude = 100,000 feet)
 - (b) Heading is approximately perpendicular to the footprint boundary (± 20 degrees)

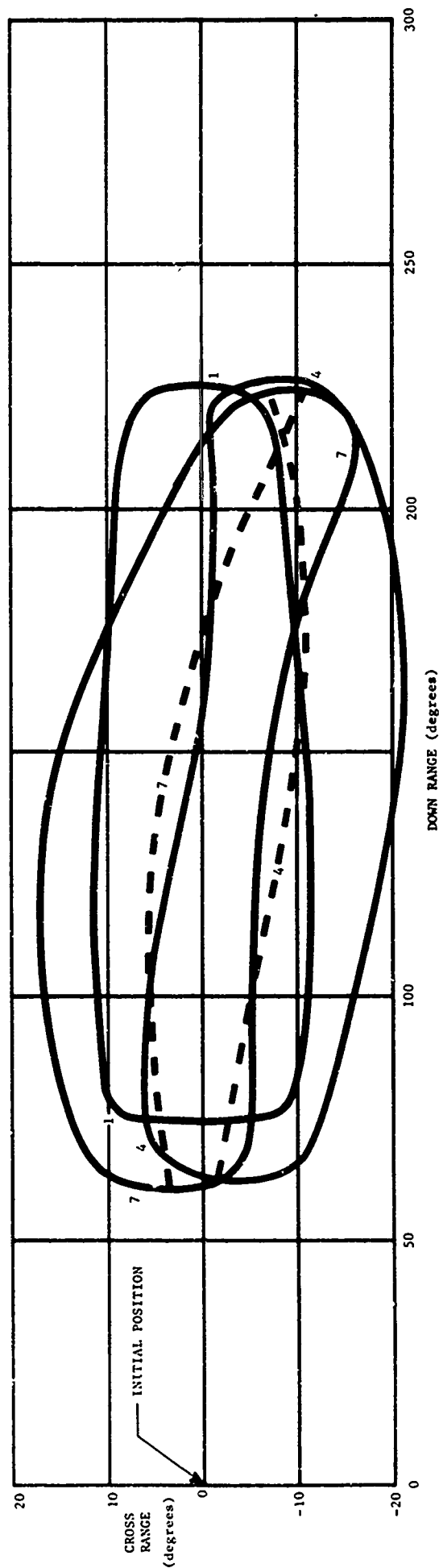
CODE NO.	INITIAL LATITUDE	INITIAL AZIMUTH	PEAK TEMPERATURE
1	0°	55°	2828°F
3	0°	55°	2716°F
5	0°	-55°	2934°F

3. Inertial conditions (relative to inertial space) at the initial position are as follows:
 - (a) Inertial Speed = 26,000 ft/sec
 - (b) Inertial Glide Angle = 1.00 degree
 - (c) Altitude = 350,000 feet
 - (d) Inertial Azimuth is value given in table; a correction must be applied (~ 2.0 degrees) to obtain the azimuth relative to a rotating Earth.

4. Solid lines are the boundaries of the footprints.

5. Broken lines are the midlines of the footprints. They show the extent of the shift in cross range due to the Earth's rotation.

FIGURE 31b CROSS RANGE VS DOWN RANGE FOR TWO INITIAL POSITIONS OVER A CIRCULAR, ROTATING EARTH



NOTES:

1. All positions of down range and cross range are given in degrees of equivalent longitude and latitude, respectively, relative to the great circle through the projection of the initial velocity vector.
2. Conditions on the footprint boundary are as follows:
 - (a) Energy of Vehicle = 250,000 ft lbf / lbm
(Nominal Speed = 3,000 ft/sec)
(Nominal Altitude = 100,000 feet)
 - (b) Heading is approximately perpendicular to the footprint boundary (±20 degrees)

CODE NO.	INITIAL LATITUDE	INITIAL AZIMUTH	PEAK TEMPERATURE
1	0°	0°	2828°F
4	0°	0°	2833°F
7	-90°	0°	2835°F

3. Inertial conditions (relative to inertial space) at the initial position are as follows:
 - (a) Inertial Speed = 26,000 ft/sec
 - (b) Inertial Glide Angle = 1.00 degree
 - (c) Altitude = 350,000 feet
 - (d) Inertial Azimuth is value given in table: the azimuth for footprint 4 is -3.4 degrees relative to a rotating Earth; no correction is necessary for footprint 7 since the relative rotational speed at the pole is zero.
4. Solid lines are the boundaries of the footprints.
5. Broken lines are the midlines of the footprints. They show the extent of the shift in cross range due to the Earth's rotation

FIGURE 31c CROSS RANGE VS DOWN RANGE FOR TWO INITIAL POSITIONS OVER A CIRCULAR, ROTATING EARTH

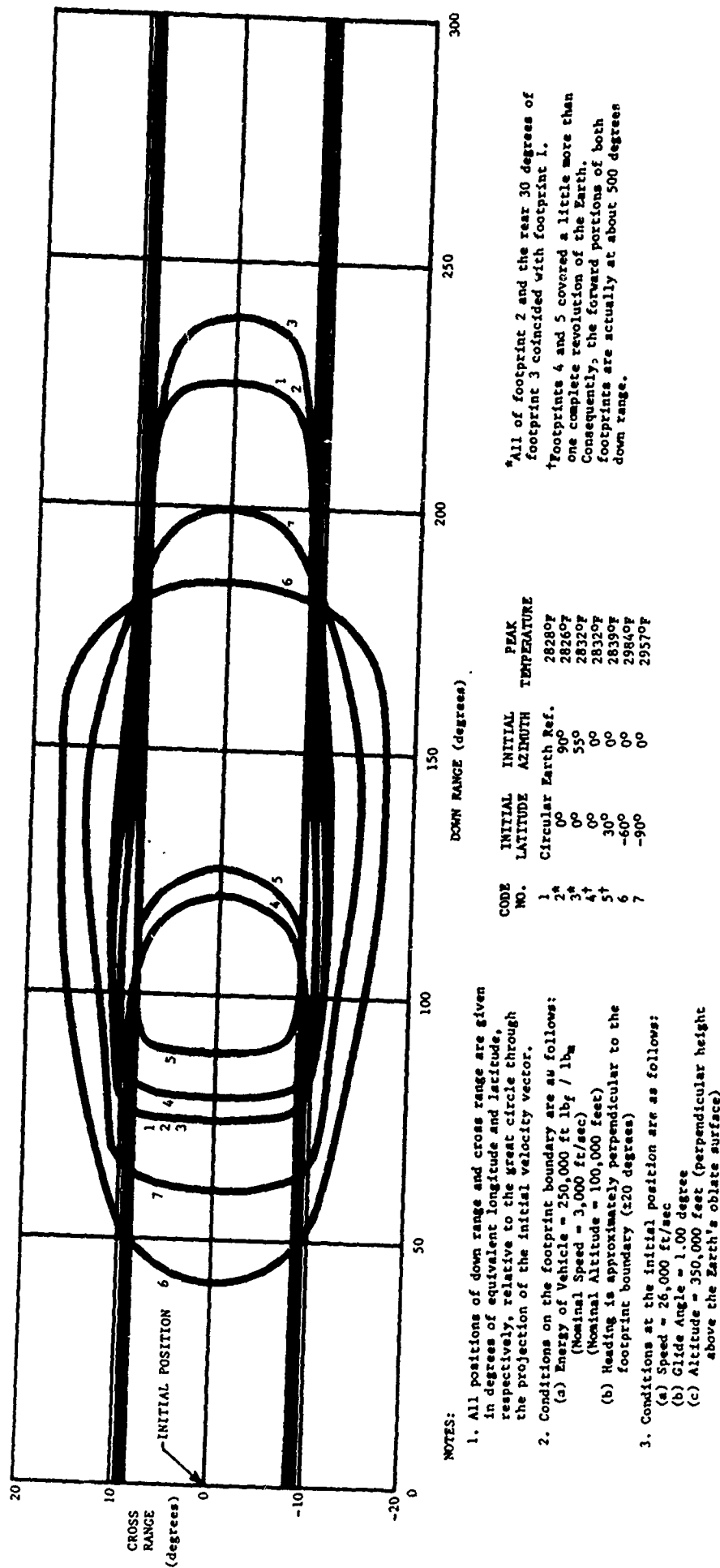
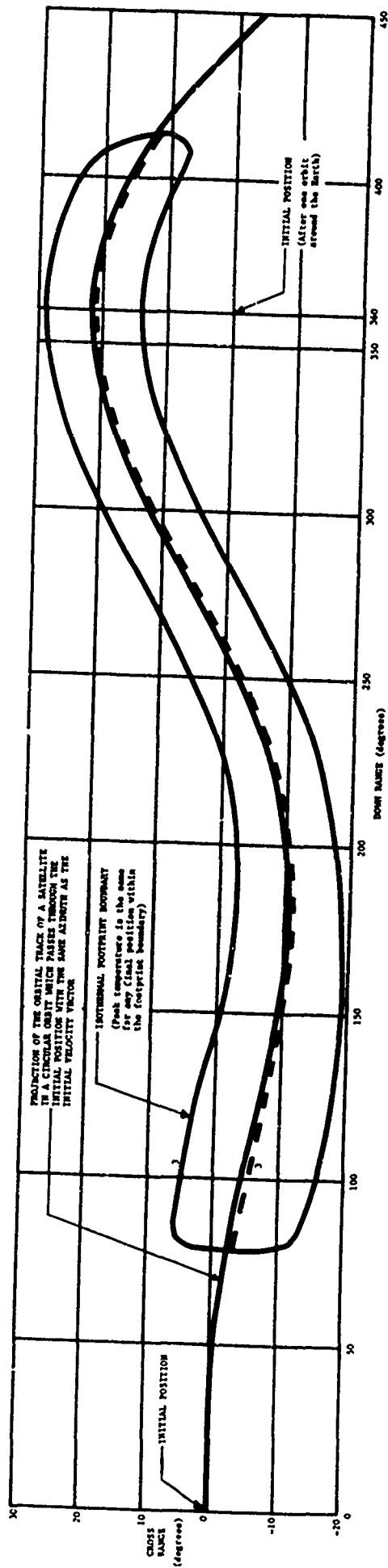


FIGURE 32 CROSS RANGE vs DOWN RANGE FOR VARIOUS INITIAL POSITIONS AND HEADINGS OVER AN OBLATE, NON-ROTATING EARTH

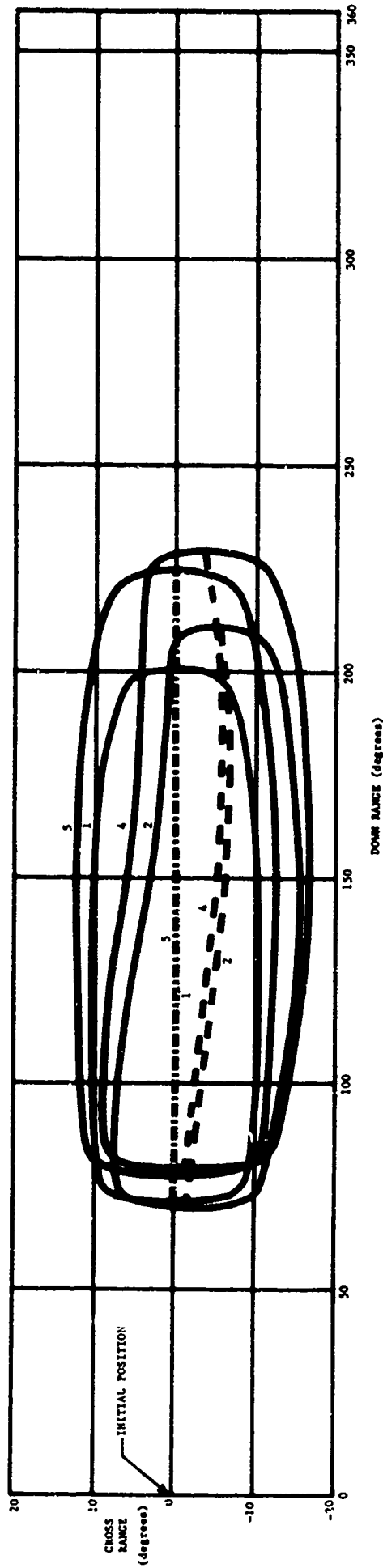


CODE NO. 3 INITIAL LATITUDE 0° INITIAL ALTITUDE 0° MAX TEMPERATURE 2811°y

NOTES:

1. All positions of down range and cross range are given in degrees of equivalent longitude and latitude, respectively, relative to the initial position through the projection of the initial velocity vector.
2. Conditions on the footprint boundary are as follows:
 - (a) Energy of Vehicle = 3,000 ft/sec
 - (b) Heading is approximately perpendicular to the footprint boundary (120 degrees)
 - (c) Altitude = 100,000 feet
 - (d) Inertial Altitude = 100,000 feet
 - (e) Inertial Speed = 3,000 ft/sec
 - (f) Inertial Altitude = 100,000 feet
 - (g) Inertial Altitude = 100,000 feet
 - (h) Inertial Altitude = 100,000 feet
 - (i) Inertial Altitude = 100,000 feet
 - (j) Inertial Altitude = 100,000 feet
 - (k) Inertial Altitude = 100,000 feet
 - (l) Inertial Altitude = 100,000 feet
 - (m) Inertial Altitude = 100,000 feet
 - (n) Inertial Altitude = 100,000 feet
 - (o) Inertial Altitude = 100,000 feet
 - (p) Inertial Altitude = 100,000 feet
 - (q) Inertial Altitude = 100,000 feet
 - (r) Inertial Altitude = 100,000 feet
 - (s) Inertial Altitude = 100,000 feet
 - (t) Inertial Altitude = 100,000 feet
 - (u) Inertial Altitude = 100,000 feet
 - (v) Inertial Altitude = 100,000 feet
 - (w) Inertial Altitude = 100,000 feet
 - (x) Inertial Altitude = 100,000 feet
 - (y) Inertial Altitude = 100,000 feet
 - (z) Inertial Altitude = 100,000 feet
3. Inertial conditions (relative to inertial space) at the initial position are as follows:
 - (a) Inertial Speed = 34,000 ft/sec
 - (b) Inertial Altitude = 100,000 feet
 - (c) Altitude = 350,000 feet (perpendicular height above Earth's surface)
 - (d) Inertial Altitude = 100,000 feet
 - (e) Inertial Altitude = 100,000 feet
 - (f) Inertial Altitude = 100,000 feet
 - (g) Inertial Altitude = 100,000 feet
 - (h) Inertial Altitude = 100,000 feet
 - (i) Inertial Altitude = 100,000 feet
 - (j) Inertial Altitude = 100,000 feet
 - (k) Inertial Altitude = 100,000 feet
 - (l) Inertial Altitude = 100,000 feet
 - (m) Inertial Altitude = 100,000 feet
 - (n) Inertial Altitude = 100,000 feet
 - (o) Inertial Altitude = 100,000 feet
 - (p) Inertial Altitude = 100,000 feet
 - (q) Inertial Altitude = 100,000 feet
 - (r) Inertial Altitude = 100,000 feet
 - (s) Inertial Altitude = 100,000 feet
 - (t) Inertial Altitude = 100,000 feet
 - (u) Inertial Altitude = 100,000 feet
 - (v) Inertial Altitude = 100,000 feet
 - (w) Inertial Altitude = 100,000 feet
 - (x) Inertial Altitude = 100,000 feet
 - (y) Inertial Altitude = 100,000 feet
 - (z) Inertial Altitude = 100,000 feet
4. Except where otherwise noted, the solid lines are the boundaries of the footprint.
5. The broken line is the midline of footprint 3. It shows the extent of the shift in cross range due to the Earth's rotation.

FIGURE 30 - COMPARISON BETWEEN THE CROSS RANGE SHIFT OF A FOOTPRINT BOUNDARY AND THE CROSS RANGE SHIFT OF THE ORBITAL TRACK OF A SATELLITE - ORBITAL, ROTATING EARTH



CODE NO. INITIAL LATITUDE INITIAL AZIMUTH PEAK TEMPERATURE

1	0°	90°	2706°
2	0°	55°	2730°
4	0°	-55°	2931°
5	0°	-90°	2936°

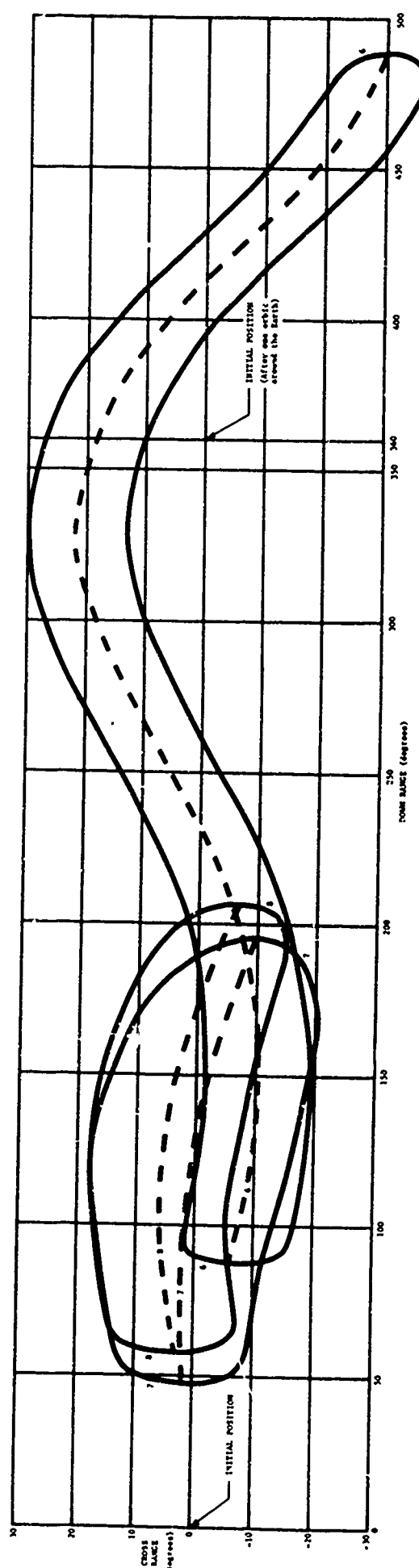
NOTES:

1. All positions of down range and cross range are given in degrees of equivalent longitude and latitude, respectively, relative to the great circle through the projection of the initial velocity vector.
2. Conditions on the footprint boundary are as follows:
 - (a) Energy of vehicle = 250,000 ft lb_g / lb_m (Nominal Speed = 3,000 ft/sec)
 - (b) Heading is approximately perpendicular to the footprint boundary (±20 degrees)

3. Inertial conditions (relative to inertial space) at the initial position are as follows:
 - (a) Inertial Speed = 26,000 ft/sec
 - (b) Inertial Glide Angle = 1.00 degree
 - (c) Altitude = 350,000 feet (perpendicular height above Earth's oblate surface)
 - (d) Inertial Azimuth is value given in table; no correction is necessary for footprints 1 and 5; a correction must be applied (±2.0 degrees) for footprints 2 and 4 to obtain the azimuth relative to a rotating Earth.

4. Solid lines are the boundaries of the footprints.
5. Broken lines are the midlines of the footprints. They show the extent of the shift in cross range due to the Earth's rotation.

FIGURE 31b CROSS RANGE VS DOWN RANGE FOR FOUR INITIAL HEADINGS OVER AN OBLATE, ROTATING EARTH



NOTES:

1. All positions of down range and cross range are given in degrees of equivalent longitude and latitude, respectively, relative to the great circle through the projection of the initial velocity vector.
2. Conditions on the footprint boundary are as follows:
 - (a) Inertial Altitude = 100,000 feet
 - (b) Inertial Altitude = 2,000 feet
 - (c) Inertial Altitude = 100,000 feet
 - (d) Inertial Altitude = 2,000 feet
 - (e) Inertial Altitude = 100,000 feet
 - (f) Inertial Altitude = 2,000 feet
3. Inertial conditions (relative to inertial space) at the initial position are as follows:
 - (a) Inertial Speed = 26,000 ft/sec
 - (b) Inertial Altitude = 100,000 feet
 - (c) Inertial Altitude = 2,000 feet
 - (d) Inertial Altitude = 100,000 feet
 - (e) Inertial Altitude = 2,000 feet
 - (f) Inertial Altitude = 100,000 feet
4. Solid lines are the boundaries of the footprint.
5. Dashed lines are the midlines of the footprint. They show the extent of the shift in cross range due to the Earth's rotation.

FIGURE 28C CROSS RANGE VS DOWN RANGE FOR THREE INITIAL POSITIONS OVER AN OBLATE, ROTATING EARTH

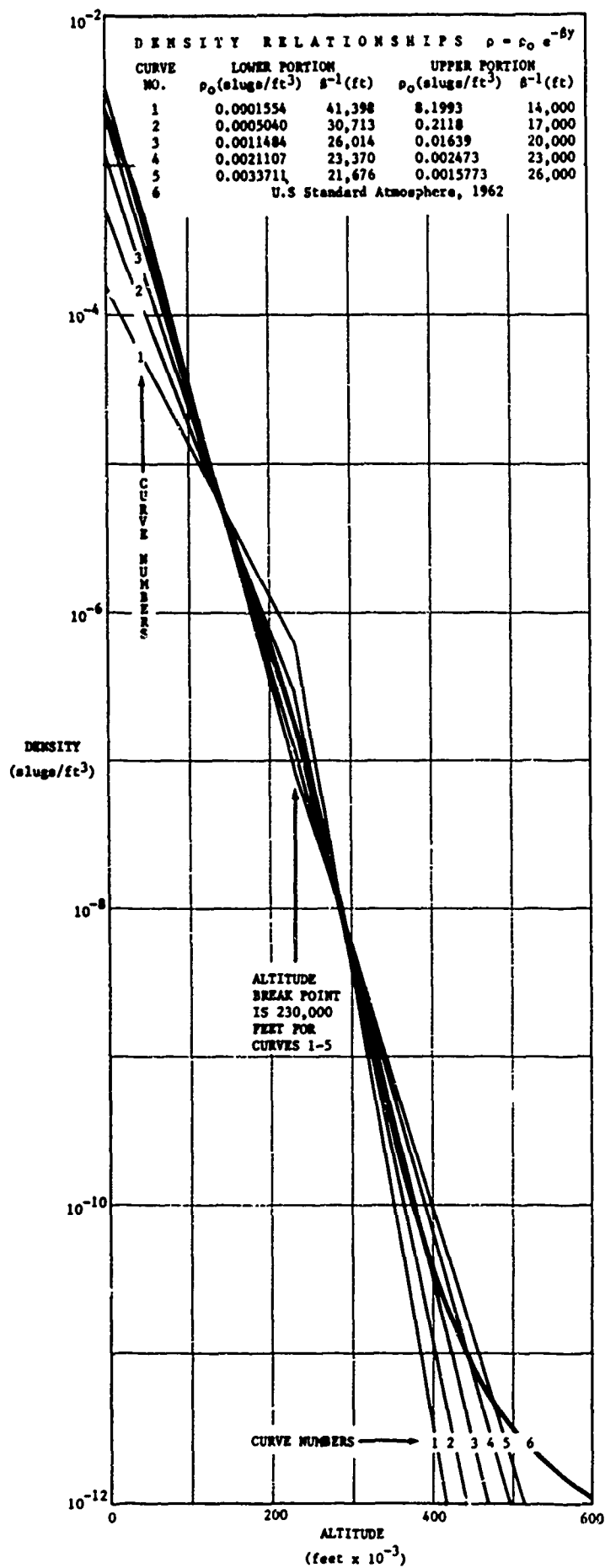


FIGURE 34 DENSITY ALTITUDE RELATIONSHIPS USED TO TEST THE PERFORMANCE OF THE CONTAC SYSTEM

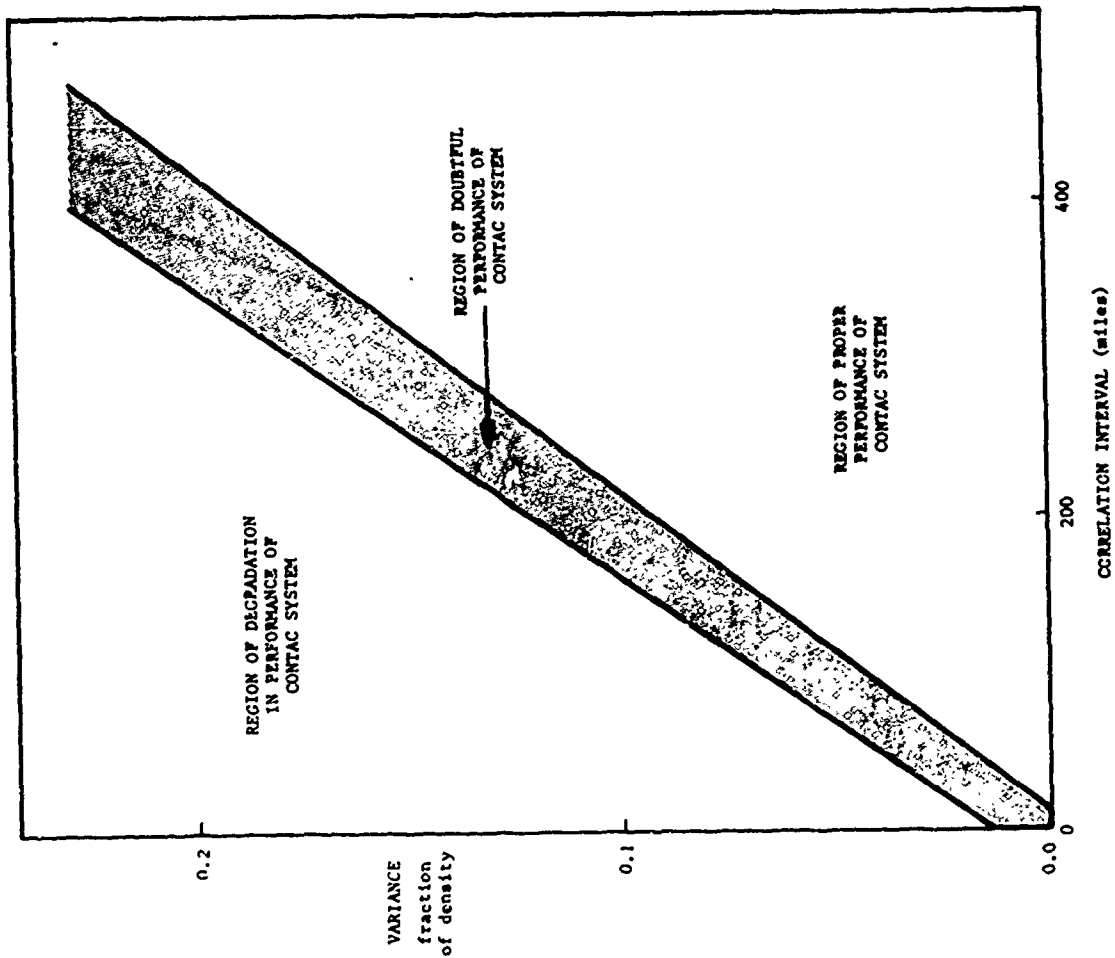


FIGURE 36 OPERATIONAL REGION OF CONTAC SYSTEM

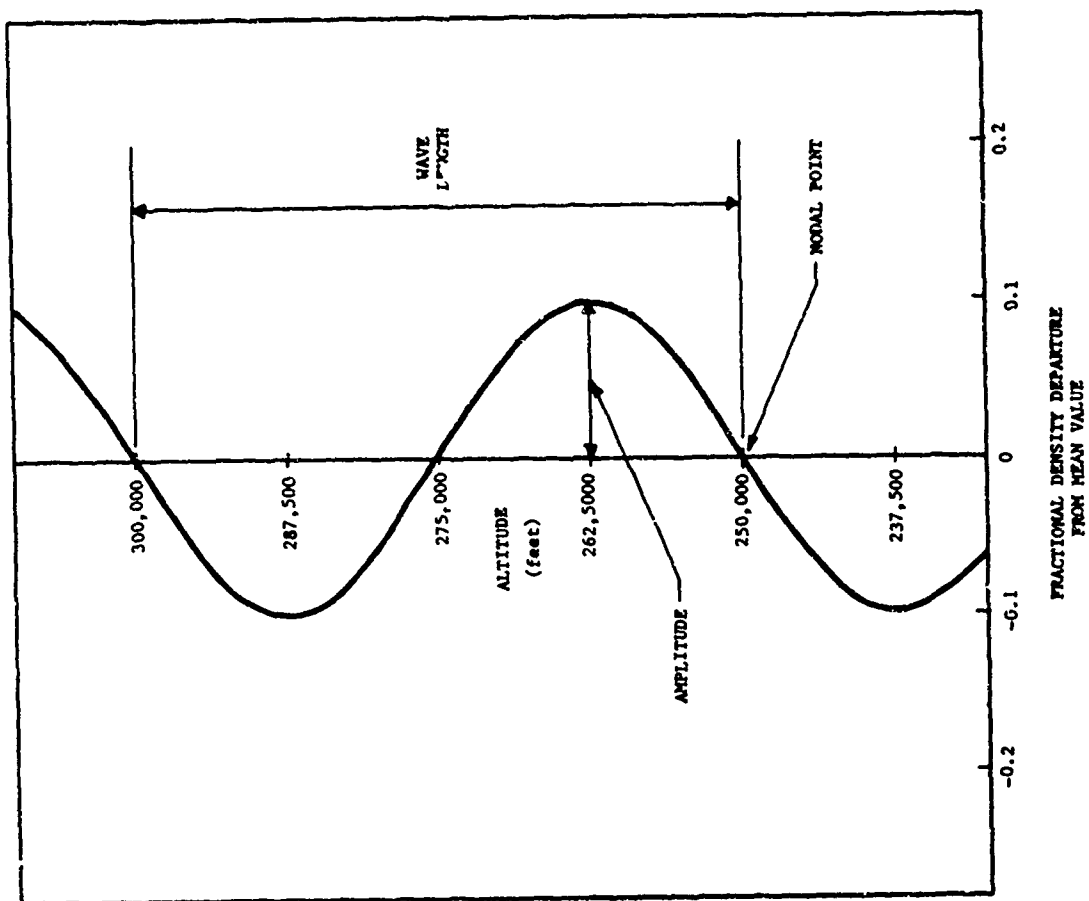


FIGURE 35 FRACTIONAL VARIATION OF DENSITY WITH ALTITUDE

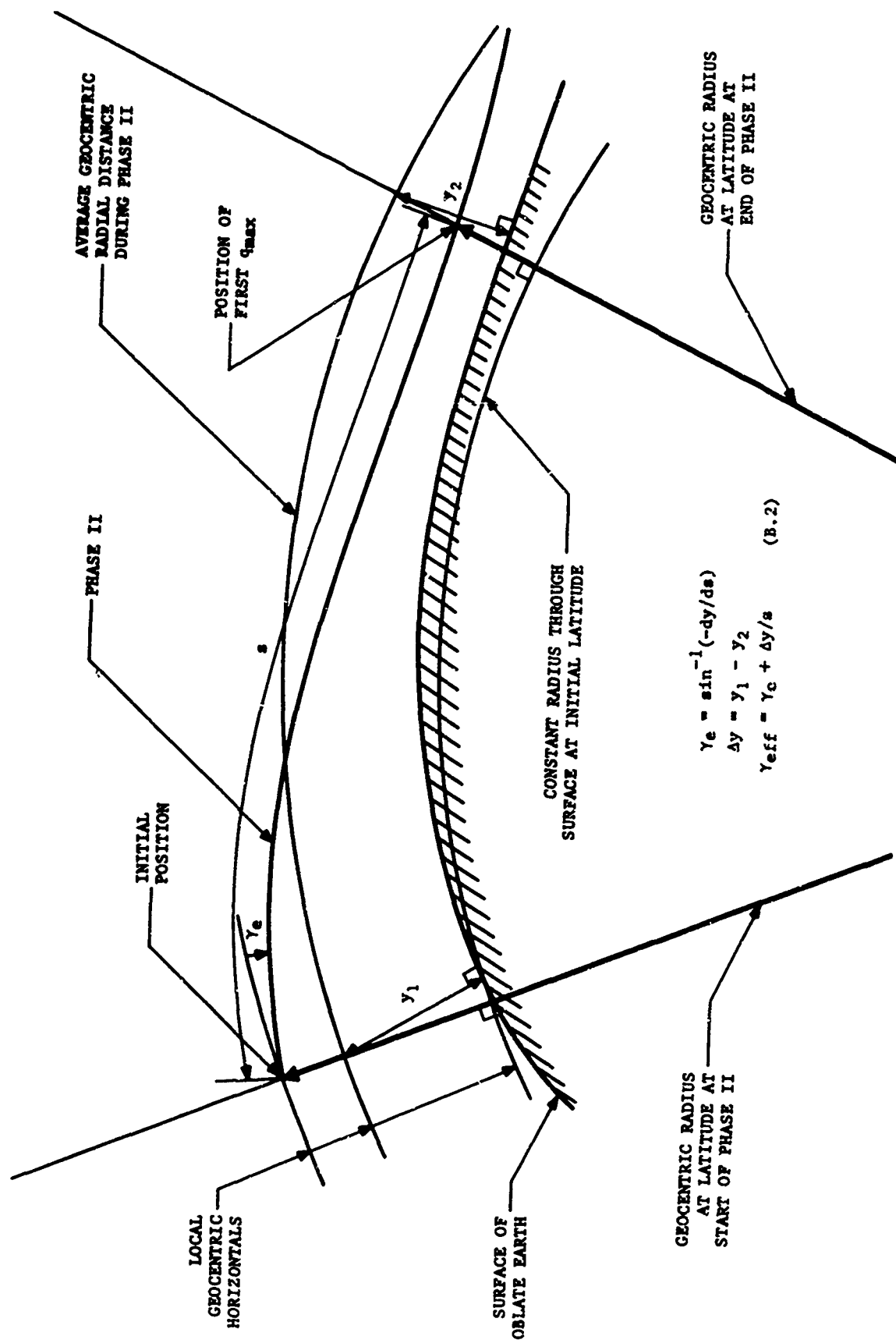


FIGURE 37 DEFINITION OF THE EFFECTIVE INITIAL GLIDE ANGLE

APPENDIX A

The Equilibrium Glide Trajectory

An equilibrium glide trajectory is a coplanar reentry during which the lift is always equal to the net difference between the gravitational and the centrifugal forces on the vehicle. Since drag is not compensated by thrust, the speed is gradually reduced thereby requiring an increase in lift to offset the loss in centrifugal force. Since the angle of attack is fixed, this requirement is met by continually descending to a lower altitude, but at a controlled rate so that the lift never becomes too large. As a consequence, the reentry is characterized by the absence of any phugoid or long period oscillations involving the exchange of speed for altitude and vice versa.

For a simple coplanar reentry over a circular non-rotating Earth, the equations of motion are given by

$$m \dot{V} + D - mg \sin \gamma = 0 \quad (A.1)$$

$$m V \dot{\gamma} + L + m \left(\frac{V^2}{r} - g \right) \cos \gamma = 0 \quad (A.2)$$

For an equilibrium glide, all the important effects of interest occur between 100,000 feet and 350,000 feet. Consequently, the values of r and g will vary by less than $\pm 1\%$ from the average values over the above altitude range. Therefore, it is reasonable to make r and g constant.

During an equilibrium glide, it is assumed that the $m V \dot{\gamma}$ term in Eq. (A.2) is negligible compared to the lift. Note that this term cannot always be equal to zero since this would require a constant glide angle.

Finally, the analysis will be restricted to the region for which $\gamma \ll 1$. (For the vehicle used in this investigation, $\gamma < 5^\circ$ until the speed drops to 4300 feet/sec at an altitude of 140,000 feet.) Also, the lift and drag are expressed in the usual manner, in terms of C_L and C_D . Equations (A.1) and (A.2) become

$$\dot{V} + C_D \frac{1}{2} \rho V^2 S/m - g \gamma = 0 \quad (A.3)$$

$$C_L \frac{1}{2} \rho V^2 S/m = \left(g - \frac{V^2}{r} \right) \quad (A.4)$$

Equation (A.4) is then rewritten to give

$$\rho = \frac{2 m}{C_L S r} \frac{1 - s^2}{s^2} \quad (A.5)$$

where the speed ratio is

$$s = V/\sqrt{rg} \quad (A.6)$$

Equation (3.7) can be used to find the temperature as a function of speed. The result is

$$T^4 = K s^{2.15} (1 - s_1^2)^{\frac{1}{2}} \quad (A.7)$$

where

$$K = \frac{17,600 (\sqrt{rg})^{3.15}}{\epsilon \sigma \sqrt{R_n} (26,000)^{3.15} \sqrt{0.002378} \frac{C_L S}{2m} r} \quad (A.8)$$

It is straightforward to show that the peak temperature occurs at

$$s^* = \sqrt{2/3} = 0.8165 \quad (A.9)$$

The use of GM and R_0 from equations (4.7) and (4.8), respectively, and using g and r for the average height of 250,000 feet gives the values at the position of the peak temperature as

$$T^* = 3035 \left(\frac{m}{\epsilon^2 R_n C_L S} \right)^{1/8} {}^\circ R \quad (A.10)$$

$$V^* = 21,050 \text{ feet/sec} \quad (A.11)$$

$$\rho^* = 4.722 \times 10^{-8} \left(\frac{m}{C_L S} \right) \text{ slugs/ft}^3 \quad (A.12)$$

Equations (A.10) to (A.12) show that the peak temperature always occurs at the same speed. Also, the height, y^* (actually the density) is dependent only on the lift coefficient and the wing loading. From Eq. (A.10), the smallest value for T^* is obtained for the maximum value of vertical force, i.e. of $C_L S/m$. Consequently, the smallest T^* is obtained by holding the vehicle at the attitude for $C_{L_{\max}}$. The expression for C_L in Eq. (3.3) is a maximum for an angle of attack of 55 degrees, which is, therefore, the optimum angle.

At the optimum angle of 55 degrees, $C_L S/m$ is 0.5417 sq.ft./slug for the subject vehicle. Substitution of this value together with $\epsilon \sqrt{R_n} = 1.0$ into Eqs. (A.10) and (A.12) yields the values in Table A.1.

An equilibrium glide can be realized very closely in practice if the proper initial conditions are achieved at the initial position. Shown on Figure 26 are the values of speed and glide angle which are required at 350,000 feet altitude above a circular, non-rotating Earth. Initially, the speed and glide angle are adjusted to produce a negligible value for $mV\dot{\gamma}$ in Eq. (A.2). It is found that the required condition of a negligible $mV\dot{\gamma}$ (relative to L) then prevails throughout the flight without any additional control. The values of T^* , V^* , ρ^* are also shown in Table A.1 for the trajectory computed from the exact equations. The value of y^* is also included for this case and may be compared to the value of $y^*(\rho^*)$ which results from Eq. (A.12) when the U.S. Standard atmosphere, 1962 is the curve of density versus altitude. The same curve was used for the numerically computed trajectory.

The agreement between the two sets of data shows that equations (A.10) to (A.12) are quite accurate. Consequently, the standard peak temperature, T^* , as given by Eq. (A.10) is shown to be independent of (L/D) . Also, the smallest value of T^* is achieved for the smallest value of $(m/\epsilon^2 R_n C_L S)$. In addition, because of the $1/8$ power, the gains to be realized from even a 50% reduction in this parameter are not large; when T^* equals 3000°F, the reduction in T^* is only 320°F or only a little more than 10%.

TABLE A1

Flight Conditions at the Position of Peak Temperature During an Equilibrium Glide

Value	Approximate Analytical Results ⁺	Numerical Integration of Exact Equations [‡]
T*	2817°F	2810°F
V*	21,050 feet/sec	20,800 feet/sec
ρ^*	8.72×10^{-8} slugs/ft ³	9.27×10^{-8} slugs/ft ³
y*	245,500 feet***	243,800 feet***

+ equations (A.10) to (A.12)

‡ initial conditions of Fig. 26

*** corresponding to ρ^* for the U.S. Standard Atmosphere, 1962

APPENDIX B

The Effective Initial Glide Angle

The definition of the effective initial glide angle over an oblate Earth is quite straightforward. It simply takes account of the effective change in height of the vehicle which occurs during Phase II of the reentry due to the change in the Earth's radius. This portion of the flight has been chosen since it is during this period that both the peak temperature and the overall down range are determined. As shown in Fig. 37, the change in the Earth's radius may be used to give

$$\sin \Delta \gamma = \frac{\Delta y}{s} \quad (\text{B.1})$$

where Δy is defined in Fig. 37.

For this investigation, both γ and $\Delta \gamma$ are always very small during Phase II. Consequently, the small angle approximation may be used to give

$$\gamma_{\text{eff}} = \gamma_e + \frac{\Delta y}{s} \quad (\text{B.2})$$

In practice, Δy is always very easy to find. It is the difference in the height over the Earth's surface when the same change that takes place during Phase II in geocentric latitude also occurs at the average geocentric radius which is used during Phase II. The value of s is the flight distance travelled during this portion of the reentry.

Program List

[illegible]

```

C THIS PROGRAM INCLUDES PROVISIONS FOR -
C 1. A VARIABLE VEHICLE ATTITUDE TO MINIMIZE TEMPERATURE AND
C ACCELERATION PEAKS AND TO MAXIMIZE CROSS RANGE
C 2. EARTH ORIENTATION
C 3. EQUIVALENT RANGE COMPUTATIONS AND THEIR OPTIMAL POINTOUT
C 4. INTERMEDIATE POINTOUTS AT SPECIFICATION POINTS
C 5. CONTINUOUS VARIABLE STEP SIZE CONTROL
C SUMMARY OF SUBROUTINES NOT INCLUDED IN SUMMARY
C
C A. THE FOLLOWING ROUTINES CONTAIN VITAL PROGRAMMING FEATURES
C WHICH MUST BE PRESENT SINCE THEY ARE ALWAYS USED -
C CALDA INITIAL COMPUTATIONS OF RANGE AND RANGE RATE
C SNGCSA SNGCRS SNGCPS SNGSPN SNGTTH AFROTH AFROCS
C APRACS APRARS APRARS APRACS APRARS APRARS APRARS APRARS
C B. THE FOLLOWING ROUTINES ARE VITAL TO THE PROGRAM SINCE
C WHICH MUST BE PRESENT IF USED. THE QUANTITY DISPLAY VALUES WILL
C halt computation if they are used instead of the actual
C routine with the proper programming features -
C SNGCRS SNGCRS SNGCRS SNGCRS SNGCRS SNGCRS SNGCRS SNGCRS
C PTBTS PTBTS RADIUS RANGE PITCH PITCH PITCH PITCH
C C. THE FOLLOWING ROUTINES ALLOW CONTROL TO PROCEED THROUGHOUT THEM
C WHEN THEY ARE USED IF NO ACTUAL VITAL PROGRAMMING FEATURES
C NECESSARY
C CMSPS DECT - DECT DECT DECT DECT DECT DECT DECT DECT
C CMSPS DECT DECT DECT DECT DECT DECT DECT DECT
C SUMMARY OF SENSITIVE CONTROL SETTINGS
C
C A. FOR PROGRAM CONTROL
C (1) AT 544 TO TERMINATE CASE WITH OR WITHOUT FIVE MORE STEPS
C (2) AT 544 TO TERMINATE CASE WITH OR WITHOUT FIVE MORE STEPS
C (3) AT 942 TO TERMINATE COMPUTATION AT END OF CURRENT CASE
C (4) AT 940 AND 976 TO POINT OPERATOR CASE MESSAGE WHEN
C KTRAX IS POS AND POSITIVE RESPECTIVELY.
C (5) AT 976 TO STOP
C WHEN KTRAX IS NEGATIVE
C
C B. FOR SPECIAL DEBUG OUTPUTS: PROGRAMMER MUST TO GIVEN STATEMENT
C WHEN LUMPING CASES TO POINT OPERATOR WHEN OR NOT THE NEXT
C STATEMENT IS EXECUTED ON SKIPPED
C
C 1001 1001 2001 3001
C 4001 4001 5001 6001
C 8001 8001
C 9001

```

PAGE 1

MAIN PROGRAM A-9	PAGE	1
-------------------------	-------------	----------

C SUMMARY OF VALUES WHICH MAY BE CHANGED UNDER CONTROL OF COSTS

C	CODE	STATEMENT	FORMAT	LIST	OF	VALUES
C	1	123	26	VHNDL	VFIND	VHNDL
C	2	126	26	PHNDL	PHNDL	PHNDL
C	4	120	26	PHNDL	PHNDL	PHNDL
C	10	152	32	APLUT	APLUT	APLUT
C	20	154	34	APLUT	APLUT	APLUT
C	40	156	34	APLUT	APLUT	APLUT
C	100	162	42	APLUT	APLUT	APLUT
C	204	166	46	APLUT	APLUT	APLUT
C	404	169	49	APLUT	APLUT	APLUT
C	1003	173	53	APLUT	APLUT	APLUT
C	2003	175	55	APLUT	APLUT	APLUT
C	4003	179	59	APLUT	APLUT	APLUT
C	10003	183	63	APLUT	APLUT	APLUT
C	20003	185	65	APLUT	APLUT	APLUT
C	40003	189	69	APLUT	APLUT	APLUT
C	100003	193	73	APLUT	APLUT	APLUT
C	200003	195	75	APLUT	APLUT	APLUT
C	400003	199	79	APLUT	APLUT	APLUT
C	1000003	203	83	APLUT	APLUT	APLUT
C	2000003	205	85	APLUT	APLUT	APLUT
C	4000003	209	89	APLUT	APLUT	APLUT
C	10000003	213	93	APLUT	APLUT	APLUT
C	20000003	215	95	APLUT	APLUT	APLUT
C	40000003	219	99	APLUT	APLUT	APLUT
C	100000003	223	103	APLUT	APLUT	APLUT
C	200000003	225	105	APLUT	APLUT	APLUT
C	400000003	229	109	APLUT	APLUT	APLUT
C	1000000003	233	113	APLUT	APLUT	APLUT
C	2000000003	235	115	APLUT	APLUT	APLUT
C	4000000003	239	119	APLUT	APLUT	APLUT
C	10000000003	243	123	APLUT	APLUT	APLUT
C	20000000003	245	125	APLUT	APLUT	APLUT
C	40000000003	249	129	APLUT	APLUT	APLUT
C	100000000003	253	133	APLUT	APLUT	APLUT
C	200000000003	255	135	APLUT	APLUT	APLUT
C	400000000003	259	139	APLUT	APLUT	APLUT
C	1000000000003	263	143	APLUT	APLUT	APLUT
C	2000000000003	265	145	APLUT	APLUT	APLUT
C	4000000000003	269	149	APLUT	APLUT	APLUT
C	10000000000003	273	153	APLUT	APLUT	APLUT
C	20000000000003	275	155	APLUT	APLUT	APLUT
C	40000000000003	279	159	APLUT	APLUT	APLUT
C	100000000000003	283	163	APLUT	APLUT	APLUT
C	200000000000003	285	165	APLUT	APLUT	APLUT
C	400000000000003	289	169	APLUT	APLUT	APLUT
C	1000000000000003	293	173	APLUT	APLUT	APLUT
C	2000000000000003	295	175	APLUT	APLUT	APLUT
C	4000000000000003	299	179	APLUT	APLUT	APLUT
C	10000000000000003	303	183	APLUT	APLUT	APLUT
C	20000000000000003	305	185	APLUT	APLUT	APLUT
C	40000000000000003	309	189	APLUT	APLUT	APLUT
C	100000000000000003	313	193	APLUT	APLUT	APLUT
C	200000000000000003	315	195	APLUT	APLUT	APLUT
C	400000000000000003	319	199	APLUT	APLUT	APLUT
C	1000000000000000003	323	203	APLUT	APLUT	APLUT
C	2000000000000000003	325	205	APLUT	APLUT	APLUT
C	4000000000000000003	329	209	APLUT	APLUT	APLUT
C	10000000000000000003	333	213	APLUT	APLUT	APLUT
C	20000000000000000003	335	215	APLUT	APLUT	APLUT
C	40000000000000000003	339	219	APLUT	APLUT	APLUT
C	100000000000000000003	343	223	APLUT	APLUT	

MAIN PROGRAM 6.9 PAGE 2

MAIN PROGRAM 4.0 PAGE 4

[illegible]

```

C      EQUIVALENCE STATEMENTS FOR GLOBAL VARIABLES
      EQUIVALENCE (V7,V20),(V10,V1),(P1,P0),(F300A,G300A),(P11,P10)
      EQUIVALENCE (V8,V21),(V11,V2),(P2,P0),(F300B,G300B),(P12,P10)
      EQUIVALENCE (V9,V22),(V12,V3),(P3,P0),(F300C,G300C),(P13,P10)
      EQUIVALENCE (V10,V23),(V13,V4),(P4,P0),(F300D,G300D),(P14,P10)
      EQUIVALENCE (V11,V24),(V14,V5),(P5,P0),(F300E,G300E),(P15,P10)
      EQUIVALENCE (V12,V25),(V15,V6),(P6,P0),(F300F,G300F),(P16,P10)
      EQUIVALENCE (V13,V26),(V16,V7),(P7,P0),(F300G,G300G),(P17,P10)
      EQUIVALENCE (V14,V27),(V17,V8),(P8,P0),(F300H,G300H),(P18,P10)
      EQUIVALENCE (V15,V28),(V18,V9),(P9,P0),(F300I,G300I),(P19,P10)
      EQUIVALENCE (V16,V29),(V19,V10),(P10,P0),(F300J,G300J),(P20,P10)
      EQUIVALENCE (V17,V30),(V20,V11),(P11,P0),(F300K,G300K),(P21,P10)
      EQUIVALENCE (V18,V31),(V21,V12),(P12,P0),(F300L,G300L),(P22,P10)
      EQUIVALENCE (V19,V32),(V22,V13),(P13,P0),(F300M,G300M),(P23,P10)
      EQUIVALENCE (V20,V33),(V23,V14),(P14,P0),(F300N,G300N),(P24,P10)
      EQUIVALENCE (V21,V34),(V24,V15),(P15,P0),(F300O,G300O),(P25,P10)
      EQUIVALENCE (V22,V35),(V25,V16),(P16,P0),(F300P,G300P),(P26,P10)
      EQUIVALENCE (V23,V36),(V26,V17),(P17,P0),(F300Q,G300Q),(P27,P10)
      EQUIVALENCE (V24,V37),(V27,V18),(P18,P0),(F300R,G300R),(P28,P10)
      EQUIVALENCE (V25,V38),(V28,V19),(P19,P0),(F300S,G300S),(P29,P10)
      EQUIVALENCE (V26,V39),(V29,V20),(P20,P0),(F300T,G300T),(P30,P10)
      EQUIVALENCE (V27,V40),(V30,V21),(P21,P0),(F300U,G300U),(P31,P10)
      EQUIVALENCE (V28,V41),(V31,V22),(P22,P0),(F300V,G300V),(P32,P10)
      EQUIVALENCE (V29,V42),(V32,V23),(P23,P0),(F300W,G300W),(P33,P10)
      EQUIVALENCE (V30,V43),(V33,V24),(P24,P0),(F300X,G300X),(P34,P10)
      EQUIVALENCE (V31,V44),(V34,V25),(P25,P0),(F300Y,G300Y),(P35,P10)
      EQUIVALENCE (V32,V45),(V35,V26),(P26,P0),(F300Z,G300Z),(P36,P10)
      EQUIVALENCE (V33,V46),(V36,V27),(P27,P0),(F300AA,G300AA),(P37,P10)
      EQUIVALENCE (V34,V47),(V37,V28),(P28,P0),(F300AB,G300AB),(P38,P10)
      EQUIVALENCE (V35,V48),(V38,V29),(P29,P0),(F300AC,G300AC),(P39,P10)
      EQUIVALENCE (V36,V49),(V39,V30),(P30,P0),(F300AD,G300AD),(P40,P10)
      EQUIVALENCE (V37,V50),(V40,V31),(P31,P0),(F300AE,G300AE),(P41,P10)
      EQUIVALENCE (V38,V51),(V41,V32),(P32,P0),(F300AF,G300AF),(P42,P10)
      EQUIVALENCE (V39,V52),(V42,V33),(P33,P0),(F300AG,G300AG),(P43,P10)
      EQUIVALENCE (V40,V53),(V43,V34),(P34,P0),(F300AH,G300AH),(P44,P10)
      EQUIVALENCE (V41,V54),(V44,V35),(P35,P0),(F300AI,G300AI),(P45,P10)
      EQUIVALENCE (V42,V55),(V45,V36),(P36,P0),(F300AJ,G300AJ),(P46,P10)
      EQUIVALENCE (V43,V56),(V46,V37),(P37,P0),(F300AK,G300AK),(P47,P10)
      EQUIVALENCE (V44,V57),(V47,V38),(P38,P0),(F300AL,G300AL),(P48,P10)
      EQUIVALENCE (V45,V58),(V48,V39),(P39,P0),(F300AM,G300AM),(P49,P10)
      EQUIVALENCE (V46,V59),(V49,V40),(P40,P0),(F300AN,G300AN),(P50,P10)
      EQUIVALENCE (V47,V60),(V50,V41),(P41,P0),(F300AO,G300AO),(P51,P10)
      EQUIVALENCE (V48,V61),(V51,V42),(P42,P0),(F300AP,G300AP),(P52,P10)
      EQUIVALENCE (V49,V62),(V52,V43),(P43,P0),(F300AQ,G300AQ),(P53,P10)
      EQUIVALENCE (V50,V63),(V53,V44),(P44,P0),(F300AR,G300AR),(P54,P10)
      EQUIVALENCE (V51,V64),(V54,V45),(P45,P0),(F300AS,G300AS),(P55,P10)
      EQUIVALENCE (V52,V65),(V55,V46),(P46,P0),(F300AT,G300AT),(P56,P10)
      EQUIVALENCE (V53,V66),(V56,V47),(P47,P0),(F300AU,G300AU),(P57,P10)
      EQUIVALENCE (V54,V67),(V57,V48),(P48,P0),(F300AV,G300AV),(P58,P10)
      EQUIVALENCE (V55,V68),(V58,V49),(P49,P0),(F300AW,G300AW),(P59,P10)
      EQUIVALENCE (V56,V69),(V59,V50),(P50,P0),(F300AX,G300AX),(P60,P10)
      EQUIVALENCE (V57,V70),(V60,V51),(P51,P0),(F300AY,G300AY),(P61,P10)
      EQUIVALENCE (V58,V71),(V61,V52),(P52,P0),(F300AZ,G300AZ),(P62,P10)
      EQUIVALENCE (V59,V72),(V62,V53),(P53,P0),(F300BA,G300BA),(P63,P10)
      EQUIVALENCE (V60,V73),(V63,V54),(P54,P0),(F300BB,G300BB),(P64,P10)
      EQUIVALENCE (V61,V74),(V64,V55),(P55,P0),(F300BC,G300BC),(P65,P10)
      EQUIVALENCE (V62,V75),(V65,V56),(P56,P0),(F300BD,G300BD),(P66,P10)
      EQUIVALENCE (V63,V76),(V66,V57),(P57,P0),(F300BE,G300BE),(P67,P10)
      EQUIVALENCE (V64,V77),(V67,V58),(P58,P0),(F300BF,G300BF),(P68,P10)
      EQUIVALENCE (V65,V78),(V68,V59),(P59,P0),(F300BG,G300BG),(P69,P10)
      EQUIVALENCE (V66,V79),(V69,V60),(P60,P0),(F300BH,G300BH),(P70,P10)
      EQUIVALENCE (V67,V80),(V70,V61),(P61,P0),(F300BI,G300BI),(P71,P10)
      EQUIVALENCE (V68,V81),(V71,V62),(P62,P0),(F300BJ,G300BJ),(P72,P10)
      EQUIVALENCE (V69,V82),(V72,V63),(P63,P0),(F300BK,G300BK),(P73,P10)
      EQUIVALENCE (V70,V83),(V73,V64),(P64,P0),(F300BL,G300BL),(P74,P10)
      EQUIVALENCE (V71,V84),(V74,V65),(P65,P0),(F300BM,G300BM),(P75,P10)
      EQUIVALENCE (V72,V85),(V75,V66),(P66,P0),(F300BN,G300BN),(P76,P10)
      EQUIVALENCE (V73,V86),(V76,V67),(P67,P0),(F300BO,G300BO),(P77,P10)
      EQUIVALENCE (V74,V87),(V77,V68),(P68,P0),(F300BP,G300BP),(P78,P10)
      EQUIVALENCE (V75,V88),(V78,V69),(P69,P0),(F300BQ,G300BQ),(P79,P10)
      EQUIVALENCE (V76,V89),(V79,V70),(P70,P0),(F300BR,G300BR),(P80,P10)
      EQUIVALENCE (V77,V90),(V80,V71),(P71,P0),(F300BS,G300BS),(P81,P10)
      EQUIVALENCE (V78,V91),(V81,V72),(P72,P0),(F300BT,G300BT),(P82,P10)
      EQUIVALENCE (V79,V92),(V82,V73),(P73,P0),(F300BU,G300BU),(P83,P10)
      EQUIVALENCE (V80,V93),(V83,V74),(P74,P0),(F300BV,G300BV),(P84,P10)
      EQUIVALENCE (V81,V94),(V84,V75),(P75,P0),(F300BW,G300BW),(P85,P10)
      EQUIVALENCE (V82,V95),(V85,V76),(P76,P0),(F300BX,G300BX),(P86,P10)
      EQUIVALENCE (V83,V96),(V86,V77),(P77,P0),(F300BY,G300BY),(P87,P10)
      EQUIVALENCE (V84,V97),(V87,V78),(P78,P0),(F300BZ,G300BZ),(P88,P10)
      EQUIVALENCE (V85,V98),(V88,V79),(P79,P0),(F300CA,G300CA),(P89,P10)
      EQUIVALENCE (V86,V99),(V89,V80),(P80,P0),(F300CB,G300CB),(P90,P10)
      EQUIVALENCE (V87,V100),(V90,V81),(P81,P0),(F300CC,G300CC),(P91,P10)
      EQUIVALENCE (V88,V101),(V91,V82),(P82,P0),(F300CD,G300CD),(P92,P10)
      EQUIVALENCE (V89,V102),(V92,V83),(P83,P0),(F300CE,G300CE),(P93,P10)
      EQUIVALENCE (V90,V103),(V93,V84),(P84,P0),(F300CF,G300CF),(P94,P10)
      EQUIVALENCE (V91,V104),(V94,V85),(P85,P0),(F300CG,G300CG),(P95,P10)
      EQUIVALENCE (V92,V105),(V95,V86),(P86,P0),(F300CH,G300CH),(P96,P10)
      EQUIVALENCE (V93,V106),(V96,V87),(P87,P0),(F300CI,G300CI),(P97,P10)
      EQUIVALENCE (V94,V107),(V97,V88),(P88,P0),(F300CJ,G300CJ),(P98,P10)
      EQUIVALENCE (V95,V108),(V98,V89),(P89,P0),(F300CK,G300CK),(P99,P10)
      EQUIVALENCE (V96,V109),(V99,V90),(P90,P0),(F300CL,G300CL),(P100,P10)
      EQUIVALENCE (V97,V110),(V100,V91),(P91,P0),(F300CM,G3
```

[illegible]

```

C  DOUBLE PRECISION STATEMENTS FOR GOPTNS VARIABLES
DOUBLE PRECISION SUMAT,SOMATP,SOMATL,SOMATL,SUMTPO
DOUBLE PRECISION TOUNIN(6)

C  EQUIVALENCE STATEMENTS FOR GOPTNS VARIABLES
EQUIVALENCE (SUMTPO,SUMTPO),(IACPR,ACCP),(IITWRP,TWRP)

```



```

C PRINT CHECK CONTROL IMPLEMENTATION SENSE SWITCH CONTROL
620 IFI SWSWT 1 6201,6203,6201
6201 IFI SWITCH(620) 1 6202,6203,6202
6202 AA = PUT
6203 CONTINUE

C POINT EVALUATION - OUTPUT TEST ON JAIL AT END OF SEQUENCE
621 V20 = V2TOMP
SD = STEMPD
GAMMA = GTEMPD
PSIO = PTEMPD
DELTA0 = DTEMPD
TMTAD = TTEMPD
TMD0 = TTEMPD
RTAD = RTEMPD
ENCLAD = ETEMPD
SO = STEMPD
PTEMP = PV
COUNT = (ANAL1) + COUNT
GASPR = GASPR + ANCLAD
ANCLD2 = SIGN1 ANAL1 AMOLD2, ACCEL2 1, TEST2 1
ALMOL2 = ANAL1 SIGN1 1.0E6, TEST2 1, ANAL1(AMOLD2,ACCEL2) 1

IFI BOLD1 MTP 1 1 622, 624, 622
IFI MTP 1 623, 625, 623
623 ON 524 IF = 1, MTP
624 TEMPO(11) = TEMPO(11) + ATPO(11)
624 TAMOL = SIGN1 ANAL1 TAMOL, TAMOL 1, TEST2 1
TAMOL = ANAL1 SIGN1 1.0E20, TEST2 1, ANAL1(TAMOL,TAMOL) 1

626 IFI ATALP = ATALP 1 627, 631, 627
627 CALL PITCHA

631 IFI IGNORE 1 632, 635, 632
632 MTP = MTP + 1
IFI 63 = MTP + MTP/100000 - IGNORE+1/100000 1 633, 636, 633
633 ICTRL = MTP/100000
JAIL = JAIL + 1
IOTCL(JAIL) = ICTRL
WRITE(6,84) MTP,MTP,(IOTCL(1),IOTCL(2),K=1,MUSL)
COUNT = COUNT + 1
LAST = COUNT / 15
IFI IOSTOP 1 634, 610, 610
634 IOSTOP = 0
635 OS = 1.0
IFI IOSTOP 1 636, 636, 637
636 IOSTOP = 0
637 MTP = MTP + 100
IFI MTP = MTP/100000 + MUSL - 65 1 638, 633, 633
638 IFI JAIL 1 610, 700, 610

```

```

C OUTPUT CONTROLS SENSE SWITCH CONTROL
600 IFI SWSWT 1 6001,6003,6001
6001 IFI SWITCH(600) 1 6002,6003,6002
6002 AA = PUT
6003 CONTINUE

C OUTPUT CONTROLS SENSE SWITCH CONTROL
601 ICPDYN = - ICPDYN
JAIL = JAIL + 1
IOTCL(JAIL) = ICTRL
IFI ILAST 1 602, 603, 620
602 ILAST = 1
PV = SORTI(21)
PV = PTEMP
GO TO 310
603 OS = 0.0
COUNT = COUNT + 1
IFI IL = JAIL 1 604, 604, 509
WRITE(6,84) MTP,MTP,(IOTCL(1),IOTCL(2),K=1,MUSL)
WRITE(6,84) JAIL,IOTCL(1),K=1,JAIL
604 FORMATE 1M0, 1N, 1N16 / ( 1N, 1N16 ) 1
PVWD = PV
ACFW = ACCEL2
TAMW = TAMOL
PV = SORTI(21)
PV = PTEMP
ACCEL2 = ACCEL AMOLD2 1
TAMOL = ACCEL TAMOL 1
LAST = 1
GO TO 610
610 PV = SORTI(2TEMP)
PV = PVWD
ACCEL2 = ACFW
TAMOL = TAMW
LAST = 1
GO TO 670

C FINAL OUTPUT CONTROL
611 JAIL = JAIL + 1
612 IOTCL(JAIL) = ICTRL
LAST = 1
GO TO 670

```

```

C OUTPUT OF INTERMEDIATE VALUES SENSE SWITCH CONTROL
610 IFI SWSWT 1 6101,6103,6101
6101 IFI SWITCH(610) 1 6102,6103,6102
6102 AA = PUT
6103 CONTINUE

C OUTPUT OF INTERMEDIATE VALUES
611 CALL OUTPUT

C INITIALIZATION OF INTERMEDIATE CONTROL VALUES
601 IFI ILAST 1 602, 602, 610
602 OS = 1.0
IGNORE = 0
JAIL = 0
MTP = 0
MUSL = 0
IFI M = MSTOP 1 200, 610, 610

C OUTPUT OF FINAL AND STORED VALUES SENSE SWITCH CONTROL
612 IFI SWSWT 1 6101,6103,6101
6101 IFI SWITCH(610) 1 6102,6103,6102
6102 AA = PUT
6103 CONTINUE

C OUTPUT OF FINAL AND STORED VALUES
611 CALL OUTPUT
612 IFI M = MSTOP 1 100, 612, 616
613 IFI SWITCH(611) 1 100, 616, 100
614 M = 0
IFI ABS(CITVLE).LT.2.0.OR.LAST.GT.0.OR.MSTOP.LE.10 1 GO TO 100
CITVLE = SIGN1 ABS(CITVLE) - 2.0, CITVLE 1
VD = DSCITE 620 3
WRITE(6,94) M,CAIF,CITVLE,VD,80
615 FORMATE 17M1 CASE NUMBER, 10, 50, 11M(CONTINUED), 120.0 /
1 7M00 CONTINUED VELOCITY = 50022.10, 0M PT/SEC., SE. /
2 1M(CONTINUED) GYROCENTRIC RADIUS = 8024.0, 7M FEET /
3 1M0, 22R, 5M(10F, 37R, 10M M G L E S O F /
4 5M VELOCITY ALTITUDE ANGLE AZIMUTH LATITUDE LONGIT /
5 11M0F TIME ATTACK ROLL NO. ACCEL TEMP(1) CNT 1
IFI BOLD(12VLE) 1 616, 616, 616
616 IFI CITVLE 1 617, 617, 618
617 WRITE(6,97)
618 FORMATE 1M0, 10M, 11M MTP MJS J, 61 4M IOT 1 /
1 23M (PT/SEC) (FEET) = 41 5M(DEC), 61 1, 0M(SEC) /
2 15M(DEC) IOTG 10'S 1 DEC-91 1
GO TO 610
619 WRITE(6,98)
619 FORMATE 1M0, 10M, 23M COMMR CROSSA PSIG /
1 23M (PT/SEC) (FEET) = 41 5M(DEC), 61 1, 0M(SEC) /
2 15M(DEC) IDECI 10'S 1 DEC-91 = 31 4M(DEC) 1 1
619 CALL OUTPUT
GO TO 700
END

```



```

C COMMON STATEMENTS FOR SUBROUTINE VARIABLES
C COMMON /CDISTF1/ DSUMF(17),PMH1(1),PMH2(2),DSUMH(11)
C /CFCAL/ F,DMH1(1),DMH2(2),DMH3(3),DMH4(4),DMH5(5),DMH6(6),DMH7(7),DMH8(8),DMH9(9),DMH10(10),DMH11(11),DMH12(12),DMH13(13),DMH14(14),DMH15(15),DMH16(16),DMH17(17),DMH18(18),DMH19(19),DMH20(20),DMH21(21),DMH22(22),DMH23(23),DMH24(24),DMH25(25),DMH26(26),DMH27(27),DMH28(28),DMH29(29),DMH30(30),DMH31(31),DMH32(32),DMH33(33),DMH34(34),DMH35(35),DMH36(36),DMH37(37),DMH38(38),DMH39(39),DMH40(40),DMH41(41),DMH42(42),DMH43(43),DMH44(44),DMH45(45),DMH46(46),DMH47(47),DMH48(48),DMH49(49),DMH50(50),DMH51(51),DMH52(52),DMH53(53),DMH54(54),DMH55(55),DMH56(56),DMH57(57),DMH58(58),DMH59(59),DMH60(60),DMH61(61),DMH62(62),DMH63(63),DMH64(64),DMH65(65),DMH66(66),DMH67(67),DMH68(68),DMH69(69),DMH70(70),DMH71(71),DMH72(72),DMH73(73),DMH74(74),DMH75(75),DMH76(76),DMH77(77),DMH78(78),DMH79(79),DMH80(80),DMH81(81),DMH82(82),DMH83(83),DMH84(84),DMH85(85),DMH86(86),DMH87(87),DMH88(88),DMH89(89),DMH90(90),DMH91(91),DMH92(92),DMH93(93),DMH94(94),DMH95(95),DMH96(96),DMH97(97),DMH98(98),DMH99(99),DMH100(100),DMH101(101),DMH102(102),DMH103(103),DMH104(104),DMH105(105),DMH106(106),DMH107(107),DMH108(108),DMH109(109),DMH110(110),DMH111(111),DMH112(112),DMH113(113),DMH114(114),DMH115(115),DMH116(116),DMH117(117),DMH118(118),DMH119(119),DMH120(120),DMH121(121),DMH122(122),DMH123(123),DMH124(124),DMH125(125),DMH126(126),DMH127(127),DMH128(128),DMH129(129),DMH130(130),DMH131(131),DMH132(132),DMH133(133),DMH134(134),DMH135(135),DMH136(136),DMH137(137),DMH138(138),DMH139(139),DMH140(140),DMH141(141),DMH142(142),DMH143(143),DMH144(144),DMH145(145),DMH146(146),DMH147(147),DMH148(148),DMH149(149),DMH150(150),DMH151(151),DMH152(152),DMH153(153),DMH154(154),DMH155(155),DMH156(156),DMH157(157),DMH158(158),DMH159(159),DMH160(160),DMH161(161),DMH162(162),DMH163(163),DMH164(164),DMH165(165),DMH166(166),DMH167(167),DMH168(168),DMH169(169),DMH170(170),DMH171(171),DMH172(172),DMH173(173),DMH174(174),DMH175(175),DMH176(176),DMH177(177),DMH178(178),DMH179(179),DMH180(180),DMH181(181),DMH182(182),DMH183(183),DMH184(184),DMH185(185),DMH186(186),DMH187(187),DMH188(188),DMH189(189),DMH190(190),DMH191(191),DMH192(192),DMH193(193),DMH194(194),DMH195(195),DMH196(196),DMH197(197),DMH198(198),DMH199(199),DMH200(200),DMH201(201),DMH202(202),DMH203(203),DMH204(204),DMH205(205),DMH206(206),DMH207(207),DMH208(208),DMH209(209),DMH210(210),DMH211(211),DMH212(212),DMH213(213),DMH214(214),DMH215(215),DMH216(216),DMH217(217),DMH218(218),DMH219(219),DMH220(220),DMH221(221),DMH222(222),DMH223(223),DMH224(224),DMH225(225),DMH226(226),DMH227(227),DMH228(228),DMH229(229),DMH230(230),DMH231(231),DMH232(232),DMH233(233),DMH234(234),DMH235(235),DMH236(236),DMH237(237),DMH238(238),DMH239(239),DMH240(240),DMH241(241),DMH242(242),DMH243(243),DMH244(244),DMH245(245),DMH246(246),DMH247(247),DMH248(248),DMH249(249),DMH250(250),DMH251(251),DMH252(252),DMH253(253),DMH254(254),DMH255(255),DMH256(256),DMH257(257),DMH258(258),DMH259(259),DMH260(260),DMH261(261),DMH262(262),DMH263(263),DMH264(264),DMH265(265),DMH266(266),DMH267(267),DMH268(268),DMH269(269),DMH270(270),DMH271(271),DMH272(272),DMH273(273),DMH274(274),DMH275(275),DMH276(276),DMH277(277),DMH278(278),DMH279(279),DMH280(280),DMH281(281),DMH282(282),DMH283(283),DMH284(284),DMH285(285),DMH286(286),DMH287(287),DMH288(288),DMH289(289),DMH290(290),DMH291(291),DMH292(292),DMH293(293),DMH294(294),DMH295(295),DMH296(296),DMH297(297),DMH298(298),DMH299(299),DMH300(300),DMH301(301),DMH302(302),DMH303(303),DMH304(304),DMH305(305),DMH306(306),DMH307(307),DMH308(308),DMH309(309),DMH310(310),DMH311(311),DMH312(312),DMH313(313),DMH314(314),DMH315(315),DMH316(316),DMH317(317),DMH318(318),DMH319(319),DMH320(320),DMH321(321),DMH322(322),DMH323(323),DMH324(324),DMH325(325),DMH326(326),DMH327(327),DMH328(328),DMH329(329),DMH330(330),DMH331(331),DMH332(332),DMH333(333),DMH334(334),DMH335(335),DMH336(336),DMH337(337),DMH338(338),DMH339(339),DMH340(340),DMH341(341),DMH342(342),DMH343(343),DMH344(344),DMH345(345),DMH346(346),DMH347(347),DMH348(348),DMH349(349),DMH350(350),DMH351(351),DMH352(352),DMH353(353),DMH354(354),DMH355(355),DMH356(356),DMH357(357),DMH358(358),DMH359(359),DMH360(360),DMH361(361),DMH362(362),DMH363(363),DMH364(364),DMH365(365),DMH366(366),DMH367(367),DMH368(368),DMH369(369),DMH370(370),DMH371(371),DMH372(372),DMH373(373),DMH374(374),DMH375(375),DMH376(376),DMH377(377),DMH378(378),DMH379(379),DMH380(380),DMH381(381),DMH382(382),DMH383(383),DMH384(384),DMH385(385),DMH386(386),DMH387(387),DMH388(388),DMH389(389),DMH390(390),DMH391(391),DMH392(392),DMH393(393),DMH394(394),DMH395(395),DMH396(396),DMH397(397),DMH398(398),DMH399(399),DMH400(400),DMH401(401),DMH402(402),DMH403(403),DMH404(404),DMH405(405),DMH406(406),DMH407(407),DMH408(408),DMH409(409),DMH410(410),DMH411(411),DMH412(412),DMH413(413),DMH414(414),DMH415(415),DMH416(416),DMH417(417),DMH418(418),DMH419(419),DMH420(420),DMH421(421),DMH422(422),DMH423(423),DMH424(424),DMH425(425),DMH426(
```

[illegible][illegible][illegible]

```

C INITIALIZATION OF ROTATIONAL AND GRAVITATIONAL TERMS
131 IF1 ACCEL GROT 1 1 172, 173, 177
172 ROTG = 0.0
      ROTP = 0.0
      ROTV = 0.0
      GO TO 176
176 IF1 GROT GROT 1 1 174, 175, 177
175 IF1 GROT 1 175, 175, 177
176 ROTG = (( SIN(COSGAMMA) * COS(COS122) + COS(DELTA)
      - COS(GAMMA) ) / COS(DELTA) ) * COS(DELTA) ) * 0
1      W2 = 0 + COS(DELTA) / W2
2      - SIN(C121) * COS(DELTA) * W / V
      ROTP = SIN(C121) * SIN(DELTA) * COS(GAMMA) + W * W * COS(DELTA) * W2
1      W2 = (( SIN(GAMMA) / COS(GAMMA) ) * COS(C121) * COS(DELTA)
2      + SIN(DELTA) ) * 0 * W / V
      ROTV = (( COS(GAMMA) * COS(C121) + SIN(DELTA)
      + SIN(GAMMA) ) * COS(DELTA) ) * 0
3      W2 = 0 + COS(DELTA) * 0 - 1.0 ?
176 GRAVED = 0.0
      GRAVX = 0.0
      GRAVY = 0.0
      GRAVZ = 0.0
      COMPMAN = 1.000
      PMO = 0.0
      PVM = 0.0
177 IF1 GRAVY 0.0 0 170, 170, 101
170 GRAVY = -1.0
177 COMPMAN = 0.0

```

SUBJ: [REDACTED]
DATE: 10/10/2001
PAGE: 1

[illegible]

C normal return from substituting initial
101 return


```

131 OVIER1) = 1      GRAYV = SING -      DGR4      = 0
132          =      GRAYV + ROTC 1) *      Z.0      = 0.05
133 OTH1) =      SPORCH      = 0.05
134 OTH1) = -      SING      = 0.05
135 OTF1) =      1.79PV      = 0.05
136 OTH1) =      CGOFA      = 0.05
332 IPI ENDR12 = ACCEL1 + ENDR21 335, 334, 334
333 IPI ACCEL2 = ENDR22 + ENDR23 334, 334, 335
334 OTH1) = ACCEL2 + ENDR42 + ENDR43 / PV      = 0.05
GO TO 337
335 OTH1) = ENDR44 + ENDR45 + ENDR46 + ENDR47 / ENDR48 / PV      = 0.05
GO TO 337
336 OTH1) = 0.0
337 IENDTV = 0

C.
INTERGRATION BY A FOURTH ORDER RUNGE-KUTTA METHOD
351 AC = ( D0113 ) + D0121 ) D0131 102.0 D0141 1) = 0.00052
AP = ( D0113 ) + D0121 ) D0131 102.0 D0141 1) = 0.00052
AD = ( D0113 ) + D0121 ) D0131 102.0 D0141 1) = 0.00052
AV2 = ( D0121 ) + D0131 ) D0141 102.0 D0151 1) = 0.00052
AR = ( D0113 ) + D0121 ) D0131 102.0 D0141 1) = 0.00052
AT = ( D0131 ) + D0141 ) D0151 102.0 D0161 1) = 0.00052
ATI = ( D0113 ) + D0121 ) D0131 102.0 D0141 1) = 0.00052
AR = ( D0113 ) + D0121 ) D0131 102.0 D0141 1) = 0.00052
AT = ( D0131 ) + D0141 ) D0151 102.0 D0161 1) = 0.00052
IPI AT1 = 1 332, 340, 352
352 OM 333 IT = 1: NTP
353 ATP11,1) = D0121,1) + D0131,1) + D0141,1) + D0151,1) + D0161,1) = 0.00052

360 IPI ENDR12 1 3401,3403,3401
3603 IPI ENDR12 1 3402,3403,3402
3602 AC = PUT
3603 ENDR12

C.
NORMAL RETURN FROM SUB-ROUTINE RUNGU
361 RETURN

C.
SPECIAL RETURN AFTER CALLING RUNGU AT STATEMENT NUMBER 407
411 RETURN

C.
SPECIAL ERROR RETURN FROM SUBROUTINE RUNGU
714 JPAR1, JPAR1 = JPAR1, JPAR1
JPAR1, JPAR1 = JPAR1, JPAR1
JPAR1 = 1
DO 720 IT = 1, 18
720 ATP11,1) = 0.0
RETURN

END

```

[illegible]

SUBROUTINE CCECR PULIST,PHAP,BO,DECK
SUBROUTINE CHECKER

C SUBROUTINE CHECKER CODE NUMBER CCECR VERSION 6.0

C THIS PROGRAM IS DESIGNED TO CHECK THE PROGRESS OF THE ALGORITHM
C CHANGE AND TO PREVENT IT FROM INCREASING BEYOND 90 DEGREES BY
C REDUCING THE GAIN ANGLE TO ZERO DEGREES

C COMMON STATEMENTS FOR GLOBAL VARIABLES
COMMON /CPVAR/ FOURN(2),PV,FOURN(22)
COMMON /CAVAR/ FOURN(30),DS,ADUMB(11)
COMMON /CCVAR/ S4DUM(11),COSPHI
COMMON /CINT/ H,N,NTP,ICPDY,IGNORE,COUNT,INTLST,ILAST,JVAL,
1 ICNTRL,NMPEV,ISTOP,COUNT,KOUNTL,NETP,MUSL,
2 NETPT,MUSL77,IT,ITSAVE
3 COMMON /CPIPS/ FOURN(2),PIB2,FOURN(7),RODGR,ROGRN,PIB2L,
FOURN(11)

C COMMON STATEMENTS FOR OPTNS VARIABLES
COMMON /COZO/ OZDUM(25),OS4IMP,OZDUM(110)

C COMMON STATEMENTS FOR SUBROUTINE VARIABLES
COMMON /COSVET/ ANGINC,OSDUM(11),DSRED,OSDUM(13)
COMMON /CPTIO/ STUMPE(1),DENSTV,PTDUM(1)
COMMON /CPRAGE/ SITYLE,OSDUM,CROSSR,PIERG,PIRGA
1 COMMON /CPTICH/ ATTACK,STATNE,ATCALP,ATRPNI,GANK,CROSSR,RMLL,
2 CHORD,COSQZM,CSSRED,MND,BRAG,MPT,MPTSP,MPTCP,
PIRING,PIERC,CSCPN,ALPHAT,PHIAT,PHIAT,BIASPM

421 IFI PML 1 422, 440, 422
422 IFI PSIRGT 1 423, 424, 428
423 IFI PSIRGT - PSIRGA - BIASPM 1 424, 440, 440
424 IFI OMI ATTACK, CROSSR 1 1 425, 427, 425
425 CSCPR = 1 / COSPHI - 1.0 / PHATE * CLSQZM
426 ATTACK = CROSSR 1 427, 424, 427
426 ATTACK = 0.0
426 CROSSR = 0.0
427 PSIRGC = PSIRB + CSCPN * DENSTV * PV
428 IFI PSIRGC - PSIRGA - BIASPM 1 429, 440, 440
429 IFI BIASPM 1 431, 432, 431
431 CALL RANGE
PSIRGA = ABS(PSIRGC - RODGR)
432 BIASPM = ANGINC
433 IFI PSIRGT 1 435, 435, 435
434 IFI PSIRGT - PSIRGA 1 434, 435, 435
434 PSIRGT = 0.0
435 IFI PSIRGC - PSIRGA 1 436, 437, 440
436 NMPEV = 436
437 IFI DSIRNP - DS 1 401, 437, 437
437 IFI PSIRGA - PIB2L 1 704, 707, 707

C NORMAL RETURN FROM SUBROUTINE CHECKER
440 RETURN

C PRINT CHECK CONTROL IMPLEMENTATION

C NO POINTS EVALUATION - OUTPUT CHECK CONTROL NOT PASSED

601 IGNORE = 1
602 DSIRNP = 0.5
603 ICPODY = 0

C SPECIAL RETURN FOR NO POINT EVALUATION

604 RETURN

C OUTPUT CONTROL VALUES RE-EVALUATION

704 ICNTRL = 704
ATRPNI = 11.0
RANK = ABS(SIGN(1.0, RMLL) * 1.0)
CSCPN = 0.0
PSIRGC = PSIRB
PSIRGT = -PIB2
GO TO 801
707 ICNTRL = 707
ATRPNI = SIGN(12.0, ATRPNI)
RANK = 0.0
RMLL = 0.0

C SPECIAL RETURN FOR OUTPUT OF INTERMEDIATE OR FINAL VALUES

801 ICPODY = -ICPODY
RETURN

END


```

C      OUTPUT CONTROL VALUES RE-EVALUATION
730  ICTRL = 730
      TPODE = TANDOE * 0.25
      TANDOE = AMAX1 ( AMAX1 ( AMIN1 ( TPODE - ABS1 ( TPODS11 ) ),
1      1      ABS1 ( TPODS12 ) ),
2      2      ABS1 ( TPODS13 ) ), 0.0 ) / 11 * 0.4, TANDOE
      TANDOE = TANDOE
      TANDOE = TPODS14
      TPODE = - 1.0
7301 IPI-THECTS = 7302,7304,7306
7302 THECTS = THECTS - 1.0
      IFI TANDOE = TANDOE / 7303,7304,7305
7303 TANDOE = AMAX1 ( AMAX1 ( AMIN1 ( TPODE - TPODS11 ),
1      1      ABS1 ( TPODS12 ) ),
2      2      ABS1 ( TPODS13 ) ), 0.0 ) / 11 * 0.4, TANDOE
      ATALP = - 1.0
      TANDOE = 1.0E20
      IFI-THECTS = 7304,7305,7306
7304 TANDOE = 0.0
7305 IPI-TCESTS = 7306,700, 700
7306 IPI-THECTS = 7307,700, 700
7307 IPI TANDOE = TANDOE / 9111,5411,7000
7308 TESTED = - 1.0
      TANDOE = TANDOE
      TANDOE = TPODS14
      IFI-THECTS = 7309,541, 541
7309 THECTS = THECTS - 1.0
      TANDOE = 0.0
      IFI-THECTS = 941, 7400,7400
740  ICTRL = 740
      TANDOE = TANDOE
      TANDOE = 1.0E20
      TANDOE = TPODS15
      TESTED = 0.7
7391 IPI-THECTS = 7392,7394,7396
7392 IPI TANDOE = TANDOE / 7393,7394,7396
7393 ATALP = 1.0
      TANDOE = 1.0E20
7394 IPI-TCESTS = 7395,7396,700
7395 IPI-THECTS = 7396,5411,700
7396 TESTED = 0.0
      TANDOE = 1.0E20
      TANDOE = TPODS15
      GO TO 941
740  ICTRL = 740
      TANDOE = MOD1 ( TANDOE, 2 )
      ATALP = 1.0
      TANDOE = 1.0E20
      IFI-TCESTS = 9411,5411,001
7410 TANDOE = 1.0E20
      GO TO 541

```

```

C      OUTPUT CONTROL MAXIMUM VALUES RE-EVALUATION
7000 ITEMP = 7000
      TANDOE = AMAX1 ( AMAX1 ( AMIN1 ( TPODE - TPODS11 ),
1      1      ABS1 ( TPODS12 ) ),
2      2      ABS1 ( TPODS13 ) ), 0.0 ) / 11 * 0.4, TANDOE
7001 ICTRL = 700
7002 TANDOE = AMAX1 ( TANDOE, 0.077 )
      TPODE = TPODE + ( TPODS14 ) - TPODE
      IFI TANDOE = TANDOE - 1.0, TANDOE / GO TO 001
      ICTRL = ICTRL - 1
      TPODE = TPODE + ( TPODS14 )
      IFI TANDOE = TANDOE - 1.0, TANDOE / GO TO 001
      ICTRL = ICTRL - 1
      TPODE = TPODE + ( TPODS14 )
      IFI TANDOE = TANDOE - 1.0, TANDOE / GO TO 001
      ICTRL = ICTRL - 1
      GO TO 001
7010 IPI TCESTS - 1.0, 2.0 / GO TO 541
      IFI TCESTS - 1.0, TCESTS / GO TO 541
      TANDOE = AMAX1 ( AMAX1 ( TPODS11 ) - TPODS12 ), - TPODS13 )
1      1      0.0 / 11 * 0.4, TANDOE
      IFI TANDOE - 1.0, TANDOE / GO TO 541
      TPODE = 7000
      TANDOE = AMAX1 ( AMAX1 ( AMIN1 ( TANDOE * 0.25 - TPODS11 ),
1      1      ABS1 ( TANDOE * 0.25 - TPODS12 ) ),
2      2      ABS1 ( TPODS13 ) ), 0.0 ) / 11 * 0.4, TANDOE
700  IPI ATTACK = 7002,7001,7002
7001 ICTRL = 700
7002 TANDOE = MOD1 ( TANDOE, 0.077 )
      TPODE = TPODE + ( TPODS14 ) - TPODE
      IFI TANDOE = TANDOE - 1.0, TANDOE / GO TO 001
      ICTRL = ICTRL - 1
      TPODE = TPODE + ( TPODS14 )
      IFI TANDOE = TANDOE - 1.0, TANDOE / GO TO 001
      ICTRL = ICTRL - 1
      TPODE = TPODE + ( TPODS14 )
      IFI TANDOE = TANDOE - 1.0, TANDOE / GO TO 001
      ICTRL = ICTRL - 1
      GO TO 001

```

C SPECIAL RETURN FOR OUTPUT OF INTERMEDIATE OR FINAL VALUES
 011 ICPDVS = - ICPDVS
 001 IISAVE = ITEMP
 012 ICOND = 0
 013 NSTP = (NSTP / 100) * 10 + MOD1 (NSTP, 100) * 1
 014 OFFUP

```

810PTE LESS FULLST,PAMP,BECK
      BLCKE DATA

C      SUBROUTINE CESSDA CODE NUMBER CESSDA                      VERSION 100.0

C      THIS PROGRAM WILL INCREASE THE SPACE RESERVED FOR LOCAL VARIABLES
C      WHICH ARE IN COMMON STATEMENTS IN SUBROUTINE OUTPUT

C      COMMON STATEMENTS FOR GLOBAL VARIABLES
COMMON /CMISS/      RMPTS,STOP

C      DATA STATEMENTS FOR GLOBAL VARIABLES
DATA      NSTMP/100/

C      COMMON STATEMENTS FOR LOCAL VARIABLES
COMMON /CINITIAL/   ISHT(1:101)/CSGHT(1:101)/SACHT(1:1)/CSHTP(1:101)/
COMMON /CINITIAL/   ISHSL(1:1)/CSGSL(1:1)/SACSL(1:1)/PCSH/PSH(1:1)/
COMMON /CFCR/       KAT(1:1)/CSTMP/STPM(1:1)/CSTP/STP(1:1)

C      TYPE STATEMENTS FOR LOCAL VARIABLES
C/PSH/11          55

```

20

```

SIOTPC ACBS          FULIST,PRAP,40,50,DECK
SUBROUTINE APMOHSI(SINAG)

C      SUBROUTINE AFFORDS CODE NUMBER ACPHOS                                VERSION 6.0

C      THIS PROGRAM WILL SEPARATE THE INTEGER AND FRACTIONAL PARTS OF A
C      SINCEDED NUMBER.
C      CNOTP = ALL CALLS TO THIS SUBROUTINE ARE ACTUALLY MADE AS
C      FUNCTION SUPPORTING CALLS = THIS IS THE REASON FOR
C      CNOTP = 0 OUT (WHICH RETURNS THE ARGUMENT IN THE ACCUMULATOR)
C      JUST BEFORE THE SINGLE RETURN STATEMENT.

C      DOUBLE PRECISION OUTUT
C      REAL COUT(2)
C      DIMENSION I(OUTS,OUTS),OUTUT,SOUT(1),I(OUT2,SOUT(2))

C      LOCAL DATA VALUES
C      DATA I(1,1),I(1,2),I(2,1),I(2,2),I(3,1),I(3,2),I(4,1),I(4,2),I(5,1),I(5,2),I(6,1),I(6,2),I(7,1),I(7,2),I(8,1),I(8,2),I(9,1),I(9,2),I(10,1),I(10,2),I(11,1),I(11,2),I(12,1),I(12,2),I(13,1),I(13,2),I(14,1),I(14,2),I(15,1),I(15,2),I(16,1),I(16,2),I(17,1),I(17,2),I(18,1),I(18,2),I(19,1),I(19,2),I(20,1),I(20,2),I(21,1),I(21,2),I(22,1),I(22,2),I(23,1),I(23,2),I(24,1),I(24,2),I(25,1),I(25,2),I(26,1),I(26,2),I(27,1),I(27,2),I(28,1),I(28,2),I(29,1),I(29,2),I(30,1),I(30,2),I(31,1),I(31,2),I(32,1),I(32,2),I(33,1),I(33,2),I(34,1),I(34,2),I(35,1),I(35,2),I(36,1),I(36,2),I(37,1),I(37,2),I(38,1),I(38,2),I(39,1),I(39,2),I(40,1),I(40,2),I(41,1),I(41,2),I(42,1),I(42,2),I(43,1),I(43,2),I(44,1),I(44,2),I(45,1),I(45,2),I(46,1),I(46,2),I(47,1),I(47,2),I(48,1),I(48,2),I(49,1),I(49,2),I(50,1),I(50,2),I(51,1),I(51,2),I(52,1),I(52,2),I(53,1),I(53,2),I(54,1),I(54,2),I(55,1),I(55,2),I(56,1),I(56,2),I(57,1),I(57,2),I(58,1),I(58,2),I(59,1),I(59,2),I(60,1),I(60,2),I(61,1),I(61,2),I(62,1),I(62,2),I(63,1),I(63,2),I(64,1),I(64,2),I(65,1),I(65,2),I(66,1),I(66,2),I(67,1),I(67,2),I(68,1),I(68,2),I(69,1),I(69,2),I(70,1),I(70,2),I(71,1),I(71,2),I(72,1),I(72,2),I(73,1),I(73,2),I(74,1),I(74,2),I(75,1),I(75,2),I(76,1),I(76,2),I(77,1),I(77,2),I(78,1),I(78,2),I(79,1),I(79,2),I(80,1),I(80,2),I(81,1),I(81,2),I(82,1),I(82,2),I(83,1),I(83,2),I(84,1),I(84,2),I(85,1),I(85,2),I(86,1),I(86,2),I(87,1),I(87,2),I(88,1),I(88,2),I(89,1),I(89,2),I(90,1),I(90,2),I(91,1),I(91,2),I(92,1),I(92,2),I(93,1),I(93,2),I(94,1),I(94,2),I(95,1),I(95,2),I(96,1),I(96,2),I(97,1),I(97,2),I(98,1),I(98,2),I(99,1),I(99,2),I(100,1),I(100,2),I(101,1),I(101,2),I(102,1),I(102,2),I(103,1),I(103,2),I(104,1),I(104,2),I(105,1),I(105,2),I(106,1),I(106,2),I(107,1),I(107,2),I(108,1),I(108,2),I(109,1),I(109,2),I(110,1),I(110,2),I(111,1),I(111,2),I(112,1),I(112,2),I(113,1),I(113,2),I(114,1),I(114,2),I(115,1),I(115,2),I(116,1),I(116,2),I(117,1),I(117,2),I(118,1),I(118,2),I(119,1),I(119,2),I(120,1),I(120,2),I(121,1),I(121,2),I(122,1),I(122,2),I(123,1),I(123,2),I(124,1),I(124,2),I(125,1),I(125,2),I(126,1),I(126,2),I(127,1),I(127,2),I(128,1),I(128,2),I(129,1),I(129,2),I(130,1),I(130,2),I(131,1),I(131,2),I(132,1),I(132,2),I(133,1),I(133,2),I(134,1),I(134,2),I(135,1),I(135,2),I(136,1),I(136,2),I(137,1),I(137,2),I(138,1),I(138,2),I(139,1),I(139,2),I(140,1),I(140,2),I(141,1),I(141,2),I(142,1),I(142,2),I(143,1),I(143,2),I(144,1),I(144,2),I(145,1),I(145,2),I(146,1),I(146,2),I(147,1),I(147,2),I(148,1),I(148,2),I(149,1),I(149,2),I(150,1),I(150,2),I(151,1),I(151,2),I(152,1),I(152,2),I(153,1),I(153,2),I(154,1),I(154,2),I(155,1),I(155,2),I(156,1),I(156,2),I(157,1),I(157,2),I(158,1),I(158,2),I(159,1),I(159,2),I(160,1),I(160,2),I(161,1),I(161,2),I(162,1),I(162,2),I(163,1),I(163,2),I(164,1),I(164,2),I(165,1),I(165,2),I(166,1),I(166,2),I(167,1),I(167,2),I(168,1),I(168,2),I(169,1),I(169,2),I(170,1),I(170,2),I(171,1),I(171,2),I(172,1),I(172,2),I(173,1),I(173,2),I(174,1),I(174,2),I(175,1),I(175,2),I(176,1),I(176,2),I(177,1),I(177,2),I(178,1),I(178,2),I(179,1),I(179,2),I(180,1),I(180,2),I(181,1),I(181,2),I(182,1),I(182,2),I(183,1),I(183,2),I(184,1),I(184,2),I(185,1),I(185,2),I(186,1),I(186,2),I(187,1),I(187,2),I(188,1),I(188,2),I(189,1),I(189,2),I(190,1),I(190,2),I(191,1),I(191,2),I(192,1),I(192,2),I(193,1),I(193,2),I(194,1),I(194,2),I(195,1),I(195,2),I(196,1),I(196,2),I(197,1),I(197,2),I(198,1),I(198,2),I(199,1),I(199,2),I(200,1),I(200,2),I(201,1),I(201,2),I(202,1),I(202,2),I(203,1),I(203,2),I(204,1),I(204,2),I(205,1),I(205,2),I(206,1),I(206,2),I(207,1),I(207,2),I(208,1),I(208,2),I(209,1),I(209,2),I(210,1),I(210,2),I(211,1),I(211,2),I(212,1),I(212,2),I(213,1),I(213,2),I(214,1),I(214,2),I(215,1),I(215,2),I(216,1),I(216,2),I(217,1),I(217,2),I(218,1),I(218,2),I(219,1),I(219,2),I(220,1),I(220,2),I(221,1),I(221,2),I(222,1),I(222,2),I(223,1),I(223,2),I(224,1),I(224,2),I(225,1),I(225,2),I(226,1),I(226,2),I(227,1),I(227,2),I(228,1),I(228,2),I(229,1),I(229,2),I(230,1),I(230,2),I(231,1),I(231,2),I(232,1),I(232,2),I(233,1),I(233,2),I(234,1),I(234,2),I(235,1),I(235,2),I(236,1),I(236,2),I(237,1),I(237,2),I(238,1),I(238,2),I(239,1),I(239,2),I(240,1),I(240,2),I(241,1),I(241,2),I(242,1),I(242,2),I(243,1),I(243,2),I(244,1),I(244,2),I(245,1),I(245,2),I(246,1),I(246,2),I(247,1),I(247,2),I(248,1),I(248,2),I(249,1),I(249,2),I(250,1),I(250,2),I(251,1),I(251,2),I(252,1),I(252,2),I(253,1),I(253,2),I(254,1),I(254,2),I(255,1),I(255,2),I(256,1),I(256,2),I(
```

Panel

[illegible]

250

[illegible]

[illegible]

PICTURE	FURTHER	TESTING	ABOUT	PICTURE
001000	C01	P01000		
	T004	P01001		
	C01	C01000		
0000	T004	C01001		
	C01	C01002		
	T004	C01003		
	C01	C01004		
001000	P01000	001000		
	T004	001001		
001000	C01	001002		
	T004	001003		
	C01	001004		
001000	T004	001005		
	C01	001006		
	T004	001007		
	C01	001008		
001000	P01000	001009		
	T004	001010		
	C01	001011		
001000	T004	001012		
	C01	001013		
001000	P01000	001014		
	T004	001015		
	C01	001016		
001000	T004	001017		
	C01	001018		
001000	P01000	001019		
	T004	001020		
	C01	001021		
001000	T004	001022		
	C01	001023		
001000	P01000	001024		
	T004	001025		
	C01	001026		
001000	T004	001027		
	C01	001028		
001000	P01000	001029		
	T004	001030		
	C01	001031		
001000	T004	001032		
	C01	001033		
001000	P01000	001034		
	T004	001035		
	C01	001036		
001000	T004	001037		
	C01	001038		
001000	P01000	001039		
	T004	001040		
	C01	001041		
001000	T004	001042		
	C01	001043		
001000	P01000	001044		
	T004	001045		
	C01	001046		
001000	T004	001047		
	C01	001048		
001000	P01000	001049		
	T004	001050		
	C01	001051		
001000	T004	001052		
	C01	001053		
001000	P01000	001054		
	T004	001055		
	C01	001056		
001000	T004	001057		
	C01	001058		
001000	P01000	001059		
	T004	001060		
	C01	001061		
001000	T004	001062		
	C01	001063		
001000	P01000	001064		
	T004	001065		
	C01	001066		
001000	T004	001067		
	C01	001068		
001000	P01000	001069		
	T004	001070		
	C01	001071		
001000	T004	001072		
	C01	001073		
001000	P01000	001074		
	T004	001075		
	C01	001076		
001000	T004	001077		
	C01	001078		
001000	P01000	001079		
	T004	001080		
	C01	00108		

STAPC DEVR PULIST,PRM,DO,DOCK
SUBROUTINE DENVAR

C SUBROUTINE DENVAR CODE NUMBER DENVAR VERSION 6.0

C THIS PROGRAM IS DESIGNED TO PRODUCE THE VARIABILITY FACTOR OF
C WHICH THE DENSITY IS OBSERVED FROM SUBROUTINE PTDS ON A SINGLE
C EXPONENTIAL WHEN STUDIED - 0.01 IS TO BE MULTIPLIED, THE
C VARIABILITY FACTOR MAY BE ANY DEPENDENT COMBINATION OF ALTITUDE
C OR RANDOM VARIATION ALONG THE FLIGHT PATH.

C COMMON STATEMENTS FOR GLOBAL VARIABLES
COMMON /COMMON/ DENSITY,ALTITUDE,DOCK,DOCK1
COMMON /CTVAR/ TOUTP,TEMP,TOUTP1
COMMON /CTVAR/ TOUTP1,TEMP,TOUTP1
COMMON /CTVAR/ TOUTP1,TEMP,TOUTP1
COMMON /CTVAR/ TOUTP1,TEMP,TOUTP1
COMMON /CTVAR/ TOUTP1,TEMP,TOUTP1
COMMON /CTVAR/ TOUTP1,TEMP,TOUTP1

C COMMON STATEMENTS FOR OPTIME VARIABLES
COMMON /COMMON/ DENSITY,ALTITUDE

C COMMON STATEMENTS FOR SUBROUTINE VARIABLES
COMMON /COMMON/ TOUTP,TEMP,TOUTP1,DOCK,DOCK1,DOCK2,DOCK3,
C TOUTP1,TEMP,TOUTP1,DOCK,DOCK1,DOCK2,DOCK3

C DOUBLE PRECISION STATEMENTS FOR LOCAL VARIABLES
DOUBLE PRECISION DENSITY,ALTITUDE

C DIMENSION STATEMENTS FOR LOCAL VARIABLES
DIMENSION DENSITY(100),ALTITUDE(100),DOCK(100),DOCK1(100),
C DENSITY(100),ALTITUDE(100),DOCK(100),DOCK1(100),DOCK2(100),
C DENSITY(100),ALTITUDE(100),DOCK(100),DOCK1(100),DOCK2(100),DOCK3(100)

C EQUIVALENCE STATEMENTS FOR LOCAL VARIABLES
EQUIVALENCE (DENSITY(1),ALTITUDE(1),DOCK(1),DOCK1(1),DOCK2(1),DOCK3(1),
C DENSITY(1),ALTITUDE(1),DOCK(1),DOCK1(1),DOCK2(1),DOCK3(1),
C DENSITY(1),ALTITUDE(1),DOCK(1),DOCK1(1),DOCK2(1),DOCK3(1))

C LOCAL DATA VALUES
DATA DENSITY(100),ALTITUDE(100),DOCK(100),DOCK1(100),DOCK2(100),DOCK3(100),
C DENSITY(100),ALTITUDE(100),DOCK(100),DOCK1(100),DOCK2(100),DOCK3(100),
C DENSITY(100),ALTITUDE(100),DOCK(100),DOCK1(100),DOCK2(100),DOCK3(100),
C DENSITY(100),ALTITUDE(100),DOCK(100),DOCK1(100),DOCK2(100),DOCK3(100)

C FORMATS
11 FORMAT(30H DENVAR 6.0 DENVAR 100, 111)

C COMPUTATION OF THE VARIABILITY FACTOR

101 IF (DOCK(100)) 102, 104, 106
102 IF (DOCK(100)) 103, 104, 106
103 IF (DOCK(100)) 104, 106, 108
104 IF (DOCK(100)) 105, 107, 109
105 IF (DOCK(100)) 106, 108, 110
106 IF (DOCK(100)) 107, 109, 111
107 IF (DOCK(100)) 108, 110, 112
108 IF (DOCK(100)) 109, 111, 113
109 IF (DOCK(100)) 110, 112, 114
110 IF (DOCK(100)) 111, 113, 115
111 IF (DOCK(100)) 112, 114, 116
112 IF (DOCK(100)) 113, 115, 117
113 IF (DOCK(100)) 114, 116, 118
114 IF (DOCK(100)) 115, 117, 119
115 IF (DOCK(100)) 116, 118, 120
116 IF (DOCK(100)) 117, 119, 121
117 IF (DOCK(100)) 118, 120, 122
118 IF (DOCK(100)) 119, 121, 123
119 IF (DOCK(100)) 120, 122, 124
120 IF (DOCK(100)) 121, 123, 125
121 IF (DOCK(100)) 122, 124, 126
122 IF (DOCK(100)) 123, 125, 127
123 IF (DOCK(100)) 124, 126, 128
124 IF (DOCK(100)) 125, 127, 129
125 IF (DOCK(100)) 126, 128, 130
126 IF (DOCK(100)) 127, 129, 131
127 IF (DOCK(100)) 128, 130, 132
128 IF (DOCK(100)) 129, 131, 133
129 IF (DOCK(100)) 130, 132, 134
130 IF (DOCK(100)) 131, 133, 135
131 IF (DOCK(100)) 132, 134, 136
132 IF (DOCK(100)) 133, 135, 137
133 IF (DOCK(100)) 134, 136, 138
134 IF (DOCK(100)) 135, 137, 139
135 IF (DOCK(100)) 136, 138, 140
136 IF (DOCK(100)) 137, 139, 141
137 IF (DOCK(100)) 138, 140, 142
138 IF (DOCK(100)) 139, 141, 143
139 IF (DOCK(100)) 140, 142, 144
140 IF (DOCK(100)) 141, 143, 145
141 IF (DOCK(100)) 142, 144, 146
142 IF (DOCK(100)) 143, 145, 147
143 IF (DOCK(100)) 144, 146, 148
144 IF (DOCK(100)) 145, 147, 149
145 IF (DOCK(100)) 146, 148, 150
146 IF (DOCK(100)) 147, 149, 151
147 IF (DOCK(100)) 148, 150, 152
148 IF (DOCK(100)) 149, 151, 153
149 IF (DOCK(100)) 150, 152, 154
150 IF (DOCK(100)) 151, 153, 155
151 IF (DOCK(100)) 152, 154, 156
152 IF (DOCK(100)) 153, 155, 157
153 IF (DOCK(100)) 154, 156, 158
154 IF (DOCK(100)) 155, 157, 159
155 IF (DOCK(100)) 156, 158, 160
156 IF (DOCK(100)) 157, 159, 161
157 IF (DOCK(100)) 158, 160, 162
158 IF (DOCK(100)) 159, 161, 163
159 IF (DOCK(100)) 160, 162, 164
160 IF (DOCK(100)) 161, 163, 165
161 IF (DOCK(100)) 162, 164, 166
162 IF (DOCK(100)) 163, 165, 167
163 IF (DOCK(100)) 164, 166, 168
164 IF (DOCK(100)) 165, 167, 169
165 IF (DOCK(100)) 166, 168, 170
166 IF (DOCK(100)) 167, 169, 171
167 IF (DOCK(100)) 168, 170, 172
168 IF (DOCK(100)) 169, 171, 173
169 IF (DOCK(100)) 170, 172, 174
170 IF (DOCK(100)) 171, 173, 175
171 IF (DOCK(100)) 172, 174, 176
172 IF (DOCK(100)) 173, 175, 177
173 IF (DOCK(100)) 174, 176, 178
174 IF (DOCK(100)) 175, 177, 179
175 IF (DOCK(100)) 176, 178, 180
176 IF (DOCK(100)) 177, 179, 181
177 IF (DOCK(100)) 178, 180, 182
178 IF (DOCK(100)) 179, 181, 183
179 IF (DOCK(100)) 180, 182, 184
180 IF (DOCK(100)) 181, 183, 185
181 IF (DOCK(100)) 182, 184, 186
182 IF (DOCK(100)) 183, 185, 187
183 IF (DOCK(100)) 184, 186, 188
184 IF (DOCK(100)) 185, 187, 189
185 IF (DOCK(100)) 186, 188, 190
186 IF (DOCK(100)) 187, 189, 191
187 IF (DOCK(100)) 188, 190, 192
188 IF (DOCK(100)) 189, 191, 193
189 IF (DOCK(100)) 190, 192, 194
190 IF (DOCK(100)) 191, 193, 195
191 IF (DOCK(100)) 192, 194, 196
192 IF (DOCK(100)) 193, 195, 197
193 IF (DOCK(100)) 194, 196, 198
194 IF (DOCK(100)) 195, 197, 199
195 IF (DOCK(100)) 196, 198, 200
196 IF (DOCK(100)) 197, 199, 201
197 IF (DOCK(100)) 198, 200, 202
198 IF (DOCK(100)) 199, 201, 203
199 IF (DOCK(100)) 200, 202, 204
200 IF (DOCK(100)) 201, 203, 205
201 IF (DOCK(100)) 202, 204, 206
202 IF (DOCK(100)) 203, 205, 207
203 IF (DOCK(100)) 204, 206, 208
204 IF (DOCK(100)) 205, 207, 209
205 IF (DOCK(100)) 206, 208, 210
206 IF (DOCK(100)) 207, 209, 211
207 IF (DOCK(100)) 208, 210, 212
208 IF (DOCK(100)) 209, 211, 213
209 IF (DOCK(100)) 210, 212, 214
210 IF (DOCK(100)) 211, 213, 215
211 IF (DOCK(100)) 212, 214, 216
212 IF (DOCK(100)) 213, 215, 217
213 IF (DOCK(100)) 214, 216, 218
214 IF (DOCK(100)) 215, 217, 219
215 IF (DOCK(100)) 216, 218, 220
216 IF (DOCK(100)) 217, 219, 221
217 IF (DOCK(100)) 218, 220, 222
218 IF (DOCK(100)) 219, 221, 223
219 IF (DOCK(100)) 220, 222, 224
220 IF (DOCK(100)) 221, 223, 225
221 IF (DOCK(100)) 222, 224, 226
222 IF (DOCK(100)) 223, 225, 227
223 IF (DOCK(100)) 224, 226, 228
224 IF (DOCK(100)) 225, 227, 229
225 IF (DOCK(100)) 226, 228, 230
226 IF (DOCK(100)) 227, 229, 231
227 IF (DOCK(100)) 228, 230, 232
228 IF (DOCK(100)) 229, 231, 233
229 IF (DOCK(100)) 230, 232, 234
230 IF (DOCK(100)) 231, 233, 235
231 IF (DOCK(100)) 232, 234, 236
232 IF (DOCK(100)) 233, 235, 237
233 IF (DOCK(100)) 234, 236, 238
234 IF (DOCK(100)) 235, 237, 239
235 IF (DOCK(100)) 236, 238, 240
236 IF (DOCK(100)) 237, 239, 241
237 IF (DOCK(100)) 238, 240, 242
238 IF (DOCK(100)) 239, 241, 243
239 IF (DOCK(100)) 240, 242, 244
240 IF (DOCK(100)) 241, 243, 245
241 IF (DOCK(100)) 242, 244, 246
242 IF (DOCK(100)) 243, 245, 247
243 IF (DOCK(100)) 244, 246, 248
244 IF (DOCK(100)) 245, 247, 249
245 IF (DOCK(100)) 246, 248, 250
246 IF (DOCK(100)) 247, 249, 251
247 IF (DOCK(100)) 248, 250, 252
248 IF (DOCK(100)) 249, 251, 253
249 IF (DOCK(100)) 250, 252, 254
250 IF (DOCK(100)) 251, 253, 255
251 IF (DOCK(100)) 252, 254, 256
252 IF (DOCK(100)) 253, 255, 257
253 IF (DOCK(100)) 254, 256, 258
254 IF (DOCK(100)) 255, 257, 259
255 IF (DOCK(100)) 256, 258, 260
256 IF (DOCK(100)) 257, 259, 261
257 IF (DOCK(100)) 258, 260, 262
258 IF (DOCK(100)) 259, 261, 263
259 IF (DOCK(100)) 260, 262, 264
260 IF (DOCK(100)) 261, 263, 265
261 IF (DOCK(100)) 262, 264, 266
262 IF (DOCK(100)) 263, 265, 267
263 IF (DOCK(100)) 264, 266, 268
264 IF (DOCK(100)) 265, 267, 269
265 IF (DOCK(100)) 266, 268, 270
266 IF (DOCK(100)) 267, 269, 271
267 IF (DOCK(100)) 268, 270, 272
268 IF (DOCK(100)) 269, 271, 273
269 IF (DOCK(100)) 270, 272, 274
270 IF (DOCK(100)) 271, 273, 275
271 IF (DOCK(100)) 272, 274, 276
272 IF (DOCK(100)) 273, 275, 277
273 IF (DOCK(100)) 274, 276, 278
274 IF (DOCK(100)) 275, 277, 279
275 IF (DOCK(100)) 276, 278, 280
276 IF (DOCK(100)) 277, 279, 281
277 IF (DOCK(100)) 278, 280, 282
278 IF (DOCK(100)) 279, 281, 283
279 IF (DOCK(100)) 280, 282, 284
280 IF (DOCK(100)) 281, 283, 285
281 IF (DOCK(100)) 282, 284, 286
282 IF (DOCK(100)) 283, 285, 287
283 IF (DOCK(100)) 284, 286, 288
284 IF (DOCK(100)) 285, 287, 289
285 IF (DOCK(100)) 286, 288, 290
286 IF (DOCK(100)) 287, 289, 291
287 IF (DOCK(100)) 288, 290, 292
288 IF (DOCK(100)) 289, 291, 293
289 IF (DOCK(100)) 290, 292, 294
290 IF (DOCK(100)) 291, 293, 295
291 IF (DOCK(100)) 292, 294, 296
292 IF (DOCK(100)) 293, 295, 297
293 IF (DOCK(100)) 294, 296, 298
294 IF (DOCK(100)) 295, 297, 299
295 IF (DOCK(100)) 296, 298, 300
296 IF (DOCK(100)) 297, 299, 301
297 IF (DOCK(100)) 298, 300, 302
298 IF (DOCK(100)) 299, 301, 303
299 IF (DOCK(100)) 300, 302, 304
300 IF (DOCK(100)) 301, 303, 305
301 IF (DOCK(100)) 302, 304, 306
302 IF (DOCK(100)) 303, 305, 307
303 IF (DOCK(100)) 304, 306, 308
304 IF (DOCK(100)) 305, 307, 309
305 IF (DOCK(100)) 306, 308, 310
306 IF (DOCK(100)) 307, 309, 311
307 IF (DOCK(100)) 308, 310, 312
308 IF (DOCK(100)) 309, 311, 313
309 IF (DOCK(100)) 310, 312, 314
310 IF (DOCK(100)) 311, 313, 315
311 IF (DOCK(100)) 312, 314, 316
312 IF (DOCK(100)) 313, 315, 317
313 IF (DOCK(100)) 314, 316, 318
314 IF (DOCK(100)) 315, 317, 319
315 IF (DOCK(100)) 316, 318, 320
316 IF (DOCK(100)) 317, 319, 321
317 IF (DOCK(100)) 318, 320, 322
318 IF (DOCK(100)) 319, 321, 323
319 IF (DOCK(100)) 320, 322, 324
320 IF (DOCK(100)) 321, 323, 325
321 IF (DOCK(100)) 322, 324, 326
322 IF (DOCK(100)) 323, 325, 327
323 IF (DOCK(100)) 324, 326, 328
324 IF (DOCK(100)) 325, 327, 329
325 IF (DOCK(100)) 326, 328, 330
326 IF (DOCK(100)) 327, 329, 331
327 IF (DOCK(100)) 328, 330, 332
328 IF (DOCK(100)) 329, 331, 333
329 IF (DOCK(100)) 330, 332, 334
330 IF (DOCK(100)) 331, 333, 335
331 IF (DOCK(100)) 332, 334, 336
332 IF (DOCK(100)) 333, 335, 337
333 IF (DOCK(100)) 334, 336, 338
334 IF (DOCK(100)) 335, 337, 339
335 IF (DOCK(100)) 336, 338, 340
336 IF (DOCK(100)) 337, 339, 341
337 IF (DOCK(100)) 338, 340, 342
338 IF (DOCK(100)) 339, 341, 343
339 IF (DOCK(100)) 340, 342, 344
340 IF (DOCK(100)) 341, 343, 345
341 IF (DOCK(100)) 342, 344, 346
342 IF (DOCK(100)) 343, 345, 347
343 IF (DOCK(100)) 344, 346, 348
344 IF (DOCK(100)) 345, 347, 349
345 IF (DOCK(100)) 346, 348, 350
346 IF (DOCK(100)) 347, 349, 351
347 IF (DOCK(100)) 348, 350, 352
348 IF (DOCK(100)) 349, 351, 353
349 IF (DOCK(100)) 350, 352, 354
350 IF (DOCK(100)) 351, 353, 355
351 IF (DOCK(100)) 352, 354, 356
352 IF (DOCK(100)) 353, 355, 357
353 IF (DOCK(100)) 354, 356, 358
354 IF (DOCK(100)) 355, 357, 359
355 IF (DOCK(100)) 356, 358, 360
356 IF (DOCK(100)) 357, 359, 361
357 IF (DOCK(100)) 358, 360, 362
358 IF (DOCK(100)) 359, 361, 363
359 IF (DOCK(100)) 360, 362, 364
360 IF (DOCK(100)) 361, 363, 365
361 IF (DOCK(100)) 362, 364, 366
362 IF (DOCK(100)) 363, 365, 367
363 IF (DOCK(100)) 364, 366, 368
364 IF (DOCK(100)) 365, 367, 369
365 IF (DOCK(100)) 366, 368, 370
366 IF (DOCK(100)) 367, 369, 371
367 IF (DOCK(100)) 368, 370, 372
368 IF (DOCK(100)) 369, 371, 373
369 IF (DOCK(100)) 370, 372, 374
370 IF (DOCK(100)) 371, 373, 375
371 IF (DOCK(100)) 372, 374, 376
372 IF (DOCK(100)) 373, 375, 377
373 IF (DOCK(100)) 374, 376, 378
374 IF (DOCK(100)) 375, 377, 379
375 IF (DOCK(100)) 376, 378, 380
376 IF (DOCK(100)) 377, 379, 381
377 IF (DOCK(100)) 378, 380, 382
378 IF (DOCK(100)) 379, 381, 383
379 IF (DOCK(100)) 380, 382, 384
380 IF (DOCK(100)) 381, 383, 385
381 IF (DOCK(100)) 382, 384, 386
382 IF (DOCK(100)) 383, 385, 387
383 IF (DOCK(100)) 384, 386, 388
384 IF (DOCK(100)) 385, 387, 389
385 IF (DOCK(100)) 386, 388, 390
386 IF (DOCK(100)) 387, 389, 391
387 IF (DOCK(100)) 388, 390, 392
388 IF (DOCK(100)) 389, 391, 393
389 IF (DOCK(100)) 390, 392, 394
390 IF (DOCK(100)) 391, 393, 395
391 IF (DOCK(100)) 392, 394, 396
392 IF (DOCK(100)) 393, 395, 397
393 IF (DOCK(100)) 394, 396, 398
394 IF (DOCK(100)) 395, 397, 399
395 IF (DOCK(100)) 396, 398, 400
396 IF (DOCK(100)) 397, 399, 401
397 IF (DOCK(100)) 398, 400, 402
398 IF (DOCK(100)) 399, 401, 403
399 IF (DOCK(100)) 400, 402, 404
400 IF (DOCK(100)) 401, 403, 405
401 IF (DOCK(100)) 402, 404, 406
402 IF (DOCK(100)) 403, 405, 407
403 IF (DOCK(100)) 404, 406, 408
404 IF (DOCK(100)) 405, 407, 409
405 IF (DOCK(100)) 406, 408, 410
406 IF (DOCK(100)) 407, 409, 411
407 IF (DOCK(100)) 408, 410, 412
408 IF (DOCK(100)) 409, 411, 413
409 IF (DOCK(100)) 410, 412, 414
410 IF (DOCK(100)) 411, 413, 415
411 IF (DOCK(100)) 412, 414, 416
412 IF (DOCK(100)) 413, 415, 417
413 IF (DOCK(100)) 414, 416, 418
414 IF (DOCK(100)) 415, 417, 419
415 IF (DOCK(100)) 416, 418, 420
416 IF (DOCK(100)) 417, 419, 421
417 IF (DOCK(100)) 418, 420, 422
418 IF (DOCK(100)) 419, 421, 423
419 IF (DOCK(100)) 420, 422, 424
420 IF (DOCK(100)) 421, 423, 425
421 IF (DOCK(100)) 422, 424, 426
422 IF (DOCK(100)) 423, 425, 427
423 IF (DOCK(100)) 424, 426, 428
424 IF (DOCK(100)) 425, 427, 429
425 IF (DOCK(100)) 426, 428, 430
426 IF (DOCK(100)) 427, 429, 431
427 IF (DOCK(100)) 428, 430, 432
428 IF (DOCK(100)) 429, 431, 433
429 IF (DOCK(100)) 430, 432, 434
430 IF (DOCK(100)) 431, 433, 435
431 IF (DOCK(100)) 432, 434, 436
432 IF (DOCK(100)) 433, 435, 437
433 IF (DOCK(100)) 434, 436, 438
434 IF (DOCK(100)) 435, 437, 439
435 IF (DOCK(100)) 436, 438, 440
436 IF (DOCK(100)) 437, 439, 441
437 IF (DOCK(100)) 438, 440, 442
438 IF (DOCK(100)) 439, 441, 443
439 IF (DOCK(100)) 440, 442, 444
440 IF (DOCK(100)) 441, 443, 445
441 IF (DOCK(100)) 442, 444, 446
442 IF (DOCK(100)) 443, 445, 447
443 IF (DOCK(100)) 444, 446, 448
444 IF (DOCK(100)) 445, 447, 449
445 IF (DOCK(100)) 446, 448, 450
446 IF (DOCK(100)) 447, 449, 451
447 IF (DOCK(100)) 448, 450, 452
448 IF (DOCK(100)) 449, 451, 453
449 IF (DOCK(100)) 450, 452, 454
450 IF (DOCK(100)) 451, 453, 455
451 IF (DOCK(100)) 452, 454, 456
452 IF (DOCK(100)) 453, 455, 457
453 IF (DOCK(100)) 454, 456, 458
454 IF (DOCK(100)) 455, 457, 459
455 IF (DOCK(100)) 456, 458, 460
456 IF (DOCK(100)) 457, 459, 461
457 IF (DOCK(100)) 458, 460, 462
458 IF (DOCK(100)) 459, 461, 463
459 IF (DOCK(100)) 460, 462, 464
460 IF (DOCK(100)) 461, 463, 465
461 IF (DOCK(100)) 462, 464, 466
462 IF (DOCK(100)) 463, 465, 467
463 IF (DOCK(100)) 464, 466, 468
464 IF (DOCK(100)) 465, 467, 469
465 IF (DOCK(100)) 466, 468, 470
466 IF (DOCK(100)) 467, 469, 471
467 IF (DOCK(100)) 468, 470, 472
468 IF (DOCK(100)) 469, 471, 473
469 IF (DOCK(100)) 470, 472, 474
470 IF (DOCK(100)) 471, 473, 475
471 IF (DOCK(100)) 472, 474, 476
472 IF (DOCK(100)) 473, 475, 477
473 IF (DOCK(100)) 474, 476, 478
474 IF (DOCK(100)) 475, 477, 479
475 IF (DOCK(100)) 476, 478, 480
476 IF (DOCK(100)) 477, 479, 481
477 IF (DOCK(100)) 478, 480, 482
478 IF (DOCK(100)) 479, 481, 483
479 IF (DOCK(100)) 480, 482, 484
480 IF (DOCK(100)) 481, 483, 485
481 IF (DOCK(100)) 482, 484, 486
482 IF (DOCK(100)) 483, 485, 487
483 IF (DOCK(100)) 484, 486, 488
484 IF (DOCK(100)) 485, 487, 489
485 IF (DOCK(100)) 486, 488, 490
486 IF (DOCK(100)) 487, 489, 491
487 IF (DOCK(100)) 488, 490, 492
488 IF (DOCK(100)) 489, 491, 493
489 IF (DOCK(100)) 490, 492, 494
490 IF (DOCK(100)) 491, 493, 495
491 IF (DOCK(100)) 492, 494, 496
492 IF (DOCK(100)) 493, 495, 497
493 IF

C INITIALIZATION ENTRY POINT
ENTRY POINT

```

721 FACTA = 0.0
    FACTA = 0.0
    FOLD = -1.0
    FOLD = -1.0
    FOLD = 100000.0 / 2 + 1
722 IF1 TWENTY = 17.10.0 GO TO 731
723 IF1 TWENTY = 17.60.0 GO TO 731
724 IF1 TWENTY = 17.70.0 GO TO 731
725 IF1 TWENTY = 17.100.0 GO TO 731
73:
    STWEND TWENTY
    STWEND = 0.0
    STWEND = 100000.0
    STWEND = TWENTY - 40.0
    STWEND = 100000.0

```

```
411 STAGE = 1.0
    YEAR = 1962.0
    ALYAR = IDNTY - 70.0
    CALL PTIME
```

```

951 IF( BOML(ALTVAR) ) 911, 902, 911
952 BAWAB = 0.0
953 IF( BOML(ANAVAR) ) 204, 504, 200
954 BFTUM

```

```

511 IF ALTVAL .GT. 9.0 GO TO 513
512 RANVAR = 0.0
    GO TO 521
513 ALTVAL = ALTVAL - 10.0
    RANVAR = 1.0

```

```

421 IF1 BOUL(ALTVAL) / 522. 905. 522
522 IF1 ALTVAL .00. 1.0 1 00 TN 531
IF1 ALTVAL .30. 2.0 1 00 TN 532
IF1 ALTVAL .40. 3.0 1 00 TN 533
IF1 ALTVAL .70. 4.0 1 00 TN 534
ALTVAL = 0.0
07 TN 403

```

```

991 ALTVAL = - 1.0
    GO TO 903
992 ALTVAL = - 0.0
    GO TO 903
993 ALTVAL = 1.0
    GO TO 903
994 ALTVAL = - 2.0
    GO TO 903

```

132


```

C      INITIALIZATION OF VALUES BASED ON 1949 US STANDARD ATMOSPHERE
301  ABO50(1:2) = ABO50(1:2)
      ISTATM = - ISTATM
      GO 327  I = 1, 14
302  VAL50(1:1) = VAL50(1:1)
303  IPI 1 = 1, 1 304, 304, 327
304  P50(1:2) = ABO50(1:2)
305  P10(1) = P10(1)
306  TMR(1) = TMR(1)
307
311  IPI  P10(1) = 912, 319, 312
312  GMRH(1:1) = GMRH(1) / P10(1)
      ISTATM(1) = - I
      GO TO 314
313  GMRH(1:1) = GMRH(1) / TMR(1)
      ISTATM(1) = 0
314  CONTINUE
307
321  IPI  ISTATM = ISTATM / 322, 325, 322
322  IPI  ISTATM = ISTATM / 371, 325, 371
323  P10(1:1) = P50(1:1)
      IPI 1 = 0 324, 324, 327
324  VAL50(1:1) = VAL50(1:1)
      GO TO 327
325  P10(1:1) = P50(1:1)
      IPI 1 = 0 326, 326, 327
326  VAL50(1:1) = VAL50(1:1)
327  CONTINUE
307
331  F0 = 0.0
      ALT00 = 0.0
      GO TO 110
307
371  WRITE(6,71) ISTATM
      WRITE(6,72) ISTATM, SECOND, ISTATM
307
381  IPI  NOLGOTHTM 1 302, IPI, 302
382  CALL GNTM
307
391  IPI  ABO50(1:2) = 2.0 1 399, 392, 399
392  READ 15,921 VAL50(1)
393  WRITE(6,921) VAL50(1)
307
399  CALL EXIT

```

[illegible]

C TRANSFER TO COMPUTATION SECTION:
NO SPECIM 1 301, 401, 501

183	PLATE	•	155.0
	WICH	•	1.0

```

C      ALGORITHM: ENTRY POINT WHICH DOES NOT REQUIRE A REG-APP
      ENTRY SEQUENCE

291  IF( WHICH = 3001, .001, .001

391  THRESH = QWESP - 1 THETA - THETA1
      TCWSP = QWESP - DELTA
      TPI04 = PSI - PSI1
      IF( OUTPUT = 031, .001, .031

401  DIFFTH = QWESP - 1 THETA - THETA1
      IF( -ABS(DELTH - DIFFTH) = 0.03, .021, .012
404  IF( ABS(DELTH - DIFFTH) = 0.00, .021, .021
406  IF( PIR02L - DIFFTH = 0.05, .031, .041
408  IF( PIR02H - DIFFTH = 0.01, .031, .031
409  IF( PIRL - DIFFTH = 0.07, .051, .041
437  IF( PIRH - DIFFTH = 0.00, .051, .051
400  QWESP1 = QWESP - 010
      THETA1 = THETA - TPI01
      PSI1 = - PSI
      QWESP = - QWESP
      IF( WHICH = 301, .001, .001

421  THRESH = QWESP - DELTA - QWESP1
      TCWSP = 0
427  TPI04 = PSI + ( QWESP2 - 1.0 ) * STOR1 PIR02, PSI1
      IF( OUTPUT = 027, .001, .027

491  THRESH = PIP - QWESP2 - DELTA - QWESP1
      TCWSP = 0
497  TPI04 = PSI + ( QWESP2 + 1.0 ) * STOR1 PIR02, PSI1
      IF( OUTPUT = 030, .001, .032

404  QWESP = STOR1 1.0, DIFFTH-PI002 ) * 1.0
      STOR1 = - QWESP1
      THRESH = QWESP - PIR02
      TCWSP = STOR1 THRESH-DIFFTH, STORP21
      THRESH = THRESH1
      IF( QWESP1 = 032, .022, .037

```

```

571 DIFTH = (THETA - THETAP) * QUESPP
572 IFI - ANGLEH - DIFTH * 903, 921, 911
573 IFI - ANGLEH - DIFTH * 904, 921, 921
574 IFI - DIFTH - DIFTH * 904, 921, 921
575 IFI - DIFTH - DIFTH * 904, 921, 921
576 IFI - DIFTH - DIFTH * 904, 921, 921
577 IFI - DIFTH - DIFTH * 904, 921, 921

511 ZETA = SIGN(PIE, ZETA) - ZETA
512 PSIP = PSIP
513 TPISIP = TPISIP
514 WHICH = 301, 401, 501

52 IFI ANGLEH - ABS(DELTA) * 522, 923, 523
521 TAMPV = ABS(SINDEL) / COSDEL
522 ANGLE2 = 0.0
523 ANGLE2 = SIGN(PIPO2, DELTA) - ZETA
524 ANGLE2 = ABS(ANGLE2)
525 GO TO 545

531 TPOVH = - DPHAN
532 TCASA = 2.0
533 TPISIP = PSI * QUESPP * (ZETA - PIPO2)
534 IFI OUTPUT 1 623, 601, 523

511 TPOVH = DIFTH - DPHAN
512 TCASA = QUESPP * (DELTA - ZETA)
513 TPISIP = PSI - PSIP
514 IFI PIPO2H - AGSITCASA * 532, 534, 534
515 SPPH = QUESPP * DELTA
516 TPOVH = TPOVH + PI
517 TCASA = SIGN(PIP - AGSITCASA), TCASA
518 TPISIP = TPISIP * SIGN(PIP, SPPH)
519 IFI OUTPUT 1 633, 601, 533
520 IFI OUTPUT 1 632, 601, 532

541 IFI ANGLEH - ABS(DELTA) * 542, 541, 541
542 SINTH = SIN(DIFTH)
543 COSH = COS(DIFTH)
544 TPOVH = SINTH / COSH
545 ANGLE1 = ATANI SINDEL / COSDEL / SINTH
546 ANGLE2 = ATANI TAMPV / ABS(SINDEL)
547 ANGLE2 = ANGLE2 - ZETA
548 ANGLE2 = ABS(ANGLE2)
549 IFI ANGLEH - ANGLE2 * 549, 571, 571
550 IFI PIPO2H - ANGLE2 * 549, 572, 572
551 IFI PIPO2H - ANGLE2 * 549, 572, 572
552 IFI PIPO2H - ANGLE2 * 549, 572, 572
553 IFI PIPO2H - ANGLE2 * 549, 572, 572

```

```

571 SPPH = - QUESPP * DELTA
572 DIFTH = QUESPP - 1.0
573 TPOVH = ATANI(TAMPV) - DPHAN
574 TCASA = 0.0
575 TPISIP = PSI * SIGN(ANGLE2, SPPH) + 0.0
576 IFI OUTPUT 1 671, 601, 571

577 OICOW = SIGN(1.0, COSH) - 1.0
578 SPPH = - QUESPP * DIFTH
579 SPPH = SIGN(1.0, DELTA) * SIGN(1.0, QUESPP * COSH) - 1.0
580 TPOVH = - OICOW * PIPO2
581 TCASA = SIGN(TPOVH - ATANI(TAMPV), SPPH)
582 TPISIP = PSI * SIGN(ANGLE2, SPPH) + 0.0
583 IFI OUTPUT 1 672, 601, 572

575 PSICOW = SIGN(1.0, CPOVH) - 1.0
576 SPPH = - QUESPP * DELTA
577 SPPH = SIGN(1.0, DELTA) * SIGN(2.0, QUESPP * COSH) - 1.0
578 TPOVH = ATANI - TAMPV - 0.0
579 TCASA = 0.0
580 TPISIP = PSI * SIGN(ANGLE2, SPPH) + 0.0
581 IFI OUTPUT 1 673, 601, 573

581 SPPH = - QUESPP * DELTA
582 SPPH = SIGN(1.0, SIGN(1.0, DELTA * ANGLE2)) * QUESPP - 1.0
583 SINH = SIGN(ANGLE2)
584 TPOVH = ATANI(COSAN) * TAMPV
585 TCASA = ATANI(SIN(TPOVH)) * SINH / COSAN * QUESPP
586 ANGLE2 = ATANI(COSAN) / ABS(SIN(TPOVH)) * TAMPV
587 TPOVH = TPOVH - DPHAN
588 TPISIP = PSI * SIGN(ANGLE2, SPPH) + 0.0
589 IFI OUTPUT 1 681, 601, 581

582 SPPH = - QUESPP * DELTA
583 PSICOW = SIGN(1.0, CPOVH) - 1.0
584 SPPH = SIGN(1.0, PI - ANGLE2)
585 SPPH = COSAN * QUESPP * QUESPP * COSH
586 SPPH = SIGN(1.0, DELTA) * SIGN(2.0, QUESPP * COSH) - 1.0
587 SINH = SIGN(ANGLE2)
588 TPOVH = ATANI(COSAN) * TAMPV - OICOW * PIPO2
589 TCASA = ATANI(SIN(TPOVH)) * SINH / COSAN * QUESPP
590 ANGLE2 = ATANI(COSAN) / SIN(TPOVH) * TAMPV
591 TPOVH = TPOVH - DPHAN
592 TPISIP = PSI * SIGN(ANGLE2, SPPH) + 0.0
593 IFI OUTPUT 1 682, 601, 582

```

```

551 IFI ANGLEH - ABS(DELTA) * 552, 553, 553
552 TAMPV = - ABS(SINDEL) / COSDEL
553 ANGLE2 = PIPO2
554 ANGLE2 = SIGN(PIPO2, DELTA) - ZETA
555 ANGLE2 = ABS(ANGLE2)
556 GO TO 545

551 TPOVH = PSI - DPHAN
552 TCASA = 0.0
553 TPISIP = PSI * QUESPP * (ZETA - PIPO2)
554 IFI OUTPUT 1 653, 601, 553

561 IFI PIPO2H - ABS(DELTA) * 562, 561, 561
562 IFI PIPO2H - ABS(DELTA) * 562, 561, 561
563 SINTH = SIN(DIFTH)
564 COSH = COS(DIFTH)
565 TPOVH = SINTH / COSH
566 SINH = TPOVH - ZETA
567 COSAN = COS(DELTA)
568 PSICOW = SIGN(1.0, CPOVH) - 1.0
569 PSICOW = QUESPP * QUESPP * COSH
570 PSICOW = SIGN(1.0, QUESPP * COSH) - 1.0
571 TPOVH = ATANI(COSAN) * TAMPV
572 TCASA = ATANI(SIN(TPOVH)) * SINH / COSAN * QUESPP
573 ANGLE2 = ATANI(COSAN) / SIN(TPOVH) * TAMPV
574 TPOVH = TPOVH - DPHAN
575 TPISIP = PSI * SIGN(ANGLE2, SPPH) + 0.0
576 IFI OUTPUT 1 653, 601, 553

561 SINTH = SIN(DIFTH)
562 COSH = COS(DIFTH)
563 TPOVH = SINTH / COSH
564 SINH = TPOVH - ZETA
565 COSAN = COS(DELTA)
566 PSICOW = SIGN(1.0, CPOVH) - 1.0
567 PSICOW = QUESPP * QUESPP * COSH
568 PSICOW = SIGN(1.0, QUESPP * COSH) - 1.0
569 TPOVH = ATANI(COSAN) * TAMPV
570 TCASA = ATANI(SIN(TPOVH)) * SINH / COSAN * QUESPP
571 ANGLE2 = ATANI(COSAN) / SIN(TPOVH) * TAMPV
572 TPOVH = TPOVH - DPHAN
573 TPISIP = PSI * SIGN(ANGLE2, SPPH) + 0.0
574 IFI OUTPUT 1 653, 601, 553

```

```

651 IFI ABS(TPOVH) - SINH * 652, 653, 653
652 TPOVH = 0.0
653 IFI ABS(TPOVH) - SINH * 652, 653, 653
654 TCASA = 0.0
655 IFI PIPO2H - ABS(TPOVH - SINH) * 656, 657, 657
656 TPISIP = TPISIP * SIGN(PIPO2, SINH - TPISIP)
657 ILOOP = 1
658 IFI ILOOP - 1, 100, 1 DO 10 658
659 ILOOP = 0
660 WRITE(6,10) DELTA, THETA, PSI, DPHAN, THETAP, ZETA
661 WRITE(6,10) DIFTH, TPOVH, TCASA, TPISIP
662 ILOOP = ILOOP + 1
663 IFI ILOOP - 10, 10, 1 LAST = 1
664 IFI OUTPUT 1 652, 601, 553
665 IFI ABS(TPOVH) - SINH * 656, 657, 657
666 TPISIP = 0.0
667 PSICOW = TPISIP
668 IFI OUTPUT 1 653, 601, 553

```

[illegible][illegible]


```

241 STANME = 0.0
242 CARRMS = C.0
    CARRMS = C.0
    R17506 = 0.0
    C12504 = C.0
    GO TO 244
243 SIGN1 = 1.29, ATTACK 1
    GO TO 242
    ATTACK = 0.0
    STANME = 2449,246, 2449
244 LEORUM = 2449
    GO TO 249
245 SIGN1 = 1.29, ATTACK 1
    IF P13241 1 2459,246, 2459
246 LEORUM = 2459
    GO TO 249
    ATTACK = 5.0
    STPMH1 = P.0
    BENDC = P.0
    HIFTEP = HIFTE
    WIFTEP = C.9
    LEORUM = PHUJ
    CPMH1 = 1.0
    RMWOT1 = RMWHT - 1
    GOFCMC = CUMPT
    PMCMG = 1.0
    GO TO 248
247 STANME = ATTACK
    P1212 = 991
    ALPMH1 = ALPHAD
    PMH1ST = PHIDEG
248 RETURN

```

```

ATTACK = ATTACK
231 1F1 M -. 1 2019.202, 2019
2019 1F0M0 0 2019
GO TO 999
202 1F1 100000 + 200 1 2019.203, 2239
2029 1F1 M = 2029
GO -. 999
235 1F1 100000 1 2029.204, 2039
2039 1F0M0 M = 2039
GO 77 999
204 1F1 0010 1 2049.211, 209
2049 1F0M0 = 2049
GO 73 999
205 1F1 = 0.0
2059 1F0M0 = AMAN1(AM05AM1) FV, FVAM1 1 1-FV1M, FV00M0
FV00FF = AMAN1(AM05AM1) FV, FV, FVAM1 1 1-FV1M, FV00M0
FV00FF = AMAN1(AM05AM1) FV, FV, FVAM1 1 1-FV1M, FV00M0
1F1 0010 = 101.0 1 211, 207, 211
1F1 0010 = 0.0
GO 71 249
211 1F1 0010 1 212, 230, 212
212 1F1 0000 1 213, 219, 213
213 1F1 0010(ATTACK) = 2.0 1 215, 234, 214
214 ATTACK = SIGNM 3%, ATTACK 1
1F1 0010 1 2149, 216, 2149
2149 1F0M0 = 2149
GO 79 999
215 ATTACK = SIGNM(1.25*AMAN1(0.625*SIGNM.0625*ATTACK),PI2ZCH1,ATTACK)
PI2ZM0 = (PI2ZM0 + SIGNM(0.5*ATTACK) = 0.5 1 AMAN1(PI2ZM0,1.0)
AMAN1(PI2ZM0,0.25 1
CPHAME = (SIGNM(1.0,1.3125*ATTACK-PI2ZCH1) + 1.0 1 CPHAME
CPHAME = 2.0000 + CPHAME
1F1 0010 1 2191,2160,791
2160 0010 = 0.0
GO TO 221
217 0010 = 0.0
0010 = 0.0
1F1 0010(ATTACK) = 2.0 1 219, 2179,2179
2179 0010 = 2179
GO TO 999
218 1F1 0010 1 222, 219, 222
219 0010 = 0.0
0010 = 0.0
GO TO 209

```

```

      GA T/ 240
267  ATTACK  *  ATTACK
240  FBI      *  FBI
      ALPSTR  *  ALPHAD
      PHISTR  *  PHIDEC
243  RETURN

```

[illegible]

```

PITCH RATE DELAY AND ADJUSTMENT
701 IPI ATSEVW 1 1 702, 710, 702
702 IPI ANDI ATSEVW, CMIOO 1 705, 705, 705
703 NMOPL = O
704 IPI ANDI ATSEVW, CMIOO 1 708, 710, 706
705 NMOPL = WMOPL O 1
706 IPI ANDI ATSEVW, CMIOO 1 708, 707, 708
707 NMOPL = O
708 GO TO 709
709 NMOPL = NMOPL + 1
710 NO = NO + 1
711 NMOPL = KOTOT O 1
712 IPI NMOPL = NO 1 712, 721, 7109
712 IPI NMOPL = NO 1 713, 721, 7109
713 NO = O
714 NMOPL = O
715 NMOPL = O
716 AWRGE = O.O
717 TINDIP = O.O
718 ALPDAT = ALPONE
719 PHINAT = PHIONE
720 IPI CMIOAL 1 710, 7109, 7101
721 ALPDAT = ALPONE
722 CMIOAL = CMIOAL
723 ALPONE = ALPDAT*ALPDAT*ALPDAT
724 IPI ALPNE*LT,ALPUM 1 CMIOAL = AMI(CMIOAL,CMIOAL)
725 PTIAPM = -ALPDAT*ALPDAT / CMIOAL
726 CMIOAL = CMIOAL + ALPDAT / CMIOAL*ALPDAT
727 PTIAPM = ALPNE / CMIOAL
728 ALPONE = (ALPDAT*ALPDAT IPI ALPDAT*ALPDAT I/CMIOAL*NO,SPATIALP
729 CMIOAL 1 710, 7109, 7102
730 PMIOST = PHIONE
731 GAINPM = CMIOAL
732 PHINAT = PHIONE*PMIOST*ALPDAT
733 PHIOCD = ABSI PHINUM 1
734 IPI PHINUM*LT,PHISUM 1 GAINPM = (SIGN(PHINUM)*PHISUM,CMIOALPM,GAINPM)
735 PTIAPM = -PMIOST*ALPDAT / GAINPM
736 CMIOAL = CMIOAL + PMIOST / GAINPM*NO,SPATIALP
737 PTIAPM = PHINE / GAINPM
738 PHINE = (PHIOAT*PMIOST IPI PHIOAT*PMIOST I/GAINPM*NO,SPATIALP
739 ATSEVW = O
740 ATALIC = CMIOAL ALPDAT*ALPDAT*ALPDAT*CMIOAL, O,077 1, PHIRAT 1
741 ATMIC = CMIOAL ALPDAT*ALPDAT*ALPDAT*CMIOAL, O,077 1, PHIRAT 1
742 IPI ATSEVW*LT, 710 I GO TO 710
743 IPI 7101 1 717, 721, 717
744 IPI 7101*CMIOAL*LT, 710 I GO TO 721
745 IPI 7101*CMIOAL*LT, 710 I GO TO 721
746 IPI 7101*CMIOAL*LT, 710 I GO TO 721
747 IPI 7101*CMIOAL*LT, 710 I GO TO 721
748 IPI 7101*CMIOAL*LT, 710 I GO TO 721
749 IPI 7101*CMIOAL*LT, 710 I GO TO 721
750 IPI 7101*CMIOAL*LT, 710 I GO TO 721
751 IPI 7101*CMIOAL*LT, 710 I GO TO 721
752 IPI 7101*CMIOAL*LT, 710 I GO TO 721
753 IPI 7101*CMIOAL*LT, 710 I GO TO 721
754 IPI 7101*CMIOAL*LT, 710 I GO TO 721
755 IPI 7101*CMIOAL*LT, 710 I GO TO 721
756 IPI 7101*CMIOAL*LT, 710 I GO TO 721
757 IPI 7101*CMIOAL*LT, 710 I GO TO 721
758 IPI 7101*CMIOAL*LT, 710 I GO TO 721
759 IPI 7101*CMIOAL*LT, 710 I GO TO 721
760 IPI 7101*CMIOAL*LT, 710 I GO TO 721
761 IPI 7101*CMIOAL*LT, 710 I GO TO 721
762 IPI 7101*CMIOAL*LT, 710 I GO TO 721
763 IPI 7101*CMIOAL*LT, 710 I GO TO 721
764 IPI 7101*CMIOAL*LT, 710 I GO TO 721
765 IPI 7101*CMIOAL*LT, 710 I GO TO 721
766 IPI 7101*CMIOAL*LT, 710 I GO TO 721
767 IPI 7101*CMIOAL*LT, 710 I GO TO 721
768 IPI 7101*CMIOAL*LT, 710 I GO TO 721
769 IPI 7101*CMIOAL*LT, 710 I GO TO 721
770 IPI 7101*CMIOAL*LT, 710 I GO TO 721
771 IPI 7101*CMIOAL*LT, 710 I GO TO 721
772 IPI 7101*CMIOAL*LT, 710 I GO TO 721
773 IPI 7101*CMIOAL*LT, 710 I GO TO 721
774 IPI 7101*CMIOAL*LT, 710 I GO TO 721
775 IPI 7101*CMIOAL*LT, 710 I GO TO 721
776 IPI 7101*CMIOAL*LT, 710 I GO TO 721
777 IPI 7101*CMIOAL*LT, 710 I GO TO 721
778 IPI 7101*CMIOAL*LT, 710 I GO TO 721
779 IPI 7101*CMIOAL*LT, 710 I GO TO 721
780 IPI 7101*CMIOAL*LT, 710 I GO TO 721
781 IPI 7101*CMIOAL*LT, 710 I GO TO 721
782 IPI 7101*CMIOAL*LT, 710 I GO TO 721
783 IPI 7101*CMIOAL*LT, 710 I GO TO 721
784 IPI 7101*CMIOAL*LT, 710 I GO TO 721
785 IPI 7101*CMIOAL*LT, 710 I GO TO 721
786 IPI 7101*CMIOAL*LT, 710 I GO TO 721
787 IPI 7101*CMIOAL*LT, 710 I GO TO 721
788 IPI 7101*CMIOAL*LT, 710 I GO TO 721
789 IPI 7101*CMIOAL*LT, 710 I GO TO 721
790 IPI 7101*CMIOAL*LT, 710 I GO TO 721
791 IPI 7101*CMIOAL*LT, 710 I GO TO 721
792 IPI 7101*CMIOAL*LT, 710 I GO TO 721
793 IPI 7101*CMIOAL*LT, 710 I GO TO 721
794 IPI 7101*CMIOAL*LT, 710 I GO TO 721
795 IPI 7101*CMIOAL*LT, 710 I GO TO 721
796 IPI 7101*CMIOAL*LT, 710 I GO TO 721
797 IPI 7101*CMIOAL*LT, 710 I GO TO 721
798 IPI 7101*CMIOAL*LT, 710 I GO TO 721
799 IPI 7101*CMIOAL*LT, 710 I GO TO 721
800 IPI 7101*CMIOAL*LT, 710 I GO TO 721

```


SUBROUTINE PATCH 6.0 PAGE 1

513PTE CELL PULSET,PMP,00,0000
SUBROUTINE PATCH

C SUBROUTINE PATCH CODE NUMBER PATCH VERSION 6.0

C THIS PROGRAM WILL ADJUST THE ALTITUDE OF THE VEHICLE SO AS TO
MINIMIZE TEMPERATURE AND ACCELERATION PEAKS AND MINIMIZE CROSS
RANGE.

C COMMON STATEMENTS FOR GLOBAL VARIABLES
COMMON /CPTD0/ PTD0(1),PTD0(2),PTD0(3)
COMMON /CSCAP/ ALPHAD,ALPDA,ALPDB,ALPDC,ALPDE,ALPDI,ALPDJ,
CSCAP
COMMON /CINTS/ ALN,HTP,LOPOT,LOHDE,LOHDT,INTST,PLAST,PAIL,
CINTS
COMMON /CPTD5/ PTD5(1),PTD5(2),PTD5(3),PTD5(4),PTD5(5),PTD5(6)

C COMMON STATEMENTS FOR SUBROUTINE VARIABLES
COMMON /CPTD0/ PTD0(1),PTD0(2),PTD0(3)
COMMON /CSCAP/ ALPHAD,ALPDA,ALPDB,ALPDC,ALPDE,ALPDI,ALPDJ,
CSCAP
COMMON /CINTS/ ALN,HTP,LOPOT,LOHDE,LOHDT,INTST,PLAST,PAIL,
CINTS
COMMON /CPTD5/ PTD5(1),PTD5(2),PTD5(3),PTD5(4),PTD5(5),PTD5(6)

C COMMON STATEMENTS FOR LOCAL VARIABLES
COMMON /CPTD0/ PTD0(1),PTD0(2),PTD0(3)
COMMON /CSCAP/ ALPHAD,ALPDA,ALPDB,ALPDC,ALPDE,ALPDI,ALPDJ,
CSCAP
COMMON /CINTS/ ALN,HTP,LOPOT,LOHDE,LOHDT,INTST,PLAST,PAIL,
CINTS
COMMON /CPTD5/ PTD5(1),PTD5(2),PTD5(3),PTD5(4),PTD5(5),PTD5(6)

C LOCAL DATA VALUES WHICH ARE FIXED
DATA PMP,HTP,LOPOT,LOHDE,LOHDT,INTST,PLAST,PAIL,
CINTS,PTD0(1),PTD0(2),PTD0(3),PTD5(1),PTD5(2),PTD5(3),PTD5(4),PTD5(5),PTD5(6)

SUBROUTINE PATCH 6.0 PAGE 3

301 IFI AMBI ATARNE, 0100 1 1 302, 301, 302
302 IFI ATARNE 1 321, 302, 331
303 IFORNE = 302
GO TO 000

321 IFI AMBI 1 321, 321, 321
322 ALPDA = ALPDA - GAINAL * PTIDIP
323 IFI ALPDA = ALPDA * PTIDIP 1 GO TO 325
324 ALPDA = ALPDA * ALPDA * ALPDA * PTIDIP - 0.5 * GAINAL * PTIDIP
GO TO 326
325 ALPDA = ALPDA * ALPDA * ALPDA * PTIDIP
326 IFI ALPDA = ALPDA * PTIDIP 1 327, 328, 331
327 ALPDA = ALPDA
328 ALPDA = 0.0
GO TO 326
329 ALPDA = ALPDA * ALPDA * ALPDA * PTIDIP
330 IFI ALPDA = ALPDA * PTIDIP 1 323, 324, 331
331 ALPDA = ALPDA
332 IFI ALPDA = ALPDA * PTIDIP 1 329, 341, 329
333 ALPDA = ALPDA
334 ALPDA = 0.0
GO TO 341

331 IFI AMBI 1 331, 331, 331
332 ALPDA = ALPDA * GAINAL * PTIDIP
333 IFI ALPDA = ALPDA * PTIDIP 1 GO TO 335
334 ALPDA = ALPDA * ALPDA * ALPDA * PTIDIP - 0.5 * GAINAL * PTIDIP
GO TO 336
335 ALPDA = ALPDA * ALPDA * ALPDA * PTIDIP - 0.5 * GAINAL * PTIDIP
336 IFI ALPDA = ALPDA * PTIDIP 1 337, 338, 341
337 ALPDA = ALPDA
338 ALPDA = 0.0
GO TO 336
339 ALPDA = ALPDA * ALPDA * ALPDA * PTIDIP
340 IFI ALPDA = ALPDA * PTIDIP 1 333, 334, 331
341 ALPDA = ALPDA
342 IFI ALPDA = ALPDA * PTIDIP 1 339, 341, 339
343 ALPDA = ALPDA
344 ALPDA = 0.0
GO TO 341

SUBROUTINE PATCH 6.0 PAGE 2

301 IFI AMBI ATARNE 1 1, 201, 1
302 IFI AMBI 1 1 000, 250, 000
303 RETURN
304
305 IFI ATTACK - ATARNE 1 250, 201, 230
306 IFI H - 2 1 200, 250, 250
307 IFORNE = 250
GO TO 000
308 IFI LOPOT 1 250, 250, 250
309 IFORNE = 250
GO TO 000
310 IFI LOHDE - LOHDT 1 250, 250, 250
311 IFORNE = 250
GO TO 000
312 IFI LOHDT - LOHDT 1 250, 250, 250
313 IFORNE = 250
GO TO 000
314 IFI ATTACK - ATARNE 1 250, 250, 250
315 IFI PHICN 1 250, 250, 250
316 IFORNE = 250
GO TO 000
317 IFI ATTACK - ATARNE 1 250, 250, 250
318 IFI PHICN 1 250, 250, 250
319 IFI PHICN = 0.0
320 IFI PHICN = PHICN
321 IFI PHICN = PHICN
322 IFI PHICN = PHICN
323 IFI PHICN = PHICN
324 IFI PHICN = PHICN
325 IFI PHICN = PHICN
326 IFI PHICN = PHICN
327 IFI PHICN = PHICN
328 IFI PHICN = PHICN
329 IFI PHICN = PHICN
330 IFI PHICN = PHICN
331 IFI PHICN = PHICN
332 IFI PHICN = PHICN
333 IFI PHICN = PHICN
334 IFI PHICN = PHICN
335 IFI PHICN = PHICN
336 IFI PHICN = PHICN
337 IFI PHICN = PHICN
338 IFI PHICN = PHICN
339 IFI PHICN = PHICN
340 IFI PHICN = PHICN
341 IFI PHICN = PHICN
342 IFI PHICN = PHICN
343 IFI PHICN = PHICN
344 IFI PHICN = PHICN
345 IFI PHICN = PHICN
346 IFI PHICN = PHICN
347 IFI PHICN = PHICN
348 IFI PHICN = PHICN
349 IFI PHICN = PHICN
350 IFI PHICN = PHICN
351 IFI PHICN = PHICN
352 IFI PHICN = PHICN
353 IFI PHICN = PHICN
354 IFI PHICN = PHICN
355 IFI PHICN = PHICN
356 IFI PHICN = PHICN
357 IFI PHICN = PHICN
358 IFI PHICN = PHICN
359 IFI PHICN = PHICN
360 IFI PHICN = PHICN
361 IFI PHICN = PHICN
362 IFI PHICN = PHICN
363 IFI PHICN = PHICN
364 IFI PHICN = PHICN
365 IFI PHICN = PHICN
366 IFI PHICN = PHICN
367 IFI PHICN = PHICN
368 IFI PHICN = PHICN
369 IFI PHICN = PHICN
370 IFI PHICN = PHICN
371 IFI PHICN = PHICN
372 IFI PHICN = PHICN
373 IFI PHICN = PHICN
374 IFI PHICN = PHICN
375 IFI PHICN = PHICN
376 IFI PHICN = PHICN
377 IFI PHICN = PHICN
378 IFI PHICN = PHICN
379 IFI PHICN = PHICN
380 IFI PHICN = PHICN
381 IFI PHICN = PHICN
382 IFI PHICN = PHICN
383 IFI PHICN = PHICN
384 IFI PHICN = PHICN
385 IFI PHICN = PHICN
386 IFI PHICN = PHICN
387 IFI PHICN = PHICN
388 IFI PHICN = PHICN
389 IFI PHICN = PHICN
390 IFI PHICN = PHICN
391 IFI PHICN = PHICN
392 IFI PHICN = PHICN
393 IFI PHICN = PHICN
394 IFI PHICN = PHICN
395 IFI PHICN = PHICN
396 IFI PHICN = PHICN
397 IFI PHICN = PHICN
398 IFI PHICN = PHICN
399 IFI PHICN = PHICN
400 IFI PHICN = PHICN

SUBROUTINE PATCH 6.0 PAGE 4

341 IFI H - 1 1 340, 342, 355
342 IFORNE = 340
GO TO 000
343 IFI LOPOT = 200 1 340, 343, 340
344 IFORNE = 340
GO TO 000
345 IFI LOHDE = LOHDT
346 IFI LOHDE = LOHDT
347 IFI LOHDE = LOHDT
348 IFI LOHDE = LOHDT
349 IFI LOHDE = LOHDT
350 IFI LOHDE = LOHDT
351 IFI LOHDE = LOHDT
352 IFI LOHDE = LOHDT
353 IFI LOHDE = LOHDT
354 IFI LOHDE = LOHDT
355 IFI LOHDE = LOHDT
356 IFI LOHDE = LOHDT
357 IFI LOHDE = LOHDT
358 IFI LOHDE = LOHDT
359 IFI LOHDE = LOHDT
360 IFI LOHDE = LOHDT
361 IFI LOHDE = LOHDT
362 IFI LOHDE = LOHDT
363 IFI LOHDE = LOHDT
364 IFI LOHDE = LOHDT
365 IFI LOHDE = LOHDT
366 IFI LOHDE = LOHDT
367 IFI LOHDE = LOHDT
368 IFI LOHDE = LOHDT
369 IFI LOHDE = LOHDT
370 IFI LOHDE = LOHDT
371 IFI LOHDE = LOHDT
372 IFI LOHDE = LOHDT
373 IFI LOHDE = LOHDT
374 IFI LOHDE = LOHDT
375 IFI LOHDE = LOHDT
376 IFI LOHDE = LOHDT
377 IFI LOHDE = LOHDT
378 IFI LOHDE = LOHDT
379 IFI LOHDE = LOHDT
380 IFI LOHDE = LOHDT
381 IFI LOHDE = LOHDT
382 IFI LOHDE = LOHDT
383 IFI LOHDE = LOHDT
384 IFI LOHDE = LOHDT
385 IFI LOHDE = LOHDT
386 IFI LOHDE = LOHDT
387 IFI LOHDE = LOHDT
388 IFI LOHDE = LOHDT
389 IFI LOHDE = LOHDT
390 IFI LOHDE = LOHDT
391 IFI LOHDE = LOHDT
392 IFI LOHDE = LOHDT
393 IFI LOHDE = LOHDT
394 IFI LOHDE = LOHDT
395 IFI LOHDE = LOHDT
396 IFI LOHDE = LOHDT
397 IFI LOHDE = LOHDT
398 IFI LOHDE = LOHDT
399 IFI LOHDE = LOHDT
400 IFI LOHDE = LOHDT

471 IF(CRSMAX) 472, 441, 472
472 IF(P379CM) 404, 247, 404

SUBROUTINE PATCH 4.0 PAGE 6

```

901 IFI 00001 BARK 1 921, 931, 941
921 C0P001 = 1.0 * (P1000A - P1000B) * PW100 / CL000 / C0N1T / P0
931 101 C0P01 = C0P001 * 520, 950, 955
941 101 1.0 - C0P001 * 500, 520, 951
950 PW100 = P010
PW100 = P010
S10001 = P010
C0P001 = 1.0
01 12 953
931 PW100 = PW100 * PW100 * P1000
00 12 957
951 C0P001 = C0P001
952 S10001 = S1000 S001: 0001 0001:0-C0P001:0-C0P001:1, P0101
PW100 = 100.0
PW100 = 200.0
101 C0P001 = 5120, 5120, 953
9520 P0000 = 0000
00 12 950
951 C0N1T001
001 00 P000

```

C FROMAT
99 FORMATI 1207 1000000 . 6115 / 11011.0 / 2012 1

[illegible]

1450

[illegible][illegible]

540

17920.853	22.2773.31	0.4391220	106.5045	31.5930	-91.3739	1860.371	41.4805	-30.8634	24	0.781	3286.811	742	122.0906	2.69241	-6.5568
16846.211	210701.23	0.439941	175.8128	30.7605	-88.1402	1923.114	38.5115	-37.8013	25	0.896	3286.433	742	125.0414	2.97866	-6.7237
15950.587	200832.97	0.745335	104.5374	30.2273	-85.8332	1082.226	36.2309	-41.2526	26	1.051	3286.714	735	127.0762	3.25756	-9.0538
15883.934	270000.	0.785192	104.4149	30.1912	-85.7755	1072.357	36.5678	-41.6888	27	1.059	3286.514	765	127.2098	3.27904	-9.2409
12810.622	152000.	0.435470	85.3957	29.2346	-77.1114	2187.669	22.7061	-40.8776	28	1.457	3070.616	765	134.6229	2.15966	-32.1019
9966.497	148000.91	0.	81.4829	29.3446	-75.1188	2222.042	22.7061	-37.3542	29	1.297	2496.583	718	135.4285	6.30612	-36.4704
9702.566	149020.12	0.	80.2937	29.3241	-75.3317	2233.501	22.7061	-36.2815	30	1.230	2837.280	713	135.6743	6.49111	-37.1725
7446.041	135036.62	1.300585	69.6153	30.0570	-72.4268	2345.418	22.7061	-26.9002	31	1.	2470.192	701	137.9847	8.28378	-49.6758
6319.113	123548.58	0.791141	64.0840	30.4405	-71.3846	2392.625	22.7061	-22.1588	32	0.750	2246.075	701	138.1848	9.06222	-55.6608
6208.525	129359.91	0.800705	63.8244	30.4584	-71.3440	2400.	22.7061	-21.9522	33	1.195	2234.786	728	138.2079	9.09386	-55.9181
5174.688	122336.66	1.895306	59.2918	30.7024	-70.6132	2455.147	22.7061	-17.1862	34	5.	1984.258	702	138.6876	9.87641	-61.8367
5000.	121152.80	2.073047	57.6823	30.9497	-70.3213	2465.899	22.7061	-16.6667	35	1.103	1959.418	703	138.7317	9.95865	-62.4958
4940.924	170546.44	2.153491	57.3931	30.9729	-70.2748	2469.096	22.7061	-16.4205	36	0.500	1947.723	701	138.7519	9.99704	-62.8034
4015.624	110635.25	7.886049	52.8822	31.3142	-69.7046	2518.194	22.7061	-12.5647	37	4.	1753.617	702	139.6078	10.53974	-67.5657
4000.	110471.34	2.891767	52.8077	31.3195	-69.6953	2519.005	22.7061	-12.5000	38	1.166	1749.992	703	139.0113	10.54792	-67.6438
3096.998	130926.40	3.769699	48.5337	31.6162	-69.2707	2567.686	22.7061	-8.7375	39	0.250	1514.011	701	139.1760	10.98794	-72.0462
3019.061	107000.	3.942087	48.2442	31.6410	-69.2379	2575.192	22.7061	-8.4128	40	1.091	1491.979	765	139.1876	11.02356	-72.5137
3000.	99707.73	4.013164	48.1582	31.6471	-69.2299	2573.292	22.7061	-8.3333	41	1.089	1486.573	703	139.1904	11.03219	-72.5033
2971.535	99416.39	4.092393	48.0300	31.6561	-69.2181	2574.957	22.7061	-8.2147	42	3.	1478.590	762	139.1945	11.04509	-72.6370
ENDURE = 0.000 912.000 = INCHES															

THE CALCULATION FOR CASE NUMBER 3312 HAS BEEN TERMINATED. TIME USED = 1 MINUTES. 36.267 SECONDS.

ADDITIONAL OUTPUT FOR CASE NUMBER 3312

NO.	GMT	COUNT	MSIP	MUS	FLIGHT	DISTANCE	BETA	MACH	NO	ACCEL	TEMP	NO	EQ	TEMP1	TEMP2	TEMP3	TEMP4	TEMP5	TEMP6
1	742	0	0	0	0	0	0.0000	29.412	0.0024	1915.412	1000.00	1000.00	1000.00	1000.00	1000.00	1000.00	1000.00	1000.00	1000.00
2	705	163	8	8	3246050.50000	8.7513	29.438	0.0354	2682.115	2248.55	2544.45	2351.83	2233.35	1515.61	2.71				
3	748	267	1	17	6559618.75000	17.5914	29.132	0.1430	3177.035	3197.59	3044.56	3044.56	3044.56	2639.63	7.70				
4	718	402	15	14	6806697.95023	18.3699	29.136	0.0368	3176.616	3165.13	3405.91	3049.46	3044.75	2721.99	8.18				
5	718	461	19	11	13663208.34521	36.9986	28.947	0.0313	3103.301	3103.23	3335.20	2982.31	2983.54	2990.51	20.51				
6	749	464	2	12	13958152.34521	37.6956	28.940	0.0313	3101.995	3103.12	3334.26	2981.53	2982.49	2988.60	21.02				
7	728	619	11	8	15472495.59521	41.7876	28.891	0.0444	3102.011	3102.01	3333.34	2981.36	2981.41	2983.59	23.63				
8	742	635	4	6	16042735.59521	43.3285	28.870	0.0444	3101.991	3102.01	3333.34	2981.37	2981.41	2982.80	24.61				
9	742	681	6	4	17928303.59521	48.9238	28.796	0.0508	3102.167	3102.16	3333.50	2981.53	2981.56	2981.82	27.87				
10	742	726	7	3	19671791.59521	53.1352	28.717	0.0576	3102.334	3102.32	3333.67	2981.69	2981.72	2981.73	30.39				
11	742	771	6	1	21256175.59521	57.4167	28.635	0.0646	3102.472	3102.45	3333.82	2981.83	2981.85	2981.80	33.65				
12	742	825	3	4	23470447.59521	63.6004	28.499	0.0756	3102.655	3102.65	3334.02	2982.01	2982.03	2981.96	37.51				
13	742	878	6	2	25423263.59521	68.9832	28.355	0.0874	3102.827	3102.81	3334.19	2982.16	2982.19	2982.12	40.94				
14	742	937	4	3	27272941.59521	73.6766	28.192	0.1007	3102.986	3102.96	3334.36	2982.31	2982.34	2982.27	44.20				
15	742	985	5	2	29039597.59521	78.5512	28.004	0.1166	3103.151	3103.13	3334.54	2982.47	2982.49	2982.42	47.33				
16	728	1028	8	11	30571773.84521	82.5922	27.807	0.1362	3103.314	3103.27	3334.69	2982.61	2982.63	2982.55	50.07				
17	742	1036	2	5	30760189.84521	83.1014	27.780	0.1366	3103.311	3103.28	3334.70	2982.62	2982.64	2982.57	50.41				
18	705	1156	8	12	34849994.09521	107.5776	23.781	0.2035	3286.559	3281.66	3527.50	3156.62	3156.26	3133.17	68.76				
19	748	1161	3	15	40144915.09521	108.4756	23.495	0.5235	3287.632	3285.24	3530.70	3159.04	3157.63	3140.48	69.51				
20	742	1317	5	4	41470995.09521	112.0642	22.264	0.5326	3287.476	3287.48	3532.55	3159.65	3159.68	3155.35	72.97				
21	742	1408	3	4	42759547.09521	115.5495	20.952	0.6055	3287.313	3287.35	3532.45	3159.50	3159.55	3158.65	76.47				
22	742	1497	5	4	43953811.09521	118.7860	19.580	0.6837	3287.101	3287.15	3532.25	3159.30	3159.35	3159.22	79.87				
23	728	1509	7	11	44066231.59521	119.9904	19.443	0.6928	3287.065	3287.13	3532.23	3159.28	3159.33	3159.23	80.20				
24	742	1620	5	3	45181751.59521	122.1121	18.035	0.7805	3286.811	3286.87	3531.96	3159.03	3159.09	3159.16	83.55				
25	742	1682	4	3	46274487.59521	125.0734	16.430	0.8958	3286.474	3286.52	3531.57	3158.67	3158.75	3158.89	87.03				
26	735	1742	2	4	47030967.59521	127.1244	15.233	1.0513	3286.214	3286.26	3531.44	3158.60	3158.61	3158.68	89.59				
27	765	1751	8	11	47088604.22021	127.5595	15.157	1.0590	3286.514	3286.41	3531.51	3158.66	3158.66	3158.69	89.76				
28	765	1839	11	7	49972386.47021	135.1098	10.075	1.4572	3070.616	3127.10	3349.86	2990.70	3002.72	3037.98	101.08				
29	718	1866	17	11	50329184.68608	136.0798	9.373	1.2969	2896.583	2988.11	3193.24	2846.95	2866.85	2965.89	102.38				
30	718	1881	10	16	50441891.19531	136.3863	9.063	1.2301	2831.280	2955.21	2729.97	2432.51	2451.07	2593.02	105.33				
31	701	1933	15	7	51402808.17184	138.9991	7.109	1.2628	2470.192	2556.21	2729.97	2432.51	2451.07	2593.02	105.33				
32	701	1967	13	6	51762251.10938	139.9767	6.088	1.2027	2246.075	2393.77	2548.49	2261.75	2291.79	2457.72	106.11				
33	728	1976	9	7	51772006.60938	140.0174	6.043	1.1950	2234.786	2385.37	2539.07	2259.23	2283.48	2451.21	106.14				
34	702	2004	8	13	52113428.78125	140.9322	5.000	1.0977	1984.258	2175.77	2304.99	2045.50	2078.64	2289.75	106.69				
35	703	2015	9	11	52147611.50000	141.0252	4.888	1.1034	1959.418	2153.58	2280.53	2043.66	2057.05	2272.07	106.74				
36	701	2027	1	11	52163500.73628	141.0685	4.836	1.1070	1947.728	2143.29	2269.27	2013.60	2044.98	2243.76	106.76				
37	702	2052	12	9	52385518.16016	141.6689	4.000	1.1659	1753.817	1991.98	2102.43	1862.32	1899.88	2142.04	107.04				
38	703	2080	8	15	52467762.28906	141.6758	3.986	1.1660	1769.992	1989.55	2099.75	1859.92	1897.49	2150.09	107.04				
39	701	2082	6	13	5249174.43750	142.1447	3.124	1.0997	1514.011	1842.24	1934.82	1703.27	1753.17	2025.93	107.21				
40	765	2093	10	8	5249236.62500	142.1821	3.047	1.0913	1491.979	1828.83	1919.75	1695.55	1739.94	2015.67	107.22				
41	703	2102	9	14	5249236.62500	142.1912	3.028	1.0893	1486.573	1825.54	1916.07	1692.21	1736.68	2013.14	107.22				
42	762	2113	11	10	52581235.33398	142.2047	3.000	1.0865	1478.450	1820.60	1910.53	1687.18	1731.81	2009.36	107.23				
TOTALS		962	824							917.000	3287.48	3532.55	3159.65	3159.68	3159.23	42			

LINE NUMBER	MAXIMUM VALUE	28	19	20	20	20	20	23	42
		1.4572	3287.632	3287.48	3532.55	3159.65	3159.68	3159.23	107.23
VALUES USED	RIKADS	=	2.00000	1.50000	1.50000	1.50000	1.47500	1.50000	1.00000
TO COMPJTE	CMDS	=	0.50000	0.50000	0.50000	0.50000	0.50000	0.50000	0.00000
TEMPERATURES	E	=	0.50000	0.50000	0.78125	0.62500	0.78125	0.00000	0.00000

EQUILIBRIUM RATIOS ARE 1.00000 1.07457 0.96112 0.96112 0.96112 0.96112 0.00000
 MAXIMUM EQUILIBRIUM TEMPERATURES ARE 3287.63 3532.79 3159.82 3159.82 3159.82 0.00

END OF OUTPUT FOR CASE NUMBER 3312

Unclassified

Security Classification

DOCUMENT CONTROL DATA - R&D		
(Security classification of title, body of abstract and indexing annotation must be entered when the overall report is classified)		
1. ORIGINATING ACTIVITY (Corporate author) Institute for Aerospace Studies, University of Toronto, Toronto, Ontario, Canada		2a. REPORT SECURITY CLASSIFICATION Unclassified
		2b. GROUP
3. REPORT TITLE AN ATTITUDE CONTROL SYSTEM TO CONSTRAIN THE SKIN TEMPERATURE OF A MANNED LIFTING SPACECRAFT DURING REENTRY INTO THE EARTH'S ATMOSPHERE		
4. DESCRIPTIVE NOTES (Type of report and inclusive dates) Scientific		
5. AUTHOR(S) (Last name, first name, initial) Fine, Jerome H.		
6. REPORT DATE July 1967	7a. TOTAL NO. OF PAGES 145	7b. NO. OF REFS 40
8a. CONTRACT OR GRANT NO. AFOSR 222-66	8a. ORIGINATOR'S REPORT NUMBER(S) UTIAS REPORT NO. 126	
a. PROJECT NO.		
c.	9b. OTHER REPORT NO(S) (Any other numbers that may be assigned this report)	
d.	AFOSR 67-0858	
10. AVAILABILITY/LIMITATION NOTICES Distribution of this document is unlimited		
11. SUPPLEMENTARY NOTES TECH, OTHER	12. SPONSORING MILITARY ACTIVITY Air Force Office of Scientific Research 1400 Wilson Blvd., Arlington, Virginia 22209	
13. ABSTRACT >An attitude control system to regulate the temperature of a manned lifting spacecraft during reentry into the Earth's atmosphere is proposed. Its use prevents the peak skin temperature that is experienced during the reentry from rising moderately beyond that which would occur during an equilibrium glide of the same vehicle. The effects of Earth rotation and oblateness upon the performance of the attitude control system were found to be moderate and predictable. The maximum temperature increment associated with them was found to be only 100F° for the worst set of initial conditions. The cross range shift of the footprint due to rotation was found to be within 70 miles of the value that would occur for the corresponding orbit in vacuum. Oblateness could generally be accounted for by using the effective initial glide angle relative to the Earth's surface rather than the geocentric initial value relative to the central coordinate system. The results of density variation in the Earth's atmosphere were not serious. Large increases in the maximum skin temperature occurred only when extremely large spatially random density disturbances were encountered by the vehicle.		

DD FORM 1473
1 JAN 64

Security Classification

Unclassified
Security Classification

14. KEY WORDS	LINK A		LINK B		LINK C	
	ROLE	WT	ROLE	WT	ROLE	WT
Reentry - heating Reentry - lifting body Reentry - temperature control Reentry - effect of earth oblateness Reentry - effect of density perturbations						

INSTRUCTIONS	
<p>1. ORIGINATING ACTIVITY: Enter the name and address of the contractor, subcontractor, grantee, Department of Defense activity or other organization (corporate author) issuing the report.</p> <p>2a. REPORT SECURITY CLASSIFICATION: Enter the overall security classification of the report. Indicate whether "Restricted Data" is included. Marking is to be in accordance with appropriate security regulations.</p> <p>2b. GROUP: Automatic downgrading is specified in DoD Directive 5200.10 and Armed Forces Industrial Manual. Enter the group number. Also, when applicable, show that optional markings have been used for Group 3 and Group 4 as authorized.</p> <p>3. REPORT TITLE: Enter the complete report title in all capital letters. Titles in all cases should be unclassified. If a meaningful title cannot be selected without classification, show title classification in all capitals in parenthesis immediately following the title.</p> <p>4. DESCRIPTIVE NOTES: If appropriate, enter the type of report, e.g., interim, progress, summary, annual, or final. Give the inclusive dates when a specific reporting period is covered.</p> <p>5. AUTHOR(S): Enter the name(s) of author(s) as shown on or in the report. Enter last name, first name, middle initial. If military, show rank and branch of service. The name of the principal author is an absolute minimum requirement.</p> <p>6. REPORT DATE: Enter the date of the report as day, month, year, or month, year. If more than one date appears on the report, use date of publication.</p> <p>7a. TOTAL NUMBER OF PAGES: The total page count should follow normal pagination procedures, i.e., enter the number of pages containing information.</p> <p>7b. NUMBER OF REFERENCES: Enter the total number of references cited in the report.</p> <p>8a. CONTRACT OR GRANT NUMBER: If appropriate, enter the applicable number of the contract or grant under which the report was written.</p> <p>8b, 8c, & 8d. PROJECT NUMBER: Enter the appropriate military department identification, such as project number, subproject number, system numbers, task number, etc.</p> <p>9a. ORIGINATOR'S REPORT NUMBER(S): Enter the official report number by which the document will be identified and controlled by the originating activity. This number must be unique to this report.</p> <p>9b. OTHER REPORT NUMBER(S): If the report has been assigned any other report numbers (either by the originator or by the sponsor), also enter this number(s).</p> <p>10. AVAILABILITY/LIMITATION NOTICES: Enter any limitations on further dissemination of the report, other than those</p>	<p>imposed by security classification, using standard statements such as:</p> <p>(1) "Qualified requesters may obtain copies of this report from DDC."</p> <p>(2) "Foreign announcement and dissemination of this report by DDC is not authorized."</p> <p>(3) "U. S. Government agencies may obtain copies of this report directly from DDC. Other qualified DDC users shall request through _____."</p> <p>(4) "U. S. military agencies may obtain copies of this report directly from DDC. Other qualified users shall request through _____."</p> <p>(5) "All distribution of this report is controlled. Qualified DDC users shall request through _____."</p> <p>If the report has been furnished to the Office of Technical Services, Department of Commerce, for sale to the public, indicate this fact and enter the price, if known.</p> <p>11. SUPPLEMENTARY NOTES: Use for additional explanatory notes.</p> <p>12. SPONSORING MILITARY ACTIVITY: Enter the name of the departmental project office or laboratory sponsoring (paying for) the research and development. Include address.</p> <p>13. ABSTRACT: Enter an abstract giving a brief and factual summary of the document indicative of the report, even though it may also appear elsewhere in the body of the technical report. If additional space is required, a continuation sheet shall be attached.</p> <p>It is highly desirable that the abstract of classified reports be unclassified. Each paragraph of the abstract shall end with an indication of the military security classification of the information in the paragraph, represented as (TS), (S), (C), or (U).</p> <p>There is no limitation on the length of the abstract. However, the suggested length is from 150 to 225 words.</p> <p>14. KEY WORDS: Key words are technically meaningful terms or short phrases that characterize a report and may be used as index entries for cataloging the report. Key words must be selected so that no security classification is required. Identifiers, such as equipment model designation, trade name, military project code name, geographic location, may be used as key words but will be followed by an indication of technical context. The assignment of links, rules, and weights is optional.</p>